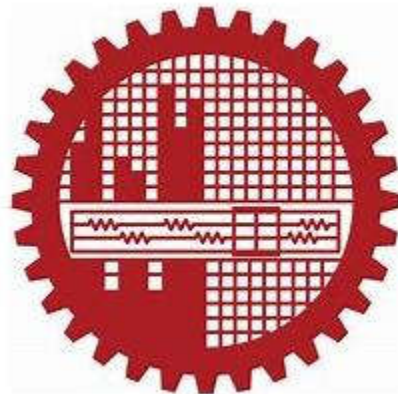


**ANALYTICAL AND NUMERICAL ANALYSIS OF GROUND
MOVEMENT ABOVE A TUNNEL UNDER SEISMIC
LOADING**

MD. FOISAL HAQUE

**MASTER OF SCIENCE IN CIVIL ENGINEERING
(GEOTECHNICAL)**



**DEPARTMENT OF CIVIL ENGINEERING
BANGLADESH UNIVERSITY OF ENGINEERING AND TECHNOLOGY
DHAKA, BANGLADESH**

DECEMBER 2019

**ANALYTICAL AND NUMERICAL ANALYSIS OF GROUND
MOVEMENT ABOVE A TUNNEL UNDER SEISMIC
LOADING**

A Thesis

by

MD. FOISAL HAQUE

MASTER OF SCIENCE IN CIVIL ENGINEERING (GEOTECHNICAL)

**DEPARTMENT OF CIVIL ENGINEERING
BANGLADESH UNIVERSITY OF ENGINEERING AND TECHNOLOGY
DHAKA**

December, 2019

**ANALYTICAL AND NUMERICAL ANALYSIS OF GROUND
MOVEMENT ABOVE A TUNNEL UNDER SEISMIC
LOADING**

A Thesis

by

Md. Faisal Haque

Submitted to the Department of Civil Engineering, Bangladesh University of Engineering
and Technology (BUET), Dhaka in partial fulfilment of the requirements for the degree

of

MASTER OF SCIENCE IN CIVIL ENGINEERING (GEOTECHNICAL)

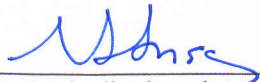
December, 2019

BANGLADESH UNIVERSITY OF ENGINEERING AND TECHNOLOGY

DHAKA

This thesis titled “ANALYTICAL AND NUMERICAL ANALYSIS OF GROUND MOVEMENT ABOVE A TUNNEL UNDER SEISMIC LOADING”, submitted by MD. FOISAL HAQUE, Roll No. 1017042204F, Session: October 2017, has been accepted as satisfactory in partial fulfilment of the requirement for the degree of Master of Science in Civil Engineering (Geotechnical) on 11th December, 2019.

BOARD OF EXAMINERS



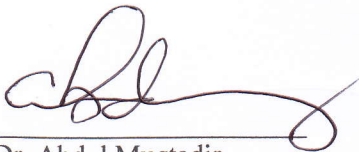
Dr. Mehedi Ahmed Ansary
Professor
Department of Civil Engineering, BUET

: Chairman
(Supervisor)



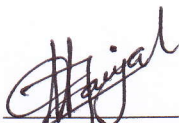
Dr. Md. Habibur Rahman
Professor and Head
Department of Civil Engineering, BUET

:Member



Dr. Abdul Muqtadir
Professor
Department of Civil Engineering, BUET

: Member



Dr. Md. Abu Taiyab
Professor
Department of Civil Engineering, DUET

: Member
(External)

CANDIDATE'S DECLARATION

It is hereby declared that this thesis or any of it has not been submitted elsewhere for the award of any degree or diploma.

(Md. Foisal Haque)

DEDICATION

This Thesis is Dedicated to My Late Father

ACKNOWLEDGEMENTS

Praise be to Almighty Allah. The author expresses his utmost gratitude to Allah for all his accomplishments.

The author would like to thank his supervisor Dr. Mehedi Ahmed Ansary, Professor, Department of Civil Engineering, Bangladesh University of Engineering and Technology (BUET) for giving this interesting topic. The idea of this thesis was initially conceived by him. The author appreciates very much his enthusiastic and enthusing support. He encouraged playful and independent thinking and gave the freedom to try out new ways. With his very positive approach he assisted in boiling the essential out of results and helped to make the work converge to a thesis. The author regards him as an outstandingly good scientific supervisor and a very nice person to work with.

The author is undoubtedly grateful to his family members and his friends for their co-operation.

ABSTRACT

Numerous methods have been used to construct a tunnel, Earth Pressure Balance Tunnel Boring Machine (EPB – TBM) method has been found to be more suitable than others. EPB – TBM has to balance earth and water pressure with the tunnel face pressure. This research deals with the movement of tunnel using EPB-TBM in homogenous sandy layer only. Ground conditions have been modelled in PLAXIS 3D software to estimate results for static (long term) and seismic loading. The site under consideration contains two layers of soil such as upper clay layer and lower sand layer respectively. Thickness of clay and sand layers are 3.5m and 24m respectively. Lateral and longitudinal dimensions of finite element models are 30m and 80m. Movement of tunnel depends on many parameters. Major parameters are relative depth (A_n/D_n) and tunnel length (y_n). Movement of tunnel is affected by surface settlements. Strain induced volume loss is an important parameter for tunnel movement. In this research, five depths of tunnel crown (A_1, A_2, A_3, A_4 and A_5), three diameters (D_1, D_2 and D_3) and three lengths (y_1, y_2 and y_3) variations have been considered to predict ground movement of tunnel under seismic and static loading. Many researches have already been done considering plain strain conditions. Previously, empirical and analytical formulas are developed based on plain strain (2D) assumption. But that method is not fully able to estimate the settlement correctly. The present researcher has modified these empirical and analytical formulas to estimate settlements. Empirical and analytical formulas results are compared with each other. Longitudinal, lateral and vertical surface settlements have varied with the variation of relative depths, diameters and phased construction modes of tunnel. Seismic loading has been applied in the model in free field condition and duration of seismic shaking used is five seconds.

PLAXIS 3D software has been used for numerical modelling in the present research. Relevant model of existing literature has been validated using PLAXIS 3D. Maximum vertical surface settlement of literature data was 8.53mm. Present researcher reanalysed the model of literature by PLAXIS 3D and obtain vertical surface settlement of 8.54mm. Also, author modified empirical and analytical formulas have been validated by using previous researchers formulae based on case study related issue. Results of settlements obtained from present study and case study are close. Results present two different types of settlements such as surface and total settlement (bottom of tunnel). Settlements of three directions varied with the variations of relative depths of tunnel. Settlements values of static loading are higher than the seismic loading because of short duration of seismic shaking. Minimum values of vertical, lateral and longitudinal surface settlements are 5mm, 2.5mm and 3mm respectively at A_5/D_1 location for static loading based on numerical analysis. Maximum value of major principle stress is 160 KN/m² at A_5/D_1 location based on static loading. Minimum value of acceleration is 0.2 m/s² at relative depth A_5 and diameter D_1 for dynamic time 0.48 seconds. Maximum vertical surface settlement is 1.2mm at 0.6s at A_5/D_1 location during seismic loading. To obtain more accuracy of results, larger model sizes and more data are required. The finding from this research offer significant new information about settlements of segmental bored tunnel such as EPB – TBM and which as guide for future implementation in geotechnical applications.

TABLE OF CONTENTS

	Page No.
DEDICATION	v
ACKNOWLEDGEMENT	vi
ABSTRACT	vii
TABLE OF CONTENT	viii
LIST OF TABLES	xii
LIST OF FIGURES	xiii
NOTATION	xvi
CHAPTER ONE GENERAL OVERVIEW	
1.1 INTRODUCTION	1
1.2 OBJECTIVE	3
1.3 OUTLINE	3
CHAPTER TWO LITERATURE REVIEW	
2.1 INTRODUCTION	4
2.2 VOLUME LOSS	4
2.3 SURFACE SETTLEMENTS	7
2.3.1 Vertical Surface Settlement (Transverse to Tunnel Axis)	7
2.3.1.1 Empirical Formulae	7
2.3.1.2 Analytical Formulae	9
2.3.2 Lateral Surface Settlement (Transverse to Tunnel Axis)	10
2.3.2.1 Empirical Formulae	10
2.3.2.2 Analytical Formulae	10
2.3.3 Longitudinal Surface Settlement (Along the Tunnel Axis)	10
2.3.3.1 Empirical Formulae	10
2.3.3.2 Analytical Formulae	11
2.4 SUB – SURFACE SETTLEMENTS	11
2.4.1 Vertical Sub – Surface Settlement (Transverse to Tunnel Axis)	11
2.4.1.1 Empirical Formulae	11
2.4.1.2 Analytical Formulae	12
2.4.2 Lateral Sub – Surface Settlement (Transverse to Tunnel Axis)	12

2.4.2.1	Empirical Formulae	12
2.4.2.2	Analytical Formulae	12
2.4.3	Longitudinal Sub – Surface Settlement (Along the Tunnel Axis)	13
2.4.3.1	Empirical Formulae	13
2.5	SEISMIC ANALOGY	13
2.5.1	Case Histories	13
2.5.2	Ground Shaking	14
2.5.3	Ground Failure	14
2.5.4	Lateral Settlement Due to Seismic Loading	15
2.5.5	Damages of TBM Tunnels Due to Seismic Loading	18
2.6	CONSTITUTIVE MODEL	20
2.7	CALCULATION PROCESS IN PLAXIS 3D	25
2.7.1	Soil Elements	25
2.7.2	Global Settings	26
2.7.3	Phased Construction	26
2.7.4	Initial Stress Generation	27
2.7.5	Plastic Calculation	29
2.7.6	Dynamic Calculation	29
2.8	STRAIN INDUCED VOLUME LOSSES	30
2.8.1	Volumetric Strains in Long Term Loading	30
2.8.2	Volumetric Strains in Seismic Shaking	31
2.9	CONCLUSIONS	31

CHAPTER THREE MODIFIED EMPIRICAL AND ANALYTICAL FORMULAS

3.1	INTRODUCTION	33
3.2	MODIFIED FORMULAS	33
3.2.1	Modified Empirical Formula for Maximum Vertical Settlement	33
3.2.2	Modified Analytical Formulae for Maximum Vertical Settlement	34
3.2.3	Modified Empirical Formulae for Maximum Lateral Settlement	34
3.2.4	Modified Analytical Formulae for Maximum Lateral Settlement	35
3.2.5	Modified Empirical Formula for Maximum Longitudinal Settlement	36
3.2.6	Modified Analytical Formulae for Strain Induced Volume Loss	36
3.3	VALIDATION OF MODIFIED FORMULAS	37
3.3.1	Validation of Modified Empirical Formula for Settlement	37
3.3.2	Validation of Modified Analytical Formula for Settlement	38
3.3.3	Validation of Modified Strain Induced Volume Loss Formula	38
3.4	IMPLEMENTATION OF MODIFIED FORMULAS IN PRESENT RESEARCH	38

3.4.1	Vertical Surface Settlements	39
3.4.2	Total Vertical Settlements	40
3.4.3	Lateral Surface Settlements	40
3.4.4	Total Lateral Settlements	41
3.4.5	Longitudinal Surface Settlements	41
3.4.6	Total Longitudinal Settlements	42
3.4.7	Strain Induced Volume Loss	42
3.5	CONCLUSIONS	43

CHAPTER FOUR RESULTS AND INTERPRETATION OF NUMERICAL ANALYSIS

4.1	INTRODUCTION	44
4.2	FINITE ELEMENT MODEL	44
4.3	MATERIAL PROPERTIES OF SOIL AND TUNNEL LINNING	45
4.4	LOADING MECHANISM OF EPB – TBM	48
4.5	MESH GENERATIONS	51
4.6	ANALYSIS PROCESS	52
4.7	MESHING EFFECTS ON THE RESULTS	53
4.8	VALIDATION OF PLAXIS 3D	54
4.9	COMPARISON AMONG PLAXIS 2D AND MODIFIED FORMULAE RESULTS WITH PLAXIS 3D RESULTS	57
4.9.1	Comparison between PLAXIS 2D and PLAXIS 3D Results	59
4.9.2	Comparison of Modified Formulae Results with PLAXIS 3D Results	60
4.10	RESULTS OF VERTICAL SETTLEMENTS	62
4.10.1	Vertical Surface Settlements	62
4.10.2	Total Vertical Settlements	66
4.11	RESULTS OF LATERAL SETTLEMENTS	70
4.11.1	Lateral Surface Settlements	70
4.11.2	Total Lateral Settlements	73
4.12	RESULTS OF LONGITUDINAL SETTLEMENTS	77
4.12.1	Longitudinal Surface Settlements	77
4.12.2	Total Longitudinal Settlements	81
4.13	RESULTS OF STRAIN INDUCED VOLUME LOSS	85
4.14	STRESS – STRAIN BEHAVIOUR OF SOIL AROUND TUNNEL	88
4.14.1	Long Term Loading	88
4.14.2	Seismic Loading	89
4.15	SURFACE ACCELERATION DURING SEISMIC SHAKING	90
4.16	SURFACE DISPLACEMENT DURING SEISMIC SHAKING	98

4.17	CONCLUSIONS	104
------	-------------	-----

CHAPTER FIVE CONCLUSIONS AND RECOMMENDATIONS

5.1	CONCLUSIONS	106
-----	-------------	-----

5.2	RECOMMENDATIONS FOR FUTURE STUDIES	108
-----	------------------------------------	-----

	REFERENCES	109
--	-------------------	-----

	APPENDIX A	113
--	-------------------	-----

	APPENDIX B	131
--	-------------------	-----

	APPENDIX C	153
--	-------------------	-----

LIST OF TABLES

		Page No.
Table 2.1:	Values of the parameters describing the recommended Type 1 elastic response spectra [Eurocode 8].	17
Table 2.2:	Values of the parameters describing the recommended Type 2 elastic response spectra [Eurocode 8].	17
Table 2.3:	Ratios (C) of ground motion at depth to motion at ground surface [Power et al. 1996].	17
Table 2.4:	Ratios of peak ground velocity to peak ground acceleration in different grounds and for increasing source to-site distance [Power et al. 1996].	18
Table 3.1:	Validation of modified empirical formula for maximum vertical surface settlement	37
Table 3.2:	Validation of modified analytical formula for maximum vertical surface Settlement	38
Table 3.3:	Validation of modified strain induced volume loss analytical formula for long term loading	38
Table 4.1:	Material properties of tunnel lining	45
Table 4.2:	Material properties of soil in the specified site and PLAXIS 3D inputting material parameters for consolidated drained test (CD)	46
Table 4.3:	Material properties of soil in the specified site and PLAXIS 3D inputting material parameters for consolidated un-drained test (CU)	47
Table 4.4:	Tunnel face pressure, grouting pressure and jacking force for CD test	50
Table 4.5:	Tunnel face pressure, grouting pressure and jacking force for CU test	51
Table 4.6:	Meshing effect on the results of this research model	53
Table 4.7:	Material Properties and Geotechnical soil parameters and the interfaces (Kilany et al. 2017)	55
Table 4.8:	Validation Results of PLAXIS 3D	56
Table 4.9:	Geotechnical specification used for soil layers of the model (salimi et. al. 2013)	58
Table 4.10:	Characteristics of segments (salimi et. al. 2013)	58
Table 4.11:	Geotechnical specification used for soil layers of the model (salimi et. al. 2013)	58
Table 4.12:	Comparison of PLAXIS 2D results with the help of PLAXIS 3D based on a case study	59
Table 4.13:	Comparison between modified formulae results and PLAXIS 3D results	60

LIST OF FIGURES

	Page No.
Figure 2.1: Circular and Oval Ground Deformation Patterns Around a Tunnel (N. Loganathan (2011) and A. Franza et al. (2018))	6
Figure 2.2: Volume loss assumption for sand (after D. Hunt, 2004)	6
Figure 2.3: Sources of volume loss for a shield driven tunnel (Cording 1991).	7
Figure 2.4: Typically representation of a tunnel.	8
Figure 2.5: Tunnelling induced ground movements (N. Loganathan, 2011).	9
Figure 2.6: Tunnel Transverse Ovaling and Racking Response to Vertically Propagating Shear Waves (Wang, 1993; Owen and Scholl, 1981)	15
Figure 2.7: Tunnel Longitudinal Axial and Curvature Response to Traveling Waves (Wang, 1993; Owen and Scholl, 1981)	16
Figure 2.8: Summary of Observed TBM Tunnel Damage under Ground Shaking Effects (Power et al., 1998)	19
Figure 2.9: Coordinate system and indication of stress components	20
Figure 2.10: Mohr – Coulomb model (Elastic – Perfectly Plastic)	21
Figure 2.11: The Mohr-Coulomb yield surface in principal stress space ($C = 0$)	23
Figure 2.12: 3D soil elements (10-node tetrahedrons)	25
Figure 3.1a: Comparison of maximum vertical surface settlement between empirical and modified empirical formula	37
Figure 3.1b: Configurations of present research tunnel and its components	39
Figure 3.2: Vertical surface settlement for long term and seismic loading based on modified formulae	40
Figure 3.3: Total vertical settlement for long term and seismic loading based on modified formulae	40
Figure 3.4: Lateral surface settlement for long term and seismic loading based on modified formulae	41
Figure 3.5: Total lateral settlement for long term and seismic loading based on modified formulae	41
Figure 3.6: Longitudinal surface settlement for long term loading based on modified formula	42
Figure 3.7: Total longitudinal settlement for long term loading based on modified formula	42
Figure 3.8: Volumetric strain for long term and seismic loading based on modified formulae	43
Figure 4.1: Finite element model based on site soil condition.	44
Figure 4.2: Input value of seismic data	48
Figure 4.3: Loading assumptions for ground and water pressures perpendicular to shield	

	(Bernhard et. al, 2011)	48
Figure 4.4:	Loading and construction mechanism of EPB – TBM of present research	49
Figure 4.5:	Relationship between the maximum thrust/jacking force, P_v and the shield diameter, D [Bernhard et. al, 2011]	49
Figure 4.6:	Fine meshing of model	52
Figure 4.7:	Meshing effect of total vertical settlement for $D_1 = 10.5\text{m}$, $A_1 = 4.5\text{m}$, $y_1 = 27\text{m}$	54
Figure 4.8:	Geotechnical soil layers (Kilany et al. 2017)	56
Figure 4.9:	PLAXIS 3D model of validation paper	57
Figure 4.10:	Material model and vertical surface settlement of case study paper	59
Figure 4.11:	Total settlement for $D_1 = 10.5\text{m}$, $A_1 = 4.5\text{m}$, $y_1 = 27\text{m}$	62
Figure 4.12:	Vertical surface settlement for long term loading based on finite element method	63
Figure 4.13:	Vertical surface settlement of long term loading effect for $A_5 = 8.5\text{m}$, $y_1 = 27\text{m}$	64
Figure 4.14a:	Vertical surface settlement for seismic loading based on finite element method	64
Figure 4.14b:	Vertical surface settlements for various frequencies under seismic loading	65
Figure 4.15:	Vertical surface settlement of seismic loading effect for $A_4 = 7.5\text{m}$, $y_1 = 27\text{m}$	66
Figure 4.16:	Total vertical settlement for long term loading based on finite element method	67
Figure 4.17:	Total vertical settlement of long term loading effect for $A_5 = 8.5\text{m}$, $y_3 = 31\text{m}$	68
Figure 4.18:	Total vertical settlement for seismic loading based on finite element method	68
Figure 4.19:	Total vertical settlement of seismic loading effect for $A_4 = 7.5\text{m}$, $y_1 = 27\text{m}$	69
Figure 4.20:	Lateral surface settlement for long term loading based on finite element method	70
Figure 4.21:	Lateral surface settlement of long term loading effect for $A_5 = 8.5\text{m}$, $y_3 = 31\text{m}$	71
Figure 4.22a:	Lateral surface settlement for seismic loading based on finite element method	72
Figure 4.22b:	Lateral surface settlements for various frequencies under seismic loading	72
Figure 4.23:	Lateral surface settlement of seismic loading effect for $A_5 = 8.5\text{m}$, $y_3 = 31\text{m}$	73
Figure 4.24:	Total lateral settlement for long term loading based on finite element method	74
Figure 4.25:	Total lateral settlement of long term loading effect for $A_5 = 8.5\text{m}$, $y_1 = 27\text{m}$	75
Figure 4.26:	Total lateral settlement for seismic loading based on finite element method	75
Figure 4.27:	Total lateral settlement of seismic loading effect for $A_1 = 4.5\text{m}$, $y_3 = 31\text{m}$	76
Figure 4.28:	Longitudinal surface settlement for long term loading based on finite element method	77
Figure 4.29:	Longitudinal surface settlement of long term loading effect for $A_3 = 6.5\text{m}$, $y_3 = 31\text{m}$	78
Figure 4.30a:	Longitudinal surface settlement for seismic loading based on finite element method	79
Figure 4.30b:	Lateral surface settlements for various frequencies under seismic loading	79

Figure 4.31:	Longitudinal surface settlement of seismic loading effect for $A_5 = 8.5\text{m}$, $y_1 = 27\text{m}$	80
Figure 4.32:	Longitudinal surface settlement profile	81
Figure 4.33:	Total longitudinal settlement for long term loading based on finite element method	82
Figure 4.34:	Total longitudinal settlement of long term loading effect for $A_3 = 6.5\text{m}$, $y_1 = 27\text{m}$	83
Figure 4.35:	Total longitudinal settlement for seismic loading based on finite element method	83
Figure 4.36:	Total longitudinal settlement of seismic loading effect for $A_2 = 5.5\text{m}$, $y_3 = 31\text{m}$	84
Figure 4.37:	Volumetric strain for long term loading based on finite element method	85
Figure 4.38:	Volumetric strain of long term loading effect for $A_4 = 7.5\text{m}$, $y_1 = 27\text{m}$	86
Figure 4.39:	Volumetric strain for seismic loading based on finite element method	87
Figure 4.40:	Volumetric strain of seismic loading effect for $A_5 = 8.5\text{m}$, $y_2 = 29\text{m}$	88
Figure 4.41:	Stress – strain behaviour of soil around tunnel for long term loading	89
Figure 4.42:	Stress – strain behaviour of soil around tunnel for seismic loading	90
Figure 4.43:	Surface acceleration during seismic loading for diameter, D_1	92
Figure 4.44:	Surface acceleration during seismic loading for diameter, D_2	93
Figure 4.45:	Surface acceleration during seismic loading for diameter, D_3	95
Figure 4.46:	Lateral surface acceleration of various relative depth during seismic loading	96
Figure 4.47:	Accelerations for $D_1 = 10.5\text{m}$, $A_4 = 7.5\text{m}$, $y_1 = 27\text{m}$	97
Figure 4.48:	Velocities for $D_1 = 10.5\text{m}$, $A_4 = 7.5\text{m}$, $y_1 = 27\text{m}$	98
Figure 4.49:	Surface displacement during seismic loading for diameter, D_1	100
Figure 4.50:	Surface displacement during seismic loading for diameter, D_2	101
Figure 4.51:	Surface displacement during seismic loading for diameter, D_3	103
Figure 4.52:	Vertical surface displacement of various relative depth during seismic loading	104

NOTATION

V_f	Face Loss
V_b	Shield Loss (Radial)
V_y, V_p	Losses attributable to mechanics of shield driving
V_u	Losses after lining erection
V_g	Losses after grouting
V_t	Tunnel volume loss
V_s	Soil volume loss
V_{sl}	Volume of the settlement trough per unit length of tunnel
V_0	Notional final area of the tunnel cross-section
ΔV	Ground loss at the tunnel periphery
D, D_n	Tunnel diameter
V_l	Percentage fraction of excavated area of tunnel
$V_{(z=0)}$	Vertical surface settlement
$V_{(z=0), \max.}$	Maximum vertical surface settlement
α	Fitting parameter
$x_{(z=0)}$	Horizontal distance from the tunnel centre line at surface
$i_{(z=0)}$	horizontal distance from the tunnel centre line to the point of inflection on the settlement trough
n	Shape function parameter
K	Factor for sands
H	Vertical distance from ground surface to tunnel centre line
ϵ	Uniform radial surface movement
δ	Long – term surface deformation due to the ovalization of tunnel lining
R	Radius of the tunnel
ν	poisson's ratio of sand
$U_{x(z=0)}$	Lateral surface settlement
$U_{y(z=0)}$	Longitudinal surface settlement
$y_{(z=0)}$	Horizontal distance from the tunnel centre line at surface
$V_{(z)}$	Vertical ground settlement
$V_{(z), \max.}$	Maximum vertical ground settlement
$x_{(z)}$	Horizontal distance from the tunnel centre line at ground
$i_{(z)}$	Horizontal distance from the tunnel centre line to the point of inflection on the settlement trough
z	Vertical distance from free surface

$U_{x(z)}$	Lateral ground settlement
$U_{y(z)}$	Longitudinal ground settlement
$Y(z)$	Horizontal distance from the tunnel centre line at ground
a_{gR}	Peak Ground Acceleration (PGA)
$a_{max,s}$	Peak Acceleration at the ground surface above a tunnel
S	Soil Factor
$a_{z,max}$	Peak Acceleration at the depth of tunnel
C	Reduction coefficient
V_s	Peak ground velocity
C_s	Apparent propagation velocity of S-wave
k	Ratio of peak ground velocity to peak ground acceleration
γ_{max}	Maximum shear deformation
Δ_{max}	Maximum lateral displacement at surface
E	Elastic modulus
ϕ	Angle of internal friction
C	Cohesion
ψ	Angle of dilatancy
ϕ'	Effective angle of internal friction
C'	Effective cohesion
ε	Total strain
ε^e	Total elastic strain
ε^p	Total plastic strain
ε_e	Effective strain
ε_e^e	Elastic effective strain
ε_e^p	Plastic effective strain
σ_e	Effective elastic stress
D^e	Elastic modulus
g	Plastic potential function
f	Yield function
λ	Plastic multiplier
$\sigma_{e1}, \sigma_{e2}, \sigma_{e3}$	Effective elastic principal stresses
J_1, J_2, J_3	Stress invariants
$\sigma_{ex}, \sigma_{ey}, \sigma_{ez}$	Elastic effective normal stresses
$\tau_{exy}, \tau_{eyz}, \tau_{ezx}$	Elastic effective shear stresses
I_e	The target element dimension
r_e	Relative element size factor
$\sigma'_{v,0}$	Initial vertical effective stress

$\sigma'_{h,0}$	Initial horizontal effective stress
K_0	Coefficient of lateral earth pressure
g	Diametric deformation
ϵ_{vl}	Volumetric strain in long term loading
ϵ_{vs}	Volumetric strain in seismic loading
V	Maximum velocity of seismic shaking
A, A_c	Maximum acceleration of seismic shaking
Y_1	Distance from neutral axis of tunnel cross section to the lining extreme fibre
$U_{(x), \max.}$	Maximum lateral ground settlement
$\Delta_{(x), \max.}$	Maximum lateral settlement
a_1	Seismic coefficient
C_d	Total depth of soil layer
$U_{(y), \max.}$	Maximum longitudinal ground settlement
t	Thickness of tunnel lining
A_n	Depth of tunnel crown
y_n	Longitudinal length of tunnel
τ_f	Tunnel face pressure
$\sigma_{h, \text{crown}}$	Lateral earth and water pressure at tunnel face
$\sigma_{h, \text{invert}}$	Lateral earth and water pressure at bottom of tunnel
τ_g	Grout pressure
$\sigma_{v, \text{crown}}$	Vertical earth and water pressure at tail of EPB – TBM.
$\sigma_{v, \text{invert}}$	Vertical earth and water pressure at tunnel axis of EPB – TBM.
$\tau_{f, \text{inc.}}$	Linear increment along depth of tunnel
$\tau_{g, \text{inc.}}$	Linear increment along peripheral depth of tunnel
τ_{jf}	Jacking force
MEF-LTL	Modified Empirical Formulae Long Term Loading
MAF-LTL	Modified Analytical Formulae Long Term Loading
MEF-SL	Modified Empirical Formulae Seismic Loading
MAF-SL	Modified Analytical Formulae Seismic Loading
BNBC	Bangladesh National Building Code

NOTE

In general, Standard SI (System International) units are used.

CHAPTER ONE

GENERAL OVERVIEW

1.1 INTRODUCTION

The word tunnel means that ‘underground passage’. Although this meaning is true, it shows the different roles in the world. Tunnels are used as various purposes such as corridors for road and rail networks, utilities, pedestrian movement etc. Shapes (e.g. oval, circular or square) of tunnel to constructed over many years using various tunnelling techniques.

Initially tunnels were constructed to carry various types of water in the major cities. Some of these tunnels are still used today for the same purpose in Egypt, Greece and Rome. In ancient, tunnels were constructed in hard rock by hand mining methods with based on the design of the arch using temporary timber supports. Hand mining method gave little safety to the workers inside the tunnels and was the cause of destructive collapses where many lives were lost. Tunnel construction method was unnecessary until Brunel. The tunnelling shield was invented in 1819. The shield was prevented to ingress of material into the face of the tunnel when constructing a tunnel under the River Thames, where soil conditions were poor. Ground movement was reduced by the shield and shield was provide greater safety for the workers within, although collapses (overlying silt and water) still occurred during the tunnel’s construction between 1825 and 1843.

Construction method of tunnel was modified slightly during its use in the 20th century and has proved to be so successful that it is still in use today. Currently says that the method is ‘open-faced’ method, due to the fact that the face is exposed during construction. Replacement of arched roof tunnels with perfectly circular tunnel linings has the advancement in tunnel design during the 20th Century. These liners expressed as excellent way for carrying soil loading.

Peoples of last thirty years, caused by an expanding global economy, are travelling in congested city centres. Space has necessitated the movement of the transport infrastructure below ground and has seen the birth and subsequent growth of many modern underground Metro systems. The increasing competition for space below ground in modern urbanised cities is almost as large as that above. Many new tunnel and sewer networks are being constructed within the vicinity of existing structures and services.

Modern day engineer has a much-improved knowledge about tunnelling projects and understanding of the possible ground movements that can occur above single tunnels. The mechanism of tunnelling has undergone many innovative changes from the early tunnelling days of Brunel. The modern engineers

consider various factors for designing new tunnels such as various sizes, depths, construction methods and soil type. This improved knowledge has helped the engineer to assess all possible risks and minimise them in order to avoid damage to existing overlying buried structures. The major risk to these structures due to ground movements (vertical, horizontal and longitudinal displacements), which will be predicted accurately than their effects may be minimised/eliminated (if possible).

Two ways to decrease these ground movements and hence decrease the risk of buildings. The first is minimisation at the face and the second is compensation in the ground as the settlements occur (Hunt 2004). Reduction of movements at the face of the tunnel can be achieved through improvement in tunnelling method (i.e tunnelling machine or the use of reinforcement methods for the soil at the face) and tunnel liner design (Hunt 2004). An example of a modern innovation in the tunnelling method has Earth Pressure Balance Machine (EPBM), which balances the forces at the tunnel face between the soil and the machine and hence reduces ground movements. Using sprayed concrete, immediately after excavation in over consolidated clay, known as the New Austrian Tunnelling Method (NATM), has also helped in reducing ground movements over the last thirty years (Hunt 2004). The second approach of ground movements as they occur is by compensation grouting (Harris et al., 2000). Overlying buildings are monitored for movements as tunnel construction occurs below. For apparent (above a specified tolerance) movement, concrete is pumped into the soil above the tunnel and below the building in order to compensate these movements. By undertaking many projects today, some or all of the minimisation methods referred to above are now adopted.

These progresses in tunnelling method have clearly helped to minimise the ground movements occurring due to tunnelling in sand operations. For new tunnel construction, the assessment of risk to existing overlying structures or sub-surface structures is only as accurate as the prediction of ground movements that are made. For many years, empirical methods have been used to predict surface and sub-surface ground movements that occur above a single tunnel.

1.2 OBJECTIVES

This research is presented according to the following objectives, which are described below:

- a. To conduct numerical analysis of tunnel to obtain immediate ground movement above tunnel under seismic loading.
- b. To conduct numerical analysis of tunnel to obtain time dependent ground movement above tunnel under static loading.
- c. To compare immediate and time dependent ground movement above tunnel under seismic and static loading.
- d. To conduct analytically initial stress state of tunnel and stress-strain behaviour of soil around tunnel under seismic loading.

1.3 OUTLINE

This research is presented according to the following chapter headings, the contents are described below:

Chapter 2 describes the literature review for predicting surface and sub-surface settlements above a tunnel in sands, seismic consideration of tunnel, calculation process in PLAXIS 3D, material model and volumetric strains.

Chapter 3 describes modified empirical and analytical formulae, validation of modified formulas, results of vertical, lateral and longitudinal ground movements by considering present research model using modified formulae, strain induced volume loss by modified formulae.

Chapter 4 describes finite element methods, material properties, loading mechanism of EPB-TBM, meshing effect, validation of PLAXIS 3D model, comparison of 2D and 3D analysis results, numerical results of ground movement for three directions, volumetric strain, stress – strain behaviour of soil around tunnel, surface acceleration and displacement during seismic shaking.

Chapter 5 describes the conclusion of this research and future recommendation for further study.

CHAPTER TWO

LITERATURE REVIEW

2.1 INTRODUCTION

Ground movements of sands are caused by the construction of bored tunnel. In practically, sands behaves as anisotropy which is more complex to analysis. So neglect complexity, constant strain induced volume loss and poisson's ratio are considered for analysis of tunnel. Horizontal and vertical movements have been reported by many authors for different tunnelling practices. The most important papers have been created by Zhou (2014), Marshall & Franza (2017), A. Franza et al., (2018), Marto et al., (2014) etc. Tunnels are lower performed under seismic shaking than ground structures such as bridges and buildings. Tunnel structures are constrained by the surrounding ground and it can't be excited independent of the ground as like the inertial response of a bridge structure during earthquakes. Another factor contributing to the reduced damage of tunnel is that the amplitude of seismic ground motion tends to reduce with depth below the ground surface. Major damage of tunnels has been experienced during earthquakes, as summarized by Sharma & Judd (1991), Pescara et al., (2011), Power et al., (1996) etc., among others. Fault rupture through a tunnel, land-sliding (especially at tunnel portals), soil liquefaction, are not considered in this thesis. The most recent Kobe earthquake (1995) in Japan that causes several damage and collapse at the Daikai and Nagata subway stations (Kobe Rapid Transit Railway). The general procedure for seismic design and analysis of tunnel structures has based primarily on the ground deformation approach (as opposed to the inertial force approach); i.e., the structures have designed to accommodate the deformations imposed by the ground. The analysis of the structural response can be conducted first by ignoring the stiffness of the structure, leading to a conservative estimate of the ground deformations. This simplified procedure is generally applicable for structures embedded in rock or very stiff/dense soil. In cases where the structure is stiff relative to the surrounding soil, the effect of soil-structure interaction must be taken into consideration. In this research, ground movements above a tunnel are influenced by variations of tunnel diameter, relative depth and tunnel length.

2.2 VOLUME LOSS

The magnitude of the ground displacements which occur above a tunnel of any diameter can be related to a parameter called the 'volume loss'. Volume loss is also known as ground loss. In plain strain condition, ground loss is represented by two parameters such as (a) tunnel volume loss, V_t , (b) soil volume loss, V_s by A. Franza et al. (2018). Cording and Hansmire (1975) considered these losses to be divided into four stages: (A) face loss, (B) shield loss, (C) losses due to erection of the shield and (D)

time dependent losses. Attewell et al., (1986) gives an empirical formula for tunnel volume loss which is given below.

$$V_t = V_f + V_b + V_p + V_y + V_u + V_g \dots \dots \dots (2.1a)$$

Where,

V_f = face loss

V_b = shield loss (radial)

V_y, V_p = losses attributable to mechanics of shield driving

V_u = losses after lining erection

V_g = losses after grouting

A. Franza et al., (2018) gives an empirical formulae for tunnel volume loss and soil volume loss which are given below.

$$V_t = (\Delta V / V_0) * 100\% \dots \dots \dots (2.1b)$$

$$V_s = (V_{s1} / V_0) * 100\% \dots \dots \dots (2.2a)$$

Where,

V_{s1} = volume of the settlement trough per unit length of tunnel

V_0 = notional final area of the tunnel cross-section

ΔV = ground loss at the tunnel periphery

British Research Establishment (BRE) and the Transport and Road Research Laboratory (TRRL) give an equation of volume loss of the surface settlement trough which is shown in below.

$$V_s = V_1 \left(\frac{\pi D^2}{4} \right) \dots \dots \dots (2.2b)$$

Where,

D is the tunnel diameter.

V_1 is percentage fraction of excavated area of tunnel.

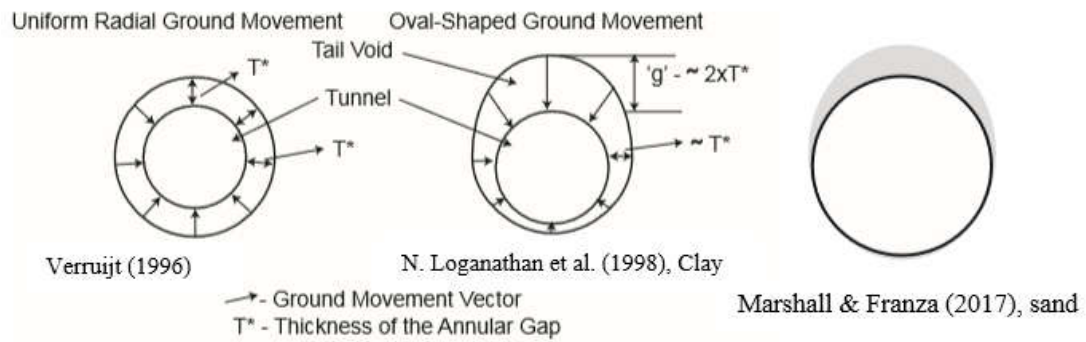


Figure 2.1: Circular and Oval Ground Deformation Patterns Around a Tunnel (N. Loganathan (2011) and A. Franza et al. (2018))

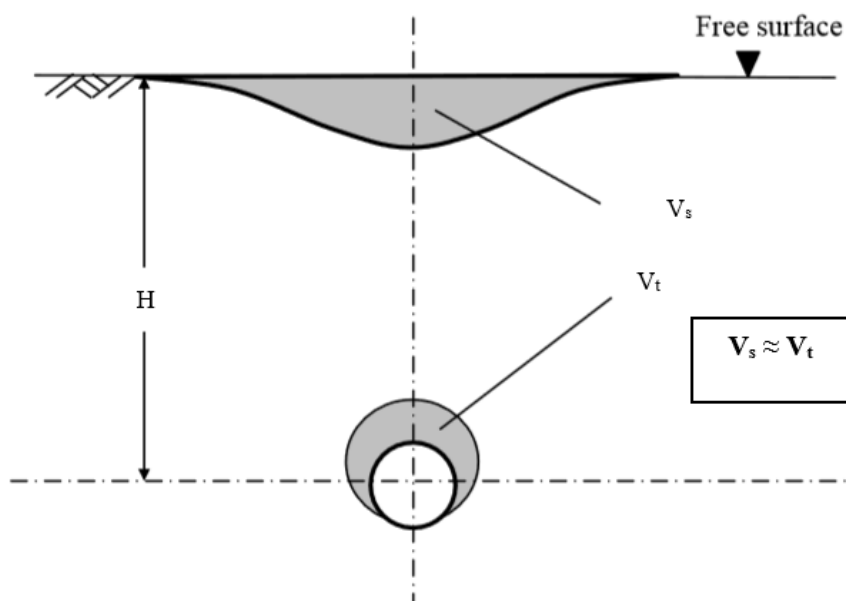


Figure 2.2: Volume loss assumption for sand (after D. Hunt, 2004)

Five main components of ground movements are associated with shield tunnelling as reported by Cording (1991) as shown in given below.

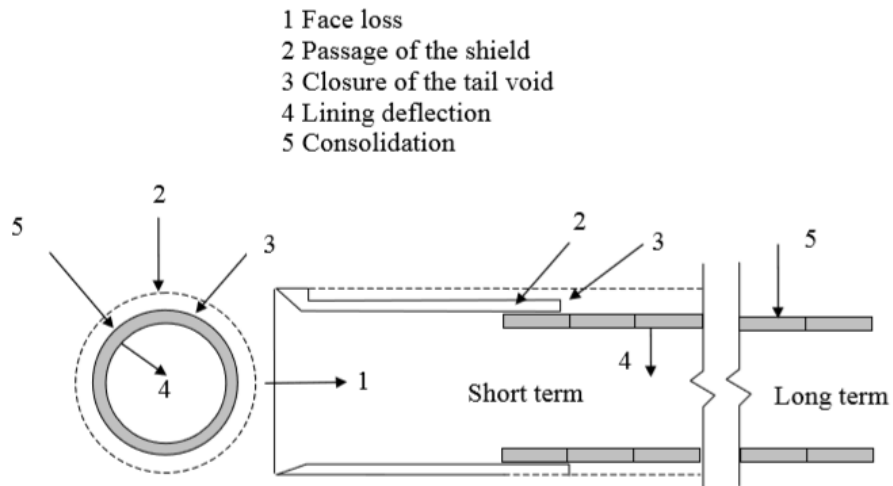


Figure 2.3: Sources of volume loss for a shield driven tunnel (Cording 1991).

2.3 SURFACE SETTLEMENTS

2.3.1 Vertical Surface Settlement (Transverse to Tunnel Axis)

2.3.1.1 Empirical Formulae

The shape of the surface settlement trough above a single tunnel has been tried to model accurately by several authors. In sandy soil, Vorster et al. (2005) suggested to find out vertical surface settlement by using modified Gaussian curve.

$$V_{(z=0)} = V_{(z=0),max} \cdot \frac{n}{(n-1) + \exp\left[\alpha \left(\frac{x_{(z=0)}}{i_{(z=0)}}\right)^2\right]} \dots \dots \dots (2.3a)$$

$$n = e^\alpha \frac{2\alpha - 1}{2\alpha + 1} + 1 \dots \dots \dots (2.3b)$$

$$i_{(z=0)} = KH \dots \dots \dots (2.3c)$$

Where,

$V_{(z=0)}$ = vertical surface settlement

$V_{(z=0),max}$ = maximum vertical surface settlement

α = fitting parameter

$x_{(z=0)}$ = horizontal distance from the tunnel centre line at surface

$i_{(z=0)}$ = horizontal distance from the tunnel centre line to the point of inflection on the settlement trough

n = shape function parameter

K = (0.25~0.45) for sands (Mair and Taylor, 1997)

H = vertical distance from ground surface to tunnel centre line.

Gaussian curve is used with the replacement of modified Gaussian curve by using $\alpha = 0.5$ (B. Zhou, 2014). Finally, the empirical equation of vertical surface settlements is given below:

$$V_{(z=0)} = V_{(z=0),max.} \frac{1}{\exp \left[0.5 \left(\frac{x_{(z=0)}}{i_{(z=0)}} \right)^2 \right]} \dots \dots \dots (2.3d)$$

Mair (1993) proposed maximum surface settlement as shown in equation (2.3e).

$$V_{(z=0),max.} = 0.313 \frac{V_s D^2}{KH} \dots \dots \dots (2.3e)$$

Earth pressure balance (EPB) and slurry machines can achieve a high degree of settlement control, particularly in sands with volume losses as low as 0.5% (Mair and Taylor, 1997).

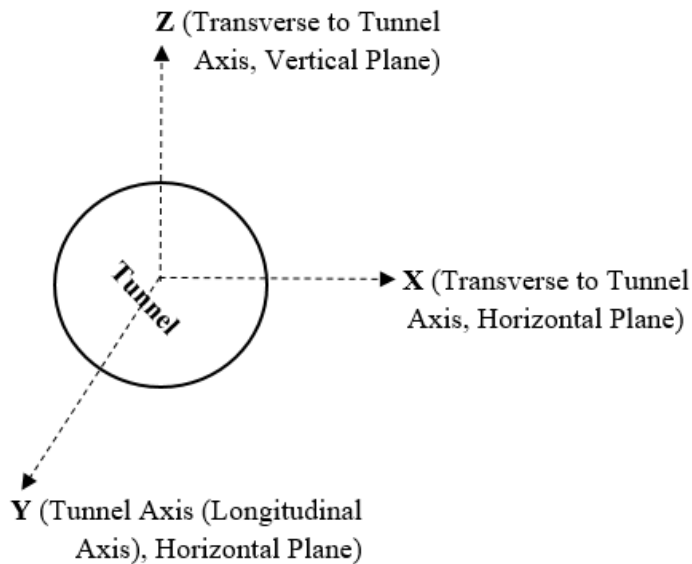


Figure 2.4: Typically representation of a tunnel.

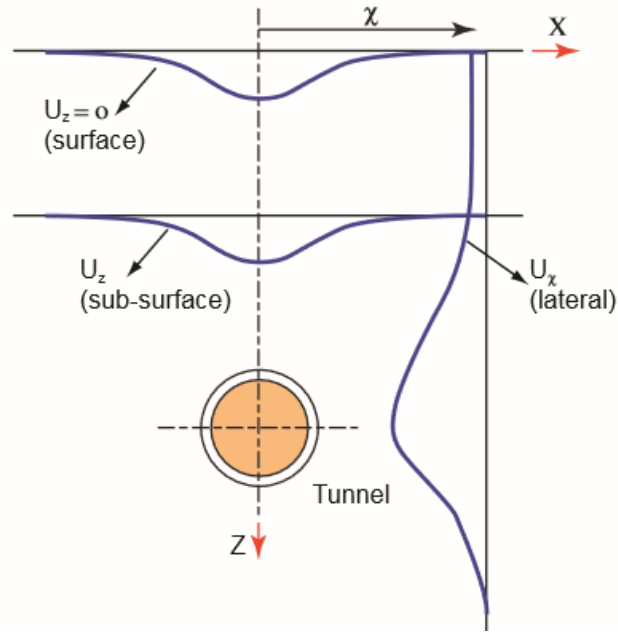


Figure 2.5: Tunnelling induced ground movements (N. Loganathan, 2011).

2.3.1.2 Analytical Formula

Verruijt and Booker (1996) gives general (sand, clay etc.) closed formed solutions for the estimation of the vertical surface settlement due to a uniform radial ground loss as shown in equation (2.4).

$$\begin{aligned}
 V_{(z=0)} = & -\varepsilon R^2 \left(\frac{z_1}{r_1^2} + \frac{z_2}{r_2^2} \right) + \delta R^2 \left[\frac{z_1(kx^2 - z_1^2)}{r_1^4} + \frac{z_2(kx^2 - z_2^2)}{r_2^4} \right] + \frac{2\varepsilon R^2}{m} \left[\frac{(m+1)z_2}{r_2^2} \right] \\
 & - 2\delta R^2 H \left[\frac{x^2 - z_2^2}{r_2^4} \right] \dots \dots \dots (2.4)
 \end{aligned}$$

Where,

ε = uniform radial surface movement as shown in Fig. 2.1

δ = long – term surface deformation due to the ovalization of tunnel lining

$z_1 = -H$

$z_2 = H$

$r_1^2 = x^2 + z_1^2$

$r_2^2 = x^2 + z_2^2$

R = radius of the tunnel

$m = 1 / (1 - 2\nu)$

$k = \nu(1 - \nu)$

ν = poisson's ratio of sand. (Assume isotropic)

2.3.2 Lateral Surface Settlement (Transverse to Tunnel Axis)

2.3.2.1 Empirical Formula

O'Reilly and New (1982) gives an empirical formulae to predict lateral surface settlement (clay, sand etc.) above a tunnel which is expressed as equation (2.5).

$$U_{x(z=0)} = V_{(z=0)} \left[\frac{x_{(z=0)}}{H} \right] \dots \dots \dots (2.5)$$

Where,

$U_{x(z=0)}$ = lateral surface settlement

2.3.2.2 Analytical Formula

Verruijt and Booker (1996) gives closed form solutions for the estimation of the lateral surface settlement in soil (sand, clay etc.) due to a uniform radial ground loss as shown in equation (2.6).

$$U_{x(z=0)} = -\varepsilon R^2 \left(\frac{x}{r_1^2} + \frac{x}{r_2^2} \right) + \delta R^2 \left[\frac{z_1(x^2 - kz_1^2)}{r_1^4} + \frac{x(x^2 - kz_2^2)}{r_2^4} \right] - \frac{2\varepsilon R^2 x}{mr_2^2} - \frac{4\delta R^2 xHz_2}{r_2^4(m+1)} \dots (2.6)$$

2.3.3 Longitudinal Surface Settlement (Along the Tunnel Axis)

2.3.3.1 Empirical Formula

Attewell and Woodman (1982) gives an empirical relation to predict longitudinal surface settlement above a tunnel in soil (sand, clay etc.).

$$U_{y(z=0)} = V_{(z=0)} \left[\frac{y_{(z=0)}}{H} \right] \dots \dots \dots (2.7)$$

Where,

$U_{y(z=0)}$ = longitudinal surface settlement

$y_{(z=0)}$ = horizontal distance from the tunnel centre line at surface

2.3.3.2 Analytical Formula

Most of tunnel has been analysed by plain strain consideration. Therefore, lack of predicting ground settlement along the tunnel axis. No suitable analytical formulae have developed to describe longitudinal ground movement above a tunnel.

2.4 SUB-SURFACE SETTLEMENTS

2.4.1 Vertical Sub Surface Settlement (Transverse to Tunnel Axis)

2.4.1.1 Empirical Formulae

The shape of the sub surface settlement trough above a single tunnel has been tried to model accurately by several authors. In sandy soil, Vorster et al. (2005) suggested to find out vertical sub surface settlement by using modified Gaussian curve.

$$V_{(z)} = V_{(z),max} \cdot \frac{n}{(n-1) + \exp\left[\alpha\left(\frac{x_{(z)}}{i_{(z)}}\right)^2\right]} \dots\dots\dots (2.8a)$$

$$n = e^\alpha \frac{2\alpha - 1}{2\alpha + 1} + 1 \dots\dots\dots (2.8b)$$

$$i_{(z)} = K(H - z) \dots\dots\dots (2.8c)$$

Where,

$V_{(z)}$ = vertical ground settlement

$V_{(z), max.}$ = maximum vertical ground settlement

$x_{(z)}$ = horizontal distance from the tunnel centre line at ground

$i_{(z)}$ = horizontal distance from the tunnel centre line to the point of inflection on the settlement trough

z = vertical distance from free surface

Gaussian curve is used with the replacement of modified Gaussian curve by using $\alpha = 0.5$ (B. Zhou, 2014). Finally, the empirical equation of vertical ground settlements is given below:

$$V_{(z)} = V_{(z),max} \cdot \frac{1}{\exp\left[0.5\left(\frac{x_{(z)}}{i_{(z)}}\right)^2\right]} \dots\dots\dots (2.8d)$$

$$V_{(z),max.} = 0.313 \frac{V_s D^2}{K(H-z)} \dots \dots \dots (2.8e)$$

2.4.1.2 Analytical Formula

Verruijt and Booker (1996) gives general (sand, clay etc.) closed form solutions for the estimation of the vertical ground settlement due to a uniform radial ground loss as shown in equation (2.9).

$$V_{(z)} = -\varepsilon R^2 \left(\frac{z_1}{r_1^2} + \frac{z_2}{r_2^2} \right) + \delta R^2 \left[\frac{z_1(kx^2 - z_2^2)}{r_1^4} + \frac{z_2(kx^2 - z_2^2)}{r_2^4} \right] \\ + \frac{2\varepsilon R^2}{m} \left[\frac{(m+1)z_2}{r_2^2} + \frac{mz(x^2 - z_2^2)}{r_2^4} \right] \\ - 2\delta R^2 H \left[\frac{x^2 - z_2^2}{r_2^4} + \frac{m}{m+1} \frac{2zz_2(3x^2 - z_2^2)}{r_2^6} \right] \dots \dots \dots (2.9)$$

Where,

$$z_1 = z - H \\ z_2 = z + H$$

2.4.2 Lateral Sub Surface Settlement (Transverse to Tunnel Axis)

2.4.2.1 Empirical Formula

O'Reilly and New (1982) gives an empirical formulae to predict lateral sub surface settlement (clay, sand etc.) above a tunnel which is expressed as in equation (2.10).

$$U_{x(z)} = V_{(z)} \left[\frac{x_{(z)}}{(H-z)} \right] \dots \dots \dots (2.10)$$

Where,

$$U_{x(z)} = \text{lateral ground settlement}$$

2.4.2.2 Analytical Formula

Verruijt and Booker (1996) gives closed form solutions for the estimation of the lateral sub surface settlement in soil (sand, clay etc.) due to a uniform radial ground loss as shown in equation (2.11).

$$U_{x(z)} = -\epsilon R^2 \left(\frac{x}{r_1^2} + \frac{x}{r_2^2} \right) + \delta R^2 \left[\frac{z_1(x^2 - kz_1^2)}{r_1^4} + \frac{x(x^2 - kz_2^2)}{r_2^4} \right] - \frac{2\epsilon R^2 x}{m} \left(\frac{1}{r_2^2} - \frac{2mzz_2}{r_2^4} \right) - \frac{4\delta R^2 xH}{(m+1)} \left[\frac{z_2}{r_2^4} + \frac{mz(x^2 - 3z_2^2)}{r_2^6} \right] \dots \dots \dots (2.11)$$

2.4.3 Longitudinal Sub Surface Settlement (Along the Tunnel Axis)

2.4.3.1 Empirical Formula

Attewell and Woodman (1982) gives an empirical relation to predict longitudinal sub surface settlement above a tunnel in soil (sand, clay etc.).

$$U_{y(z)} = V_{(z)} \left[\frac{y(z)}{L(H-z)} \right] \dots \dots \dots (2.12)$$

Where,

$U_{y(z)}$ = longitudinal ground settlement

$y(z)$ = horizontal distance from the tunnel centre line at ground

2.5 SEISMIC ANALOGY

Accelerations on surface and depth of tunnel axis are major important parameters to evaluate stability of tunnel under seismic loading.

2.5.1 Case Histories

In previous, seismic analysis has been conducted for surface structures. Some data are available to introduce damage of tunnels after earthquake before 70's. Sharma & Judd (1991) was collected a total number of 192 cases for 85 different earthquakes which described some factors such as tunnel cover, subsoil type, peak ground acceleration, magnitude of the earthquake, distance from the epicentre and type of lining support. Most of the damages (60%) occurred in the shallow tunnels (depth lower than 100m) by Sharma & Judd (1991). Several earthquakes were occurred in different countries such as California, Japan, Taiwan, Turkey, Italy etc. have a moment magnitude of 6.7 to 7.8. Power et al. (1996) were collected 217 cases of bored tunnels only which described damage of tunnels during the extremely severe earthquake of Kobe (1995).

2.5.2 Ground Shaking

Ground shaking refers to the vibration of the ground produced by seismic waves propagating through the earth's crust. The area experiencing this shaking may cover hundreds of square miles in the vicinity of the fault rupture. The intensity of the shaking attenuates with distance from the fault rupture. Ground shaking motions are composed of two different types of seismic waves, each with two sub-types, described as follows:

- (a) Body waves traveling within the earth's material. They may be either longitudinal P waves or transverse shear S waves and they can travel in any direction in the ground.
- (b) Surface waves traveling along the earth's surface. They may be either Rayleigh waves or Love waves.

As the ground is deformed by the traveling waves, any tunnel structure in the ground will also be deformed, since tunnel structures are constrained by the surrounding medium (soil or rock). As long as the ground (i.e., the surrounding medium) is stable, the structures cannot move independently of the ground. Therefore, the design and analysis of underground structures is based on ground deformations/strains rather than ground acceleration values. If the magnitude of ground deformation during earthquakes is small, the seismic effect on tunnels is negligible. In loose or soft soil deposits, on the other hand, the soil deformation developed during the design earthquake(s) should be estimated and used for the structure's design and analysis. In general the potential effects of ground shaking range from minor cracking of a concrete liner to collapse of the liner and major caving of geologic materials into the tunnel.

2.5.3 Ground Failure

Ground failure broadly includes various types of ground instability such as fault rupture, tectonic uplift and subsidence, land-sliding, and soil liquefaction. Each of these hazards may be potentially catastrophic to tunnel structures, although the damages are usually localized.

If an active fault crosses the tunnel alignment, there is a hazard of direct shearing displacement through the tunnel in the event of a moderate to large magnitude earthquake. Such displacements may range from a few inches to greater than ten feet and, in many cases, may be concentrated in a narrow zone along the fault. Fault rupture can and has had very damaging effects on tunnels.

Land-sliding through a tunnel, whether statically or seismically induced, can result in large, concentrated shearing displacements and either full or partial collapse of tunnel cross sections.

For tunnels located in soils below the groundwater table, there could be a potential for liquefaction if loose to medium-dense cohesion less soils (sands, silts, gravels) are adjacent to the tunnel.

Neglecting complexity, these types of failure during tunnelling under seismic loading will not be considered to analysing tunnel.

2.5.4 Lateral Settlement Due to Seismic Loading

An underground tunnel structure undergoes three primary modes of deformation during seismic shaking (M. Pescara, 2011) as shown in **Figure 2.6** and **Figure 2.7**.

- (a) ovaling deformation
- (b) axial deformation
- (c) curvature deformation

The ovaling deformation means that seismic waves propagating perpendicular to the tunnel longitudinal axis. The definition of axial and curvature deformations are components of seismic waves that propagate along the longitudinal axis or spatially varying ground motions resulting from local soil / site effects.

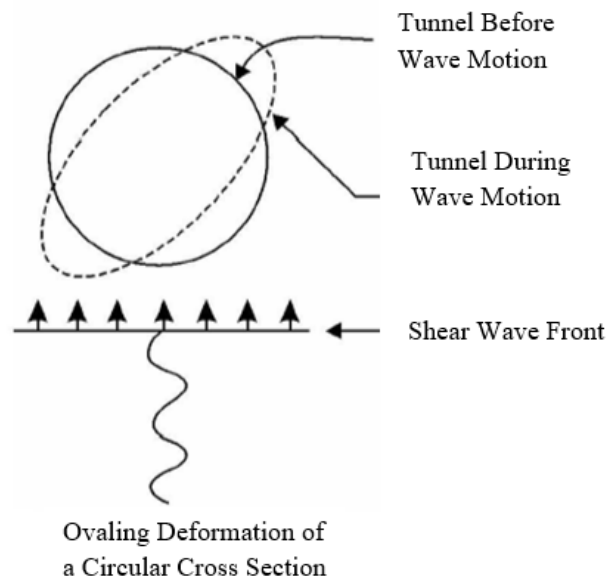


Figure 2.6: Tunnel Transverse Ovaling and Racking Response to Vertically Propagating Shear Waves (Wang, 1993; Owen and Scholl, 1981)

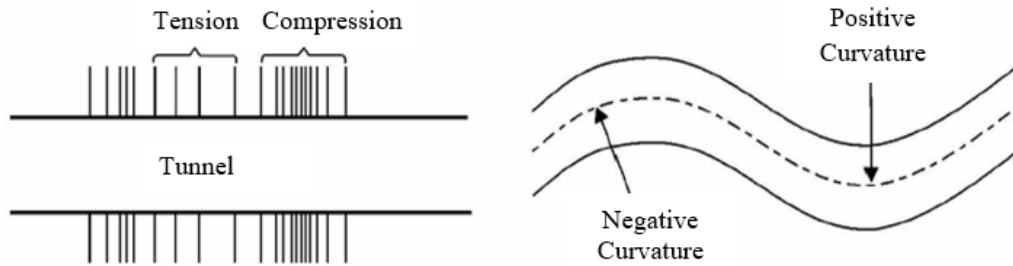


Figure 2.7: Tunnel Longitudinal Axial and Curvature Response to Traveling Waves (Wang, 1993; Owen and Scholl, 1981)

Effect of the seismic loadings on the tunnel stability is the free-field shear deformation method [Wang, 1993, Power et al. 1996; Hashash et al. 2001], which has most conservative. This approach assumes that deformation of the structure and soil are coincide in the free-field under the design earthquakes.

The site-specific Peak Ground Acceleration ($a_{max,s}$) is given by the equation (2.13), where S is the soil factor, defined in terms of the ground type [Eurocode 8]:

$$a_{max,s} = S * a_{gR} \dots \dots \dots (2.13)$$

Where,

a_{gR} = Peak Ground Acceleration (PGA)

$a_{max,s}$ = Peak Acceleration at the ground surface above a tunnel

S = Soil Factor

[Hashash et al., 2001] was considered the depth of tunnel to define the peak acceleration $a_{z,max}$, this consists in the determination of a reduction coefficient C for the peak acceleration on the surface depending on the depth of the tunnel (Table 2.3) as for equation (2.14):

$$a_{z,max} = C * a_{max,s} \dots \dots \dots (2.14)$$

Where,

$a_{z,max}$ = Peak Acceleration at the depth of tunnel

C = reduction coefficient

The value of S as shown in given below, suggested in Eurocode 8, is based on the types of elastic response spectra.

- Table 2.1 refer to conditions characterized by $M_w < 5.5$.
- Table 2.2 refer to conditions characterized by $M_w \geq 5.5$.

Table 2.1: Values of the parameters describing the recommended Type 1 elastic response spectra [Eurocode 8].

Ground type	S	T_B (s)	T_C (s)	T_D (s)
A	1,0	0,05	0,25	1,2
B	1,35	0,05	0,25	1,2
C	1,5	0,10	0,25	1,2
D	1,8	0,10	0,30	1,2
E	1,6	0,05	0,25	1,2

Table 2.2: Values of the parameters describing the recommended Type 2 elastic response spectra [Eurocode 8].

Ground type	S	T_B (s)	T_C (s)	T_D (s)
A	1,0	0,15	0,4	2,0
B	1,2	0,15	0,5	2,0
C	1,15	0,20	0,6	2,0
D	1,35	0,20	0,8	2,0
E	1,4	0,15	0,5	2,0

Table 2.3: Ratios (C) of ground motion at depth to motion at ground surface [Power et al. 1996].

Tunnel depth (m)	Ratio of ground motion at tunnel depth to motion at ground surface
≤ 6	1.0
6–15	0.9
15–30	0.8
> 30	0.7

M. Pescara, (2011) gives some empirical relations which is shown in below.

$$\gamma_{max} = \frac{V_s}{C_s} \dots \dots \dots (2.15)$$

$$V_s = k * a_{z,max} \dots \dots \dots (2.16)$$

$$\Delta_{max} = \gamma_{max}(H) \dots \dots \dots (2.17)$$

Where,

V_s = peak ground velocity

C_s = apparent propagation velocity of S-wave, several authors [O'Rourke & Liu, 1999; Power et al., 1996; Paolucci & Pitilakis, 2007] have suggested values between 1 and 5km/s.

k = ratio of peak ground velocity to peak ground acceleration, as shown in Table 2.4.

γ_{max} = maximum shear deformation

Δ_{\max} = Maximum lateral displacement at surface.

Table 2.4: Ratios of peak ground velocity to peak ground acceleration in different grounds and for increasing source to-site distance [Power et al. 1996].

Moment magnitude (M_w)	Ratio of peak ground velocity (cm/s) to peak ground acceleration (g)		
	Source-to-site distance (km)		
	0–20	20–50	50–100
<i>Rock^a</i>			
6.5	66	76	86
7.5	97	109	97
8.5	127	140	152
<i>Stiff soil^a</i>			
6.5	94	102	109
7.5	140	127	155
8.5	180	188	193
<i>Soft soil^a</i>			
6.5	140	132	142
7.5	208	165	201
8.5	269	244	251

^aIn this table, the sediment types represent the following shear wave velocity ranges: rock ≥ 750 m/s; stiff soil is 200–750 m/s; and soft soil < 200 m/s. The relationship between peak ground velocity and peak ground acceleration is less certain in soft soils.

2.5.5 Damages of TBM Tunnels Due to Seismic Loading

In this section, damage guidelines of TBM tunnels are presented considering empirical observations of tunnel performance during earthquakes. **Figure 2.8** represents a summary of empirical observations of the effects of seismic ground shaking on the performance of TBM tunnels. The figure is from the study by Power et al. (1998), which updates earlier presentations of tunnel performance data by Dowding and Rozen (1978), Owen and Scholl (1981), and Sharma and Judd (1991). The data are for damage due only to shaking; damage that was definitely or probably attributed to fault rupture, landsliding, and liquefaction is not included.

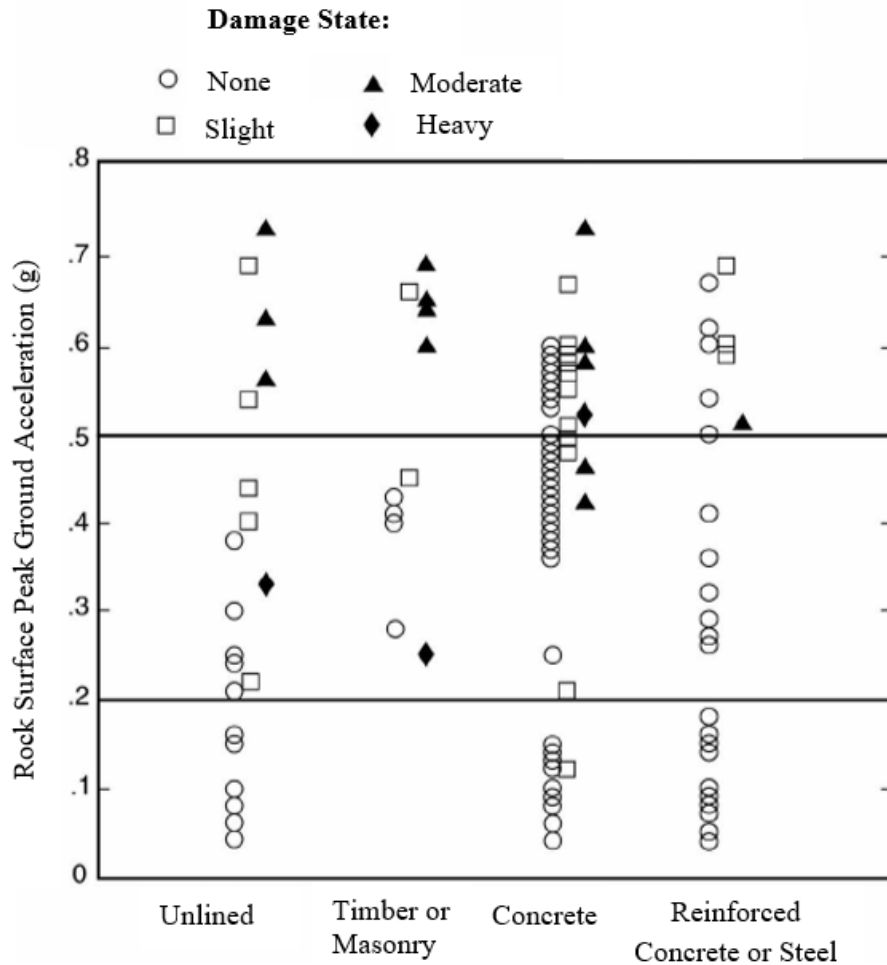


Figure 2.8: Summary of Observed TBM Tunnel Damage under Ground Shaking Effects (Power et al., 1998)

Figure 2.8 incorporates observations for 192 tunnels from ten moderate to large magnitude earthquakes (moment magnitude M_w 6.6 to 8.4) in California, Japan, and Alaska. Ninety-four of the observations are from the moment magnitude M_w 6.9, 1995 Kobe, Japan earthquake. This earthquake produced by far the most observations for moderate to high levels of shaking (estimated peak ground accelerations, PGA, at ground surface above the tunnels in the range of about 0.4 g to 0.6 g for the Kobe data). Peak ground accelerations in **Figure 2.8** are estimated for actual or hypothetical outcropping rock conditions at ground surface above the tunnel. Other observations are from moderate to large (M_w 6.7 to 8.4) earthquakes in California and Japan. **Figure 2.8** shows the level of damage induced in tunnels with different types of linings subjected to the indicated levels of ground shaking. Damage was categorized into four states: none for no observable damage; slight for minor cracking and spalling; moderate for major cracking and spalling, falling of pieces of lining and rocks; and heavy for major cave-ins, blockage, and collapse. The figure indicates the following trends:

- (a) For PGA equal to or less than 0.2 g, ground shaking caused essentially no damage in tunnels.

- (b) For PGA in the range of 0.2 g to 0.5 g, there are some instances of damage ranging from slight to heavy. Note that the three instances of heavy damage are all from the 1923 Kanto, Japan, earthquake. For the 1923 Kanto earthquake observation with PGA equal to 0.25 g shown on **Figure 2.8** the investigations for this tunnel indicated the damage may have been due to landsliding. For the other two Kanto earthquake observations, collapses occurred in the shallow portions of the tunnels.
- (c) For PGA exceeding about 0.5 g, there are a number of instances of slight to moderate damage (and one instance of heavy damage noted above for the Kanto earthquake).
- (d) Tunnels with stronger linings appear to have performed better, especially those tunnels with reinforced concrete and/or steel linings.

2.6 CONSTITUTIVE MODEL

Constitutive model is most important for understanding about failure mechanism of any material. 3D model has better performance over 2D model. In this thesis, Mohr – Coulomb failure criteria has been discussed. In PLAXIS 3D, stresses are based on Cartesian coordinate system as shown in **Figure 2.9**.

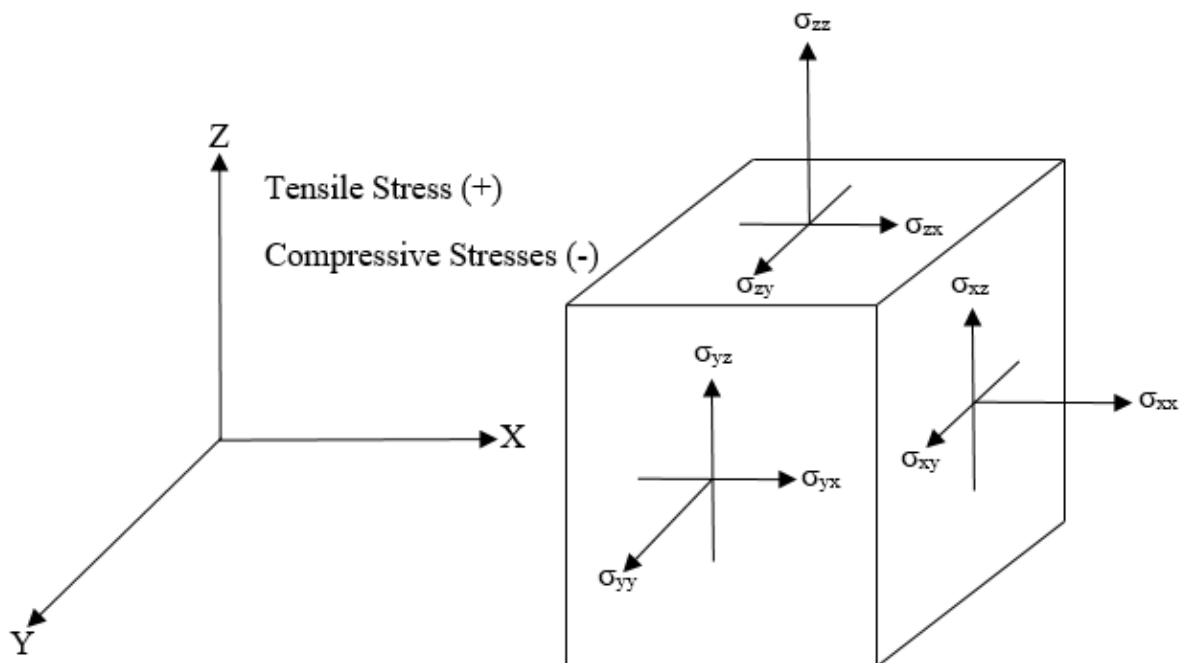


Figure 2.9: Coordinate system and indication of stress components

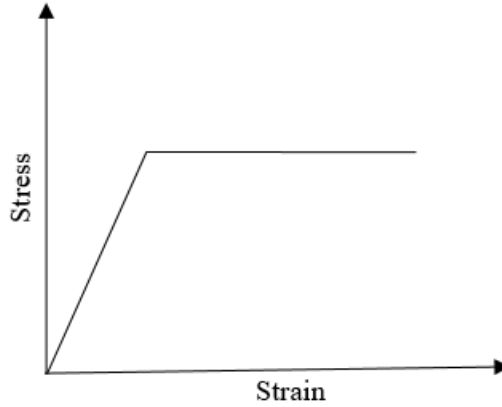


Figure 2.10: Mohr – Coulomb model (Elastic – Perfectly Plastic)

Mohr-Coulomb model consists of five parameters such as elastic modulus (E), poisson’s ratio (ν), angle of internal friction (ϕ), cohesion (C) and angle of dilatancy (ψ). These model describes ‘first – order’ approximation of soil behaviour. For first analysis of any problem, to use this model. Only one constant average stiffness calculates for each layer and stiffness increases linearly with depth. Elastic part of Mohr-Coulomb model is based on Hooke’s law of isotropic elasticity and perfectly plastic part is based on the Mohr-Coulomb failure criterion, formulated in a non-associated plasticity framework.

Linear elastic perfectly-plastic Mohr-Coulomb model describes only limited features of soil in reality. Although variation of stiffness with depth can be taken into account, the Mohr-Coulomb model does neither include stress-dependency nor stress-path dependency nor strain-dependency of stiffness or anisotropic stiffness. Effective stress state at failure are well described using Mohr-Coulomb failure criterion with effective strength parameters ϕ' and C' .

In elastoplasticity model, strains and strain rates are decomposed into an elastic part and a plastic part:

$$\varepsilon = \varepsilon^e + \varepsilon^p \dots \dots \dots (2.18)$$

$$\varepsilon_e = \varepsilon_e^e + \varepsilon_e^p \dots \dots \dots (2.19)$$

Where, ε , ε^e , ε^p , ε_e , ε_e^e , ε_e^p are the total strain, total elastic strain, total plastic strain, effective strain, elastic effective strain and plastic effective strain. Hooke’s law established relationship between elastic stress rates to the elastic strain rates.

$$\sigma_e = D^e(\varepsilon_e - \varepsilon_e^p) \dots \dots \dots (2.20)$$

Where, σ_e , D^e are the effective elastic stress and elastic modulus. According to the classical theory of plasticity Hill (1950), plastic strain rates are proportional to the derivative of the yield function with

respect to the stresses. This means that the plastic strain rates can be represented as a vectors perpendicular to the yield surface. This classical form of theory is referred to as associated plasticity. However, for Mohr-Coulomb type yield function, the theory of associated plasticity overestimates dilatancy. Therefore, in addition to the yield function, a plastic potential function g is introduced. The case $g \neq f$ is denoted as non – associated plasticity. In general, the plastic strain rates are written as:

$$\varepsilon_e^p = \lambda \frac{\partial g}{\partial \sigma_e} \dots \dots \dots (2.21)$$

In which λ is a plastic multiplier. For purely elastic behaviour λ is zero, whereas in the case of plastic behaviour λ is positive:

$$\lambda = 0 \quad \text{for:} \quad f < 0 \quad \text{or:} \quad \frac{\partial f^T}{\partial \sigma_e} D^e \varepsilon_e \leq 0 \quad (\text{Elasticity}) \dots \dots \dots (2.22a)$$

$$\lambda > 0 \quad \text{for:} \quad f = 0 \quad \text{and:} \quad \frac{\partial f^T}{\partial \sigma_e} D^e \varepsilon_e > 0 \quad (\text{Plasticity}) \dots \dots \dots (2.22b)$$

The full Mohr-Coulomb yield condition consists of six yield functions when formulated in terms of principal stresses (Smith & Griffiths, 1982):

$$f_{1a} = \frac{1}{2}(\sigma_{e2} - \sigma_{e3}) + \frac{1}{2}(\sigma_{e2} + \sigma_{e3})\sin\varphi - C\cos\varphi \leq 0 \dots \dots \dots (2.23a)$$

$$f_{1b} = \frac{1}{2}(\sigma_{e3} - \sigma_{e2}) + \frac{1}{2}(\sigma_{e3} + \sigma_{e2})\sin\varphi - C\cos\varphi \leq 0 \dots \dots \dots (2.23b)$$

$$f_{2a} = \frac{1}{2}(\sigma_{e3} - \sigma_{e1}) + \frac{1}{2}(\sigma_{e3} + \sigma_{e1})\sin\varphi - C\cos\varphi \leq 0 \dots \dots \dots (2.23c)$$

$$f_{2b} = \frac{1}{2}(\sigma_{e1} - \sigma_{e3}) + \frac{1}{2}(\sigma_{e1} + \sigma_{e3})\sin\varphi - C\cos\varphi \leq 0 \dots \dots \dots (2.23d)$$

$$f_{3a} = \frac{1}{2}(\sigma_{e1} - \sigma_{e2}) + \frac{1}{2}(\sigma_{e1} + \sigma_{e2})\sin\varphi - C\cos\varphi \leq 0 \dots \dots \dots (2.23e)$$

$$f_{3b} = \frac{1}{2}(\sigma_{e2} - \sigma_{e1}) + \frac{1}{2}(\sigma_{e2} + \sigma_{e1})\sin\varphi - C\cos\varphi \leq 0 \dots \dots \dots (2.23f)$$

Where, σ_{e1} , σ_{e2} , σ_{e3} are the effective elastic principal stresses. The two plastic model parameters appearing in the yield functions are well known friction angle (φ) and cohesion (C). The condition $f_i =$

0 for all yield functions together (where f_i is used to denote each individual yield function) represents a fixed hexagonal cone in principal stress space as shown in **Figure 2.11**.

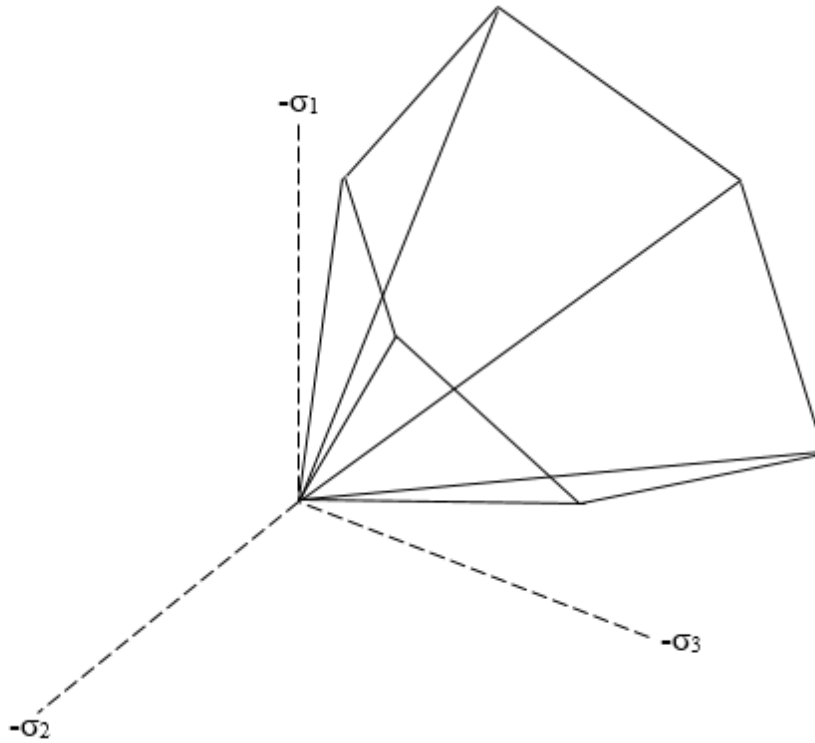


Figure 2.11: The Mohr-Coulomb yield surface in principal stress space ($C = 0$)

In addition to the yield functions, six plastic potential functions are defined for the Mohr-coulomb model:

$$g_{1a} = \frac{1}{2}(\sigma_{e2} - \sigma_{e3}) + \frac{1}{2}(\sigma_{e2} + \sigma_{e3})\sin\psi \dots \dots \dots (2.24a)$$

$$g_{1b} = \frac{1}{2}(\sigma_{e3} - \sigma_{e2}) + \frac{1}{2}(\sigma_{e3} + \sigma_{e2})\sin\psi \dots \dots \dots (2.24b)$$

$$g_{2a} = \frac{1}{2}(\sigma_{e3} - \sigma_{e1}) + \frac{1}{2}(\sigma_{e3} + \sigma_{e1})\sin\psi \dots \dots \dots (2.24c)$$

$$g_{2b} = \frac{1}{2}(\sigma_{e1} - \sigma_{e3}) + \frac{1}{2}(\sigma_{e1} + \sigma_{e3})\sin\psi \dots \dots \dots (2.24d)$$

$$g_{3a} = \frac{1}{2}(\sigma_{e1} - \sigma_{e2}) + \frac{1}{2}(\sigma_{e1} + \sigma_{e2})\sin\psi \dots \dots \dots (2.24e)$$

$$g_{3b} = \frac{1}{2}(\sigma_{e2} - \sigma_{e1}) + \frac{1}{2}(\sigma_{e2} + \sigma_{e1})\sin\psi \dots \dots \dots (2.24f)$$

The plastic potential functions contain a third plasticity parameter, the dilatancy angle ψ . This parameter is required to model positive plastic volumetric strain increments (dilatancy) as actually observed for dense soils. When implementing the Mohr-Coulomb model for general stress states, special treatment is required for the intersection of two yield surfaces. In PLAXIS 3D, however, the exact form of the full Mohr-Coulomb model is implemented, using a sharp transition from one yield surface to another.

For $C > 0$, the standard Mohr-Coulomb criterion allows for tension. In fact allowable tensile stresses increase with cohesion. In reality, soil can sustain none or only very small tensile stresses. This behaviour is expressed as tension cut-off in PLAXIS 3D. In this case, Mohr circles with positive principle stresses are not allowed. The tension cut-off introduces three additional yield functions, defined as:

$$f_4 = (\sigma_{e1} - \sigma_t) \leq 0 \dots \dots \dots (2.25a)$$

$$f_5 = (\sigma_{e2} - \sigma_t) \leq 0 \dots \dots \dots (2.25b)$$

$$f_6 = (\sigma_{e3} - \sigma_t) \leq 0 \dots \dots \dots (2.25c)$$

Where, σ_t is the allowable tensile stress. For stress states within yield surface, the behaviour is elastic and obeys Hooke's law for isotropic linear elasticity. And outside the yield surface, the behaviour is plastic.

$$J_1 = \sigma_{e1} + \sigma_{e2} + \sigma_{e3} \dots \dots \dots (2.26)$$

$$J_2 = -(\sigma_{e1}\sigma_{e2} + \sigma_{e2}\sigma_{e3} + \sigma_{e3}\sigma_{e1}) \dots \dots \dots (2.27)$$

$$J_3 = \sigma_{e1}\sigma_{e2}\sigma_{e3} \dots \dots \dots (2.28)$$

Where, J_1, J_2, J_3 are the first, second and third stress invariants. For simplicity to consider that the principal directions as the directions of the co-ordinate axes.

$$J_1 = \sigma_{ex} + \sigma_{ey} + \sigma_{ez} \dots \dots \dots (2.29)$$

$$J_2 = \tau_{exy}^2 + \tau_{eyz}^2 + \tau_{ezx}^2 - (\sigma_{ex}\sigma_{ey} + \sigma_{ey}\sigma_{ez} + \sigma_{ez}\sigma_{ex}) \dots \dots \dots (2.30)$$

$$J_3 = \sigma_{ex}\sigma_{ey}\sigma_{ez} + 2\tau_{exy}\tau_{eyz}\tau_{ezx} - (\sigma_{ex}\tau_{eyz}^2 + \sigma_{ey}\tau_{ezx}^2 + \sigma_{ez}\tau_{exy}^2) \dots \dots \dots (2.31)$$

Where, σ_{ex} , σ_{ey} , σ_{ez} , τ_{exy} , τ_{eyz} , τ_{ezx} are the elastic effective normal and shear stresses in X, Y and Z directions. Invariants are the function of co-ordinate stresses as well as principle stresses. Principle stresses are physical quantities and obviously do not depend on the co-ordinate axes chosen.

2.7 CALCULATION PROCESS IN PLAXIS 3D

2.7.1 Soil Elements

The basic soil elements of the 3D finite element mesh are the 10-node tetrahedral elements as shown in **Figure 2.12**. In addition to the soil elements, special types of elements are used to model structural behaviour. For beams, 3-node line elements are used, which are compatible with the 3-node edge of a soil element. In addition, 6-node plate and geogrid elements are used to simulate the behaviour of plates and geogrid respectively. Moreover, 12-node interface elements are used to simulate soil-structure interaction behaviour.

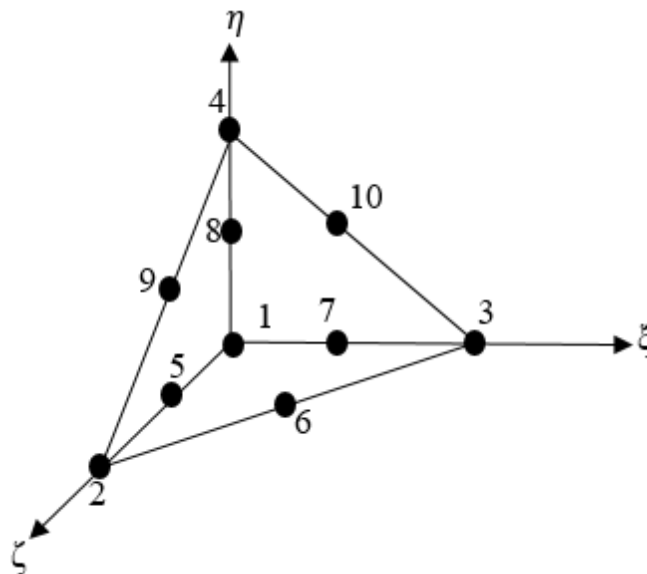


Figure 2.12: 3D soil elements (10-node tetrahedrons)

The 10-node tetrahedral elements are created in the 3D mesh procedure. This type of element provides a second-order interpolation of displacements. For tetrahedral elements there are three local co-ordinates (ξ , η and ζ). The shape function N_i have the property that the function value is equal to unity at node i and zero at the other nodes.

2.7.2 Global Settings

The mesh generator requires a global meshing parameter that represents the target element size, I_e . In PLAXIS 3D this parameter is calculated from the outer geometry dimensions (x_{min} , x_{max} , y_{min} , y_{max} , z_{min} , z_{max}). The target element dimension is calculated according to the formulae:

$$I_e = \frac{r_e}{20} \sqrt{(x_{max} - x_{min})^2 + (y_{max} - y_{min})^2 + (z_{max} - z_{min})^2} \dots \dots \dots (2.32)$$

The target element dimension or average element size, (I_e) is based on a parameter called relative element size factor (r_e). Regarding the element distribution, distinction is made between five global levels. The values of the parameter, r_e for the element distributions predefined in the PLAXIS 3D are given below:

- Very coarse: $r_e = 2.0$
- Coarse: $r_e = 1.5$
- Medium: $r_e = 1.0$
- Fine: $r_e = 0.7$
- Very fine: $r_e = 0.5$

The exact number of elements depends on the shape of the geometry and optional local refinement settings. The number of cores is set to 256 for these model.

2.7.3 Phased Construction

Tunnel structure have been excavated with the several phases. In this research, three phase have to be consider for excavation. Each calculation phase corresponds to a particular loading or construction stage. The construction stages can be defined in the staged construction mode. The phases have the settings of the parent unless they are defined differently. In this case it is required that the next phase is fully redefined, since the start conditions have changed. This may also have consequences for the phases thereafter. The name of the phases is determined consecutively by the program and it cannot be modified. The order of calculation phases is defined by selecting the reference phase (parent phase) first and then adding a phase, or selecting the reference phase.

2.7.4 Initial Stress Generation

A lot of analysis problems in geotechnical engineering require the specification of a set of initial stresses. The initial stresses of a soil body are influenced by the weight of the material and the history of its formation. This stress state is usually characterised by an initial vertical effective stress ($\sigma'_{v,0}$). The initial horizontal effective stress $\sigma'_{h,0}$ is related to the initial vertical effective stress by the coefficient of lateral earth pressure K_0 ($\sigma'_{h,0} = K_0 \sigma'_{v,0}$). In PLAXIS 3D, initial stresses may be generated by using K0 procedure or by using gravity loading. To generate and inspect results from initial stresses first before defining and executing other calculation phases.

K0 Procedure: K0 procedure is special calculation method available in PLAXIS 3D to define the initial stresses for the model, taking into account the loading history of the soil. Two K_0 values can be specified, one for the x-direction and one for the y-direction.

$$K_{0,x} = \sigma_{xx}^e / \sigma_{zz}^e \dots \dots \dots (2.33a)$$

$$K_{0,y} = \sigma_{yy}^e / \sigma_{zz}^e \dots \dots \dots (2.33b)$$

Where, σ_{xx}^e , σ_{yy}^e , σ_{zz}^e are effective stress components of X, Y and Z directions. In practice, the value of K_0 for a normally consolidated soil is often assumed to be related to the friction angle by Jaky's empirical expressions:

$$K_0 = 1 - \sin\varphi \dots \dots \dots (2.34)$$

In an over-consolidated soil, K_0 would be expected to be larger than the value given by the expression. Using very low or very high K_0 values in the K0 procedure may lead to stresses that violate the Mohr-Coulomb failure condition. In this case software automatically reduces the lateral stresses such that the failure condition is obeyed. Hence, these stress points are in plastic state and are thus indicated as plastic points. Although the corrected stress state obeys the failure condition, it may results in stress field which is not in equilibrium. It is generally preferable to generate an initial stress field that does not contain Mohr-Coulomb plastic points. For a sand, it can be easily be shown that to avoid Mohr-Coulomb plasticity, the value of K_0 is bounded by:

$$\frac{1-\sin\varphi}{1+\sin\varphi} < K_0 < \frac{1+\sin\varphi}{1-\sin\varphi} \dots \dots \dots (2.35)$$

When K0 procedure is adopted, software will generate vertical stresses that are in equilibrium with the self-weight of the soil. Horizontal stresses, however, are calculated from the specified value of K₀. Even if the value of K₀ is chosen such that plasticity does not occur, the K0 procedure does not ensure that the complete stress field is in equilibrium. Full equilibrium is only obtained for a horizontal soil surface with any soil layers parallel to this surface and a horizontal phreatic level. Therefore, the K0 procedure is not recommended when dealing with non-horizontal surfaces. If the stress field requires only small equilibrium corrections, then these may be carried out using the K0 procedure followed by a plastic nil-step. If the stresses are substantially out of equilibrium, then the K0 procedure should be abandoned in favour of the gravity loading procedure.

Gravity Loading: Gravity loading is a type of plastic calculation, in which the initial stresses are generated based on the volumetric weight of the soil. If gravity loading is adopted, then the initial stresses are set up by applying the soil self-weight in the first calculation phase. In this case, when using an elastic perfectly-plastic soil model such as Mohr-Coulomb model, the ratio of horizontal effective stress over vertical effective stress, K₀, depends strongly on the assumed values of poisson's ratio. It is important to choose values of poisson's ratio that give realistic values of K₀. If necessary, separate material data sets may be used with poisson's ratio adjusted to provide the proper K₀-value during gravity loading. These sets may be changed by other material sets in subsequent calculations. For one-dimensional compression an elastic computation will give:

$$K_0 = \frac{\nu}{1-\nu} \dots \dots \dots (2.36)$$

If a value of K₀ of 0.5 is required, for example, then it is necessary to specify a value of poisson's ratio of 0.333. As a poisson's ratio must be lower than 0.5, it is not straightforward to generate K₀ values larger than 1 using gravity loading. If K₀ values larger than 1 are desired, it is necessary to simulate the loading history and use different poisson's ratio for loading and unloading or use the K0 procedure. In some cases plastic points will be generated during the gravity loading procedure. For sand, in one-dimensional compression, for example, plastic Mohr-Coulomb points will be generated unless the following inequality is satisfied:

$$\frac{1 - \sin\phi}{1 + \sin\phi} < \frac{\nu}{1 - \nu} < 1 \dots \dots \dots (2.37)$$

Results: After the generation of initial stresses the plot of the initial effective stresses can be inspected. It is also useful to view the plot of plastic points. Using K₀ values that differ substantially from unity may sometimes lead to an initial stress state that violates the Mohr-Coulomb criterion. If the plot of the

plastic points shows many red plastic points (Mohr-Coulomb points), the value of K_0 should be chosen closer to 1.0. If there are a small number of plastic points, it is advisable to perform a plastic nil-step.

2.7.5 Plastic Calculation

A plastic calculation is used to carry out an elastic-plastic deformation analysis in which it is not necessary to take the change of pore pressure with time into account. The stiffness matrix in a normal plastic calculation is based on the original un-deformed geometry. This type of calculation is appropriate in most practical geotechnical applications. A fully drained analysis can assess the settlements on the long term. This will give a reasonably accurate prediction of final situation, although the precise loading history is not followed and the processes consolidation is not dealt with explicitly. An elastic-plastic deformation analysis where the un-drained (A) behaviour is temporarily ignored and the stiffness of water is not taken into account.

In a plastic calculation loading can be defined in the sense of changing the load combination, stress state, weight, strength or stiffness of elements, activated by changing the load and geometry configuration or pore pressure distribution by means of staged construction. In this case, the total load level that is to be reached at the end of the calculation phase is defined by specifying a new geometry and load configuration, and/or pore pressure distribution, in the staged construction mode.

2.7.6 Dynamic Calculation

In PLAXIS 3D it is possible to perform a dynamic analysis after a series of plastic calculations. The applied dynamic load is the product of the input value of the defined dynamic load and corresponding dynamic load multiplier. Besides the activation of the dynamic load or dynamic prescribed displacement, absorbent (viscous) boundary conditions can be defined for a dynamic calculation. In a dynamic calculation loading can be defined in the sense of applying a predefined combination of external loads as dynamic forces using dynamic multipliers activated in the staged construction mode. The basic equation for the time-dependent movement of a volume under the influence of a (dynamic) load is:

$$M\ddot{u} + C\dot{u} + Ku = F \dots \dots \dots (2.38)$$

Here, M is the mass matrix, u is the displacement vector, C is the damping matrix, K is the stiffness matrix and F is the load vector. The displacement, u , the velocity, \dot{u} and the acceleration, \ddot{u} , can vary with time. The last two terms in equation (2.38) ($Ku = F$) correspond to the static deformation. Here the theory is described on the bases of linear elasticity. In the matrix M , the mass of materials (soil + water + any construction) is taken into account. In this software, the mass matrix is implemented as a lumped

matrix. The matrix C represents the material damping of the materials. In reality, material damping is caused by friction or by irreversible deformations (plasticity or viscosity).

In the case of static deformation analysis, prescribed boundary displacements are introduced at the boundaries of a finite element model. The boundaries can be completely free or fixities can be applied in one or two directions. Particularly the vertical boundaries of a mesh are often non-physical (synthetic) boundaries that have been chosen so that they do not actually influence the deformation behaviour of the construction to be modelled. In other words: the boundaries are ‘far away’. For dynamic calculations, the boundaries should in principle be much further away than those for static calculation, because, otherwise, stress waves will be reflected leading to distortions in the computed results. However, locating the boundaries far away requires many extra elements and therefore a lot of extra memory and calculating time. For the implementation of dynamic effects in these software the viscous boundaries are created with the use of viscous boundaries (dampers).

The natural frequency of vibration of a soil deposit may be calculated from the following equation (page 261 of Kramer, 1996).

$$f_n = \frac{V_s}{4H}(2n + 1) \dots \dots \dots (2.39)$$

Where, V_s is the shear wave velocity, H is the thickness of soil layer, f_n is the n^{th} natural frequency of the soil deposit in Hz and $n = 0,1,2,\dots\dots n$.

2.8 STRAIN INDUCED VOLUME LOSSES

Volumetric strains are influenced to the ground movement due to tunnelling in soil. These types of strains are represented as the volume losses. Two types of volumetric strains are seen due to tunnel construction such as strain due to long term loading and seismic shaking.

2.8.1 Volumetric Strains in Long Term Loading

N.Loganathan, 2011 gives an analytical formulae for calculating volumetric strain in plain strain consideration. These types of strain behaves as non-linearly around tunnel soil interface (N.Loganathan, 2011). This equation is shown in below:

$$\varepsilon_{v1} = \frac{2gD + g^2}{D^2} \exp \left\{ - \left[\frac{1.38x^2}{\left(H + \frac{D}{2}\right)^2} + \frac{0.69z^2}{H^2} \right] \right\} \dots \dots \dots (2.40)$$

Where, g is the diametric deformation (**Figure 2.1**), x is the any distance from tunnel centre line along lateral direction and ε_{v1} is the long term volumetric strain.

2.8.2 Volumetric Strains in Seismic Shaking

Volumetric strain due to seismic loading has expressed that the combination of the axial and curvature deformations of the ground in the free-field (i.e., without the presence of the tunnel). St. John and Zahrah (1987) developed solutions for these strains due to compression seismic waves. This equation is shown in below:

$$\varepsilon_{vs} = \frac{V}{C} \sin\varphi \cos\varphi + Y_1 \frac{A}{C^2} \cos^3\varphi \dots \dots \dots (2.41)$$

Where, ε_{vs} is the volumetric strain under seismic shaking, V is the maximum velocity of seismic shaking, A is the maximum acceleration of seismic shaking, C is the velocity of apparent propagation which varies 2 to 4 km/s (FHWA-NHI-10-034), Y_1 is the distance from neutral axis of tunnel cross section to the lining extreme fibre, φ is the angle at which seismic waves propagate in the horizontal plane with respect to the tunnel axis.

2.9 CONCLUSIONS

This chapter is highlighted of behaviour of sands for construction of a single tunnel and is reviewed the previous empirical and analytical methods for prediction of ground displacements. Empirical methods are developed based on field observation. Horizontal and vertical displacements above a tunnel are estimated by empirical formulae. Finite element methods are expressed more accurate settlements profile than empirical and analytical formulae. However, this method is expensive in terms of resources and still has a long way to go in predicting accurately the actual magnitudes of displacement that occur above a tunnel in the field. Mohr-Coulomb material model contains some limitation but it's more suitable for finite element analysis. Volumetric strains based on numerical analysis are expressed more accurate behaviour than empirical and analytical formulae. These formulae are provided by different authors. Behaviour of soil around tunnel are evaluated from volumetric strains. Seismic analysis is advance technology for construction of underground tunnel. Underground structures are less damage than surface structures under seismic loading during tunnelling. It has necessary for analysis to evaluate

transverse racking effect and longitudinal movement of tunnel under seismic loading. Transverse racking effect is dangerous for tunnel structures. Large amounts of lateral spreading occurs due to racking effects. Empirical and analytical formulae are not expressed properly of racking effects and longitudinal movements of tunnel. That is why, numerical analysis has necessary to evaluate proper behaviour of tunnel under seismic loading.

CHAPTER THREE
MODIFIED EMPIRICAL AND ANALYTICAL FORMULAS

3.1 INTRODUCTION

This chapter deals with modified empirical and analytical formulae. Modified formulae contains some short terms such as MEF-LTL (Modified Empirical Formulae Long Term Loading), MAF-LTL (Modified Analytical Formulae Long Term Loading), MEF-SL (Modified Empirical Formulae Seismic Loading), MAF-SL (Modified Analytical Formulae Seismic Loading). Long term loading means static loading. Firstly, modified formulae are validated than it is implemented to the present research. In present research, some parameters are – lengths of tunnel ($y_1 = 27\text{m}$, $y_2 = 29\text{m}$, $y_3 = 31\text{m}$), diameters of tunnel ($D_1 = 10.5\text{m}$, $D_2 = 10.8\text{m}$, $D_3 = 11.0\text{m}$) and depths of tunnel crown ($A_1 = 4.5\text{m}$, $A_2 = 5.5\text{m}$, $A_3 = 6.5\text{m}$, $A_4 = 7.5\text{m}$ and $A_5 = 8.5\text{m}$). Relative depths are expressed by A_n/D_n . Pre-cast concrete segments are used for ring of tunnel. Width of ring is 2m. Shape of ring is circular. Most of the case, results are nearly close of empirical and analytical formulae.

3.2 MODIFIED FORMULAS

Modified formulas are two types such as empirical and analytical. By using these formulae to get the value of maximum settlements and strain induced ground losses.

3.2.1 Modified Empirical Formula for Maximum Vertical Settlement

Practically, maximum value is most important than others value. Most of the case, maximum value is critical for design purpose. Vertical ground settlements are most important during tunnelling under static and seismic loading. In present research, modified Mair (1993) maximum ground settlement formula with the consideration of 0.5 percent uniform volume loss (Mair and Taylor, 1997) and 35 percent of K factor (Mair and Taylor, 1997) as shown in given below:

$$V_{(z),max.} = 0.0045 \frac{D^2}{(H - z)} \dots \dots \dots (3.1)$$

Where, D , H , z , $V_{(z),max.}$ are represented by inner diameter of tunnel (m), vertical distance (m) from free surface to tunnel centre line, any distance (m) from free surface and maximum vertical settlement (m). For surface settlement, z is equal to zero and for total settlement z is equal to summation of depth of tunnel crown and outer diameter of tunnel.

3.2.2 Modified Analytical Formulae for Maximum Vertical Settlement

Verruijt and Booker (1996) shows a closed formed general solutions for the calculation of the vertical ground settlement under uniform radial ground loss. In present research, modified this formula for static and seismic loading for 0.5 percent volume loss. Long term ground deformation is taken 1mm based on following authors observations (Rankin, 1988 (Damage Risk Chart) and N.Loganathan et.al 1998). Maximum ground settlement for long term and seismic loading are expressed as equations (3.2) and (3.3) which is shown in below:

$$\begin{aligned}
 V_{(z)max.} = & -0.005R^2 \left(\frac{z_1}{r_1^2} + \frac{z_2}{r_2^2} \right) + 0.001R^2 \left[\frac{z_1(-z_2^2)}{r_1^4} + \frac{z_2(-z_2^2)}{r_2^4} \right] \\
 & + \frac{0.01R^2}{m} \left[\frac{(m+1)z_2}{r_2^2} + \frac{mz(-z_2^2)}{r_2^4} \right] \\
 & - 0.002R^2H \left[\frac{-z_2^2}{r_2^4} + \frac{m}{m+1} \frac{2zz_2(-z_2^2)}{r_2^6} \right] \dots \dots \dots (3.2)
 \end{aligned}$$

$$V_{(z)max.} = -0.005R^2 \left(\frac{z_1}{r_1^2} + \frac{z_2}{r_2^2} \right) + \frac{0.01R^2}{m} \left[\frac{(m+1)z_2}{r_2^2} + \frac{mz(-z_2^2)}{r_2^4} \right] \dots \dots \dots (3.3)$$

Where, $z_1 = z - H$, $z_2 = z + H$, $r_1^2 = z_1^2$, $r_2^2 = z_2^2$, $R = D/2$, $m = 1/(1 - 2v)$, $k = v(1 - v)$. v is the poisson's ratio of soil. Long term ground deformation due to ovalization is equal to zero for seismic loading.

3.2.3 Modified Empirical Formulae for Maximum Lateral Settlement

Maximum lateral settlement is most important for practical purpose. Surface structures have to be design based on maximum settlements above a tunnel. Lateral ground settlements are disturbed surface structures and underground facilities. O'Reilly and New (1982) gives an empirical formula to predict lateral surface settlement. In present research, modified this formula which is shown in below:

$$U_{(x),max.} = V_{(z),max.} \frac{A + D}{4(H - z)} \dots \dots \dots (3.4)$$

Maximum lateral ground settlement (m) and distance (m) from free surface to tunnel crown are expressed by $U_{(x),max.}$ and A in equation (3.4).

A lot of seismic analysis have been performed for surface structures. A few amount of data are available to express damage of tunnels after earthquake before 70's. M. Pescara, (2011) gives an empirical relations to predict lateral settlement under seismic loading by using Eurocode 8. In present research, modified M. Pescara, (2011) formula which is shown in below:

$$\Delta_{(x),max.} = f \frac{a_1 g S C k}{C_s} (C_d - (H - z)) \dots \dots \dots (3.5)$$

Where, $\Delta_{(x),max.}$, a_1 , g , S , C , k , C_d , f and C_s are represented by maximum lateral settlement (mm), seismic coefficient such as 0.15 (Bangladesh National Building Code (BNBC) 2006), gravitational acceleration (9.81m/s²), soil factor (1.15) based on Eurocode 8 which equivalent to BNBC 2006, factor of ground motion (0.9) (Power et.al 1996), factor which depends upon seismic data (142) (Power et.al 1996), total depth (27.5m), modified factor (10) and apparent propagation velocity of S-wave. Several authors [O'Rourke & Liu, 1999; Power et al., 1996; Paolucci & Pitilakis, 2007] have suggested values between 1 and 5km/s for apparent propagation velocity of S-wave.

3.2.4 Modified Analytical Formulae for Maximum Lateral Settlement

Verruijt and Booker (1996) gives a closed form general solutions for the calculation of the lateral ground settlement under uniform radial ground loss. In present research, modified this formula for 0.5 percent volume loss based on Hunt (2004) and Zhou (2014) consideration of lateral distance from tunnel axis (lateral distance equal to twenty five percent of summation of tunnel diameter and depth of tunnel crown) for static and seismic loading which is shown in below:

$$\begin{aligned} U_{(x),max.} = & 0.00125R^2 \left(\frac{(A + D)}{r_1^2} + \frac{(A + D)}{r_2^2} \right) \\ & - 0.0000625R^2 \left[\frac{z_1((A + D)^2 - 16kz_1^2)}{r_1^4} + \frac{((A + D)^3 - (A + D)16kz_2^2)}{4r_2^4} \right] \\ & + \frac{0.0025(A + D)R^2}{m} \left(\frac{1}{r_2^2} - \frac{2mzz_2}{r_2^4} \right) \\ & + \frac{0.001R^2(A + D)H}{(m + 1)} \left[\frac{z_2}{r_2^4} + \frac{mz((A + D)^2 - 48z_2^2)}{16r_2^6} \right] \dots \dots \dots (3.6) \end{aligned}$$

$$U_{(x),max.} = 0.00125R^2 \left(\frac{(A + D)}{r_1^2} + \frac{(A + D)}{r_2^2} \right) + \frac{0.0025(A + D)R^2}{m} \left(\frac{1}{r_2^2} - \frac{2mzz_2}{r_2^4} \right) \dots \dots \dots (3.7)$$

Where, equation (3.6) represents the maximum lateral settlement for static loading and equation (3.7) represents the maximum lateral settlement for seismic loading.

3.2.5 Modified Empirical Formula for Maximum Longitudinal Settlement

Two dimensional plain strain analysis can't described the length effect of tunnel. Settlement along length of tunnel is necessary. In previous, most of tunnelling analysis has been completed based on plain strain consideration which are not included longitudinal settlement profile of tunnel. A few amount of research are expressed in longitudinal settlement above a tunnel based on field observations. Attewell and Woodman (1982) gives an empirical relation to predict longitudinal ground settlement above a tunnel. In present research, modified this formula which is shown in below:

$$U_{(y),max.} = \frac{V_{(z),max.}}{(H - z)} \dots \dots \dots (3.8)$$

Where, $U_{(y),max.}$ expresses maximum longitudinal ground settlement (m). Unit length is considered along the length of tunnel.

3.2.6 Modified Analytical Formulae for Strain Induced Volume Loss

Settlement of tunnel is caused by the strain induced volume loss. N.Loganathan et.al. (1998) provided a formula of strain induced volume loss for static loading. In present research, modified this formula based on some considerations such as 0.5 percent volume loss, maximum surface settlement (N.Loganathan et.al. (1998)). This modified formula is shown in below:

$$\varepsilon_{vl} = 0.01003 \exp \left[- \frac{0.69}{\left(1 + \frac{t}{A} + \frac{D}{2A}\right)^2} \right] \dots \dots \dots (3.9)$$

Where, t is the thickness of tunnel lining (pre-cast concrete segment) and ε_{vl} is the strain induced volume loss for static loading. St. John and Zahrah (1987) gives an analytical formula to evaluate strain induced ground loss for seismic loading. In this formula, following considerations have been taken such as apparent propagation of velocity (3km/s, FHWA-NHI-10-034), seismic wave propagation angle in horizontal plane with the tunnel axis (45° , D.M.Workey, Open-File Report 01-0440, USGS). In present research, modified this formula based on above considerations.

$$\varepsilon_{vs} = \frac{V}{6000} + \frac{A_c(2t + D)}{36000000\sqrt{2}} \dots \dots \dots (3.10)$$

Where, V is the maximum velocity of seismic shaking, A_c is the maximum acceleration of seismic shaking, ϵ_{vs} is the volumetric strain due to seismic shaking.

3.3 VALIDATION OF MODIFIED FORMULAS

Validation of modified formulas will be required for comparison between actual and modified formula. Validation has been performed some terms such as modified empirical formula for maximum vertical surface settlement, modified analytical formula for maximum vertical surface settlement and modified analytical formula for strain induced volume loss. Maximum lateral and longitudinal settlements are the function of maximum vertical settlement. Validation results are very close with each other for every case.

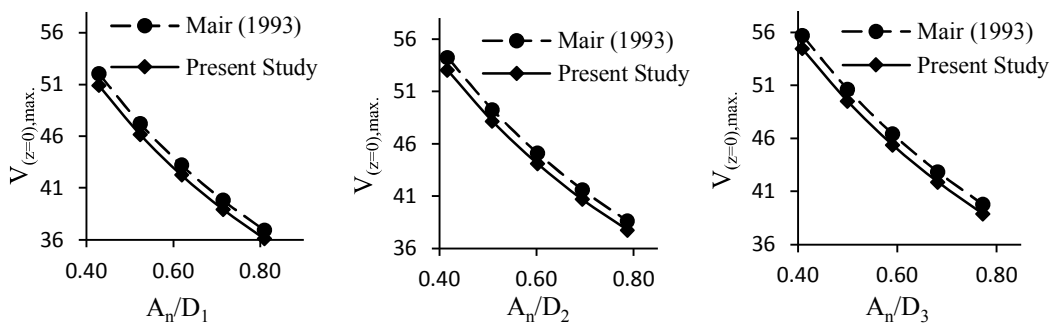


Figure 3.1a: Comparison of maximum vertical surface settlement between empirical and modified empirical formula.

Difference of settlement between Mair (1993) formula and present study (modified) formula is 2 percent for every location of relative depth of tunnel in **Figure 3.1a**. This variation indicates good accuracy of modified formula of present research.

3.3.1 Validation of Modified Empirical Formula for Settlement

Table 3.1: Validation of modified empirical formula for maximum vertical surface settlement

Location of Case Study	Tunnel Depth, H (m)	Tunnel Diameter, D (m)	Maximum vertical surface settlement (mm)			Reference
			Mair et al. (1981)	Clough et al. (1981)	Present Study (Eq. 3.1)	
Barcelona Subway Network Extension Tunnel, Barcelona	10	8	29	30.3	28.8	Loganathan Poulos (1998)

3.3.2 Validation of Modified Analytical Formula for Settlement

Table 3.2: Validation of modified analytical formula for maximum vertical surface settlement

Location of Case Study	Tunnel Depth, H (m)	Tunnel Diameter, D (m)	Maximum vertical surface settlement (mm)		Reference
			Loganathan et al. (1998)	Present Study (Eq. 3.2)	
Barcelona Subway Network Extension Tunnel, Barcelona	10	8	23.2	24.6	Loganathan and Poulos, (1998)

3.3.3 Validation of Modified Strain Induced Volume Loss Formula

Table 3.3: Validation of modified strain induced volume loss analytical formula for long term loading

Location of Case Study	Tunnel Depth, H (m)	Tunnel Diameter, D (m)	Volume Loss (%)		Reference
			Loganathan et al. (1998)	Present Study (Eq. 3.9)	
Barcelona Subway Network Extension Tunnel, Barcelona	10	8	0.8	0.78	Loganathan and Poulos, (1998)

3.4 IMPLEMENTATION OF MODIFIED FORMULAS IN PRESENT RESEARCH

It is necessary to implement modified formulas in present research for observe settlements and volumetric strains with the variation of diameters, lengths and relative depths of tunnel. Results of modified formulas deals with two types of settlements such as surface and total settlements. Total

settlements defined as the overall settlements of tunnel which occurs bottom of tunnel. Present research model of tunnel and its various parameters are shown below:

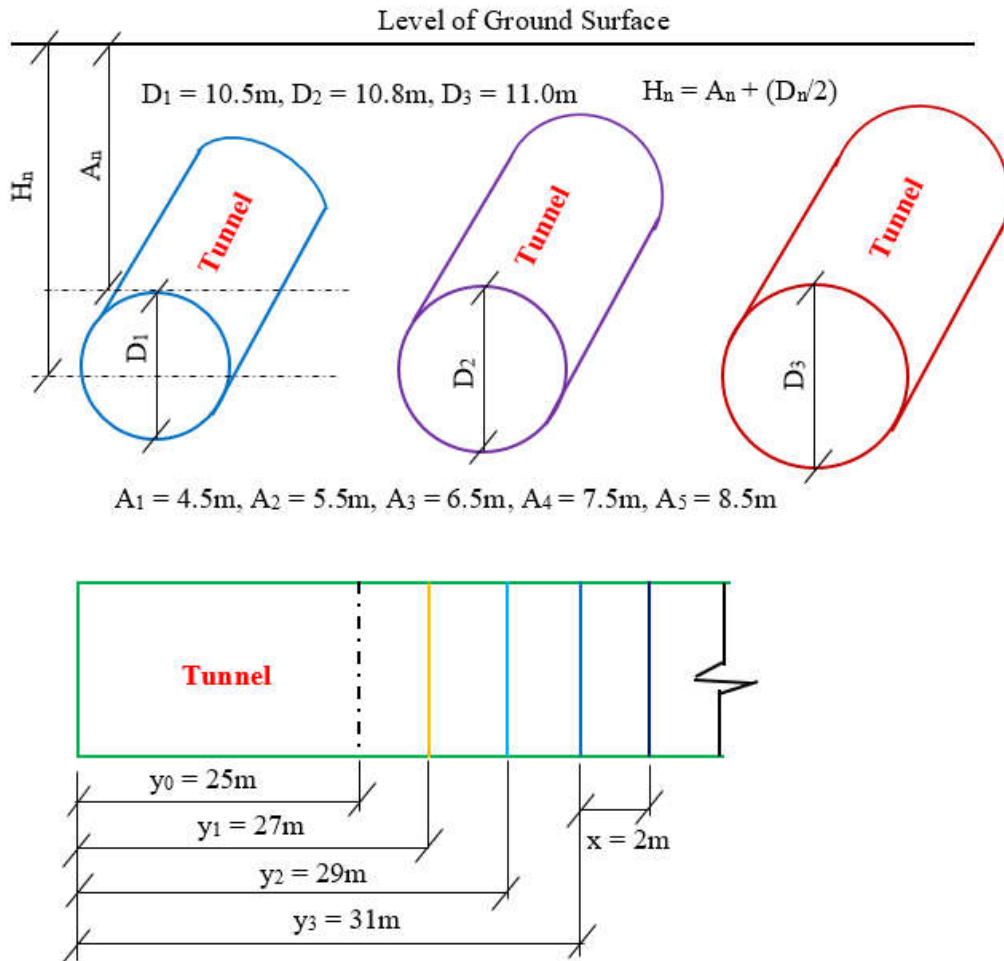


Figure 3.1b: Configurations of present research tunnel and its components.

3.4.1 Vertical Surface Settlements

Surface settlements are important for surface structures. If surface has to be settle due to tunnelling than surface structures must be settle which is dangerous for human and others. Empirical and analytical formulas express surface settlements based on plain strain condition. Variation of depths of tunnel crown are influenced surface settlements. Surface settlements are varied with the variation of relative depths of tunnel. Such types of settlements are expressed by modified empirical and analytical formulas.

Maximum values of vertical surface settlements are decreasing gradually with the increment of relative depths as shown in **Figure 3.2**. Decreasing rates are similar for three diameters. Difference between MEF-LTL and MAF-LTL are less than 5 mm. During seismic loading, settlements values are low but difference of decreasing rates are high. Minimum settlement is located at A_5/D_1 . So this location is suitable for construction of tunnel based on modified empirical and analytical formulae.

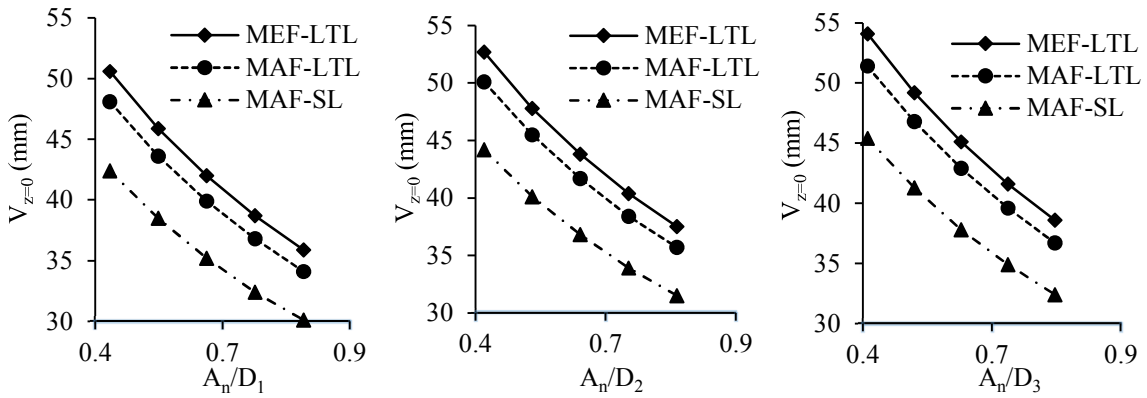


Figure 3.2: Vertical surface settlement for long term and seismic loading based on modified formulae

3.4.2 Total Vertical Settlements

Total vertical settlements are represented as the settlements of bottom of tunnel. **Figure 3.3** shows settlements of tunnel based on empirical and analytical formulae. MEF-LTL and MAF-SL are expressed constant settlements with the variation of relative depths. On the other hand, MAF-LTL shows linear variations of settlements for various diameters. Settlements values are negative which means uplift.

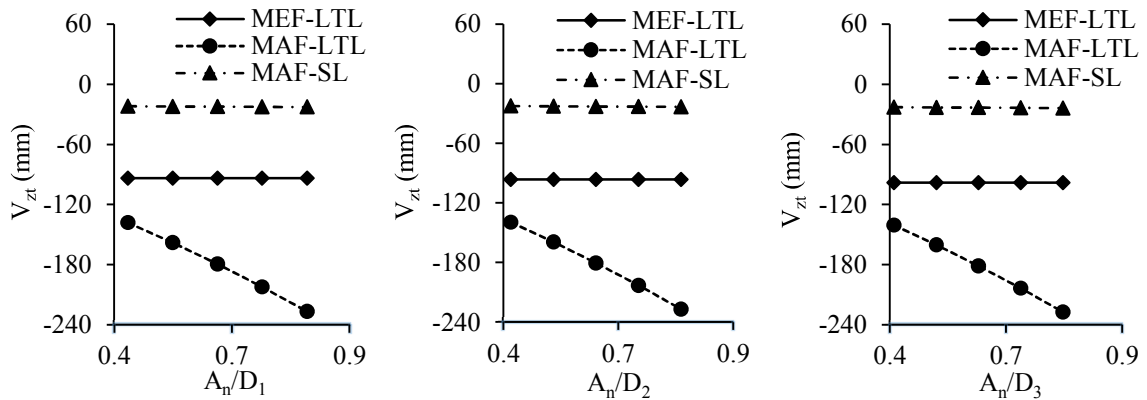


Figure 3.3: Total vertical settlement for long term and seismic loading based on modified formulae

3.4.3 Lateral Surface Settlements

Lateral surface settlements above a tunnel consists of lateral movements of surface structures. Lateral surface settlements are shown in **Figure 3.4** based on modified empirical and analytical formulae. MAF-LTL and MAF-SL are expressed very similar results of settlements for diameters D_1 , D_2 and D_3 .

MEF-LTL and MEF-SL are expressed little difference of settlements for all diameter. A_5/D_1 indicates the minimum lateral settlement.

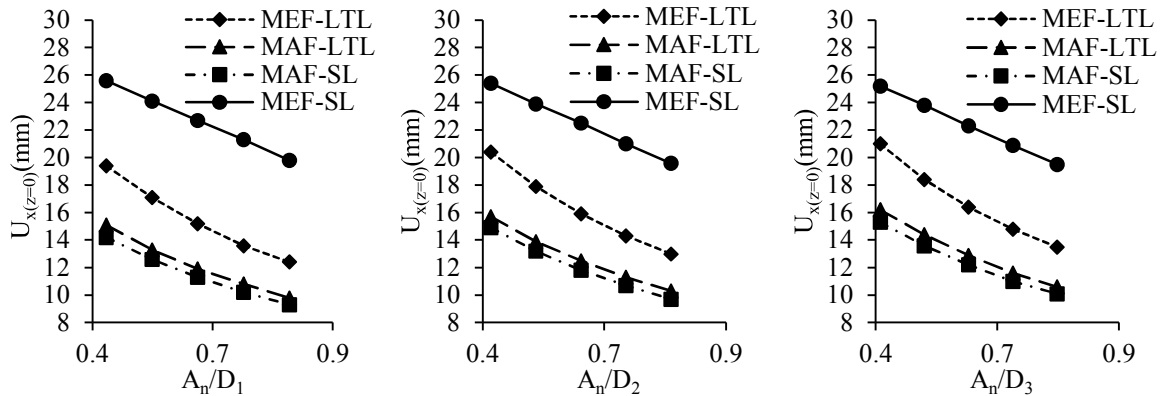


Figure 3.4: Lateral surface settlement for long term and seismic loading based on modified formulae

3.4.4 Total Lateral Settlements

Total lateral settlements are expressed overall settlements of tunnel structures. **Figure 3.5** represents lateral settlements based on modified empirical and analytical formulae. MEF-SL shows straight line variation of settlements. MAF-LTL and MAF-SL are very close to each other and slightly increase with the increment of relative depths. MEF-LTL shows linear increment of settlements for all diameter. Minimum settlement is 10 mm at A_5/D_1 .

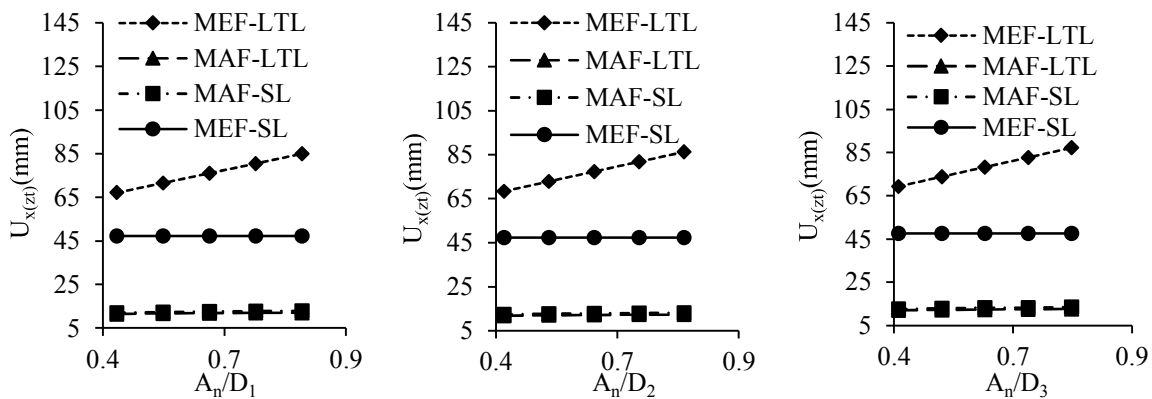


Figure 3.5: Total lateral settlement for long term and seismic loading based on modified formulae

3.4.5 Longitudinal Surface Settlements

Modified empirical formula deals with the longitudinal surface settlements of various diameters as shown in **Figure 3.6**. Longitudinal surface settlements are decreasing gradually with the increment of

depth of tunnel crown for diameters D_1 , D_2 and D_3 . Three diameters are shown nearly similar settlement profile. Minimum settlement is 2.6 mm at A_5/D_1 .

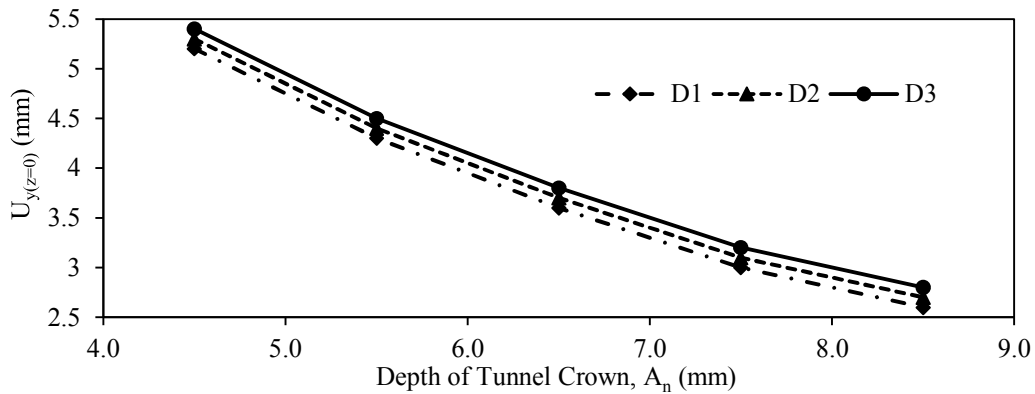


Figure 3.6: Longitudinal surface settlement for long term loading based on modified formula

3.4.6 Total Longitudinal Settlements

Total longitudinal settlements of tunnel are shown in **Figure 3.7** based on modified empirical formula. Constant variations of settlements show with the increment of depth of tunnel crown for diameters D_1 , D_2 and D_3 . These types of settlements can't vary with relative depths. Settlements are decreasing gradually with increment of diameters. Minimum settlement is 16.25mm for diameter, D_3 .

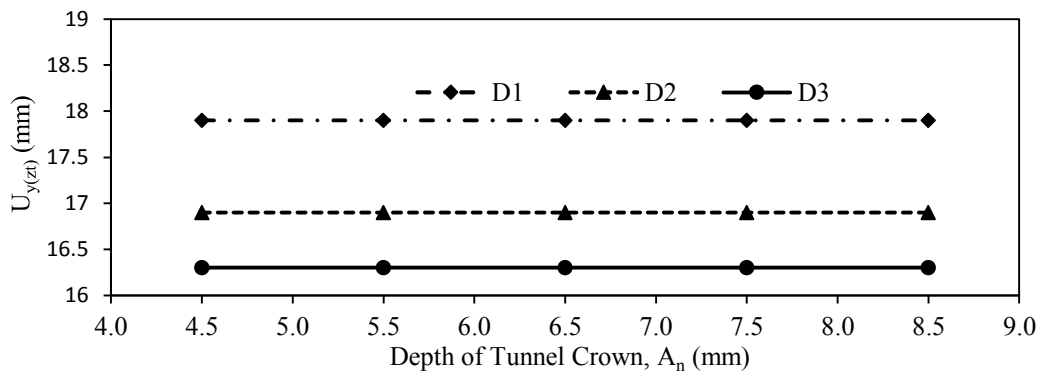
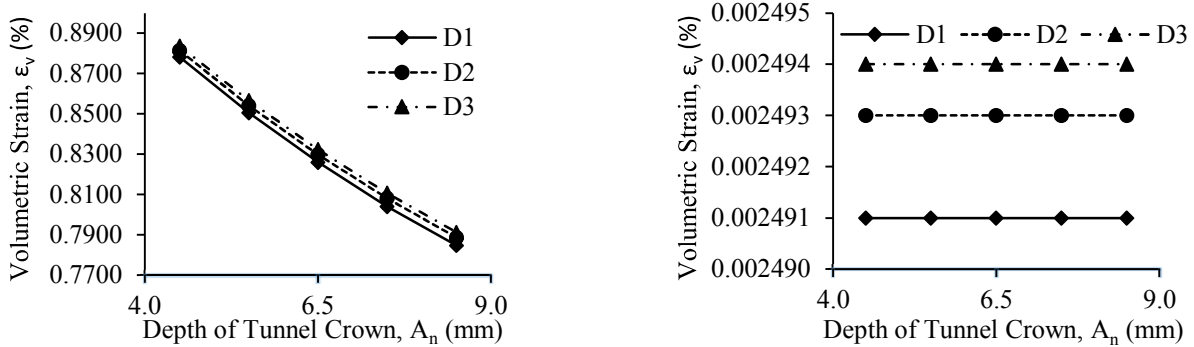


Figure 3.7: Total longitudinal settlement for long term loading based on modified formula

3.4.7 Strain Induced Volume Loss

Volume loss at the face of tunnel causes settlements of tunnel in any directions. Volume loss of tunnel are discussed here with consideration of modified formula as shown in **Figure 3.8**. Volumetric strain does not vary with the increment of depth of tunnel crown for seismic loading. Minimum volumetric

strain is 0.78 percent for diameter, D_1 under long term loading and minimum volumetric strain is 0.002491 percent for diameter, D_1 under seismic loading.



(a) Long term loading

(b) Seismic loading

Figure 3.8: Volumetric strain for long term and seismic loading based on modified formulae

3.5 CONCLUSIONS

Results are nearly close for modified empirical and analytical formulae. Difference of vertical surface settlement between modified empirical and analytical formula has been found to be 4.7% under static loading. Minimum vertical surface settlement is 30 mm at A_5/D_1 location based on modified analytical formula of seismic loading. Difference of settlement between static and seismic loading has been found to be less than 1% at relative depth, A_5/D_1 using modified analytical formulae. Minimum lateral surface settlement is 9 mm at A_5/D_1 based on modified analytical formula of seismic loading. Minimum value of total lateral settlement is 10 mm at A_5/D_1 based on modified analytical formulae of seismic and long term loading. Differences of settlements among various diameters have been obtained to be 2% under static loading. Minimum longitudinal surface settlement is 2.6 mm at A_5 for diameter D_1 based on modified empirical formula. Differences of strain induced volume losses among various diameters have been found to be 0.5%. under static loading. Minimum difference of strain induced volume loss between diameters D_2 and D_3 has been obtained to be less than 0.1% under seismic loading. Minimum value of volumetric strain is 0.78 percent at A_5/D_1 based on modified formula for long term loading.

Based on above analysis results, it has to be noted that suitable depth of tunnel crown and tunnel diameter are 8.5 m (A_5) and 10.5 m (D_1). Good accuracy has been performed of validation results. Results differences are very small between modified empirical and analytical formulas. That is why, modified formulas will be used in practical work for optimise time of engineers, workers and others.

CHAPTER FOUR

RESULTS AND INTERPRETATION OF NUMERICAL ANALYSIS

4.1 INTRODUCTION

In this chapter contains numerical modelling and analysis of tunnel under static and seismic loading. Numerical analysis is more accurate than 2D plain strain analysis. Two types of tri-axial tests have been performed in laboratory such as consolidated drained (CD) and consolidated un-drained (CU). Both tests results are implemented in the present research. Numerical analysis is performed by PLAXIS 3D, finite element based commercial package software. Firstly, PLAXIS 3D model is validated than it is used for present research. In this chapter deals with some terms such as numerical model, soil parameters, mesh generations, mesh effects, analysis process and results. Numerical model contains some short terms such as lengths of tunnel ($y_1 = 27\text{m}$, $y_2 = 29\text{m}$, $y_3 = 31\text{m}$), diameters ($D_1 = 10.5\text{m}$, $D_2 = 10.8\text{m}$, $D_3 = 11.0\text{m}$), depths of tunnel crown ($A_1 = 4.5\text{m}$, $A_2 = 5.5\text{m}$, $A_3 = 6.5\text{m}$, $A_4 = 7.5\text{m}$, $A_5 = 8.5\text{m}$) and relative depth (A_n/D_n). Seismic analysis is performed to consider effective portion of seismic duration which is five seconds. Numerical analysis results are expressed some terms such as settlements, strain induced volume loss, stress – strain behaviour of soil around tunnel, accelerations and displacement under static and seismic loading. In this research, long term loading means static loading and total settlement means overall settlement (settlement of bottom) of tunnel.

4.2 FINITE ELEMENT MODEL

Numerical model is created for analysis based on practical site condition. Fixed parameters of this model are soil volume, material properties of soil, location of bore hole etc. Similarly, variable parameters are tunnel length, diameter and depth of tunnel crown. Finite element model is shown in below:

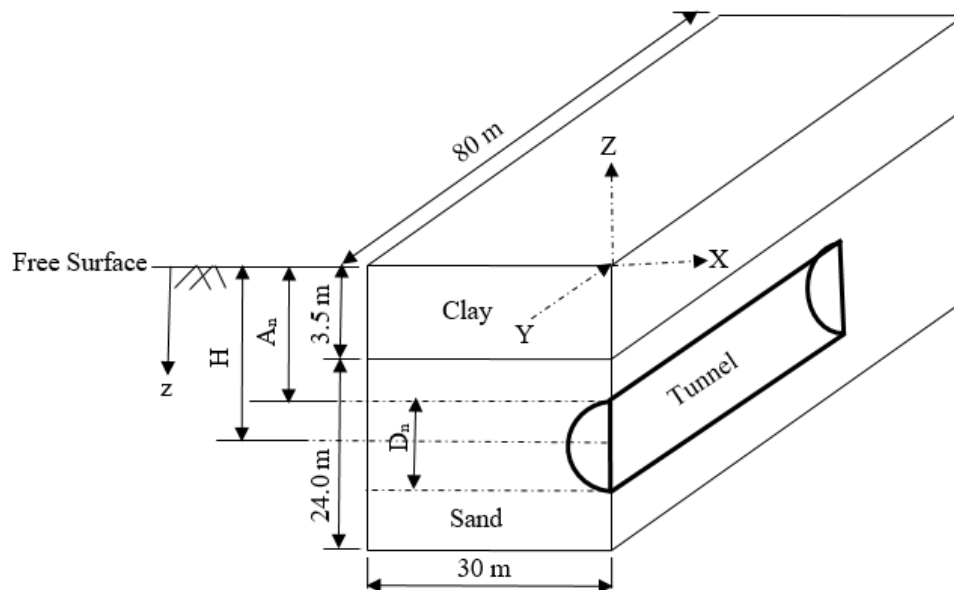


Figure 4.1: Finite element model based on site soil condition.

Here, X, Y, Z are the model co-ordinate axes and its directions are positive. Tunnel passage through a homogeneous sand layer with no seismic fault region. Neglecting seismic refraction phenomena in two layers such as upper clay and lower sand layer. Any depth from free surface is represented by z. Distance between free surface to centre line of tunnel is H. A_n is the depth of free surface to tunnel top surface (depth of tunnel crown). The fixed thickness of clay and sand layers are shown in **Figure 4.1** which are selected from construction site. D_n is the diameter of tunnel. Half circle is considered for analysis because of symmetry. Initial length of tunnel is 25m. Ring (pre-cast concrete segment) width is 2m. This model is used for static and seismic loading. Length and width of soil are shown in **Figure 4.1** which are fixed. Thickness of tunnel lining (pre-cast concrete segment) is 0.5m.

4.3 MATERIAL PROPERTIES OF SOIL AND TUNNEL LINING

Sample was collected from site and tri-axial test was performed in laboratory. Tri-axial tests are two types such as consolidated drained (CD) for static loading and consolidated un-drained (CU) for seismic loading. Mohr-Coulomb material model is considered for analysis in PLAXIS 3D. Material properties of CD and CU test are shown below:

Table 4.1: Material properties of tunnel lining

Parameter	Name	TBM	Unit
Lining Thickness	d	0.50	m
Unit weight	γ	24	kN/m ³
Material behavior	-	Linear, Isotropic	-
Young's modulus	E'	2.8×10^7	kN/m ²
Poission's ratio	ν'	0.20	-
Shear modulus	G	1.17×10^7	kN/m ²
Width of ring (Excavation phase)	x	2.0	m

Table 4.2: Material properties of soil in the specified site and PLAXIS 3D, inputting material parameters for consolidated drained test (CD)

Parameter	Name	Upper silty clay	Lower fine sand	Lining segment (Concrete)	Units
Material Model	Model	Mohr-Coulomb	Mohr-Coulomb	Linear elastic	-
Drainage Type	Type	Drained	Drained	Non porous	-
Bulk unit weight	γ_{unsat}	16.40	18.6	24	kN/m ³
Saturated unit weight	γ_{sat}	18.90	20	-	kN/m ³
Young's Modulus	E'	14400	26097	2.8 x 10 ⁷	kN/m ²
Poisson's Ratio	ν'	0.310	0.250	0.20	-
Cohesion	C'_{ref}	30	1.0	-	kN/m ²
Friction Angle	ϕ'	23	36	-	degree (°)
Dilatancy Angle	ψ	0	6 [($\psi = \phi' - 30$), Bolton, (1986)]	-	degree (°)
Interface Strength	Rigid	Rigid	Rigid	Rigid	-
K ₀ determination	Automatic	Automatic	Automatic	Automatic	-

Table 4.3: Material properties of soil in the specified site and PLAXIS 3D, inputting material parameters for consolidated un-drained test (CU)

Parameter	Name	Upper silty clay	Lower fine sand	Lining segment (Concrete)	Units
Material Model	Model	Mohr-Coulomb	Mohr-Coulomb	Linear elastic	-
Drainage Type	Type	Undrained (A)	Undrained (A)	Non porous	-
Bulk unit weight	γ_{unsat}	17.00	19.00	24	kN/m ³
Saturated unit weight	γ_{sat}	19.00	20	-	kN/m ³
Young's Modulus	E_u'	22450	40818	2.8×10^7	kN/m ²
Poission's Ratio	ν_u'	0.310	0.250	0.20	-
Cohesion	C'_{ref}	30	1.0	-	kN/m ²
Friction Angle	ϕ'	23	29	-	degree (°)
Dilatancy Angle	ψ	0	0	-	degree (°)
Interface Strength	Rigid	Rigid	Rigid	Rigid	-
K_0 determination	Automatic	Automatic	Automatic	Automatic	-

PLAXIS 3D is considered effective stress during analysis. Mohr-Coulomb material model consists of two parts such as linear elastic and perfectly plastic. Seismic data has been collected from respective site. Rayleigh damping coefficient α and β are related with earthquake frequency and damping ratio. Range of earthquake frequency is less than 20Hz. In this research, damping ratio is taken 5% and seismic frequency is taken 4Hz, 8Hz and 12Hz.

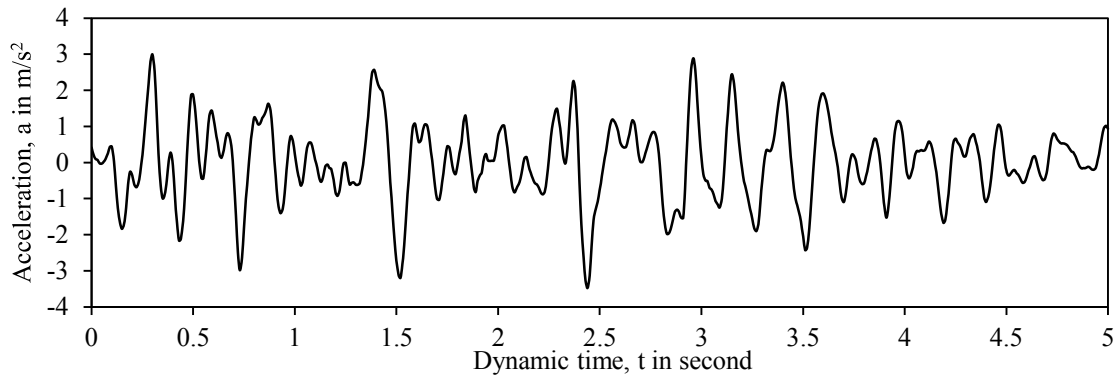


Figure 4.2: Input value of seismic data

4.4 LOADING MECHANISM OF EPB – TBM

Mainly three types of loads are applied to the tunnel during construction such as tunnel face pressure, grout pressure and jacking force. Analysis of tunnel in PLAXIS 3D consists of full construction mechanism. Loading mechanism and calculation process are shown in below:

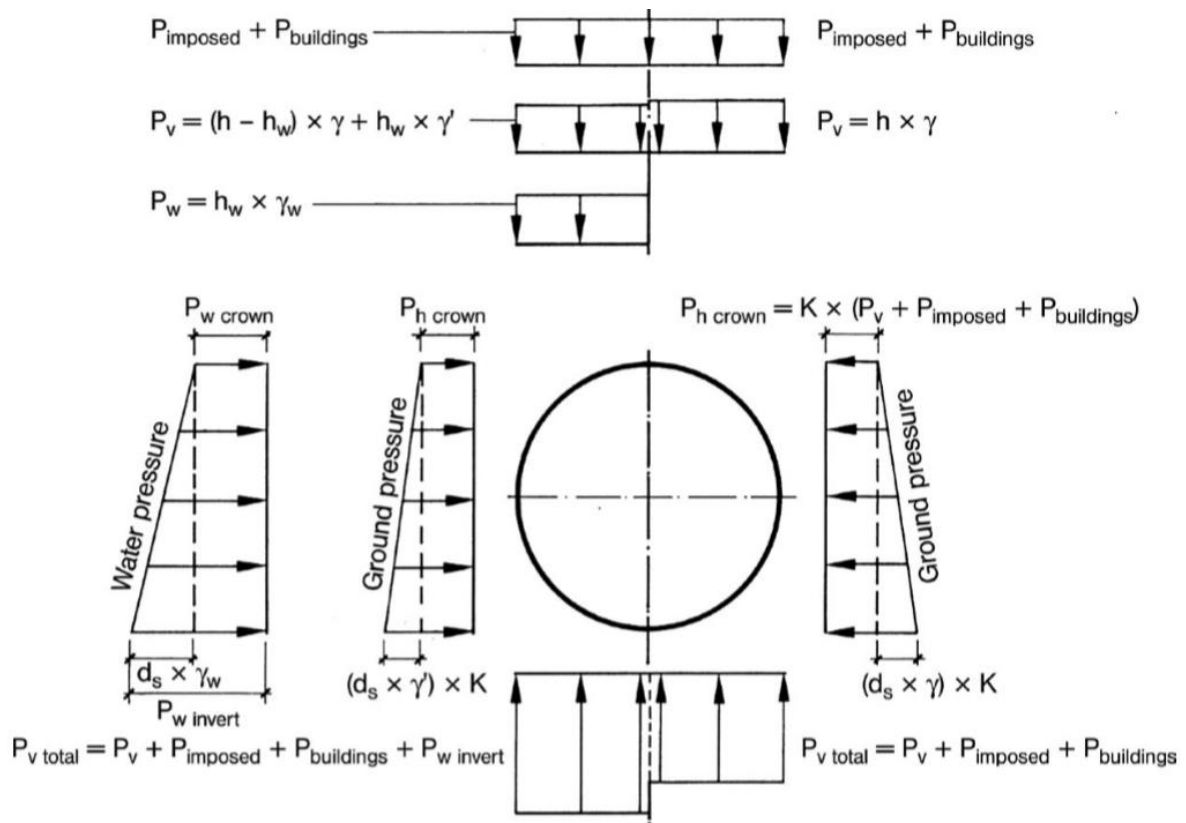


Figure 4.3: Loading assumptions for ground and water pressures perpendicular to shield (Bernhard et. al, 2011)

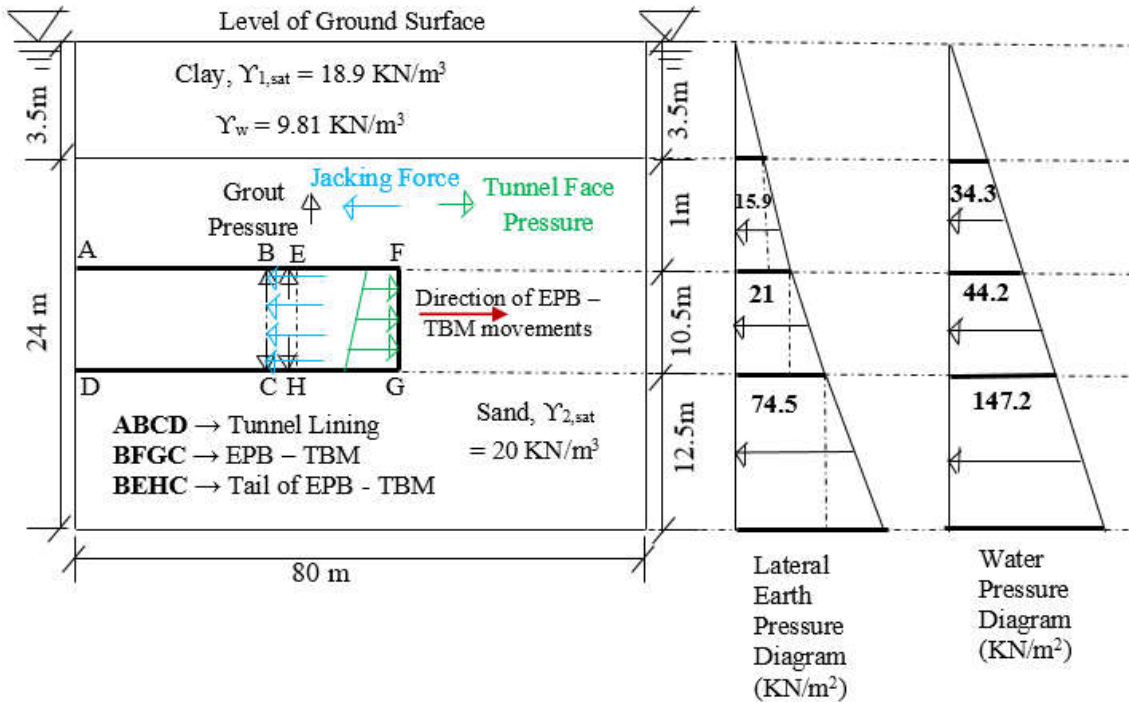


Figure 4.4: Loading and construction mechanism of EPB – TBM of present research.

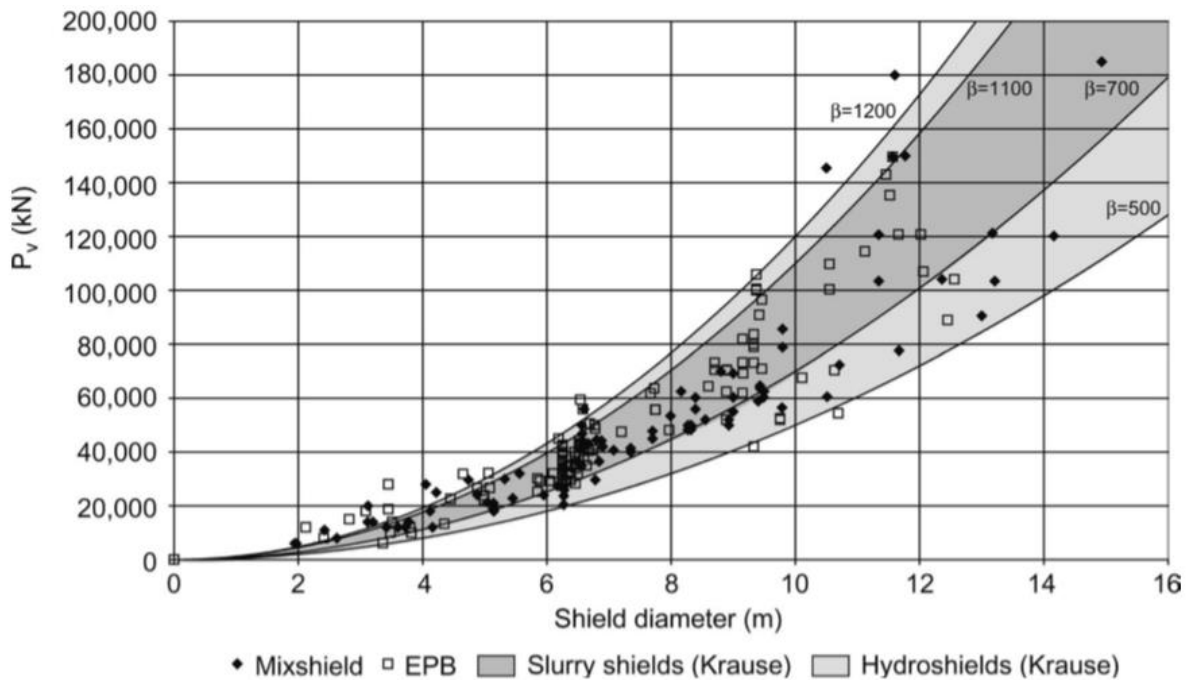


Figure 4.5: Relationship between the maximum thrust/jacking force, P_v and the shield diameter, D (Bernhard et. al, 2011)

Length of EPB – TBM is 12m which is used in this research. 0.5 percent volume loss of tunnel has to be consider in this thesis with axial increment of 0.05 percent.

Table 4.4: Tunnel face pressure, grouting pressure and jacking force for CD test

Tunnel Diameter, D_n (m)	Depth of tunnel crown, A_n (m)	Area, m^2	Quarter perimeter, (m)	Tunnel face pressure (kN/m^2)	Increment of face pressure (kN/m^2)	Grout pressure (kN/m^2)	Increment of grout pressure (kN/m^2)	Jacking Force (kN/m^2)
10.5	4.5	86.6	8.25	65.1	14.9	86.2	20	785.3
	5.5			80.1	14.9	106.2	20	
	6.5			95.0	14.9	126.2	20	
	7.5			109.9	14.9	146.2	20	
	8.5			124.8	14.9	166.2	20	
10.8	4.5	91.6	8.48	65.1	14.9	86.2	20	775.0
	5.5			80.1	14.9	106.2	20	
	6.5			95.0	14.9	126.2	20	
	7.5			109.9	14.9	146.2	20	
	8.5			124.8	14.9	166.2	20	
11.0	4.5	95.0	8.64	65.1	14.9	86.2	20	599.8
	5.5			80.1	14.9	106.2	20	
	6.5			95.0	14.9	126.2	20	
	7.5			109.9	14.9	146.2	20	
	8.5			124.8	14.9	166.2	20	

Table 4.5: Tunnel face pressure, grouting pressure and jacking force for CU test

Tunnel Diameter, D_n (m)	Depth of tunnel crown, A_n (m)	Area, m^2	Quarter perimeter, (m)	Tunnel face pressure (kN/m^2)	Increment of face pressure (kN/m^2)	Grout pressure (kN/m^2)	Increment of grout pressure (kN/m^2)	Jacking Force (kN/m^2)
10.5	4.5	86.6	8.25	65.3	14.9	86.5	20	785.3
	5.5			80.2	14.9	106.5	20	
	6.5			95.1	14.9	126.5	20	
	7.5			110.0	14.9	146.5	20	
	8.5			124.9	14.9	166.5	20	
10.8	4.5	91.6	8.48	65.3	14.9	86.5	20	775.0
	5.5			80.2	14.9	106.5	20	
	6.5			95.1	14.9	126.5	20	
	7.5			110.0	14.9	146.5	20	
	8.5			124.9	14.9	166.5	20	
11.0	4.5	95.0	8.64	65.3	14.9	86.5	20	599.8
	5.5			80.2	14.9	106.5	20	
	6.5			95.1	14.9	126.5	20	
	7.5			110.0	14.9	146.5	20	
	8.5			124.9	14.9	166.5	20	

4.5 MESH GENERATIONS

Model geometry is divided into finite elements for calculations. A composition of the finite element is called a mesh. The mesh is created in the mesh mode. Fine mesh is used for analysis to obtain accurate numerical results. On the other hand, very fine meshes are avoided because of it's taken to excessive calculation times. The PLAXIS 3D programme allows automatic mesh generation. The mesh generation process takes into account the soil stratigraphy as well as all structural objects, loads and boundary conditions. Analysis is continuing until convergence achieved.

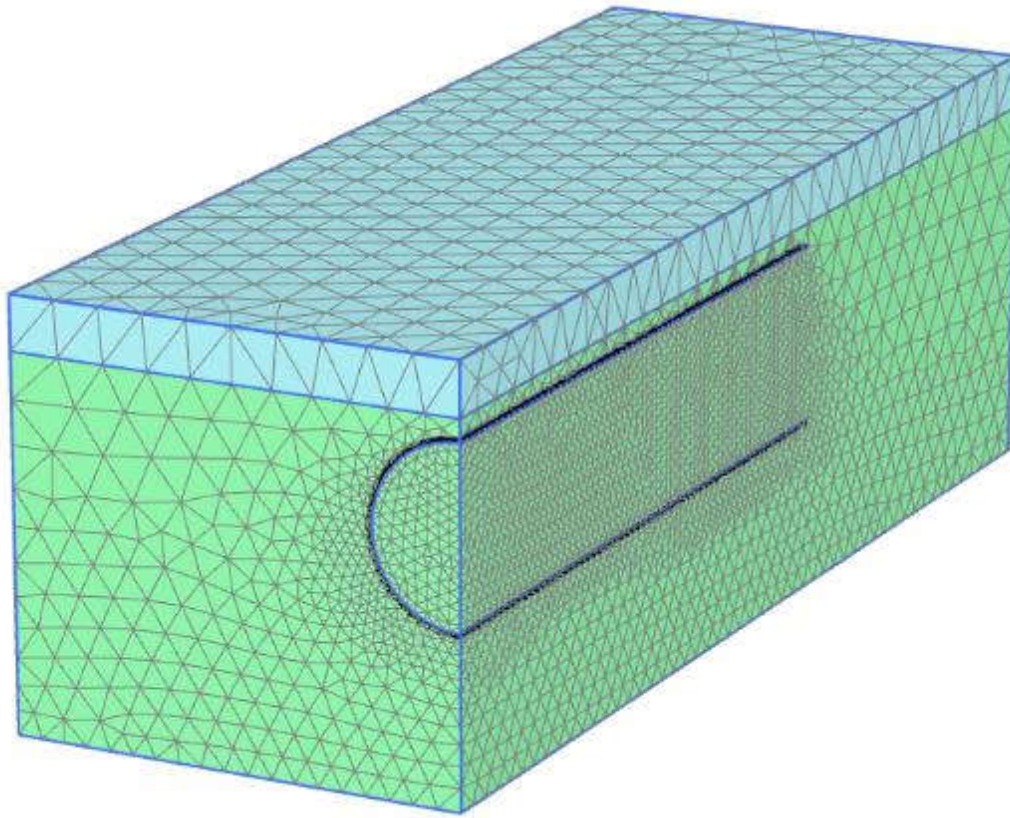


Figure 4.6: Fine meshing of model

4.6 ANALYSIS PROCESS

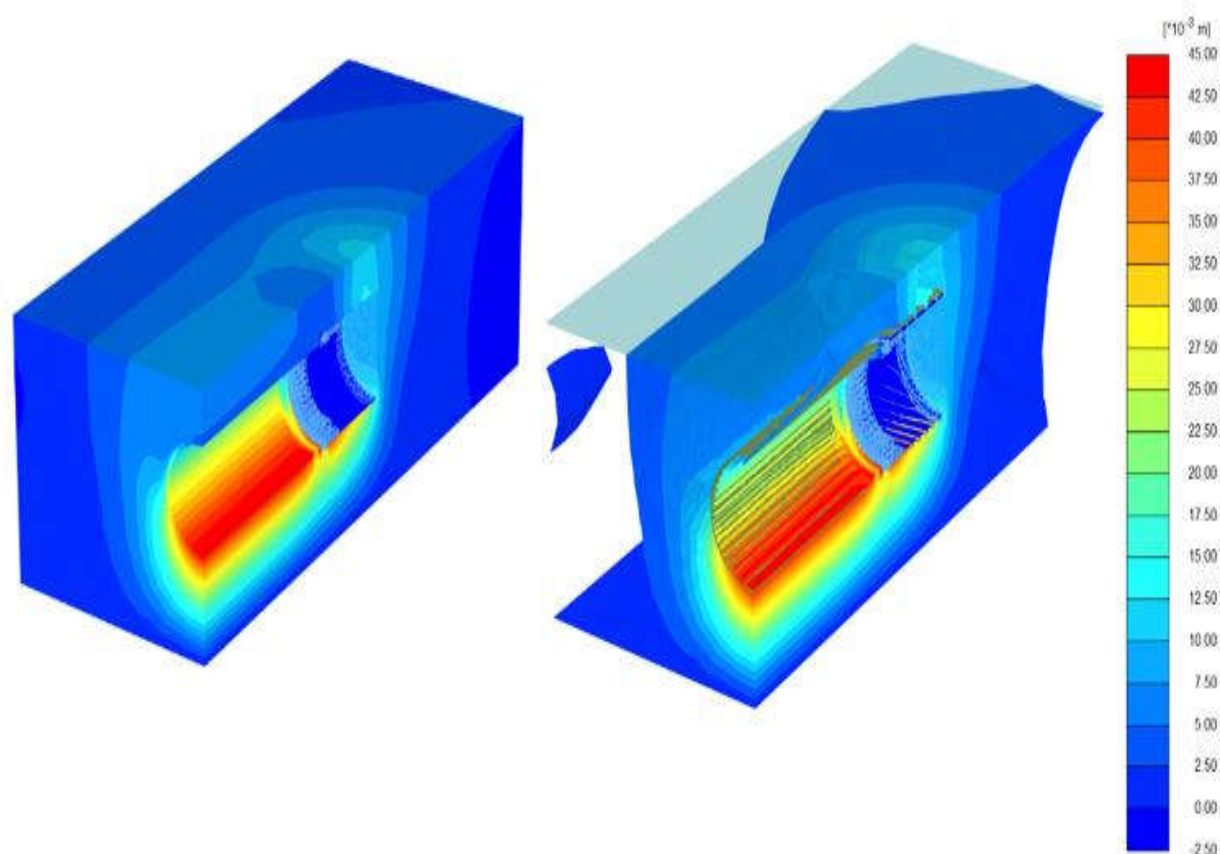
Firstly, static analysis is performed and secondly, performed seismic analysis with considering appropriate boundary conditions. In static analysis, software automatically selected suitable parameters which maintain analysis process. In dynamic analysis, different parameters are selected by user. In this research, free-field boundary condition has to be consider along lateral direction of tunnel and other two directions have to be consider fixed boundary condition. Seismic source is located far away from the tunnel. Dynamic displacement multipliers are provided along lateral directions of tunnel which are contained accelerations with drift. Static analysis consists of minimum two and maximum four phases. Completing static analysis, dynamic analysis is started which connects with first phase. Duration of seismic analysis is five seconds.

4.7 MESHING EFFECTS ON THE RESULTS

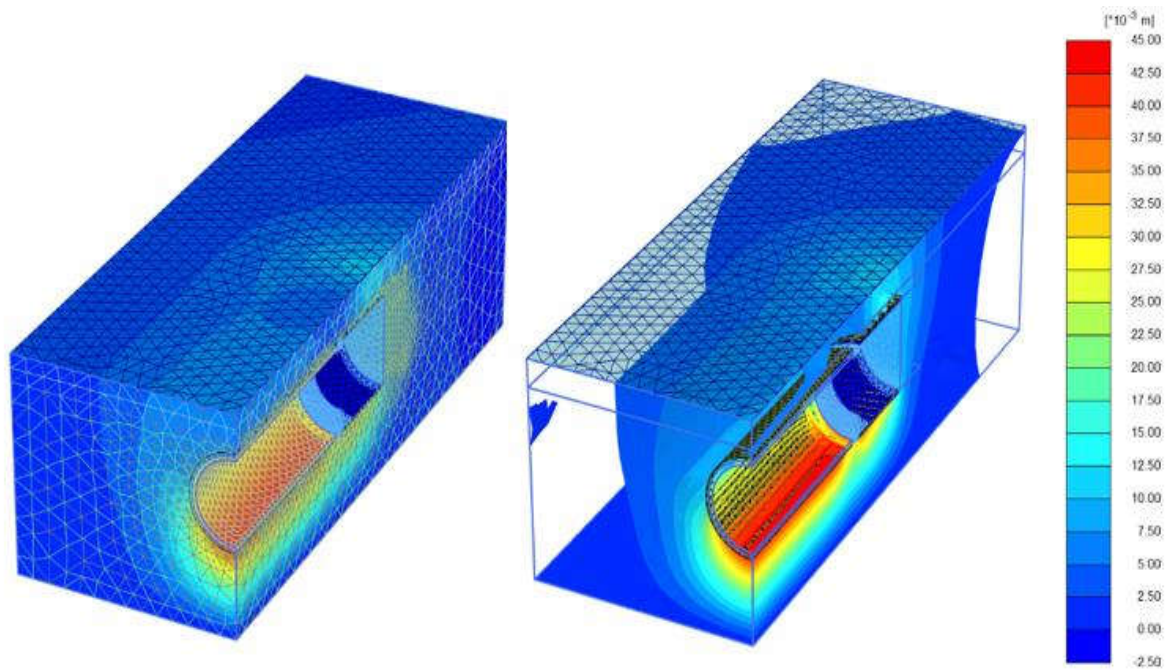
Mesh is the most important for finite element analysis. Medium and fine meshes are contained more accurate analysis than coarse mesh. On the other hand, very fine mesh takes longer time to complete analysis than other types which seems to be difficult to solve full scale model for used in practical purpose. Meshing effects are shown in **Table 4.6** and **Figure 4.7**.

Table 4.6: Meshing effect on the results of this research model

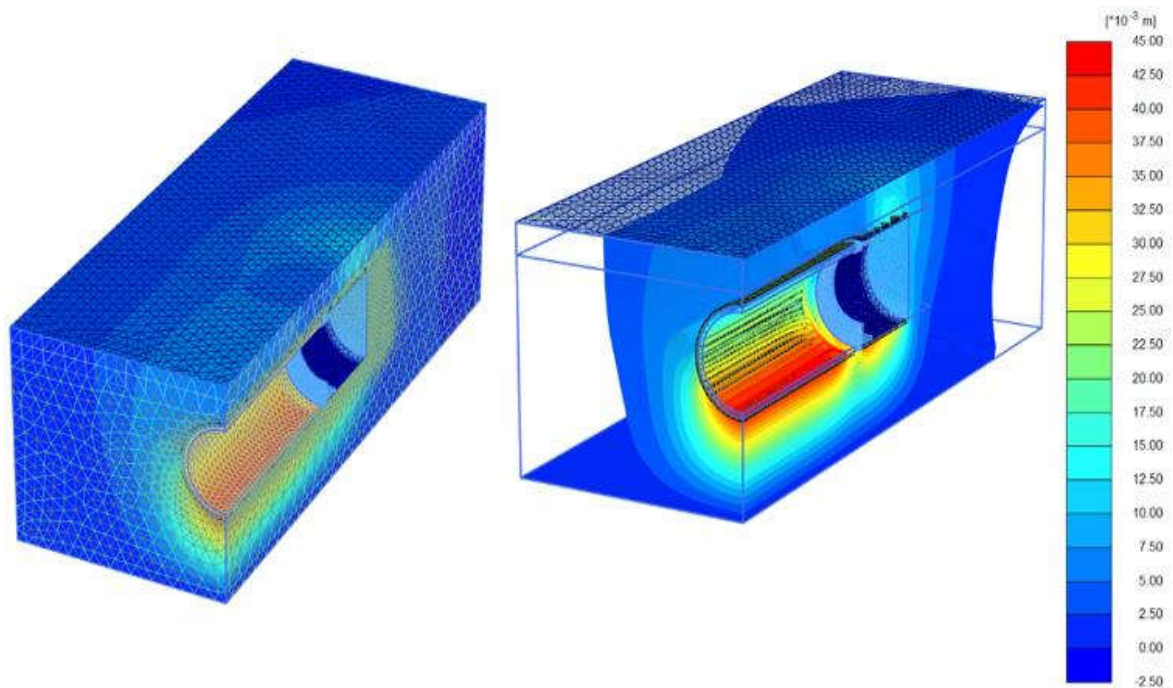
Tunnel length, y_1 (m)	A_1/D_1	Maximum total vertical settlement ($V_{(zt)}$) in (mm)		
		Coarse	Medium	Fine
27	0.4286	-44.7	-44.5	-44.5



(a) Coarse mesh



(b) Medium mesh



(c) Fine mesh

Figure 4.7: Meshing effect of total vertical settlement for $D_1 = 10.5\text{m}$, $A_1 = 4.5\text{m}$, $y_1 = 27\text{m}$

4.8 VALIDATION OF PLAXIS 3D

Validation of PLAXIS 3D model is performed by existing literature (Kilany et al. 2017). Existing literature consists of under construction tunnel of Cairo Metro–Line III in Egypt. Most of the length of

this line were constructed by Tunnel Boring Machine (TBM). Outer diameter of tunnel was 8m and thickness was 0.40m. Length of EPB – TBM was 6m. Length of tunnel was 6m. In this analysis, only considered tunnel face pressure. Volume loss of tunnel was 0.5 percent and axial increment of volume loss along length of TBM was 0.10 percent. Mohr – Coulomb material model was used in this analysis and 10 – noded tetrahedral soil element was used for finite element analysis. Along length of tunnel dimension of model was 18m and other horizontal dimension was 30m. Lining segment of tunnel was concrete whose modulus of elasticity, unit weight and poisson’s ratio were 2.8×10^7 kN/m², 24 kN/m³ and 0.15. In present research, validated above mentioned literature with considering its parameters.

Table 4.7: Material Properties and Geotechnical soil parameters and the interfaces (Kilany et al. 2017)

Parameter	Name	Fill	Sand-1	Clay-1	Sand-2	Gravel	Sand-3	Clay-2	Sand-4	Units
Drainage Type	Type	Drained	Drained	Drained	Drained	Drained	Drained	Drained	Drained	-
Bulk unit weight	γ_{unsat}	15	16	15	17	18	18	16.5	17	kN/m ³
Saturated unit weight	γ_{sat}	17	18	17	19	20	20	18.5	19	kN/m ³
Young’s Modulus	E_u'	2.5	35	12	40	100	40	14	45	Mpa
Poisson’s Ratio	ν_u'	0.3	0.3	0.3	0.3	0.3	0.3	0.3	0.3	-
Cohesion	C'_{ref}	5	5	75	5	1	5	150	5	kN/m ²
Friction Angle	ϕ'	25	37	20	39	42	38	20	40	degree
Dilatancy Angle	ψ	0	7	0	9	12	8	0	10	degree
Interface Strength	Rigid									
K_0 determination	Automatic									

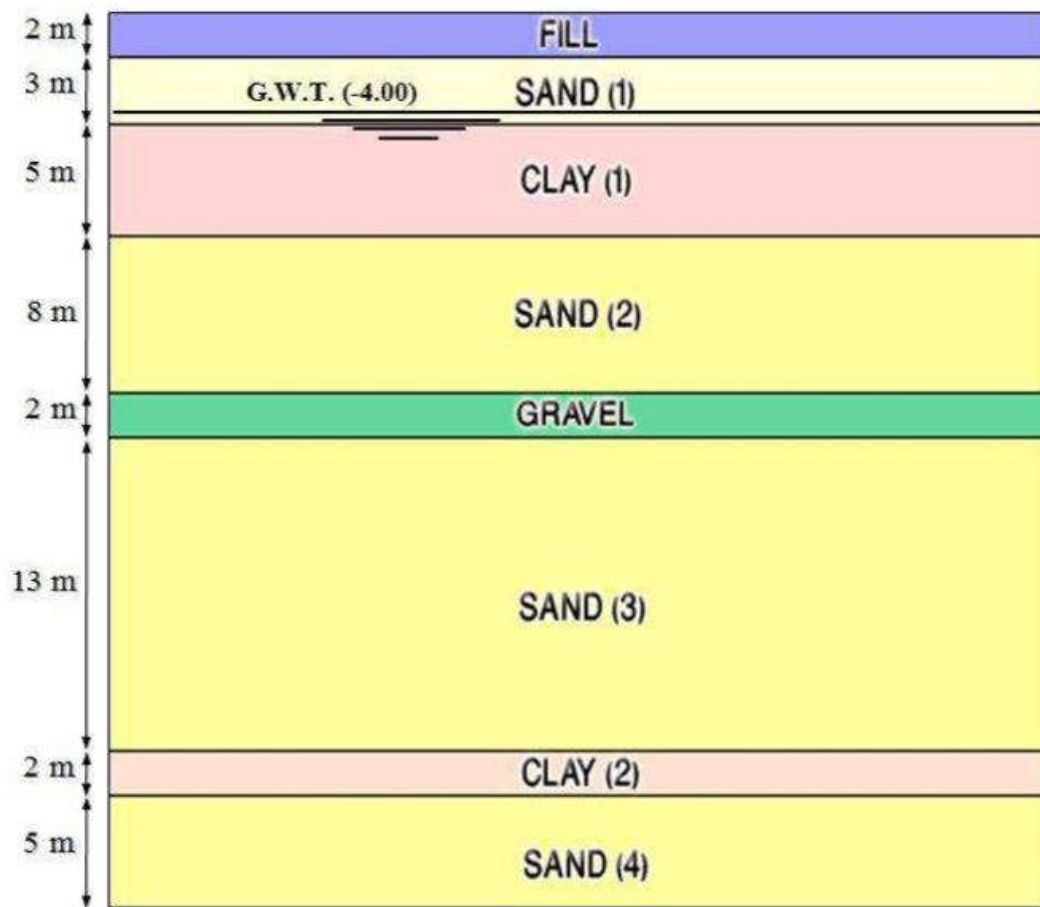


Figure 4.8: Geotechnical soil layers (Kilany et al. 2017)

Table 4.8: Validation Results of PLAXIS 3D

Type	Kilany et al. (2017) [3D analysis using PLAXIS]	Present Research [PLAXIS 3D]
Maximum Vertical Surface Settlement (mm)	8.53	8.54

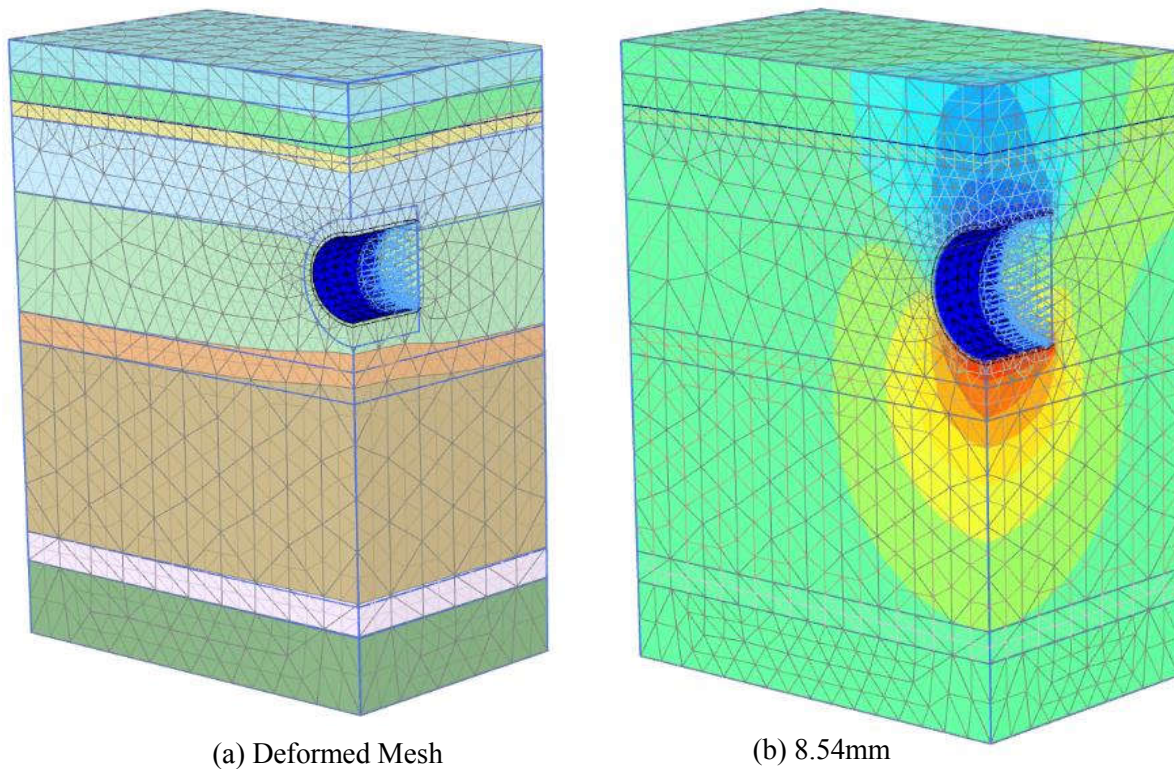


Figure 4.9: PLAXIS 3D model of validation paper

4.9 COMPARISON AMONG PLAXIS 2D AND MODIFIED FORMULAE RESULTS WITH PLAXIS 3D RESULTS

4.9.1 Comparison between PLAXIS 2D and PLAXIS 3D Results

A case study was performed by salimi et. al. 2013 which was located in Sanat square in the route of seventh line (w7 section) of Tehran subway in Iran. This case study was performed by numerically in PLAXIS 2D. In this research, compare PLAXIS 2D results with PLAXIS 3D results.

Tunnelling method was Earth Pressure Balance Tunnel Boring Machine (EPB – TBM). Shield length and machine weight were 9m and 1250ton. Inner diameter was 8.29m and thickness of concrete lining segment was 0.35m. In that section, depth of tunnel and water were 16.1m and 6.6m with the unit weight of dry, total and saturation of soil 16.30KN/m³, 19KN/m³ and 20KN/m³ respectively. Loads including the surface weight and traffic load were considered in modelling in terms of distributed loads such as 40Kpa in 16m lengths. Material model was Mohr-Coulomb. It specifications were elastic module (2.25×10^7 kN/m²), axial stiffness (EA) (3.66×10^6 kN/m) and bending stiffness (EI) (3.74×10^4 kN-m).

Table 4.9: Geotechnical specification used for soil layers of the model (Salimi et. al., 2013)

Internal friction angle (degree)	Cohesion (MPa)	Young Module (MPa)	Poisson Ratio	Soil material (BSCS classification)	Soil depth (m)
32.5	29.42	64.74	0.285	CLG/GCL	0-1.7
30	29.42	49.03	0.30	CLG	1.7-4
35	29.42	78.45	0.27	GCL	4-10
32.5	29.42	63.74	0.285	CLG/GCL	10-18
27	39.23	29.42	0.35	CL	18<

Table 4.10: Characteristics of segments (Salimi et. al., 2013)

Density (T/m3)	Poisson Ratio	Unconfined Compression Strength (MPa)	Young Module (GPa)
2.4	0.15	34.32	22.5

Table 4.11: Geotechnical specifications used for soil layers of the model (Salimi et. al., 2013)

Type	Elastic Module (Kpa)	Poisson Ratio	Cohesion (KPa)		Internal Friction Angle		Deep (m)
			Dry	Saturated	Dry	Saturated	
Upper Gravel	40000	0.28	25	20	30	18	4
Gravel and Clay	7845	0.28	29.4	22	30	22	4
Deep Gravel and Clay	6374	0.285	29.4	22.5	27.5	21	27

In present research, used previous paper (Salimi et. al., 2013) data for analysis in PLAXIS 3D. The variation of results is shown in below. PLAXIS 3D model and results are shown in **Figure 4.10**.

Table 4.12: Comparison of PLAXIS 2D results with the help of PLAXIS 3D based on a case study

Types of settlements	Salimi et. al., (2013) [PLAXIS 2D]	Present research [PLAXIS 3D]
Maximum vertical surface settlement	5cm	3.6cm

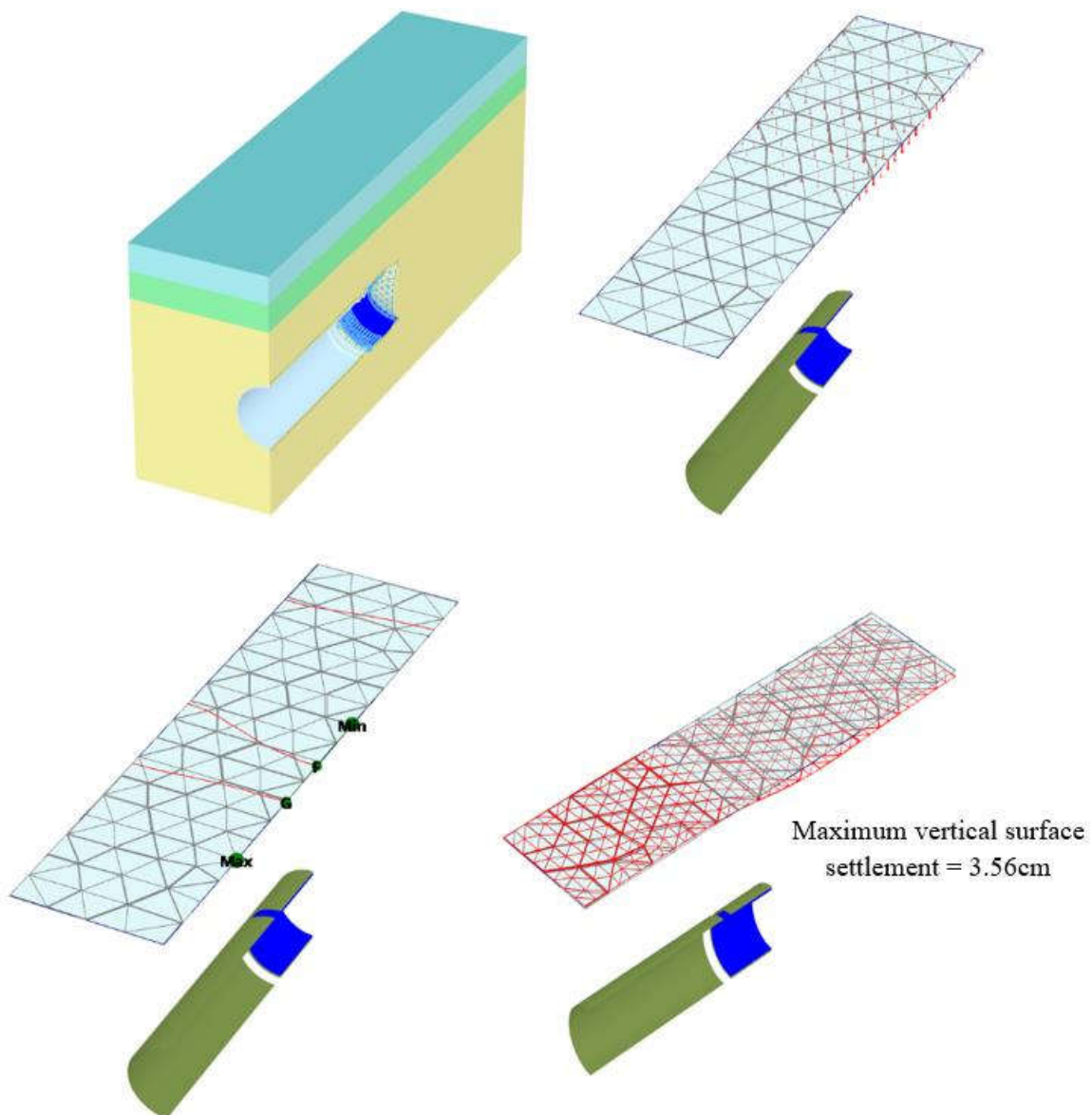


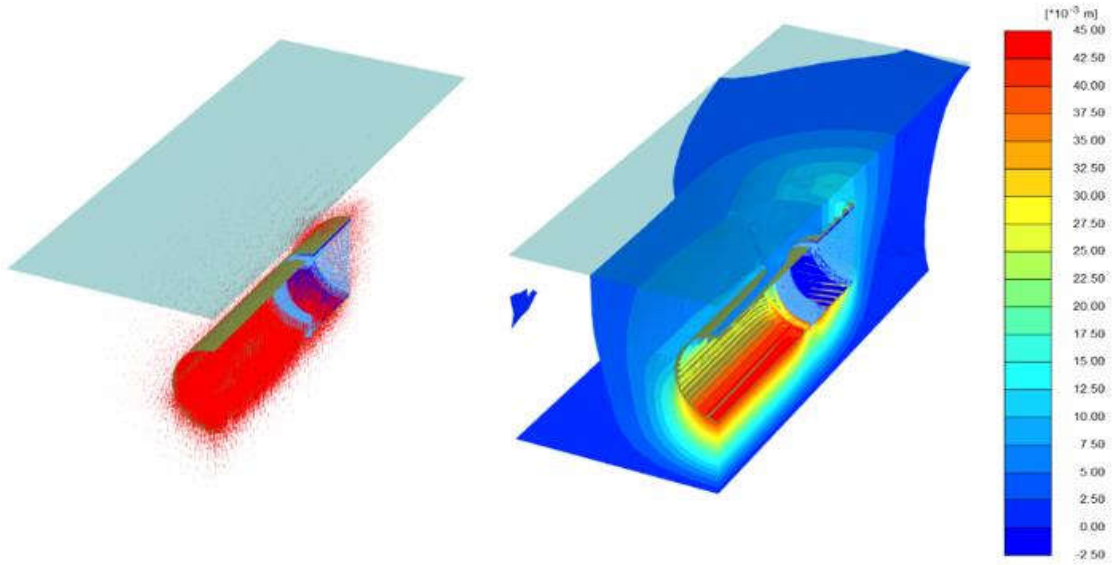
Figure 4.10: Material model and vertical surface settlement of case study paper

4.9.2 Comparison of Modified Formulae Results with PLAXIS 3D Results

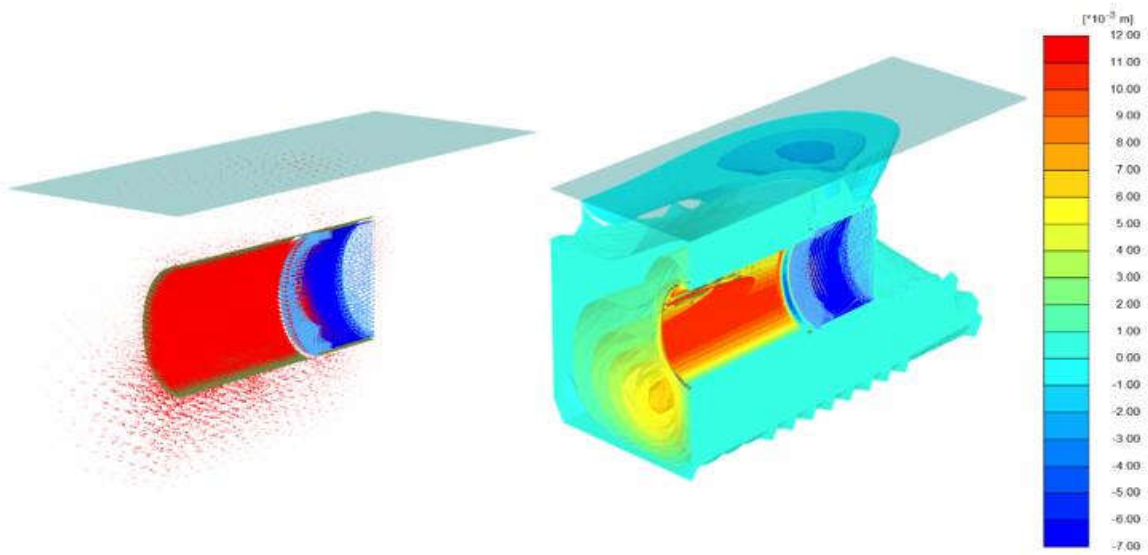
Modified formulae have been developed by considering lot of assumptions. Numerical method gives more accurate results than plain strain analysis. In this research, comparison are performed for modified empirical and analytical formulae with numerical results. Representation of PLAXIS 3D results are shown in **Figure 4.11**.

Table 4.13: Comparison between modified formulae results and PLAXIS 3D results

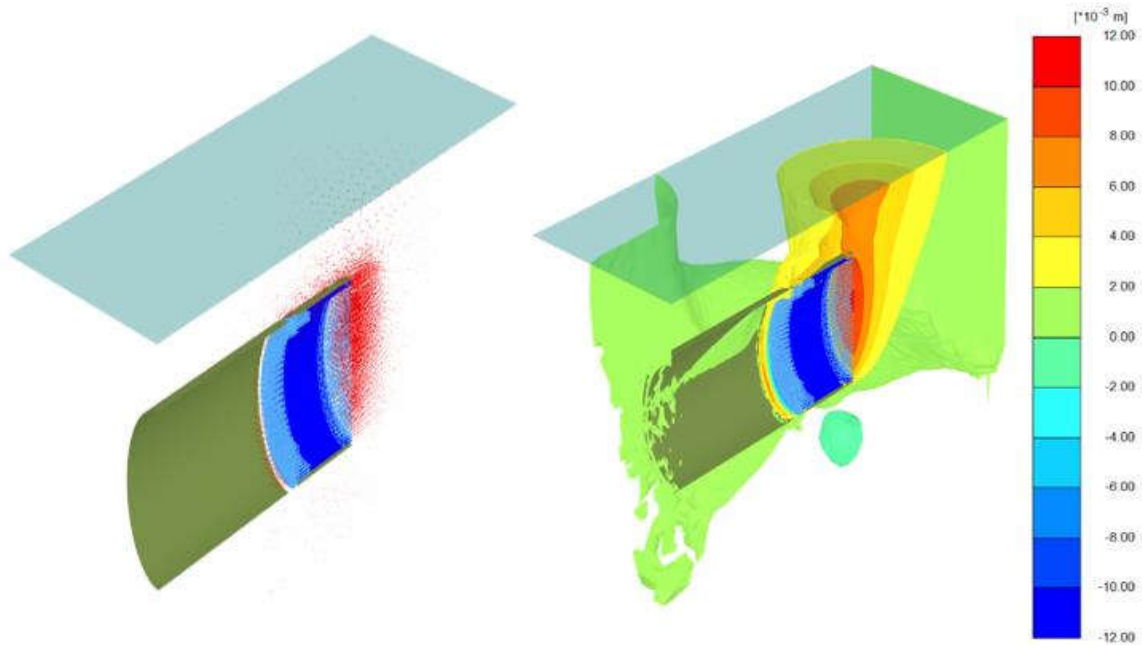
Types of settlements	Results of maximum settlements in (mm)					
	Vertical	Lateral		Longitudi nal	Numerical	
	Modified Analytical Formula – Seismic Loading (Equation, (3.3))	Modified Analytical Formula – Seismic Loading (Equation, (3.7))	Modified Analytical Formula – Long Term Loading (Equation, (3.6))	Modified Empirical Formula – Long Term Loading (Equation, (3.8))	PLAXIS 3D (Long Term Loading)	PLAXIS 3D (Seismic Loading)
Total vertical settlement for diameter, 10.5m at depth of tunnel crown 4.5m	-30				-44	-15
Total lateral settlement for diameter, 10.5m at depth of tunnel crown 4.5m		12	12		12	9
Longitudinal surface settlement for diameter, 10.5m at depth of tunnel crown 4.5m				5.25	6.5	1



(a) Total vertical settlement



(b) Total lateral settlement



(c) Total longitudinal settlement

Figure 4.11: Total settlement for $D_1 = 10.5\text{m}$, $A_1 = 4.5\text{m}$, $y_1 = 27\text{m}$

4.10 RESULTS OF VERTICAL SETTLEMENTS

4.10.1 Vertical Surface Settlements

Numerical results are more accurate than empirical and analytical results because empirical and analytical formulae are developed by considering lot of assumptions. Finite element analysis results are shown in **Figure 4.12**. **Figure 4.13** expresses vertical surface settlements profile. Settlements profiles are maintained symmetric Gaussian curve. Plain strain analysis has not expressed the uplift effects when structures stand on soft soil. Uplift is maximum when length of tunnel is 31m. Diameter, D_2 represents this uplift. Vertical surface settlement is less than 10 mm at A_5 for various diameters. Settlements are match at A_5 for all diameter. Also, A_5 expresses minimum value of settlement for diameter D_1 . This value is 5mm. Settlements jumps are observed some locations such as A_2/D_1 at second construction phase, A_3/D_2 at three construction phases. In these locations, shear strength of sands are much lower than others locations because of various types of loss TBM tunnel. So, soil particles are not sustain external load and suddenly occurs larger settlement either uplift.

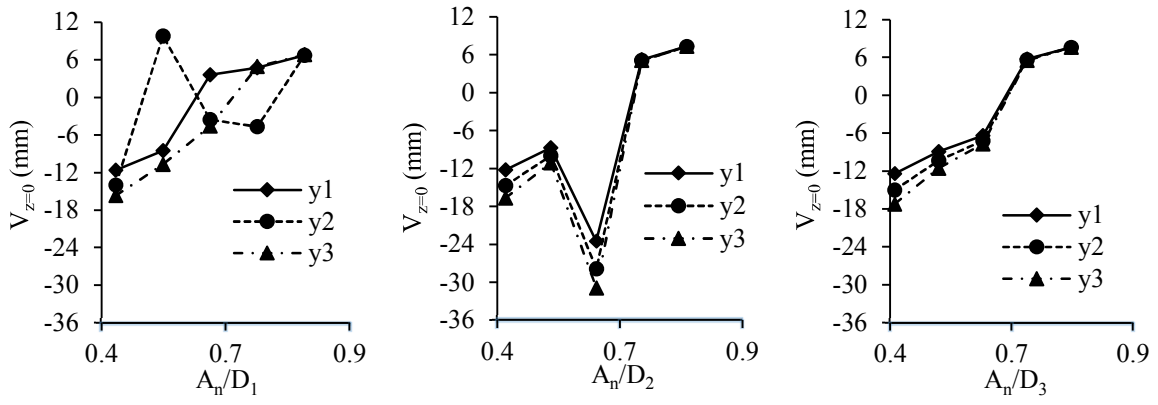
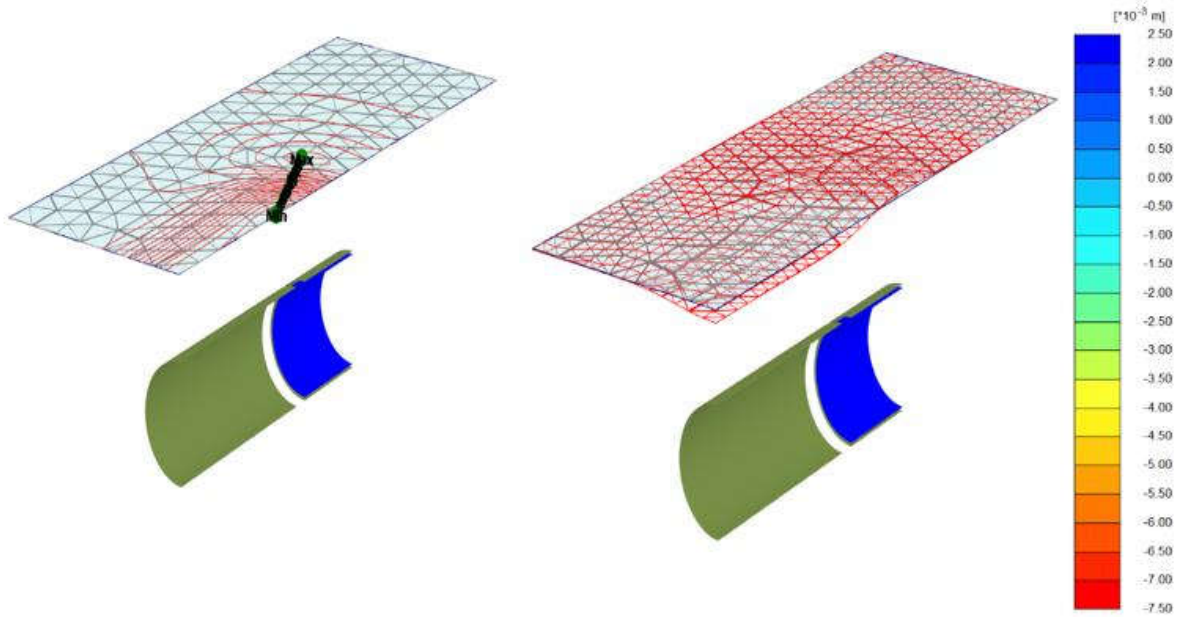
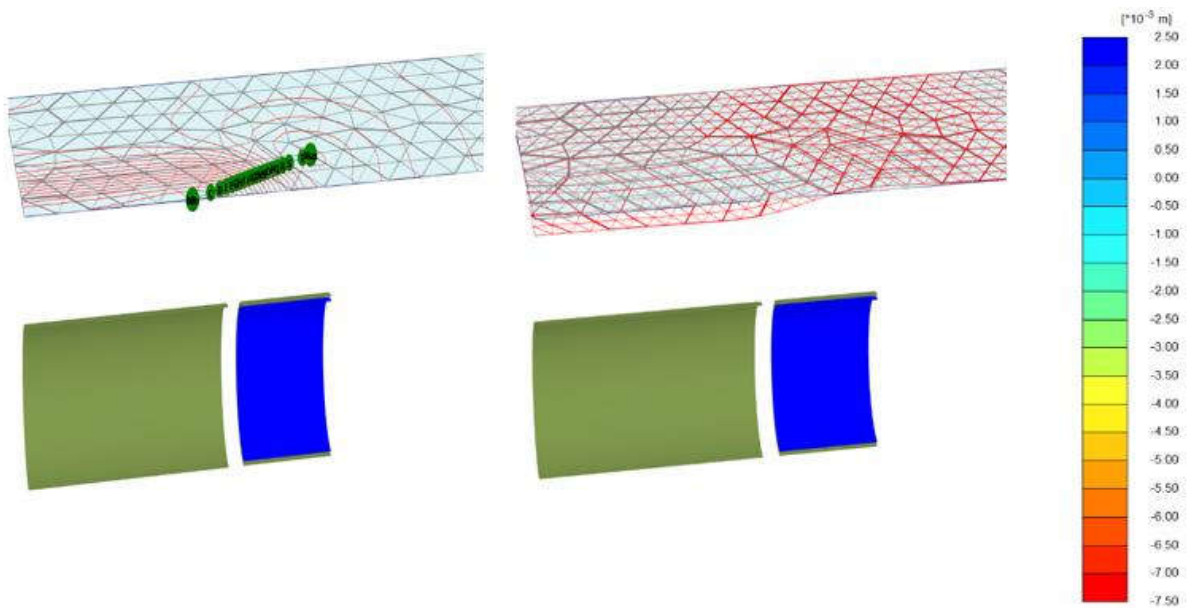


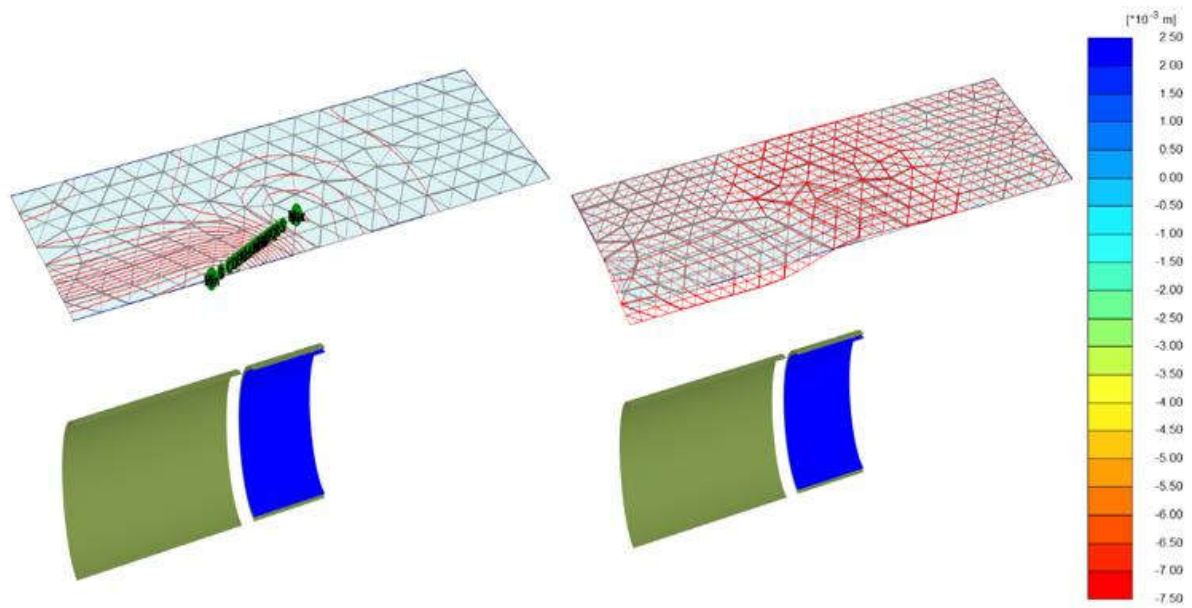
Figure 4.12: Vertical surface settlement for long term loading based on finite element method



(a) Diameter, $D_1 = 10.5\text{m}$



(b) Diameter, $D_2 = 10.8\text{m}$



(c) Diameter, $D_3 = 11.0\text{m}$

Figure 4.13: Vertical surface settlement of long term loading effect for $A_5 = 8.5\text{m}$, $y_1 = 27\text{m}$

Seismic loading is applied along lateral directions of the tunnel in free field conditions. Variation of settlements are shown in **Figure 4.14a** and **Figure 4.15**. Uplift shows when length of tunnel is 31m. Uplift also occurs for two various lengths of tunnel such as 27m and 29m. Minimum value of uplift is less than 3mm at relative depth A_1/D_1 . Minimum value of settlement is 2mm at A_5 for diameter D_1 . **Figure 4.14b** represents vertical surface settlements of various frequencies. Difference of settlements among various seismic frequencies are very low which is 4 percent. This difference is constant along various depths of tunnel crown and diameters. So, in this case liquefaction of soil layers is not occurred during seismic shaking.

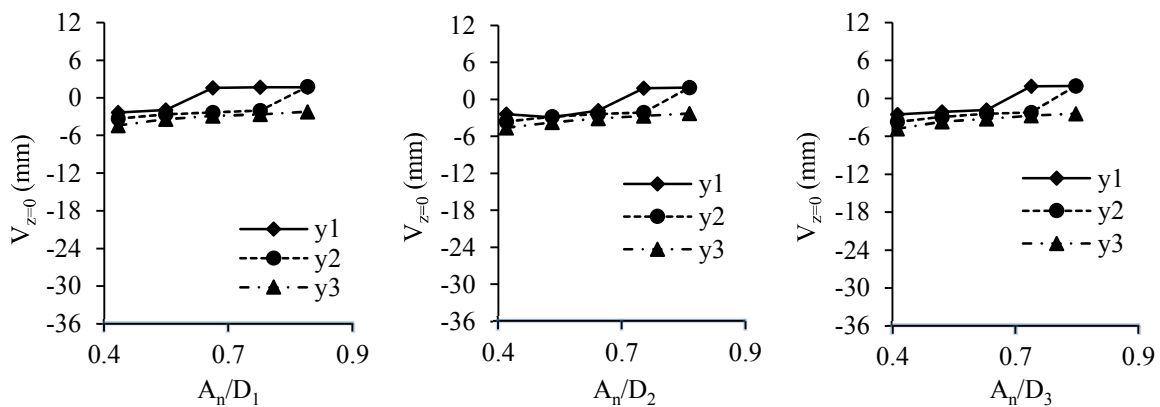


Figure 4.14a: Vertical surface settlement for seismic loading based on finite element method

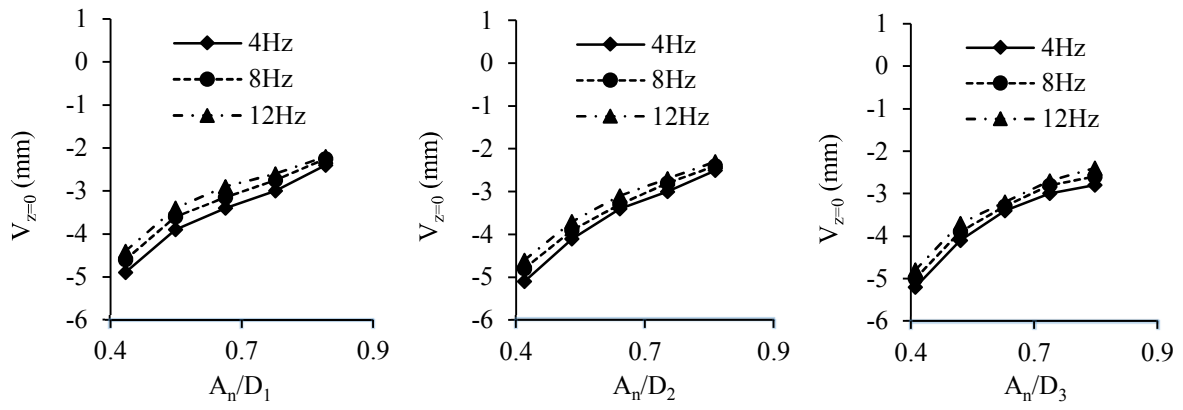
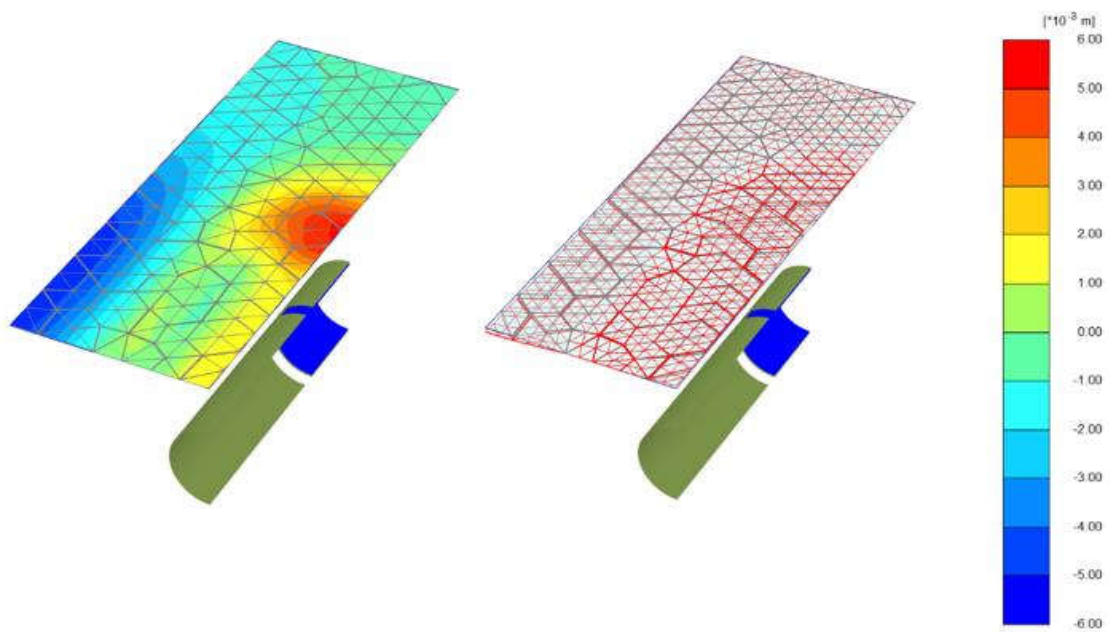
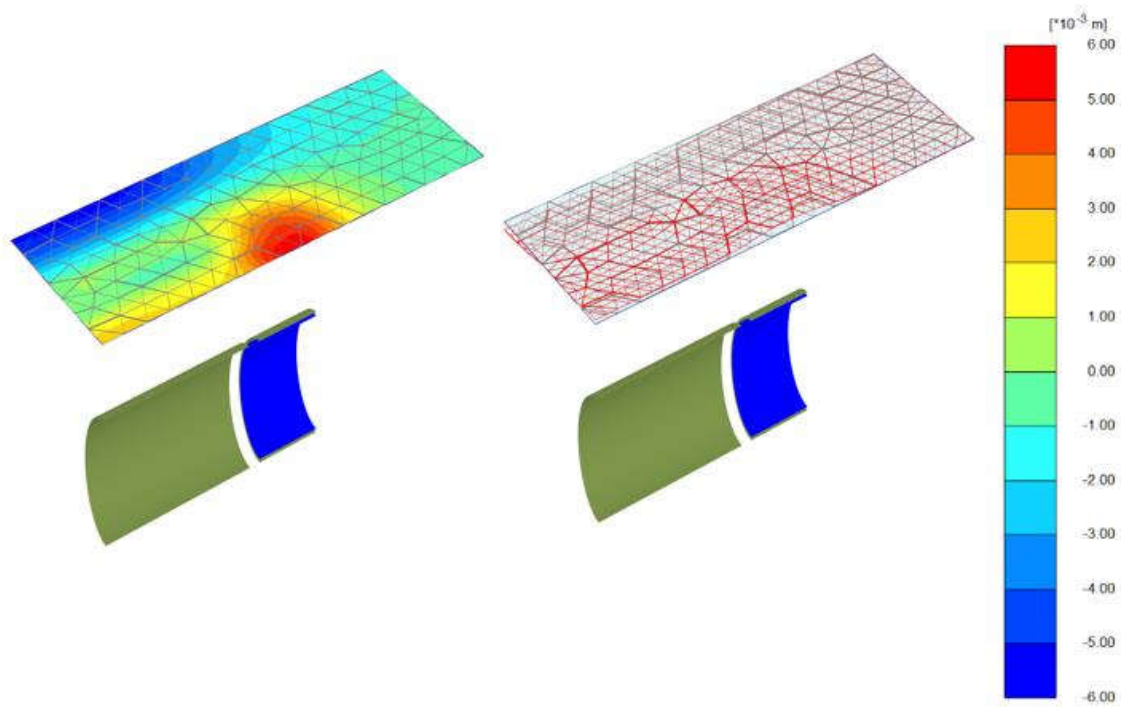


Figure 4.14b: Vertical surface settlements for various frequencies under seismic loading

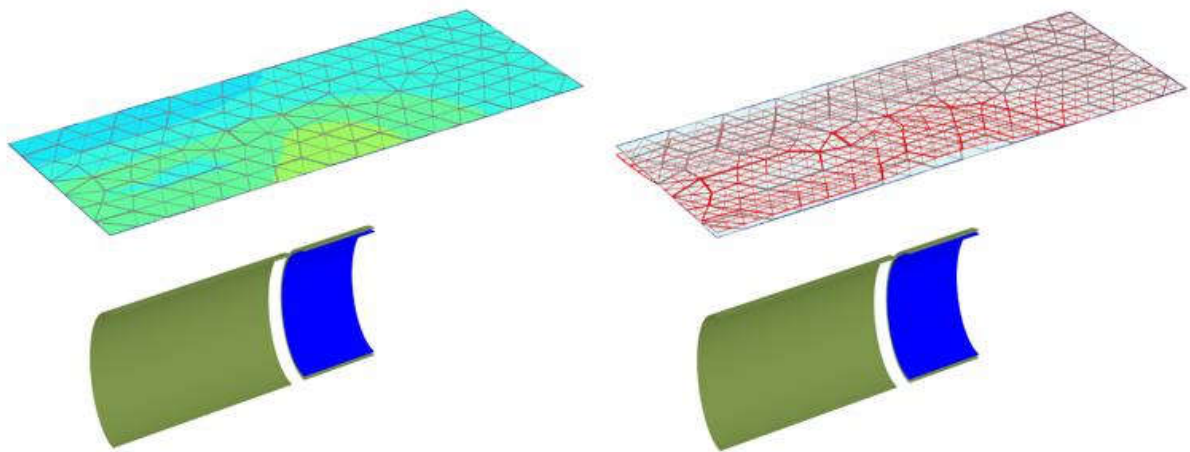
Figure 4.15 represents vertical surface settlements profiles. These settlements curve do not maintain symmetric Gaussian curve. Also, settlements are observed at opposite side from tunnel alignment.



(a) Diameter, $D_1 = 10.5\text{m}$



(b) Diameter, $D_2 = 10.8\text{m}$



(c) Diameter, $D_3 = 11.0\text{m}$

Figure 4.15: Vertical surface settlement of seismic loading effect for $A_4 = 7.5\text{m}$, $y_1 = 27\text{m}$

4.10.2 Total Vertical settlement

Plain strain analysis can't described the length variations of tunnel. Numerical analysis results are described in **Figure 4.16**, **Figure 4.17**, **Figure 4.18** and **Figure 4.19**. **Figure 4.16** represents results for long term loading and **Figure 4.17** expresses PLAXIS 3D representation. Uplifts occurs static loading for all diameter. Uplift gradually decreases with the increment of relative depths except A_3/D_2 and

A_5/D_3 . Uplift increases with the increment of lengths of tunnel for all diameter. Minimum uplift is 38mm at A_5/D_1 .

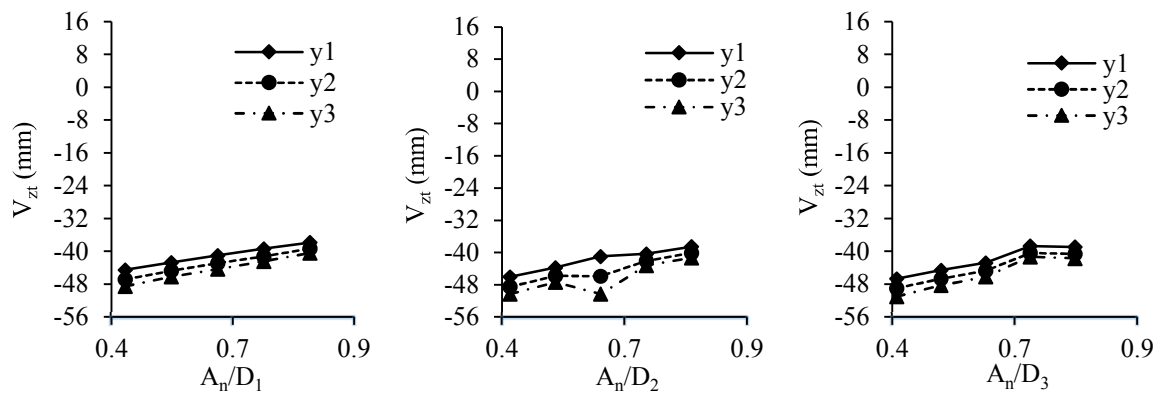
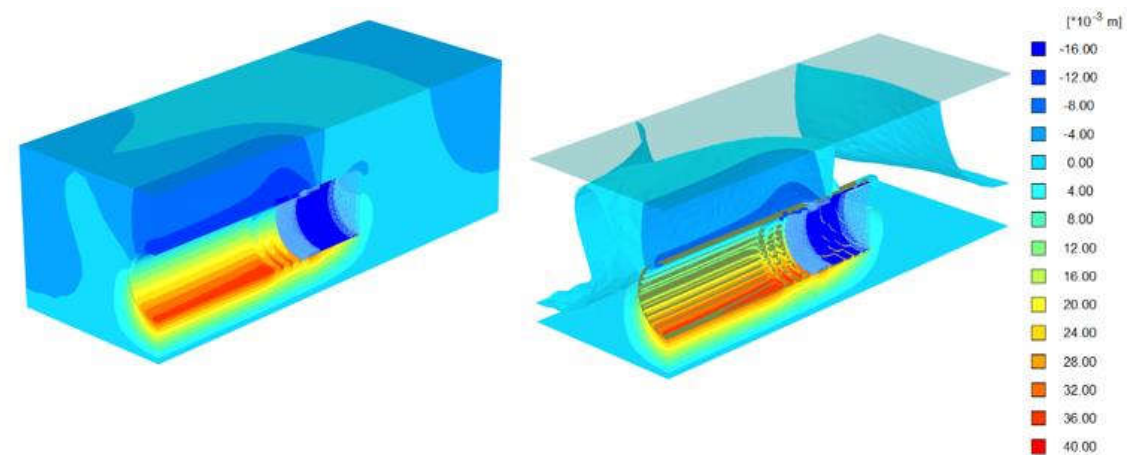
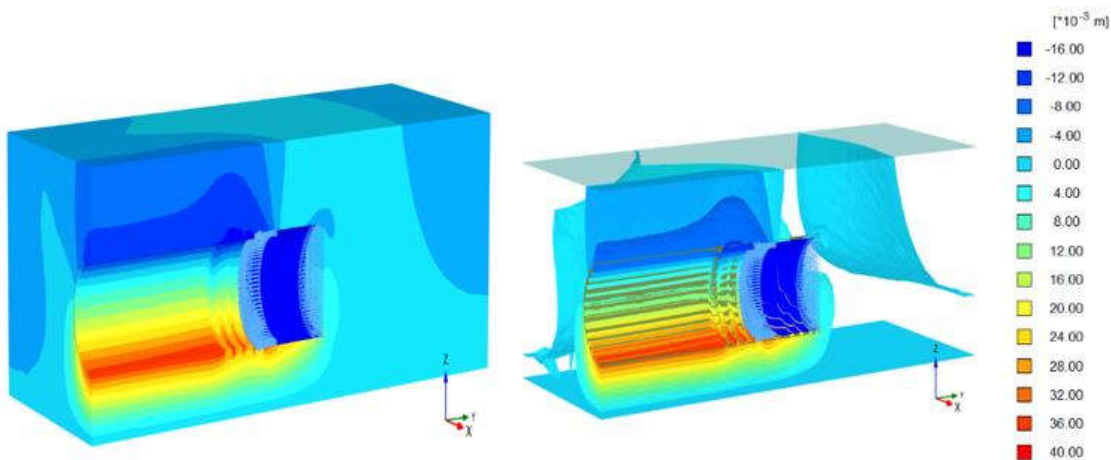


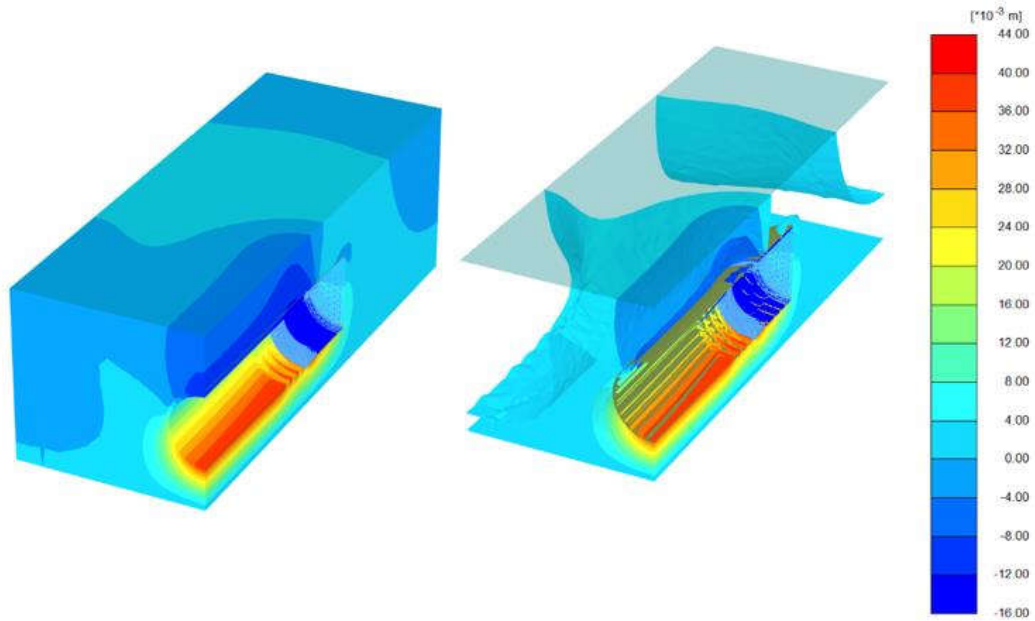
Figure 4.16: Total vertical settlement for long term loading based on finite element method



(a) Diameter, $D_1 = 10.5\text{m}$



(b) Diameter, $D_2 = 10.8\text{m}$



(c) Diameter, $D_3 = 11.0\text{m}$

Figure 4.17: Total vertical settlement of long term loading effect for $A_5 = 8.5\text{m}$, $y_3 = 31\text{m}$

Completing static analysis, seismic analysis is performed. Settlements are recorded at various locations of tunnel as shown in **Figure 4.18**. **Figure 4.19** represents total vertical settlements profiles for all diameter. These profiles are formed under seismic loading. Settlements are expressed by two various lengths of tunnel such as 27m and 29m. Settlements are decreasing gradually for diameter D_2 and D_3 when lengths of tunnel are 27m and 29m. Minimum uplift is nearly 8mm at A_5/D_1 . Minimum settlement is nearly 7mm at A_4/D_3 .

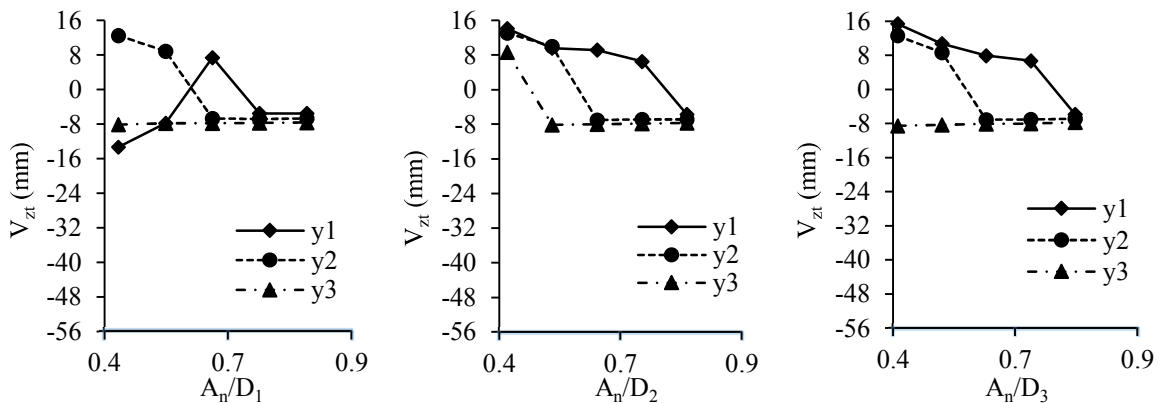
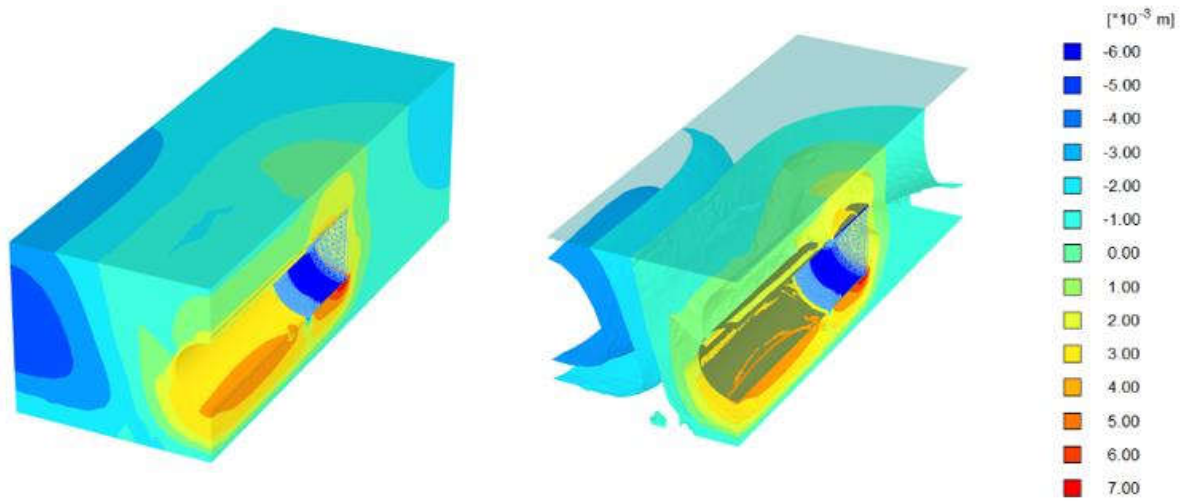
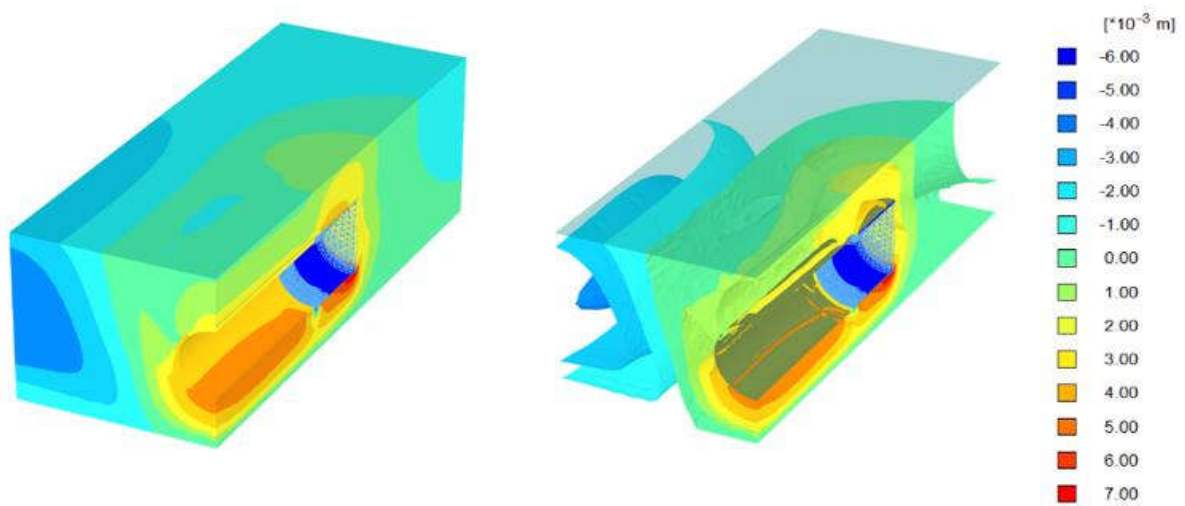


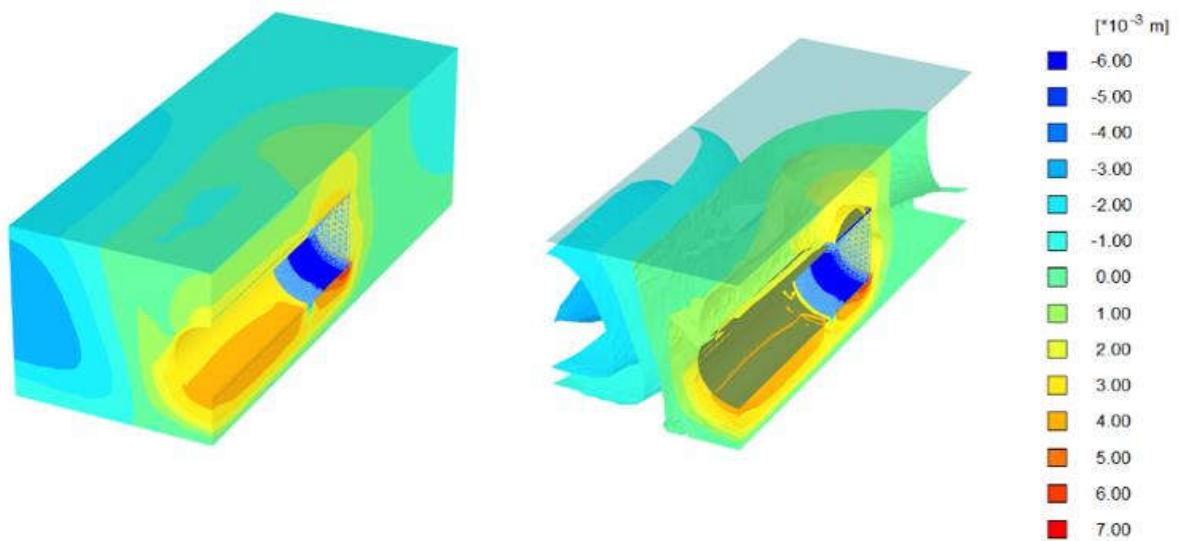
Figure 4.18: Total vertical settlement for seismic loading based on finite element method



(a) Diameter, $D_1 = 10.5\text{m}$



(b) Diameter, $D_2 = 10.8\text{m}$



(c) Diameter, $D_3 = 11.0\text{m}$

Figure 4.19: Total vertical settlement of seismic loading effect for $A_4 = 7.5\text{m}$, $y_1 = 27\text{m}$

4.11 RESULTS OF LATERAL SETTLEMENTS

4.11.1 Lateral Surface Settlement

Figure 4.20 represents lateral surface settlements for long term loading. Figure 4.21 represents settlements profiles. PLAXIS 3D gives these settlements profiles. Settlements are increasing with the increment of relative depths. Maximum settlement is 14mm at A_3/D_2 . One direction settlements are increasing with the increment of lengths of tunnel. Another direction settlements are decreasing with the increment of lengths of tunnel. Minimum settlement is 2.5mm at A_5/D_1 . Settlements jumps are observed at A_3/D_2 for three construction phases. In this locations, shear strength of sands are much lower than others locations because of various types of loss TBM tunnel. So, soil particles are not sustain external load and suddenly occurs larger settlement.

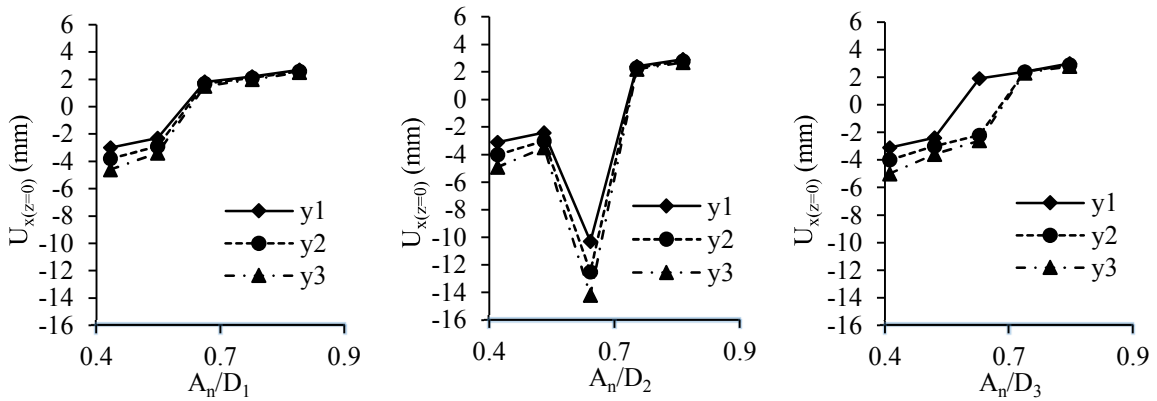
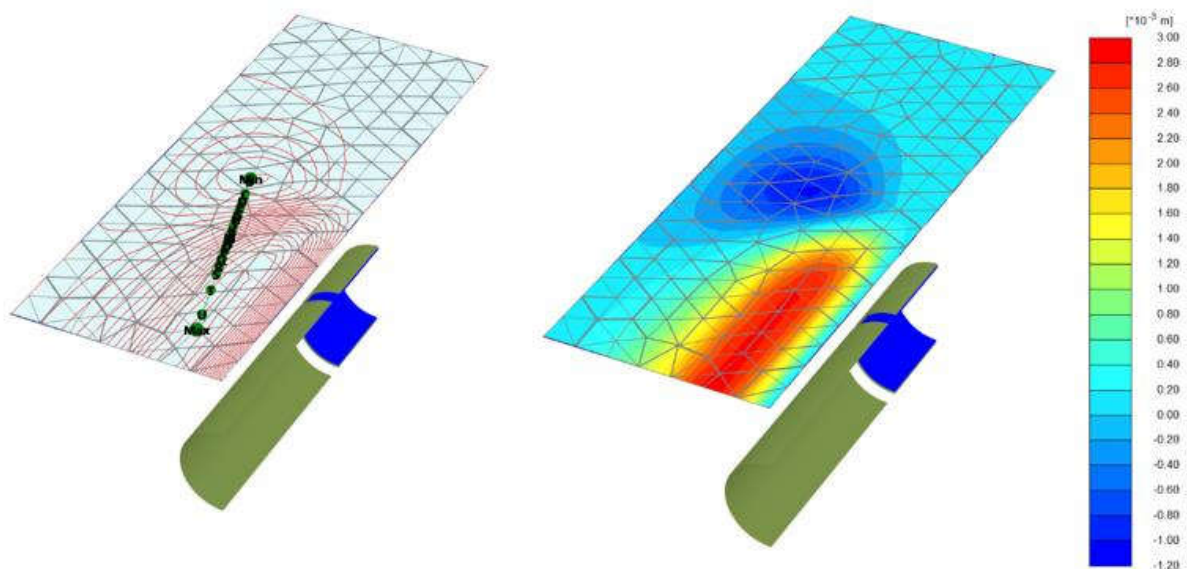
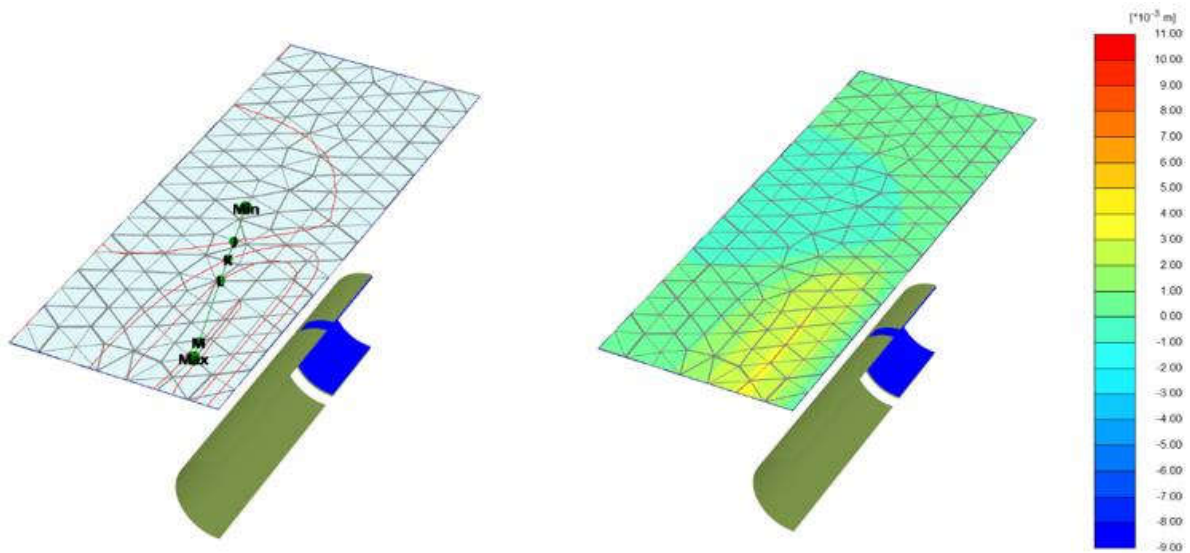


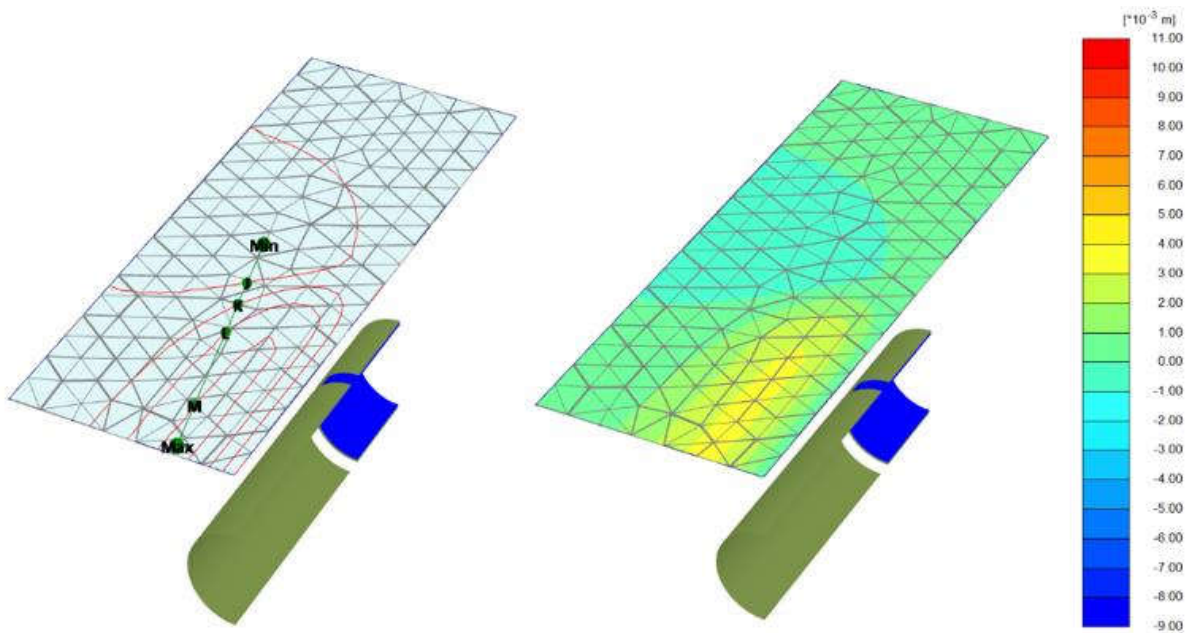
Figure 4.20: Lateral surface settlement for long term loading based on finite element method



(a) Diameter, $D_1 = 10.5\text{m}$



(b) Diameter, $D_2 = 10.8\text{m}$



(c) Diameter, $D_3 = 11.0\text{m}$

Figure 4.21: Lateral surface settlement of long term loading effect for $A_5 = 8.5\text{m}$, $y_3 = 31\text{m}$

Seismic shaking is provided in software after long term loading. Lateral surface settlements are shown in **Figure 4.22a**. **Figure 4.23** expresses PLAXIS 3D representation. Lateral settlements are nearly constant for all length and diameter of tunnel. Minimum lateral settlement is 1.8mm at A_5/D_1 . Settlements are similar for all length of tunnel. Settlements are almost constant with the increment of relative depths. **Figure 4.22b** represents lateral surface settlements of various frequencies. Difference of settlements among various seismic frequencies are very low which is 4.8 percent. This difference is constant along various depths of tunnel crown and dimeters. So, in this case liquefaction of soil layers is not occurred during seismic shaking.

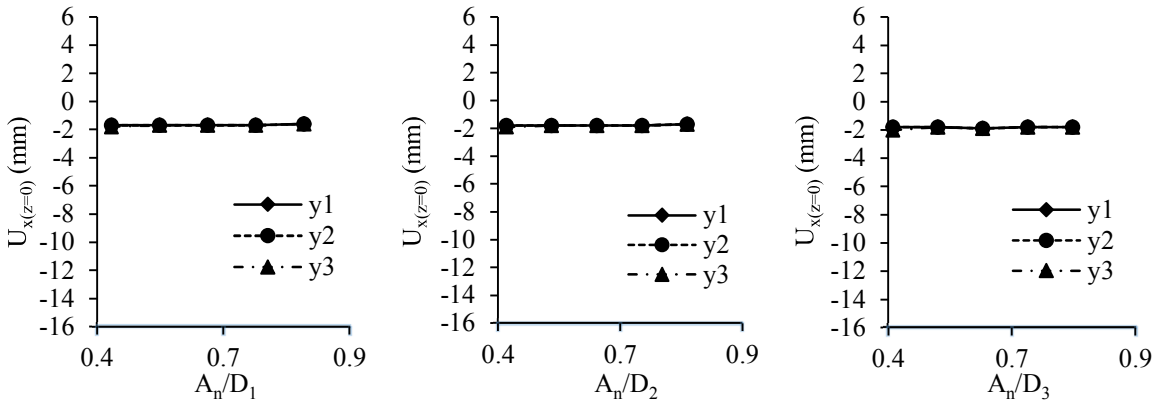


Figure 4.22a: Lateral surface settlement for seismic loading based on finite element method

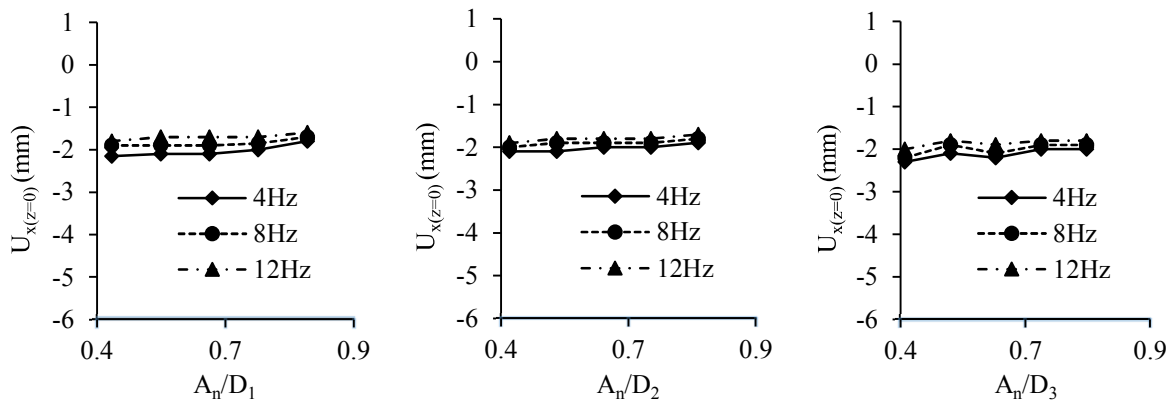
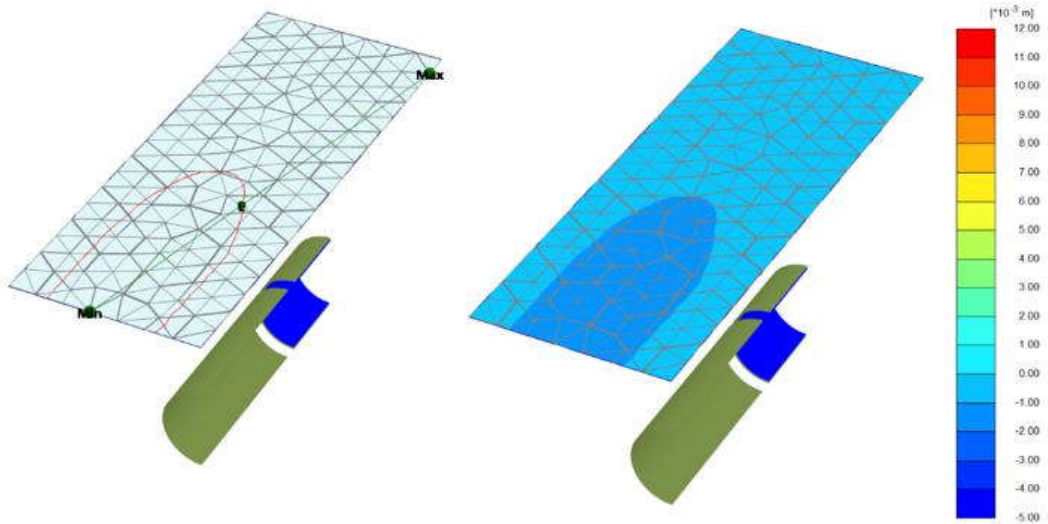
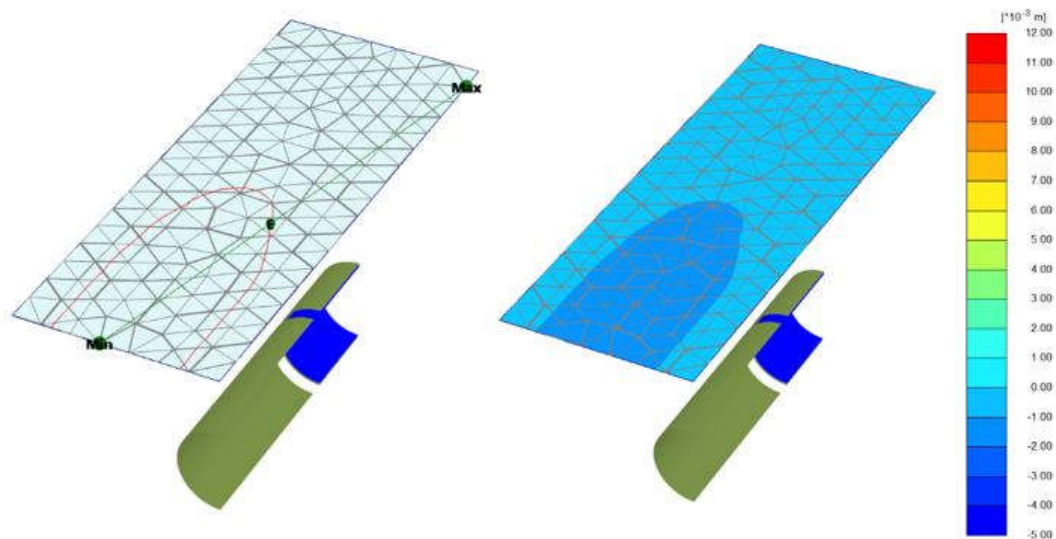


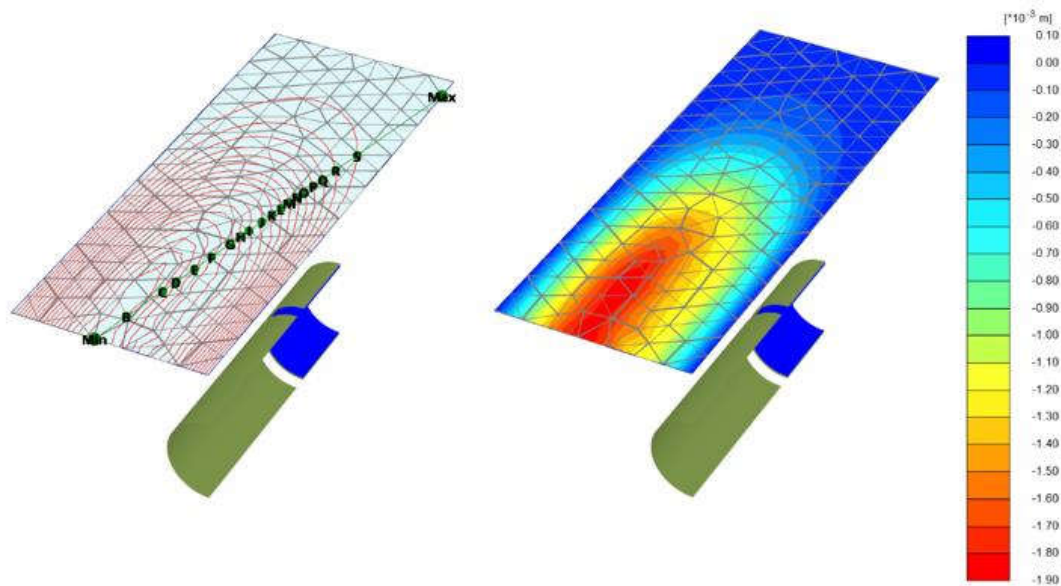
Figure 4.22b: Lateral surface settlements for various frequencies under seismic loading



(a) Diameter, $D_1 = 10.5\text{m}$



(b) Diameter, $D_2 = 10.8\text{m}$



(c) Diameter, $D_3 = 11.0\text{m}$

Figure 4.23: Lateral surface settlement of seismic loading effect for $A_5 = 8.5\text{m}$, $y_3 = 31\text{m}$

4.11.2 Total Lateral Settlement

Variation of lengths of tunnel are called phased construction. Phased constructions are influenced by lateral movements. Variations of lateral settlements are shown in **Figure 4.24**. **Figure 4.25** expresses PLAXIS 3D representation. Red zone of soil cluster indicates maximum settlements of tunnel. Total lateral settlements are decreasing gradually with the increment of relative depths except some points such as A_3/D_2 , A_4/D_2 . Settlements are match at A_3/D_1 . Fluctuation of settlements are observed for diameter D_2 . Minimum total lateral settlement is 10mm at A_5/D_1 . Settlements jumps are observed some locations such as A_5/D_2 at third construction phase, A_3/D_2 at three construction phases. In these

locations, shear strength of sands are much lower than others locations because of various types of loss TBM tunnel. So, soil particles are not sustain external load and suddenly occurs larger settlement.

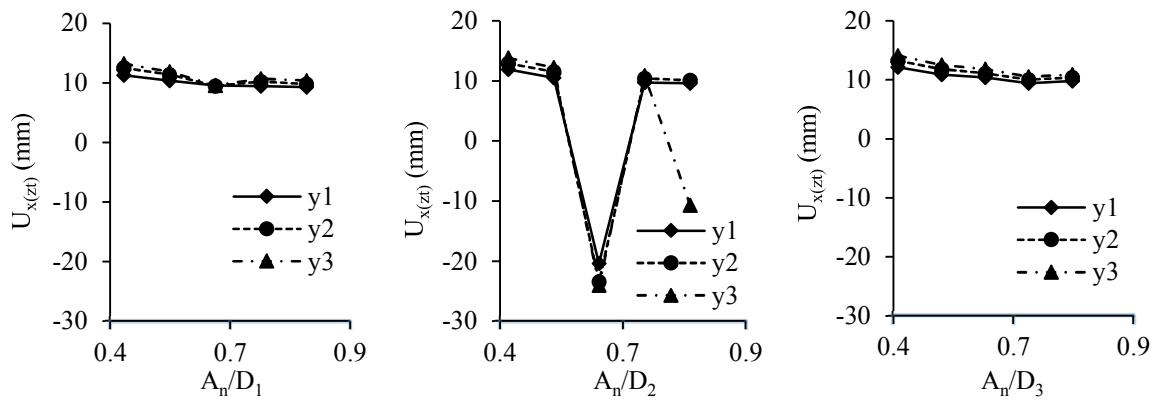
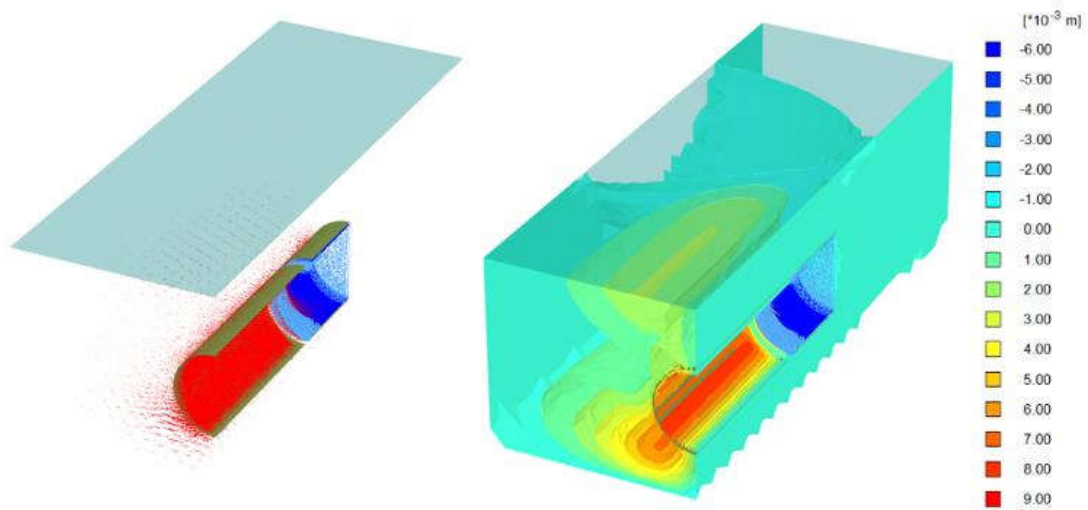
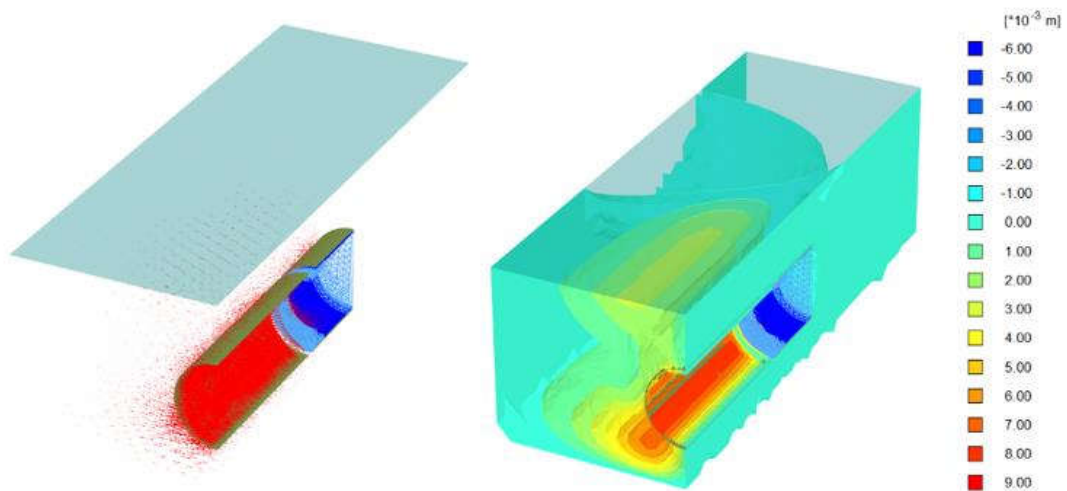


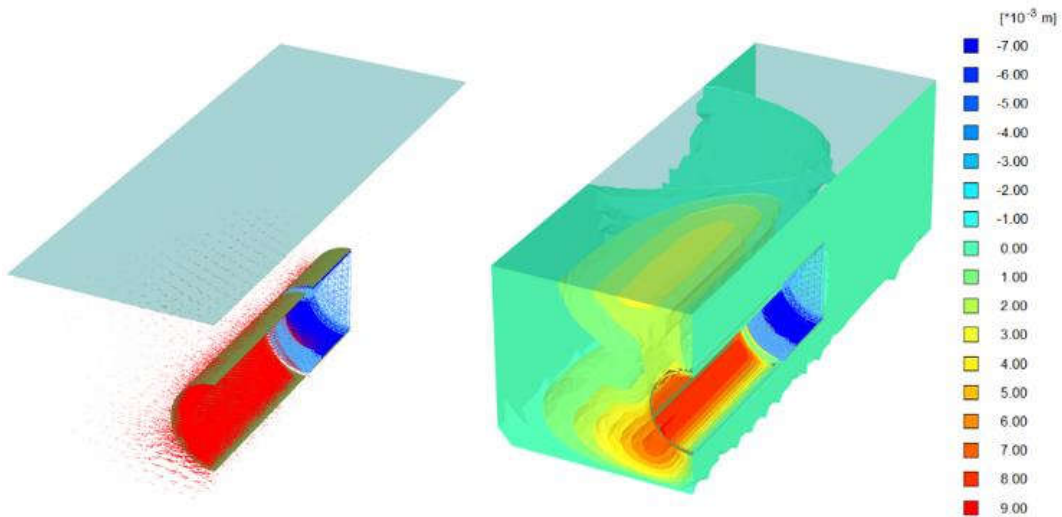
Figure 4.24: Total lateral settlement for long term loading based on finite element method



(a) Diameter, $D_1 = 10.5\text{m}$



(b) Diameter, $D_2 = 10.8\text{m}$



(c) Diameter, $D_3 = 11.0\text{m}$

Figure 4.25: Total lateral settlement of long term loading effect for $A_5 = 8.5\text{m}$, $y_1 = 27\text{m}$

Lateral settlements are occurred by seismic loading. **Figure 4.26** represents total lateral settlements for various diameters and lengths of tunnel. **Figure 4.27** expresses PLAXIS 3D representation. Change of soil cluster are similar for all diameter. Settlements are varied linearly for diameters D_2 and D_3 . For these diameters, settlements are nearly same for variations of lengths of tunnel. Minimum total lateral settlement is 10mm at A_5/D_1 . Settlements jumps are observed some locations at A_3/D_1 for three construction phases. In this locations, shear strength of sands are much lower than others locations because of various types of loss TBM tunnel. So, soil particles are not sustain external load and suddenly occurs larger settlement.

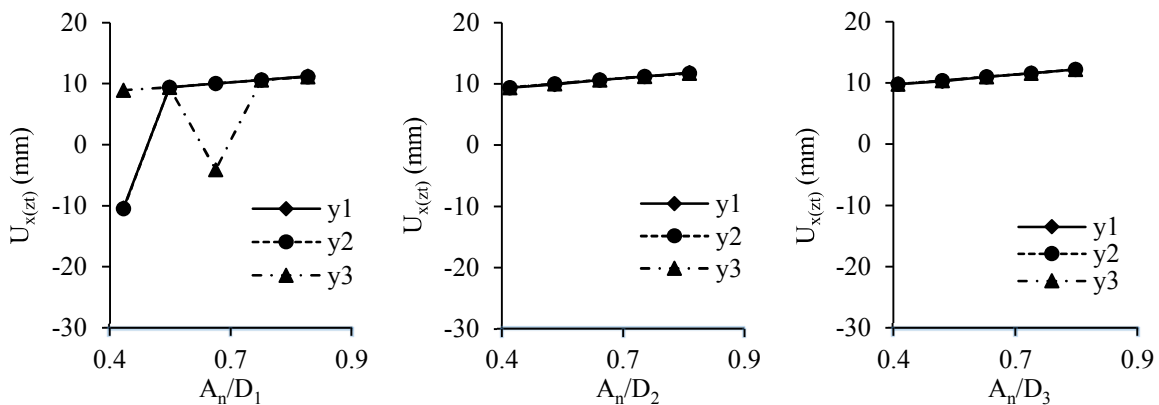
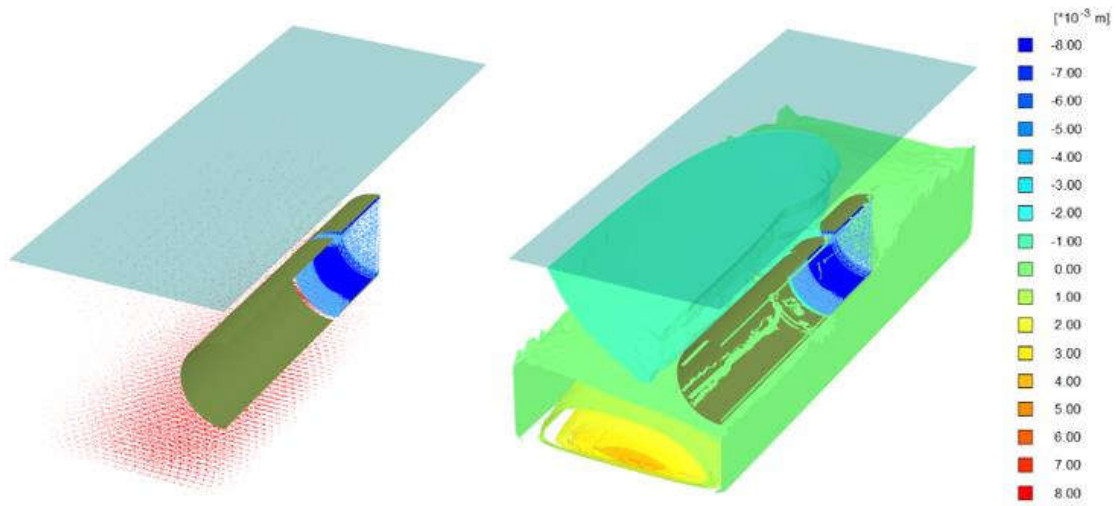
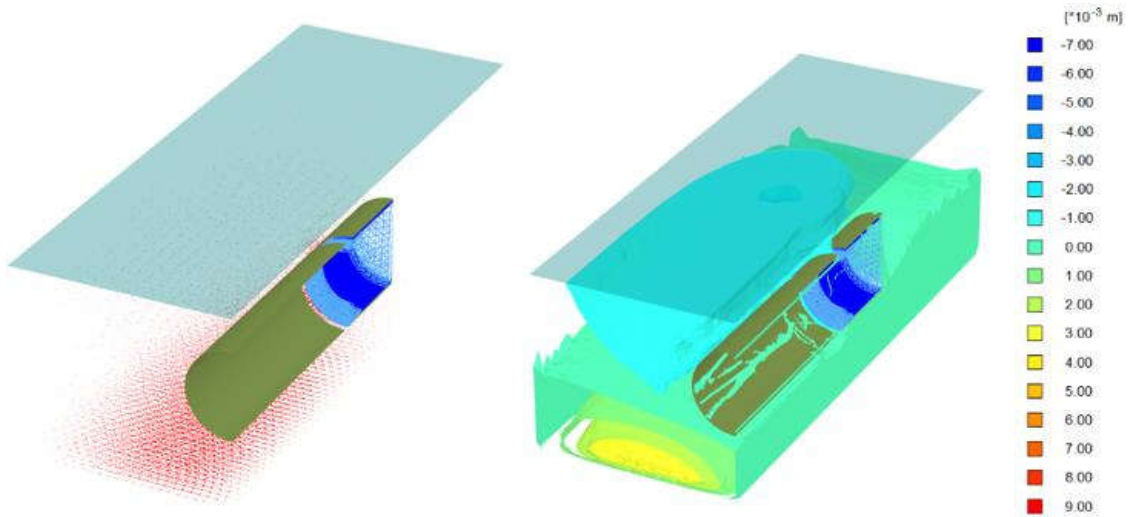


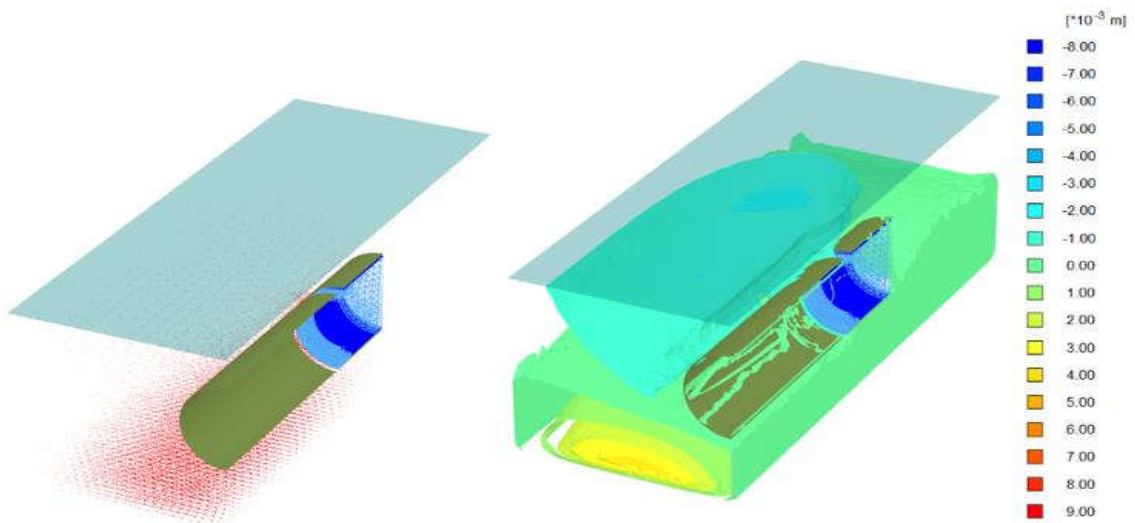
Figure 4.26: Total lateral settlement for seismic loading based on finite element method



(a) Diameter, $D_1 = 10.5\text{m}$



(b) Diameter, $D_2 = 10.8\text{m}$



(c) Diameter, $D_3 = 11.0\text{m}$

Figure 4.27: Total lateral settlement of seismic loading effect for $A_1 = 4.5\text{m}$, $y_3 = 31\text{m}$

4.12 RESULTS OF LONGITUDINAL SETTLEMENTS

4.12.1 Longitudinal Surface Settlement

Modified methods can't describe extension and contraction of length of tunnel. Numerical method expresses extension and contraction of length of tunnel. **Figure 4.28** expresses longitudinal surface settlements for long term (static) loading. Also, **Figure 4.29** expresses PLAXIS 3D representation. Contour line indicates maximum and minimum settlements on surface. Longitudinal settlements are decreasing gradually with the increment of relative depths except some locations. Settlements are decreasing with the increasing of tunnel lengths. Positive settlements called extension and negative settlements called compression. Extension converts compression with the increment of relative depths. Extension means the settlements along the tunnel axis and compression means the settlements along the tunnel axis in reverse direction. Minimum value of extension is 2mm at A_3/D_1 and minimum value of compression is 3.0mm at A_5/D_1 . Compression settlements are more effective than extension settlements. Settlements jumps are observed some locations at A_3/D_2 for three construction phases. In this locations, shear strength of sands are much lower than others locations because of various types of loss TBM tunnel. So, soil particles are not sustain external load and suddenly occurs larger settlement.

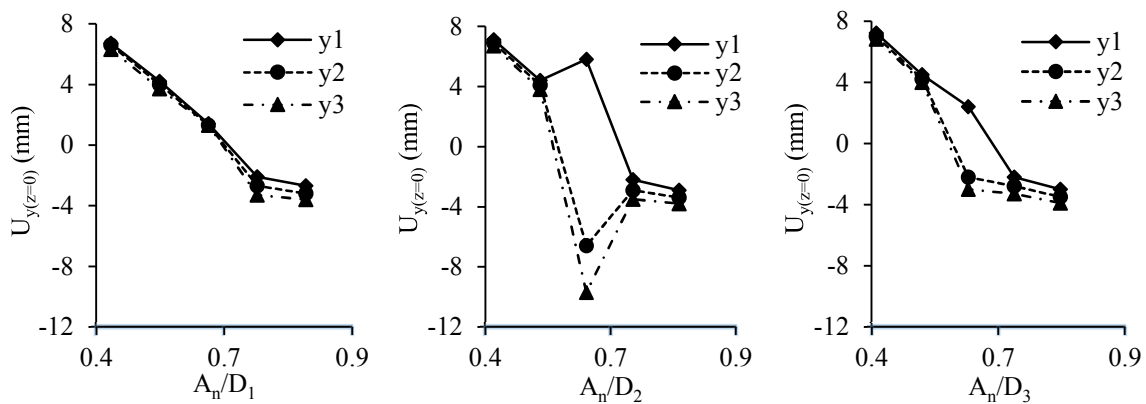
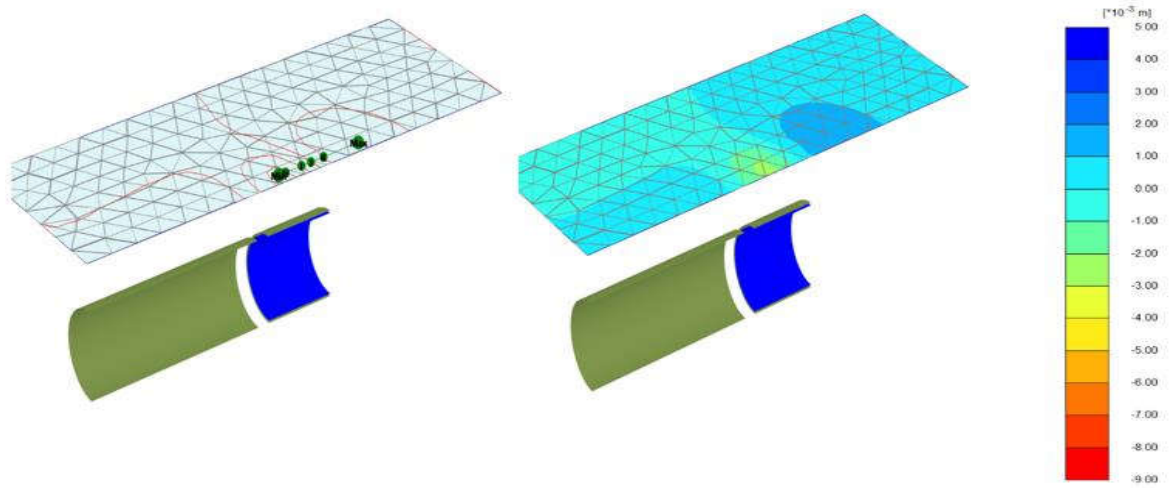
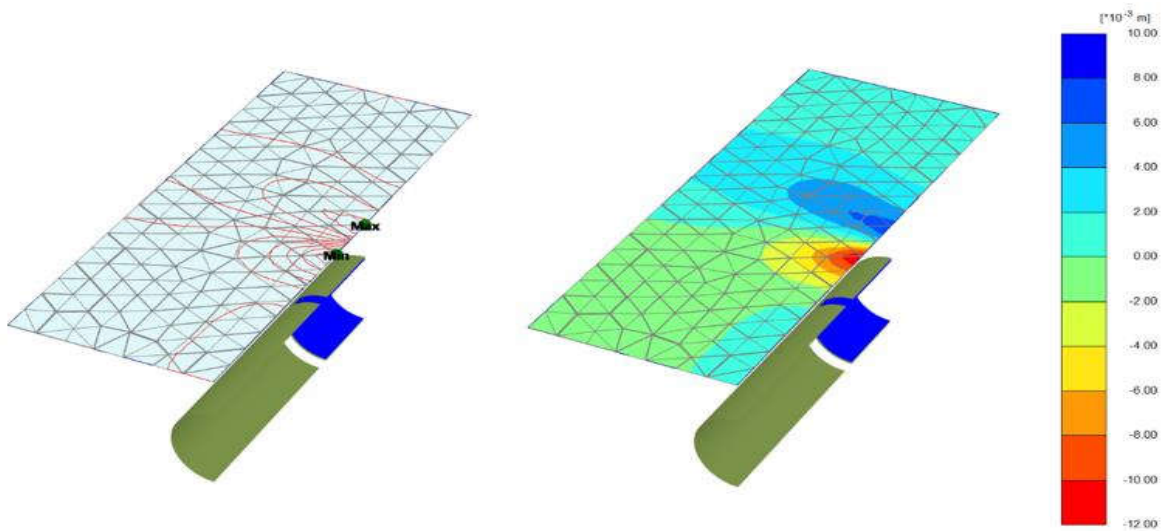


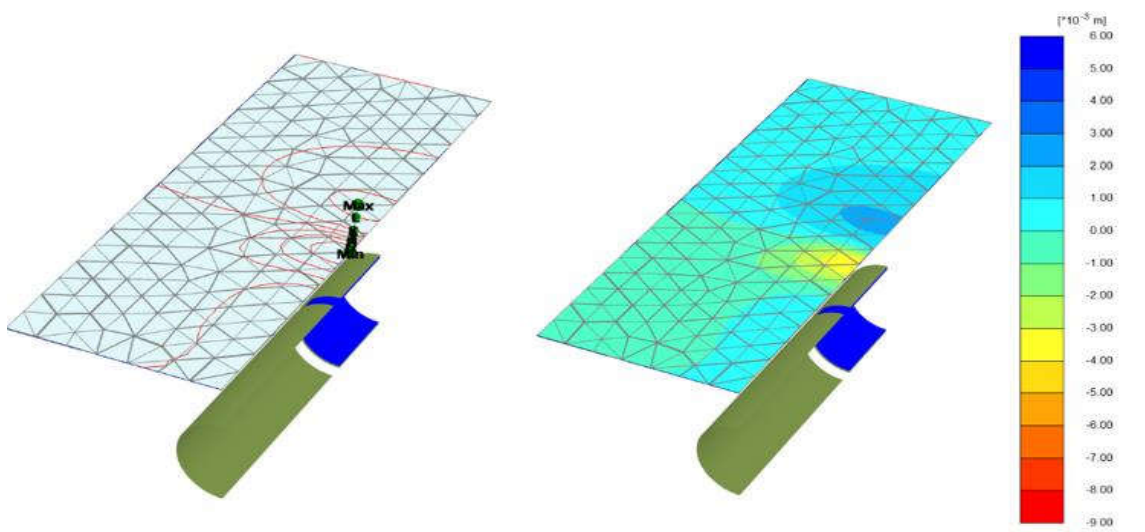
Figure 4.28: Longitudinal surface settlement for long term loading based on finite element method



(a) Diameter, $D_1 = 10.5\text{m}$



(b) Diameter, $D_2 = 10.8\text{m}$



(c) Diameter, $D_3 = 11.0\text{m}$

Figure 4.29: Longitudinal surface settlement of long term loading effect for $A_3 = 6.5\text{m}$, $y_3 = 31\text{m}$

Seismic analysis has necessary to evaluate longitudinal settlements of soil at surface above a tunnel. Longitudinal surface settlements are expressed by **Figure 4.30a**. **Figure 4.31** expresses graphical representation of PLAXIS 3D. Contour line indicates amount of settlements on surface. Longitudinal surface settlements are decreasing gradually with the increment of relative depths of tunnel. Settlements are very close with the variations of lengths of tunnel. Minimum value of compressive longitudinal settlement is 0.2mm at A_5/D_1 . **Figure 4.30b** represents longitudinal surface settlements of various frequencies. Difference of settlements among various seismic frequencies are very low which is 4.8 percent. This difference is constant along various depths of tunnel crown and dimeters. So, in this case liquefaction of soil layers is not occurred during seismic shaking.

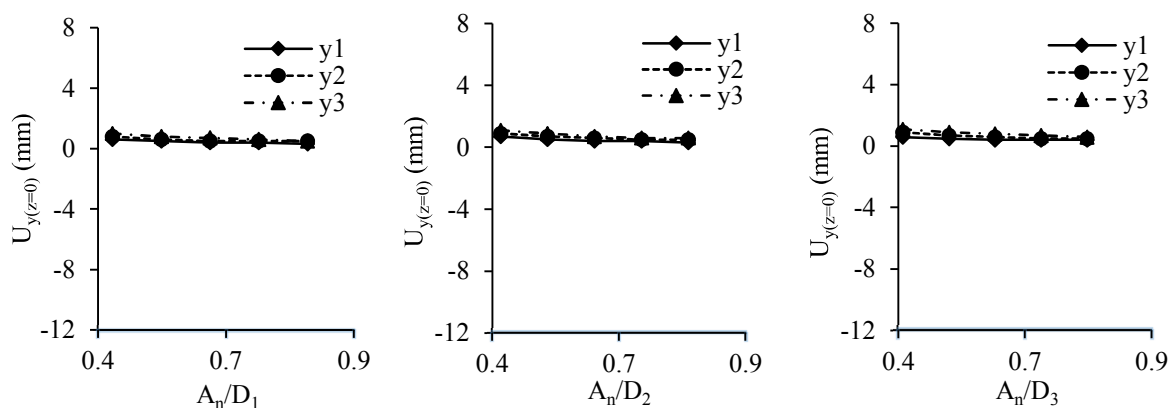


Figure 4.30a: Longitudinal surface settlement for seismic loading based on finite element method

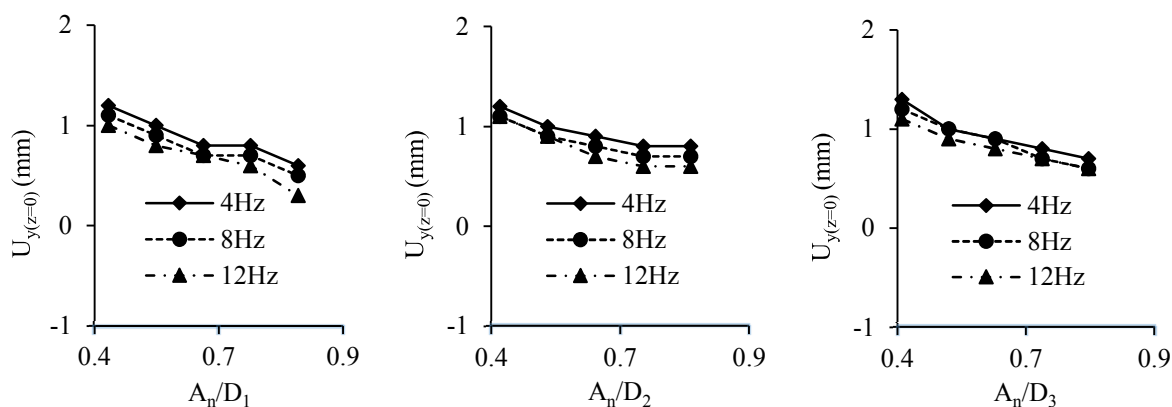
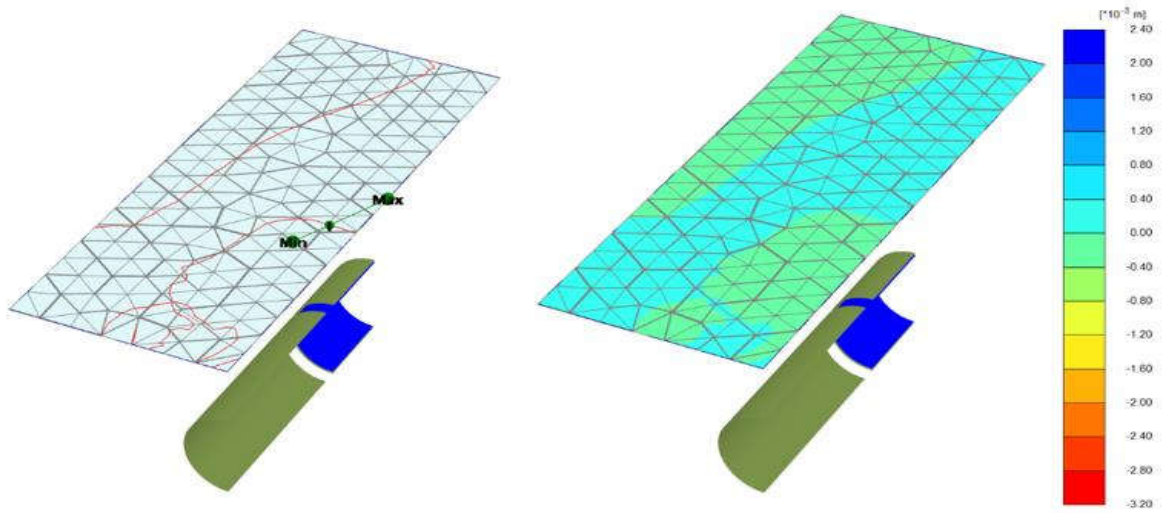
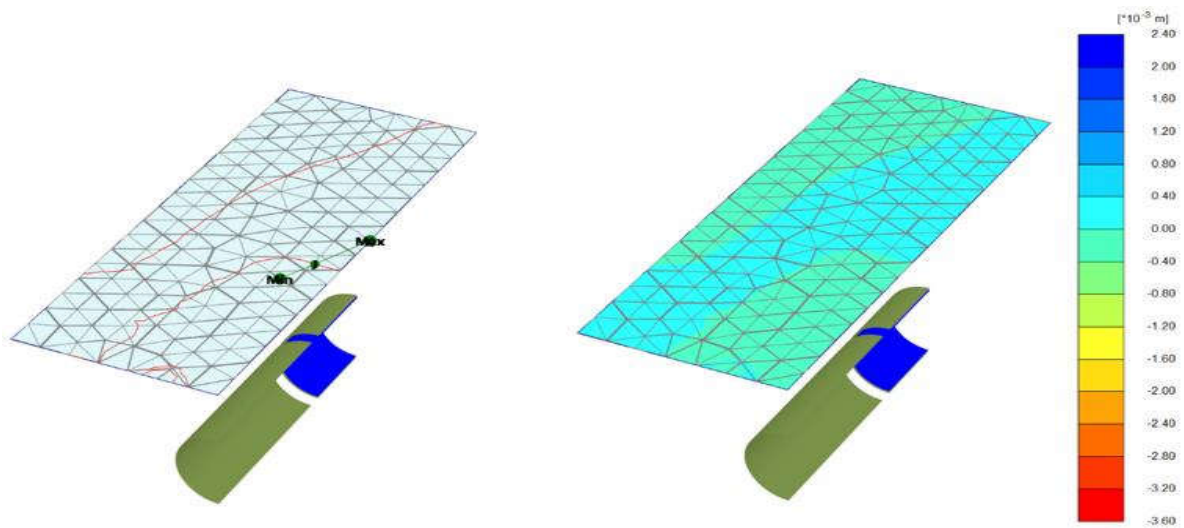


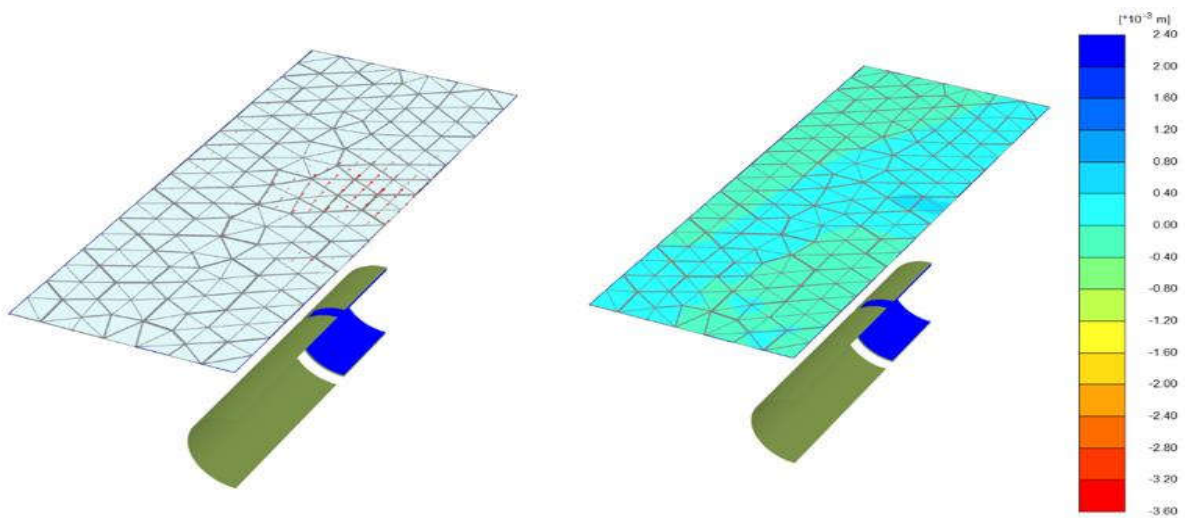
Figure 4.30b: Lateral surface settlements for various frequencies under seismic loading



(a) Diameter, $D_1 = 10.5\text{m}$



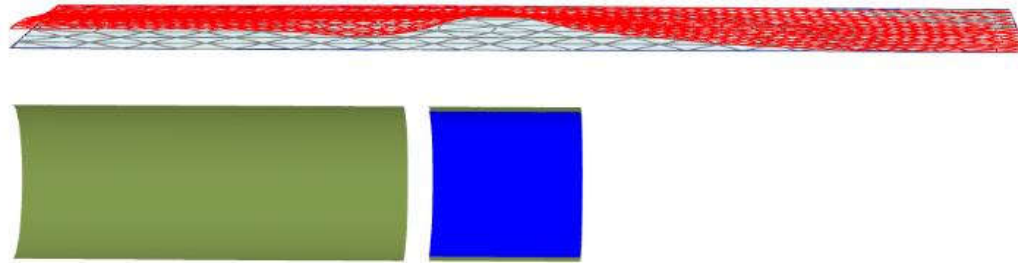
(b) Diameter, $D_2 = 10.8\text{m}$



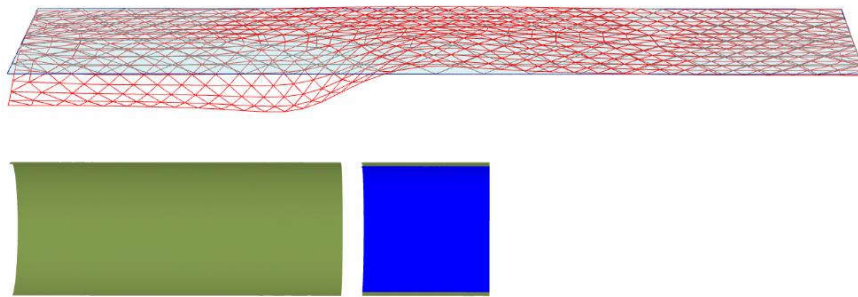
(c) Diameter, $D_3 = 11.0\text{m}$

Figure 4.31: Longitudinal surface settlement of seismic loading effect for $A_5 = 8.5\text{m}$, $y_1 = 27\text{m}$

Figure 4.32 (a) shows the upward settlements along the length of tunnel. These types of settlements occur for presence of upper clay. **Figure 4.32 (b)** shows the settlements which maintains symmetric Gaussian curve.



(a) Uplift along length of tunnel



(b) Settlement along length of tunnel

Figure 4.32: Longitudinal surface settlement profile

4.12.2 Total Longitudinal Settlement

Numerical methods are described the settlements with the variation of relative depths. Numerical methods can be solved the limitation of empirical and analytical formulae. Plain strain analysis can't expresses the compression settlements of tunnel. **Figure 4.33** expresses the total longitudinal settlements of long term (static) loading. PLAXIS 3D representations are shown in **Figure 4.34**. For diameter D_3 , compressive settlements are decreasing with the increment of relative depths except A_5/D_3 . Diameter D_1 and D_2 are expressed settlements due to compression and extension. Minimum settlement due to compression is 11mm at A_5/D_1 . Minimum settlement due to extension is 8mm at A_3/D_2 . Settlements jumps are observed some locations such as A_5/D_1 at second construction phase, A_3/D_2 at first construction phases. In these locations, shear strength of sands are much lower than others locations because of various types of loss TBM tunnel. So, soil particles are not sustain external load and suddenly occurs larger settlement.

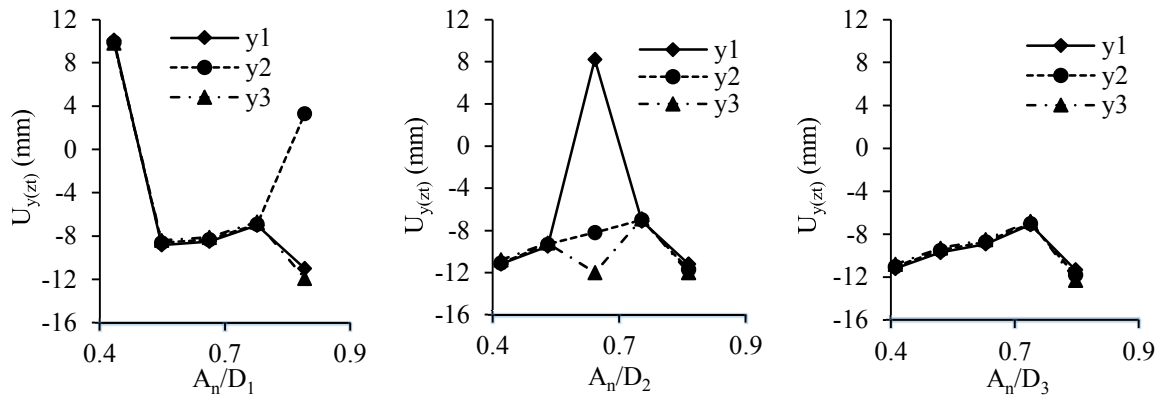
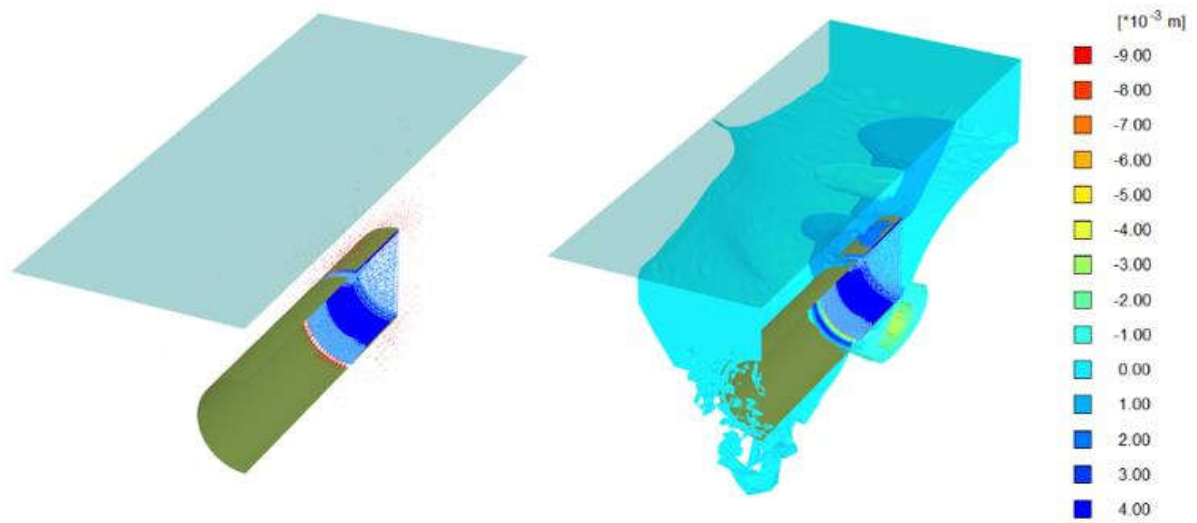
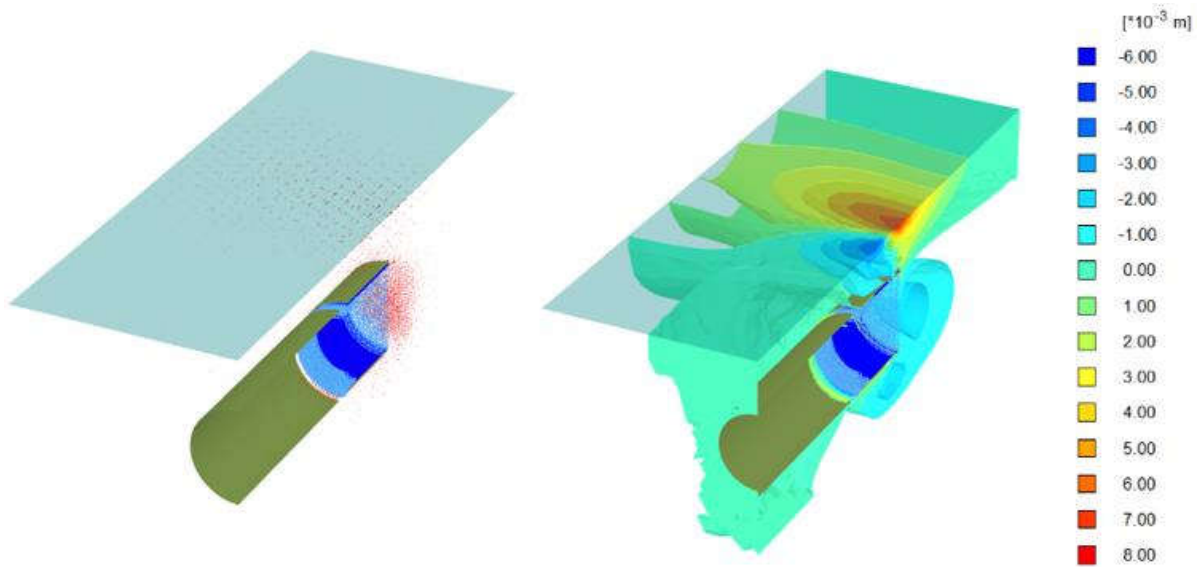


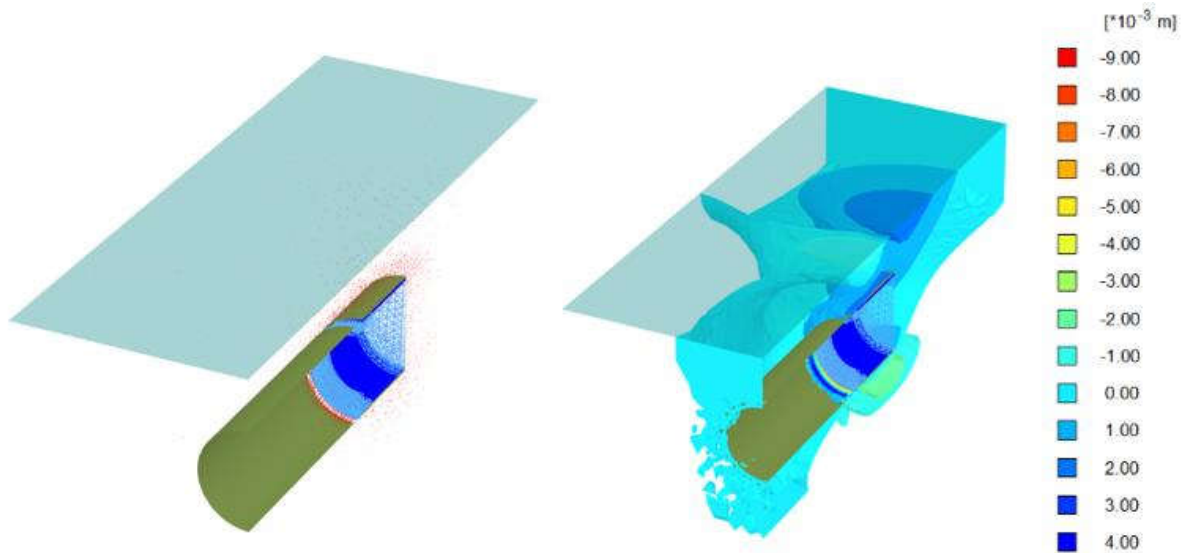
Figure 4.33: Total longitudinal settlement for long term loading based on finite element method



(a) Diameter, $D_1 = 10.5\text{m}$



(b) Diameter, $D_2 = 10.8\text{m}$



(c) Diameter, $D_3 = 11.0\text{m}$

Figure 4.34: Total longitudinal settlement of long term loading effect for $A_3 = 6.5\text{m}$, $y_1 = 27\text{m}$

Total longitudinal settlements under seismic loading are presented by **Figure 4.35**. **Figure 4.36** expresses PLAXIS 3D representation of settlements. Total settlements are decreasing gradually with the variation of relative depths. Minimum settlement due to compression is 3mm at A_5/D_1 . Minimum settlement due to extension is 3mm at A_2/D_1 .

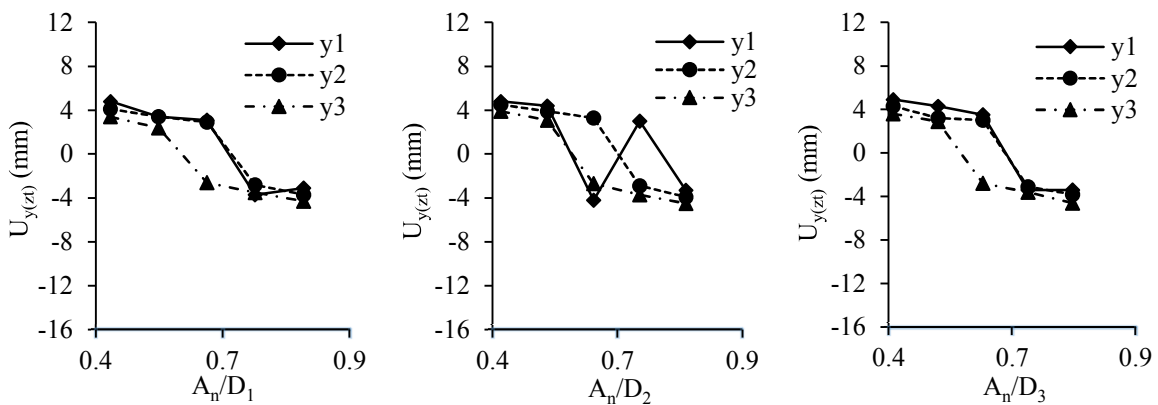
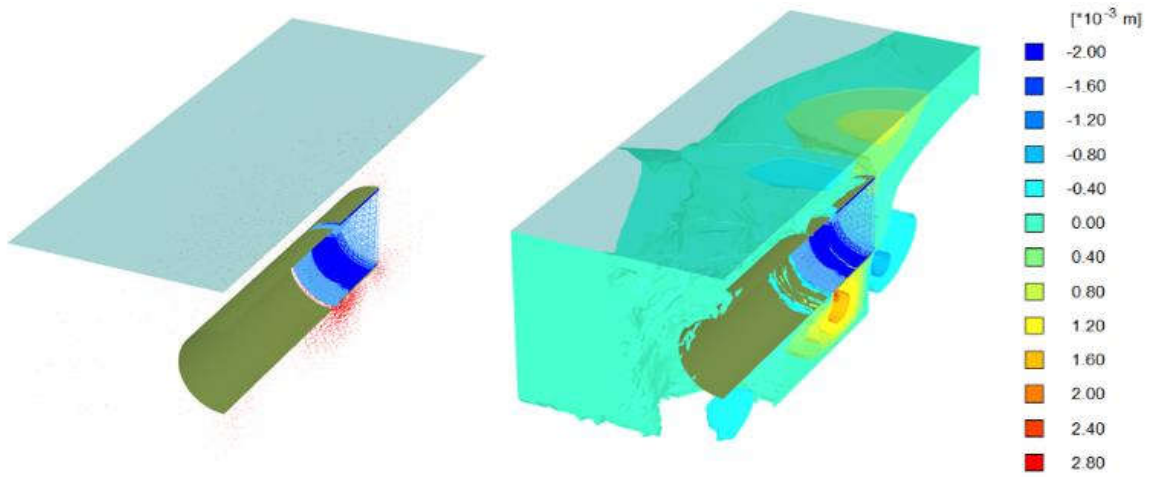
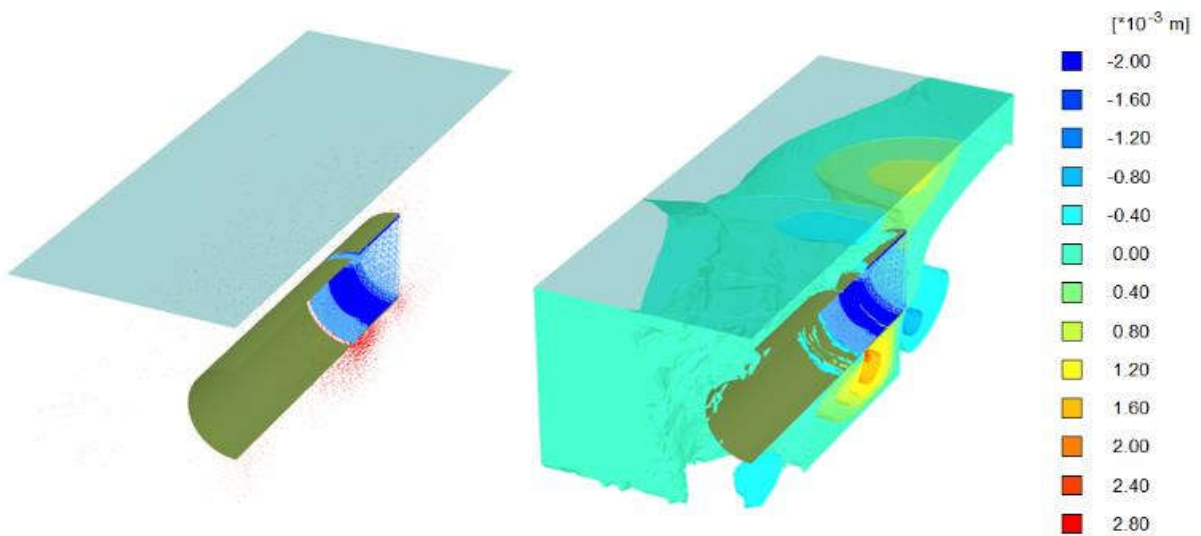


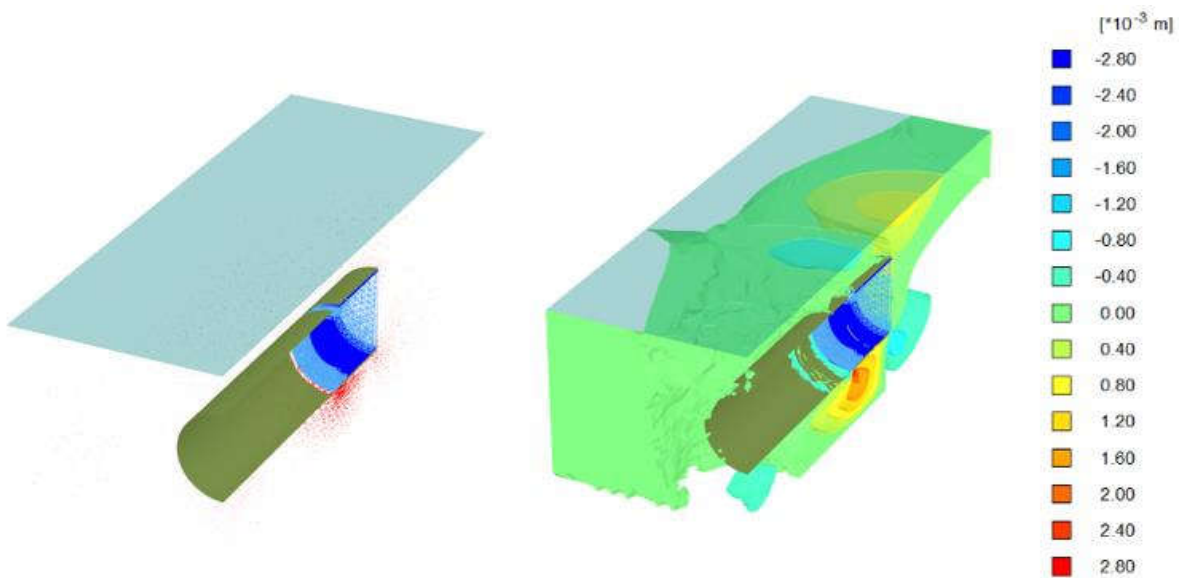
Figure 4.35: Total longitudinal settlement for seismic loading based on finite element method



(a) Diameter, $D_1 = 10.5\text{m}$



(b) Diameter, $D_2 = 10.8\text{m}$



(c) Diameter, $D_3 = 11.0\text{m}$

Figure 4.36: Total longitudinal settlement of seismic loading effect for $A_2 = 5.5\text{m}$, $y_3 = 31\text{m}$

4.13 RESULTS OF STRAIN INDUCED VOLUME LOSS

Numerical methods are described the volumetric strains which are shown in **Figure 4.37** and **Figure 4.38**. **Figure 4.38** expresses PLAXIS 3D representation. Soil clusters are similar for all diameter. Numerical methods solve the limitation of modified formula. Modified analytical formula is developed based on plain strain assumptions which is not described the length effects of tunnel. For diameter D_1 , volumetric strains are decreasing gradually with the increment of relative depths. Other two diameter express the fluctuation of settlement with the variation of relative depths and lengths of tunnel. Minimum volumetric strain is 1.5 percent at A_5/D_1 .

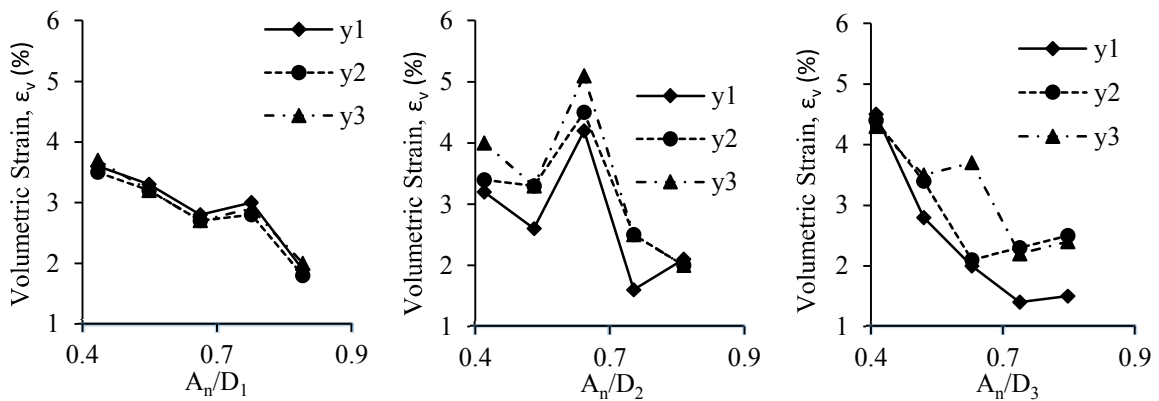
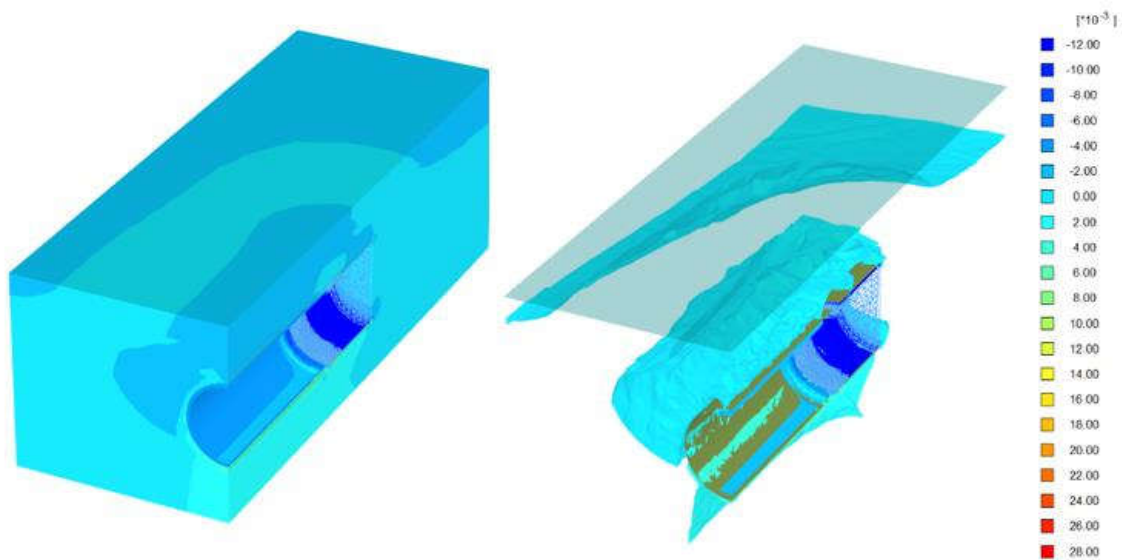
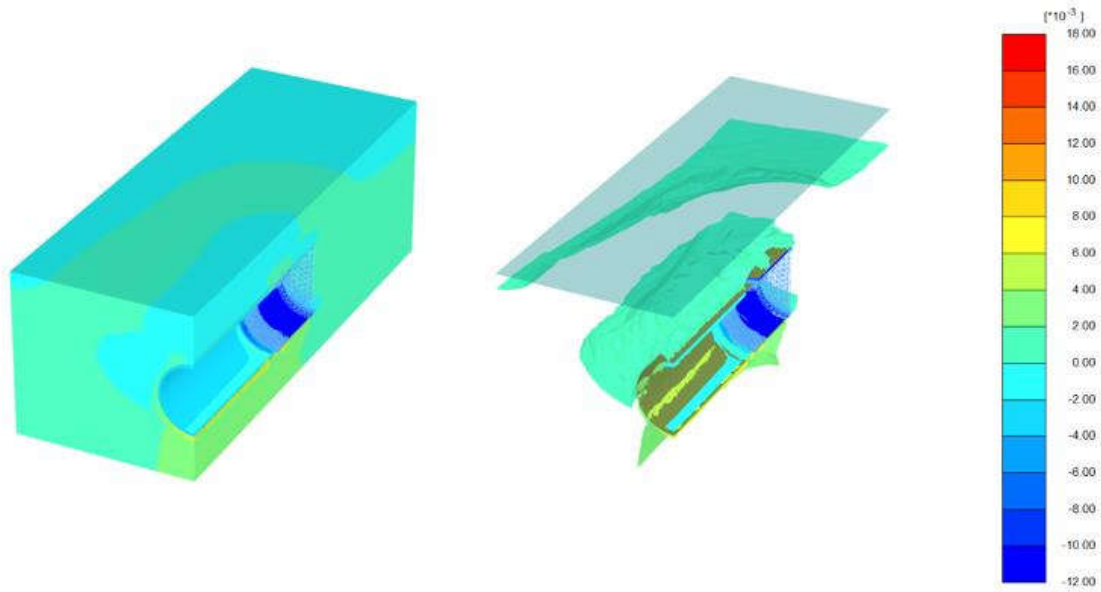


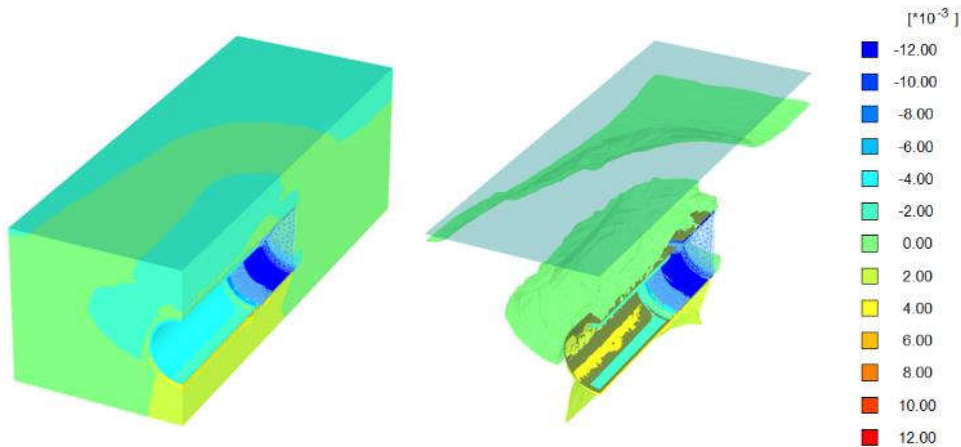
Figure 4.37: Volumetric strain for long term loading based on finite element method



(a) Diameter, $D_1 = 10.5\text{m}$



(b) Diameter, $D_2 = 10.8\text{m}$



(c) Diameter, $D_3 = 11.0\text{m}$

Figure 4.38: Volumetric strain of long term loading effect for $A_4 = 7.5\text{m}$, $y_1 = 27\text{m}$

Figure 4.39 and **Figure 4.40** represent the volumetric strain under seismic loading. **Figure 4.40** expresses PLAXIS 3D representation of volumetric strains. Soil clusters are nearly same for all diameter. Volumetric strains are fluctuating with change of relative depths. Volumetric strain represents two types of strain induced volume loss such as extension and contraction. Extension means positive volume loss and contraction means negative volume loss. Minimum value of volumetric strain is 0.03 percent due to contraction at A_5/D_1 . Minimum value of volumetric strain is 0.03 percent due to extension at A_5/D_2 . Volumetric strains jumps are observed some locations such as A_2/D_1 at second construction phase, A_2/D_2 at second construction phase, A_5/D_2 at three construction phases, A_1/D_3 at first construction phase and A_5/D_3 at three construction phases. In these locations, shear strength of sands are much lower than others locations because of various types of loss TBM tunnel. So, soil particles are not sustain external load and suddenly occurs larger settlement.

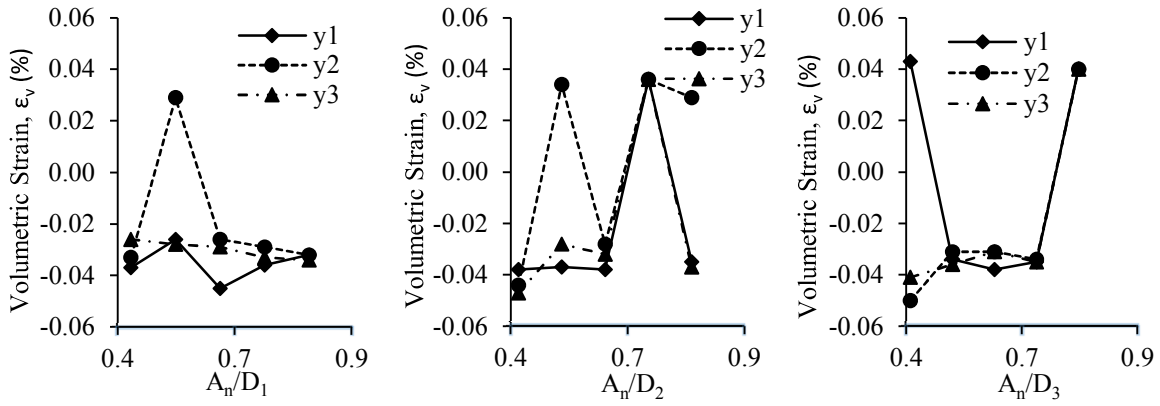
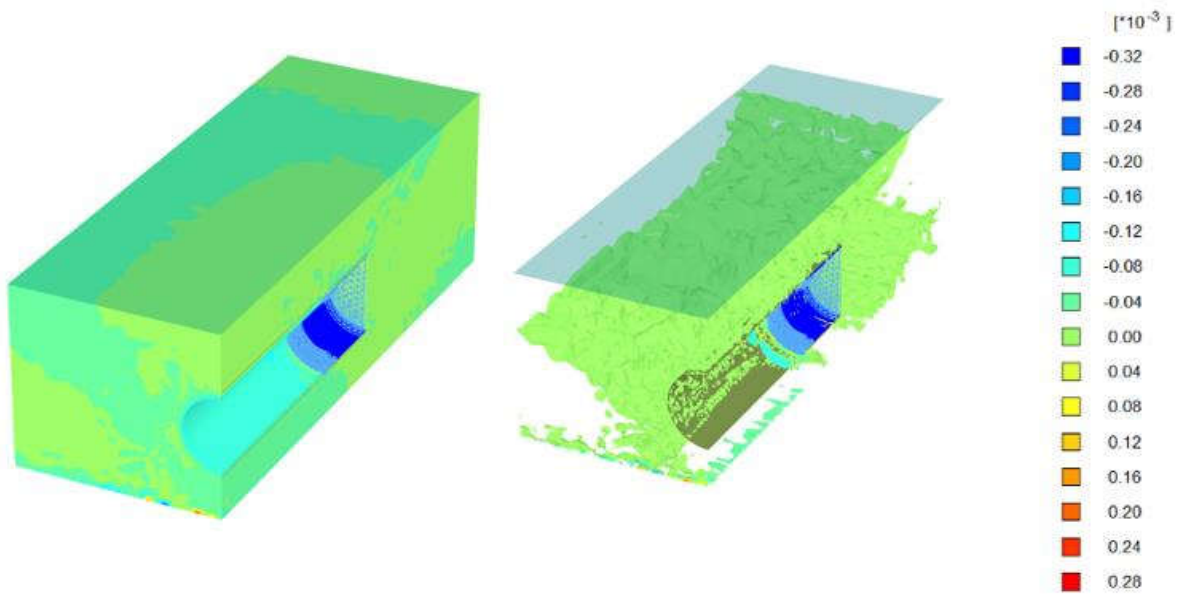
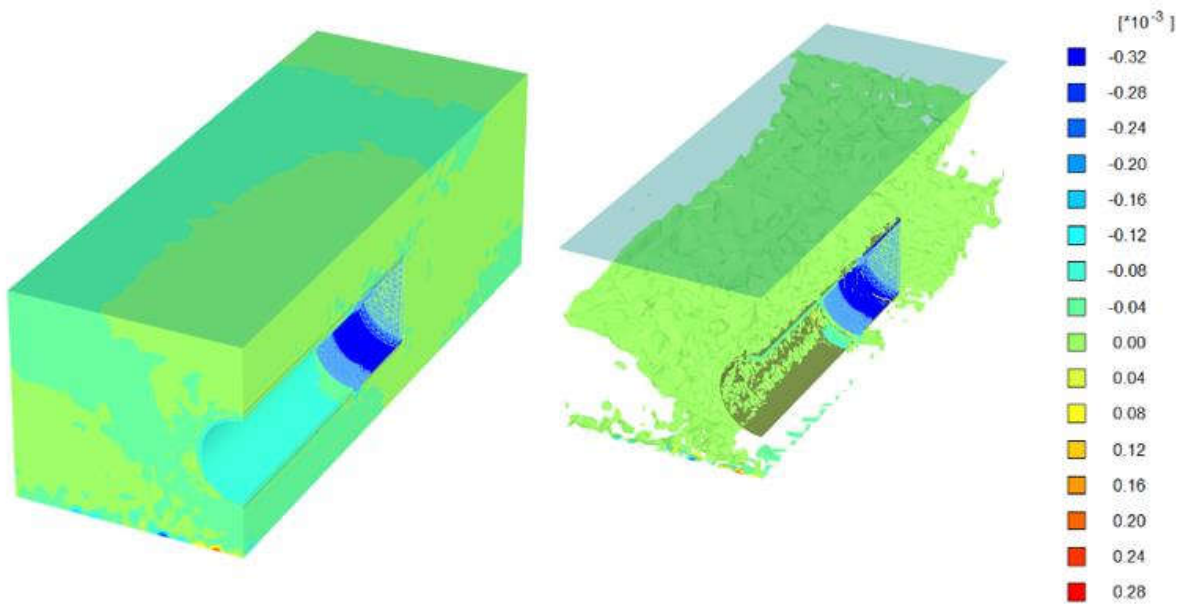
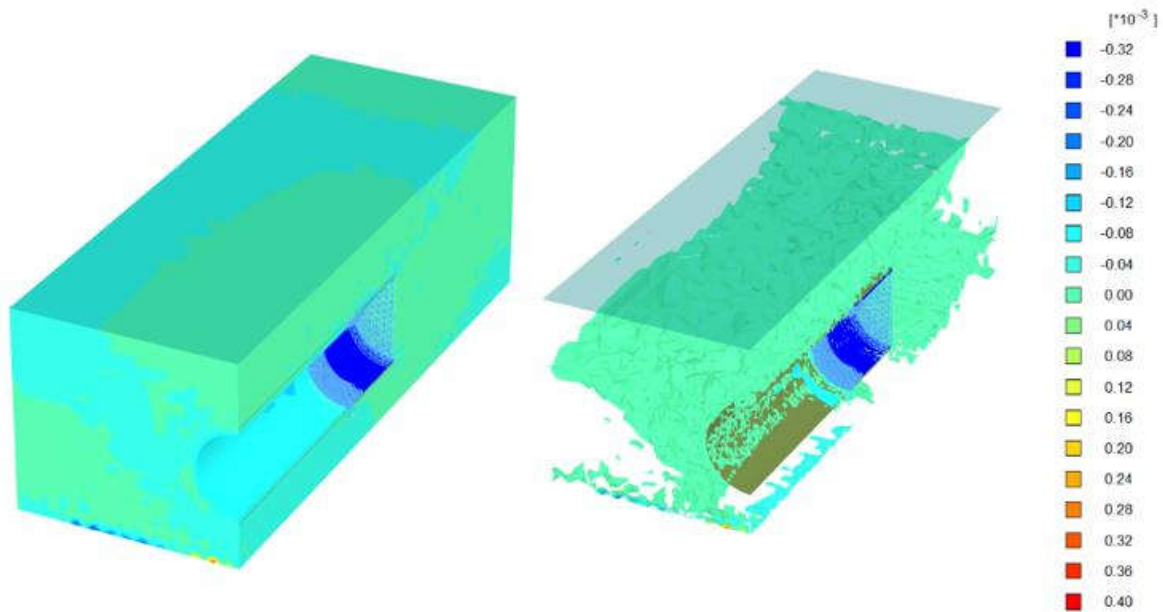


Figure 4.39: Volumetric strain for seismic loading based on finite element method





(c) Diameter, $D_3 = 11.0\text{m}$

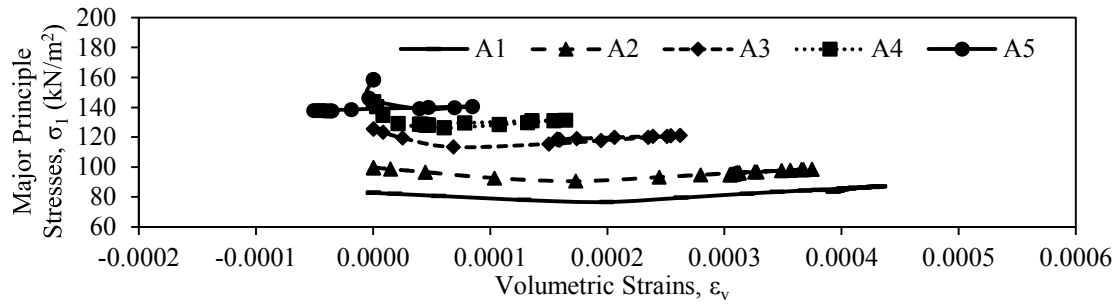
Figure 4.40: Volumetric strain of seismic loading effect for $A_5 = 8.5\text{m}$, $y_2 = 29\text{m}$

4.14 STRESS – STRAIN BEHAVIOUR OF SOIL AROUND TUNNEL

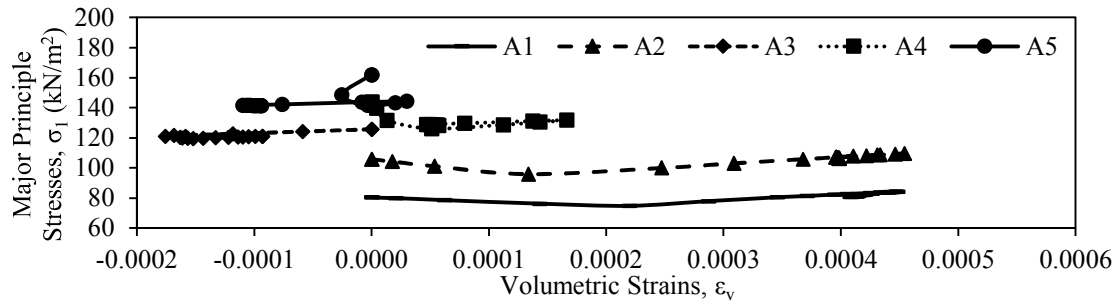
Stress – strain behaviour of soil around tunnel expresses stability of tunnel under long term and seismic loading. Stress – strain varies with soil particle to particle. This behaviour is not same in every particle of soil. Strain induced volume loss of soil particles are evaluated by this behaviour. In long term (static) loading, simultaneous loading-unloading –reloading has not possible but in seismic loading these mechanism has possible. In this paper, stress – strain behaviour of soil around tunnel describes only for one point (0, 20) of various depths of tunnel crown. These points are indicating the change of major principle stresses with the variation of volumetric strains. Volumetric strains are defined the strain induced volume losses.

4.14.1 Long Term Loading

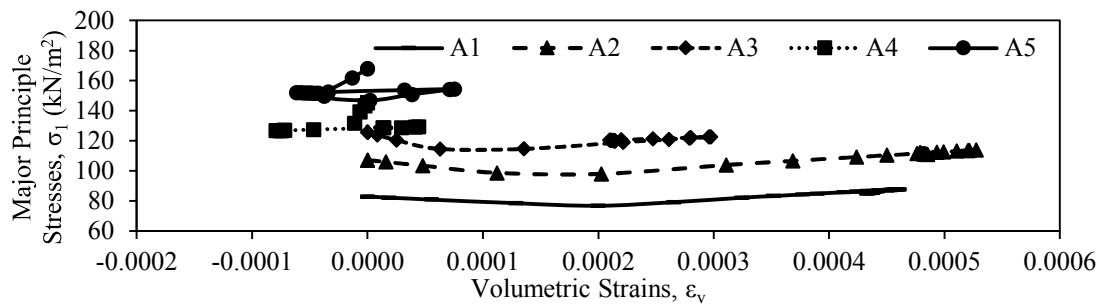
Stress – strain varies with long term (static) loading. These variations are not same at surface and a point around tunnel. Volumetric strains and major principle stresses are shown in **Figure 4.41**. Stress – strain behaviour changes with the variation of diameters. Major principle stresses are increasing gradually with the increment of depths of tunnel crown. Major principle stresses are decreasing with the increment of volumetric strain. Major principle stress and strain are 140 kN/m^2 and 0.0095 percent at A_5 for diameter D_1 which indicates the critical highest stress against lowest strain value. Maximum value of stress is 160 kN/m^2 at A_5 for D_1 . Minimum volumetric strain is 0.0045 percent due to extension at A_5 for D_2 . Minimum volumetric strain is 0.002 percent due to contraction at A_5 for D_3 . Extension means positive volumetric strain and contraction means negative volumetric strain.



(a) Diameter, D_1



(b) Diameter, D_2

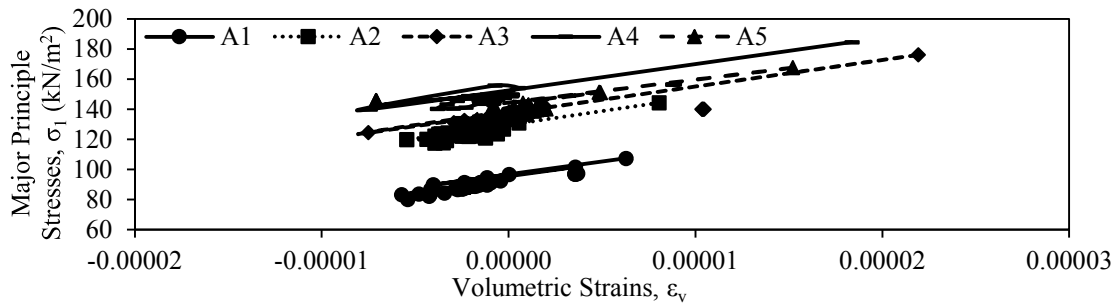


(c) Diameter, D_3

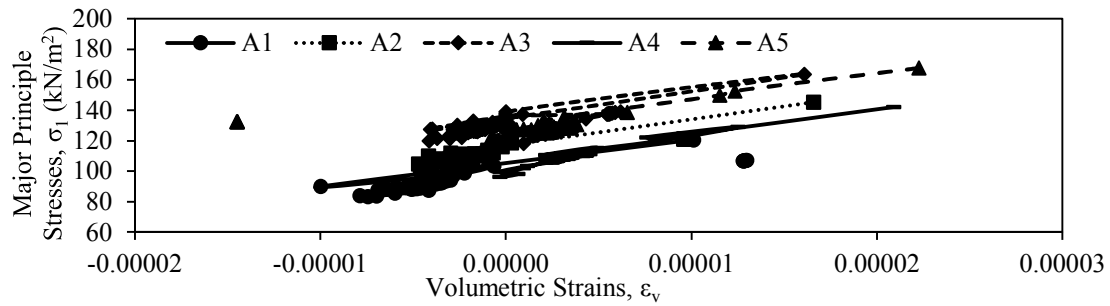
Figure 4.41: Stress – strain behaviour of soil around tunnel for long term loading

4.14.2 Seismic Loading

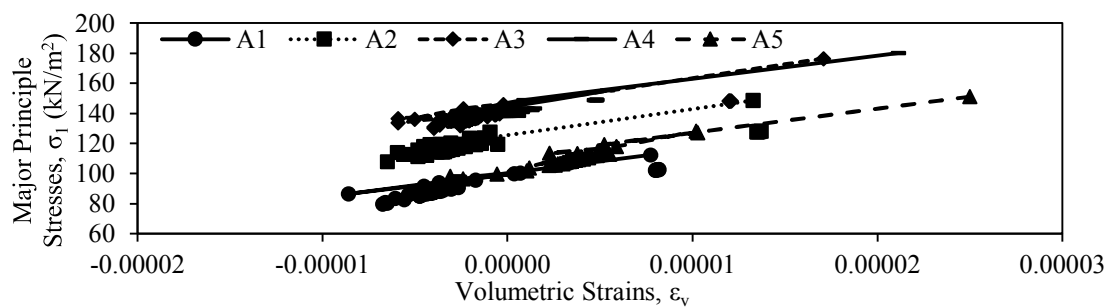
Seismic loading deals loading-unloading-reloading mechanism as shown in **Figure 4.42**. More yield points are created under seismic loading. Stresses and strains are fluctuating for various relative depths and diameters. Maximum major principle stress is 158 kN/m^2 at A_5 for D_1 . Rate of volumetric strain is very low. Minimum volumetric strain is less than 0.0005 percent for various relative depths and diameters.



(a) Diameter, D_1



(b) Diameter, D_2

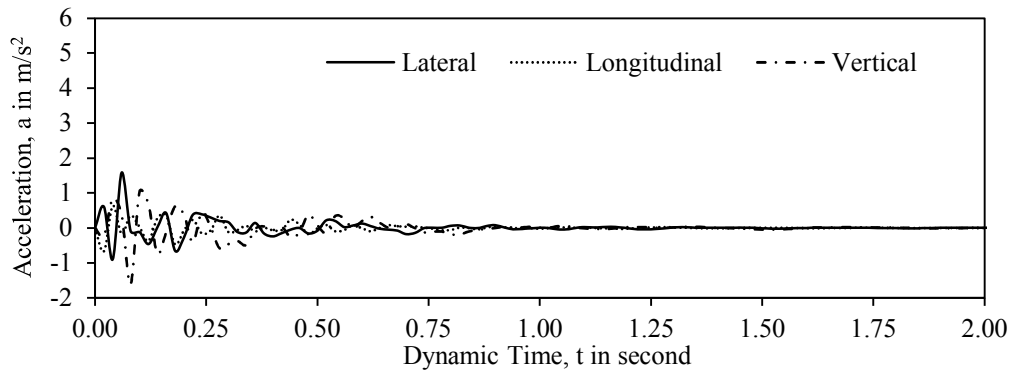


(c) Diameter, D_3

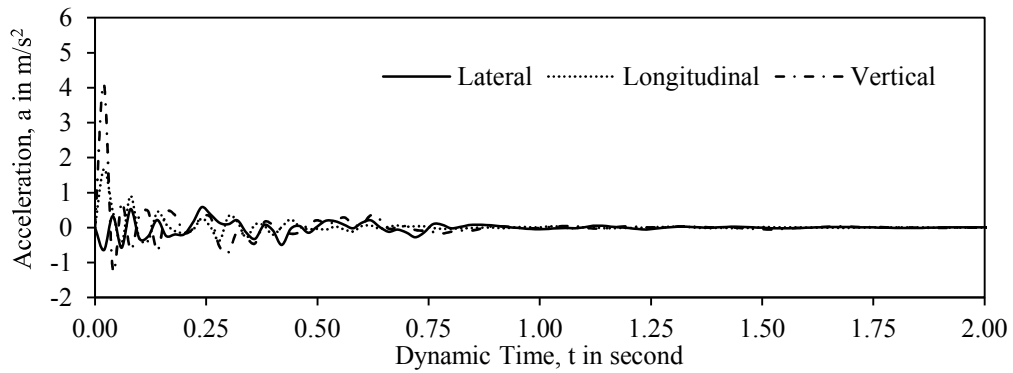
Figure 4.42: Stress – strain behaviour of soil around tunnel for seismic loading

4.15 SURFACE ACCELERATION DURING SEISMIC SHAKING

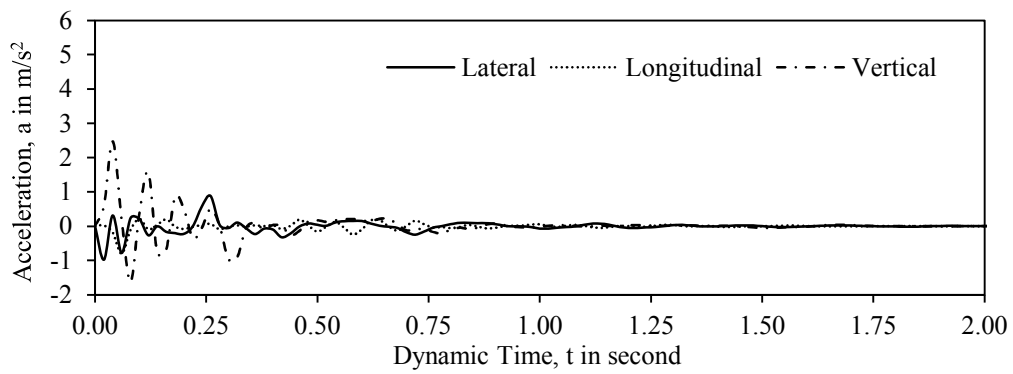
Accelerations are taken at a fixed point in surface. After one second, accelerations are almost constant because of failure of soil particle at this point but overall not. Soil cluster not fail in case of failure of only one particle. So seismic shaking is not further proceed for this point. Surface accelerates gradually during seismic shaking. Super structures stands on the surface, so it has necessary to evaluate how much accelerate under seismic loading. Accelerations diagram are shown in **Figure 4.43** at various depths of tunnel crown. Acceleration takes at a point (-3.5, 15.5, -1.5) for various diameters and relative depths. Accelerations are decreasing gradually with the increment of dynamic times. Vertical accelerations are major part under seismic loading. Lateral, longitudinal and vertical accelerations at 0.25s are 0.9m/s^2 , -0.05m/s^2 and 0.1m/s^2 at A_5 location for diameter, D_1 .



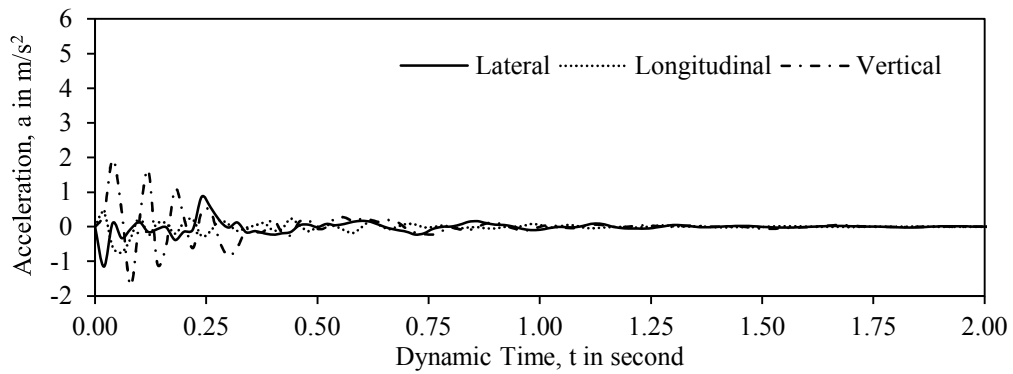
(a) Depth of tunnel crown, A_1



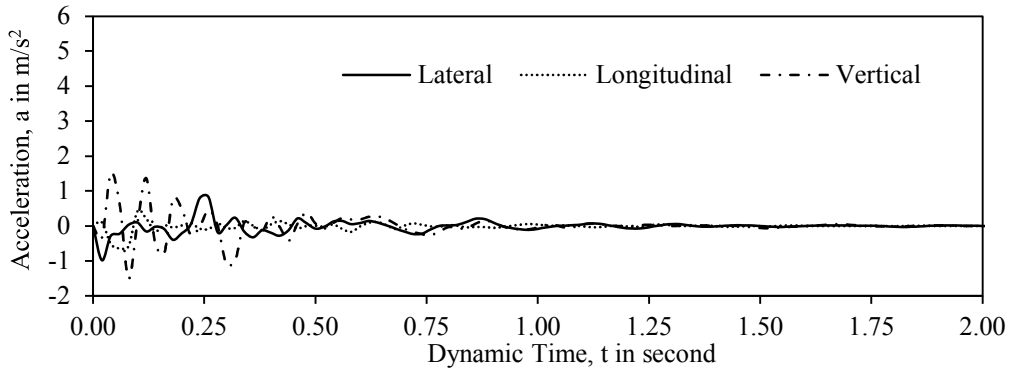
(b) Depth of tunnel crown, A_2



(c) Depth of tunnel crown, A_3



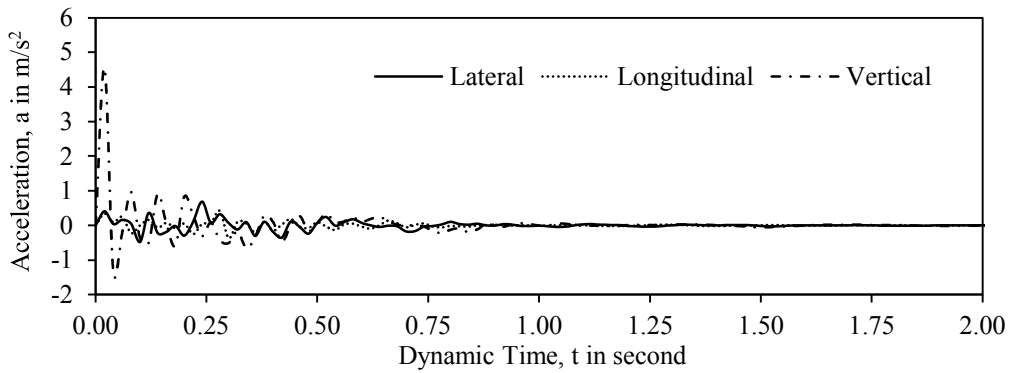
(d) Depth of tunnel crown, A_4



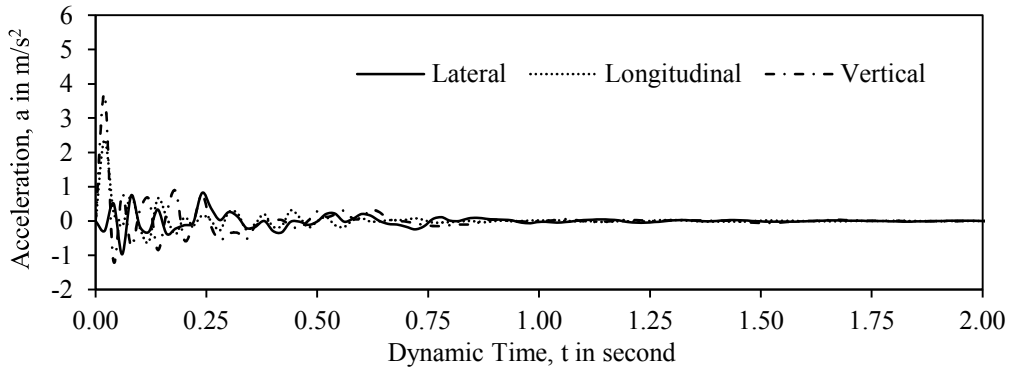
(e) Depth of tunnel crown, A_5

Figure 4.43: Surface acceleration during seismic loading for diameter, D_1

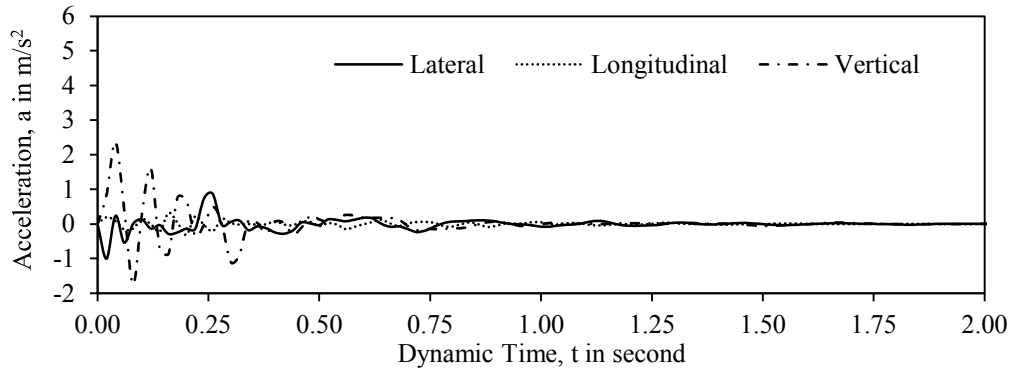
Variation of accelerations with dynamic time are shown in **Figure 4.44** for diameter D_2 . Maximum vertical acceleration is 4.5m/s^2 at A_1 for diameter D_2 . Accelerations of lateral, longitudinal and vertical directions are 0.9m/s^2 , -0.05m/s^2 and 0.7m/s^2 in 0.25s at A_5 location for diameter, D_2 .



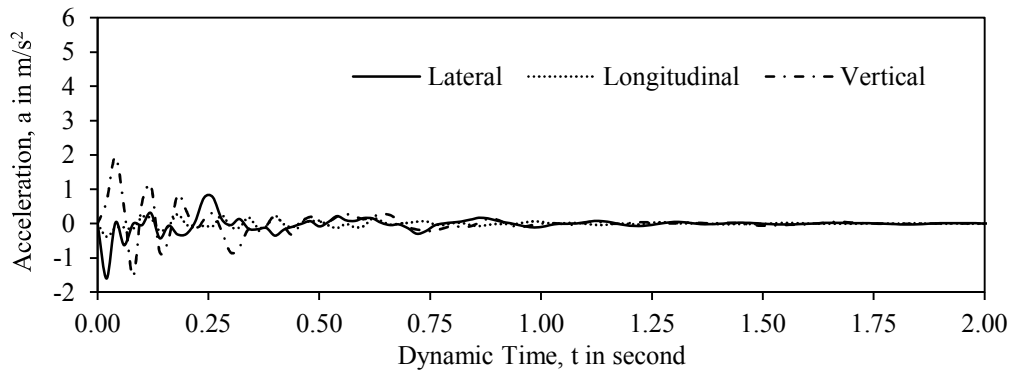
(a) Depth of tunnel crown, A_1



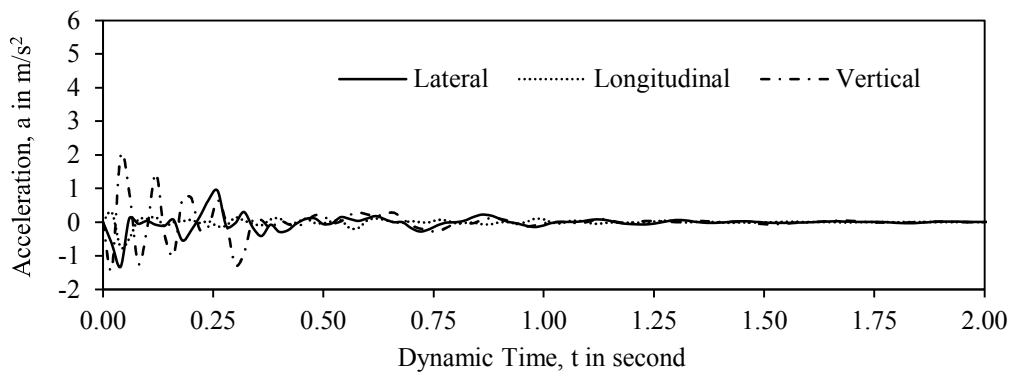
(b) Depth of tunnel crown, A_2



(c) Depth of tunnel crown, A_3



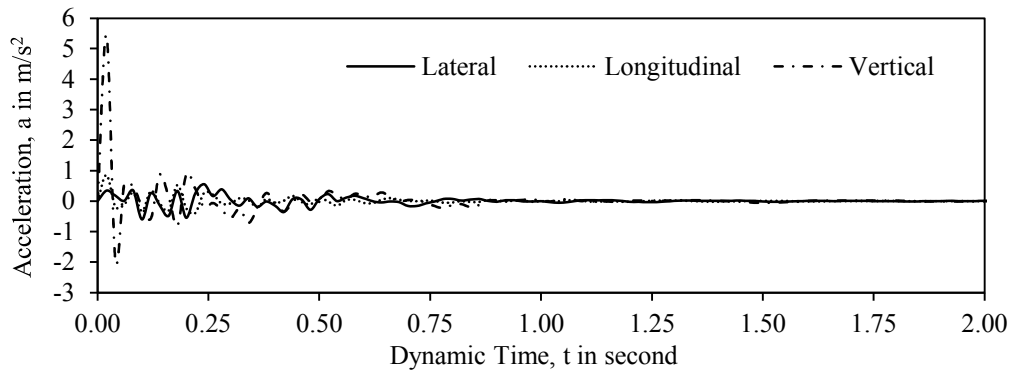
(d) Depth of tunnel crown, A_4



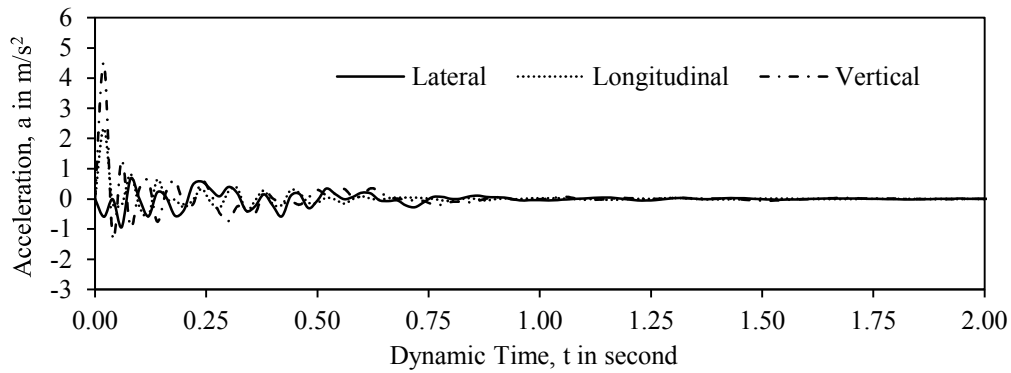
(e) Depth of tunnel crown, A_5

Figure 4.44: Surface acceleration during seismic loading for diameter, D_2

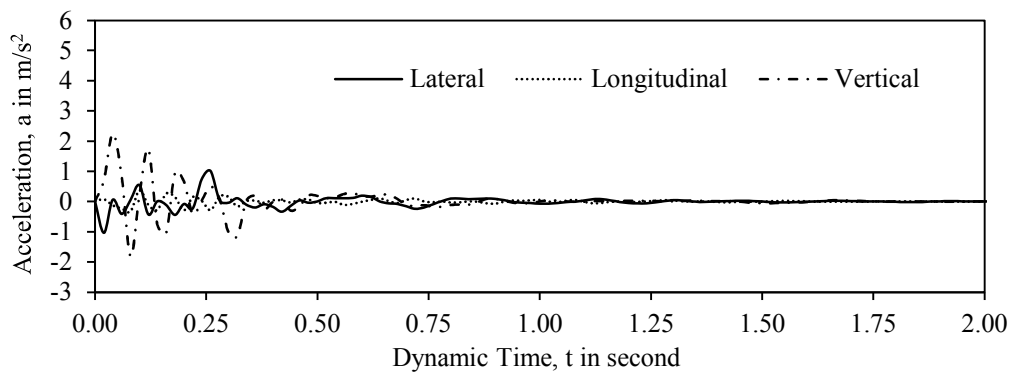
Variations of accelerations of various depths of tunnel crown are shown in **Figure 4.45** for diameter D_3 . Maximum acceleration is 5.4 m/s^2 at A_1 for diameter, D_3 . Acceleration is nearly zero after one second for all depth of tunnel crown. Accelerations of lateral, longitudinal and vertical directions are 1.0 m/s^2 , -0.1 m/s^2 and 0.7 m/s^2 in 0.25s at A_5 for diameter, D_3 .



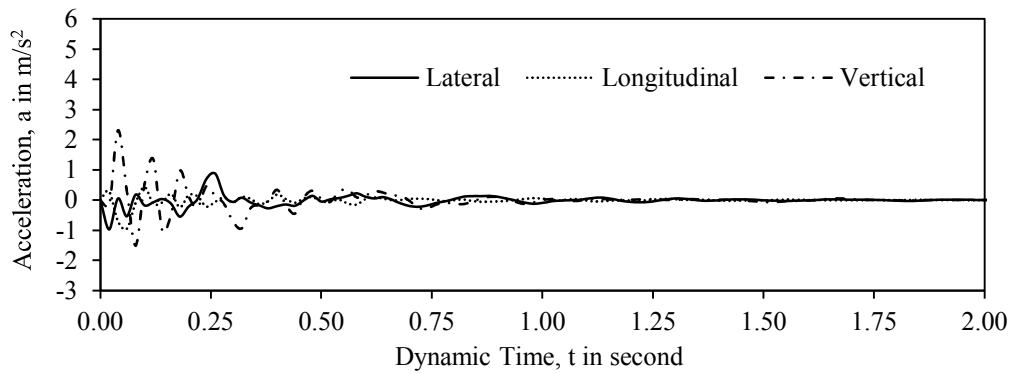
(a) Depth of tunnel crown, A_1



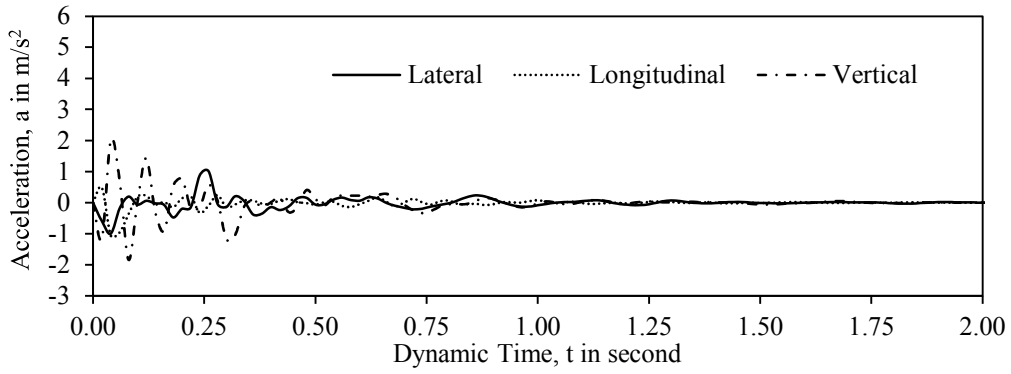
(b) Depth of tunnel crown, A_2



(c) Depth of tunnel crown, A_3



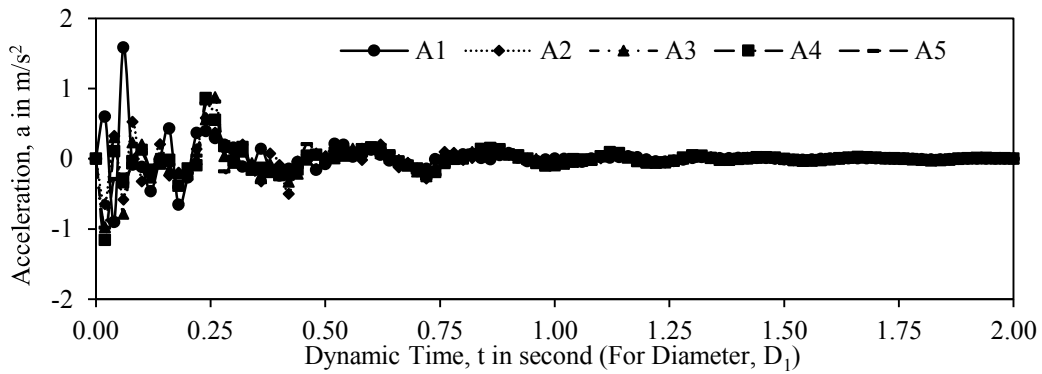
(d) Depth of tunnel crown, A_4



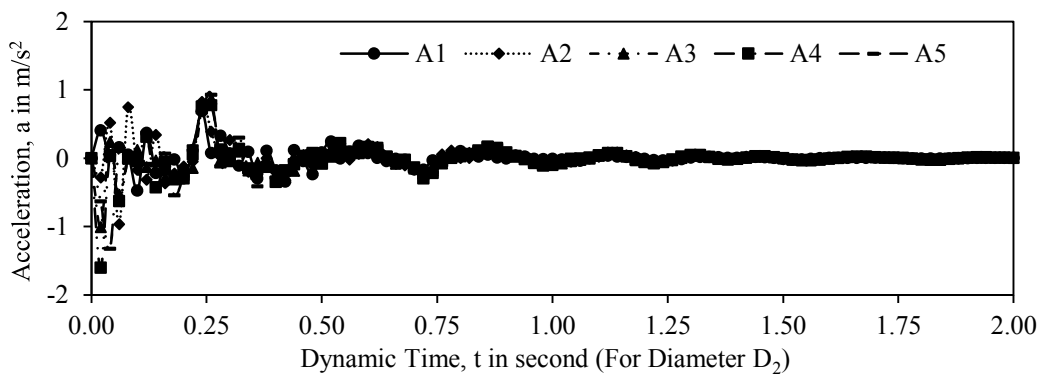
(e) Depth of tunnel crown, A_5

Figure 4.45: Surface acceleration during seismic loading for diameter, D_3

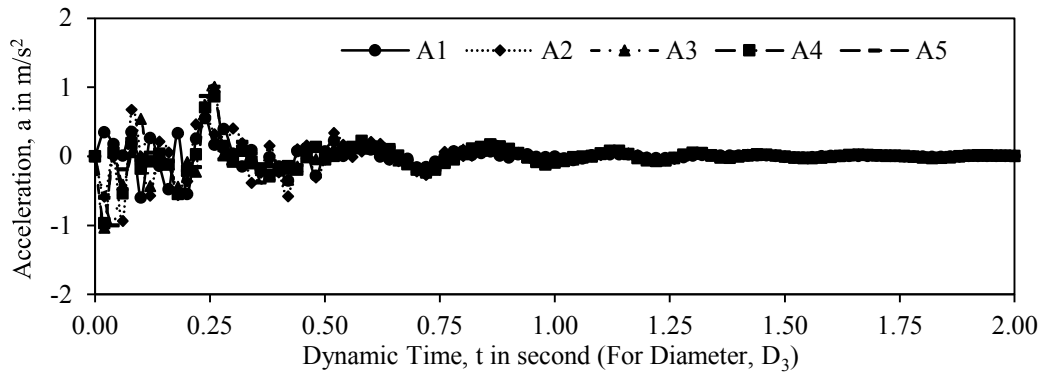
Variations of accelerations in lateral direction are expressed for various depths of tunnel crown and diameters which are shown in **Figure 4.46**. Accelerations are decreasing gradually with the increment of dynamic time. Maximum acceleration is 1.8 m/s^2 at A_1 for diameter, D_1 and is -1.8 m/s^2 at A_4 for diameter, D_2 . Acceleration is 0.9 m/s^2 in 0.25 s at A_4 for diameter, D_1 .



(a) Diameter, D_1



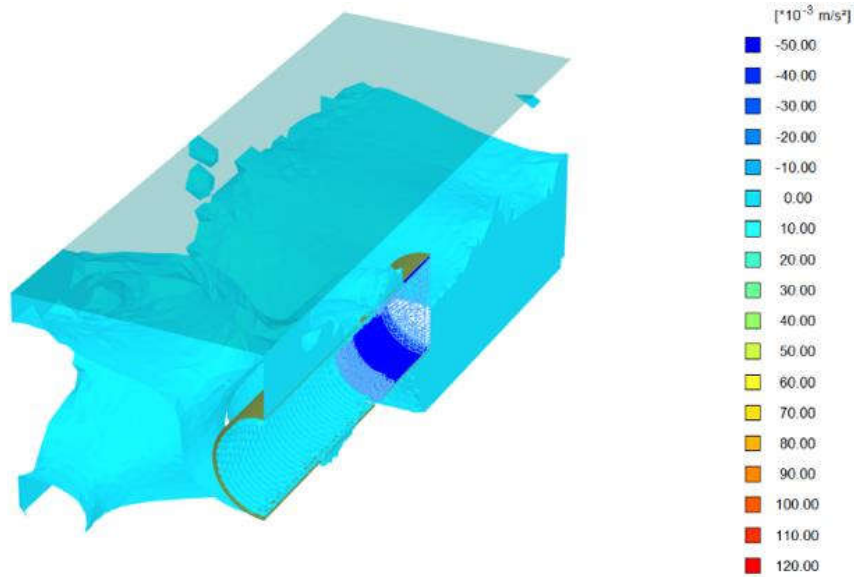
(b) Diameter, D_2



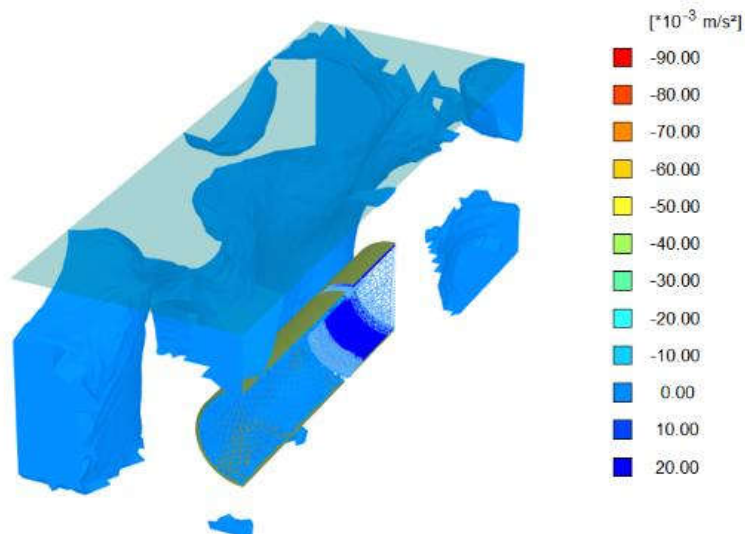
(c) Diameter, D_3

Figure 4.46: Lateral surface acceleration of various relative depth during seismic loading

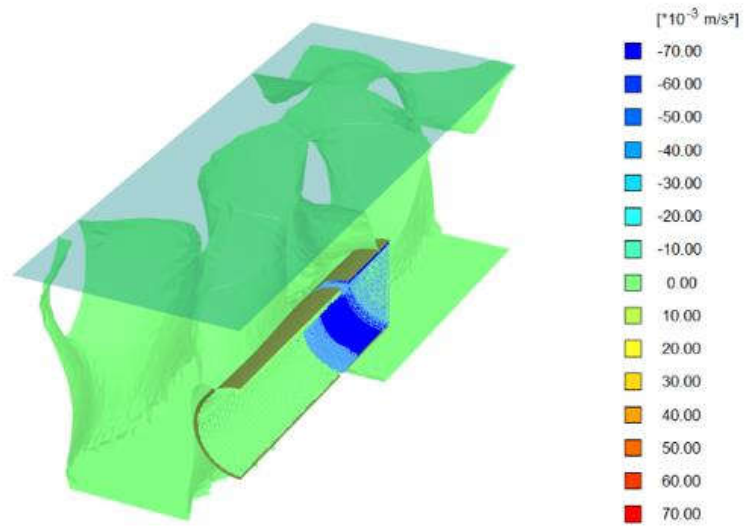
Analysis results of PLAXIS 3D are shown in **Figure 4.47** and **Figure 4.48** for accelerations and velocities in lateral, longitudinal and vertical directions respectively.



(a) Lateral acceleration

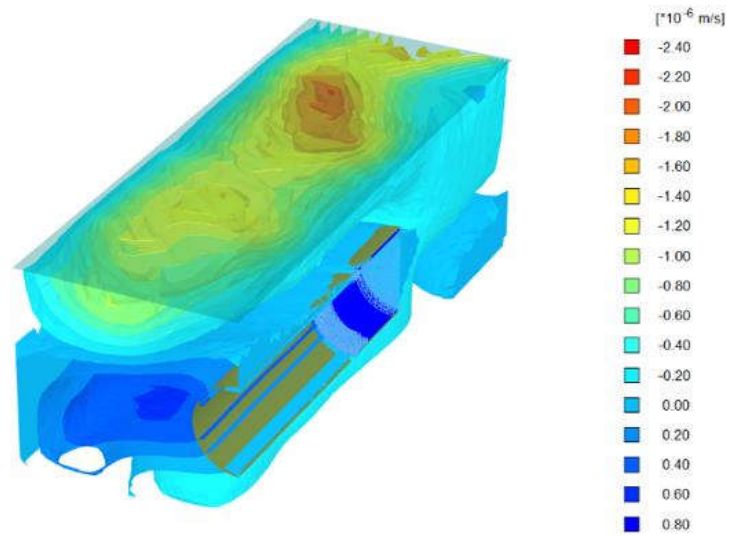


(b) Longitudinal acceleration

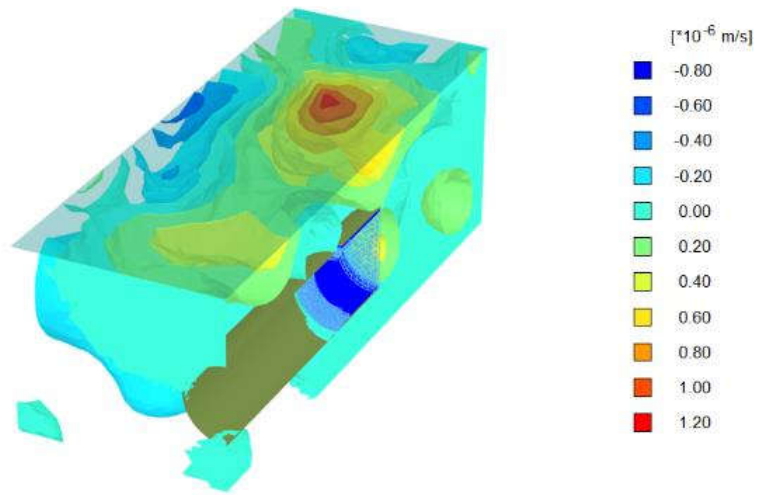


(c) Vertical acceleration

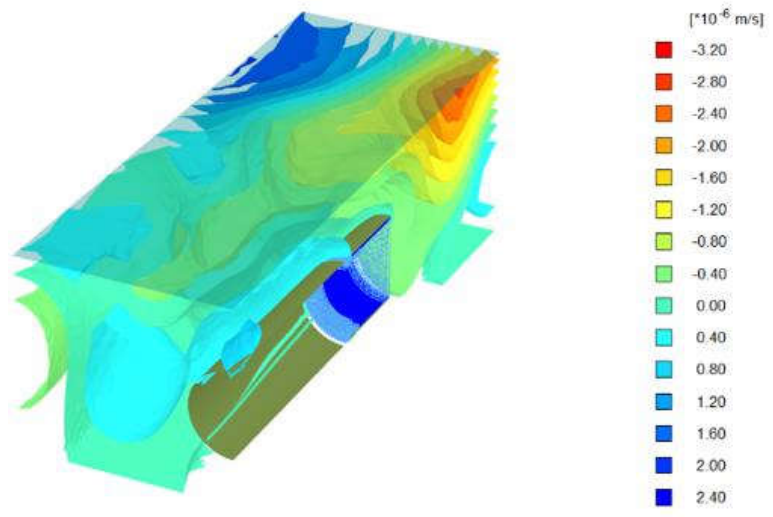
Figure 4.47: Accelerations for $D_1 = 10.5\text{m}$, $A_4 = 7.5\text{m}$, $y_1 = 27\text{m}$



(a) Lateral velocity



(b) Longitudinal velocity



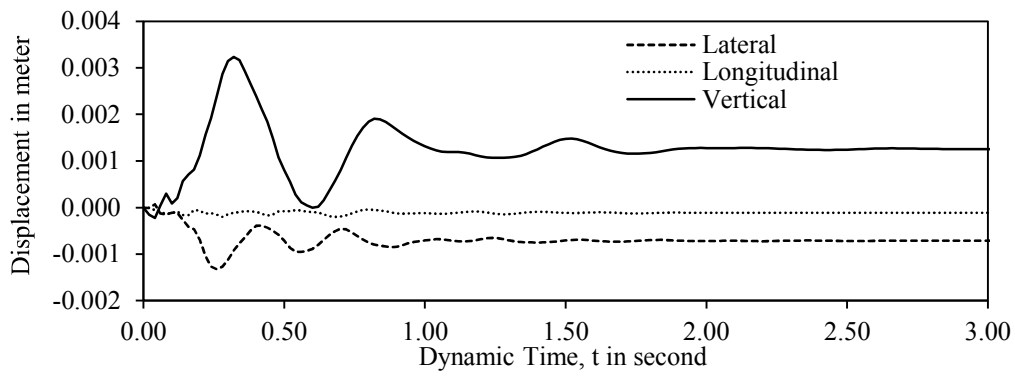
(c) Vertical velocity

Figure 4.48: Velocities for $D_1 = 10.5\text{m}$, $A_4 = 7.5\text{m}$, $y_1 = 27\text{m}$

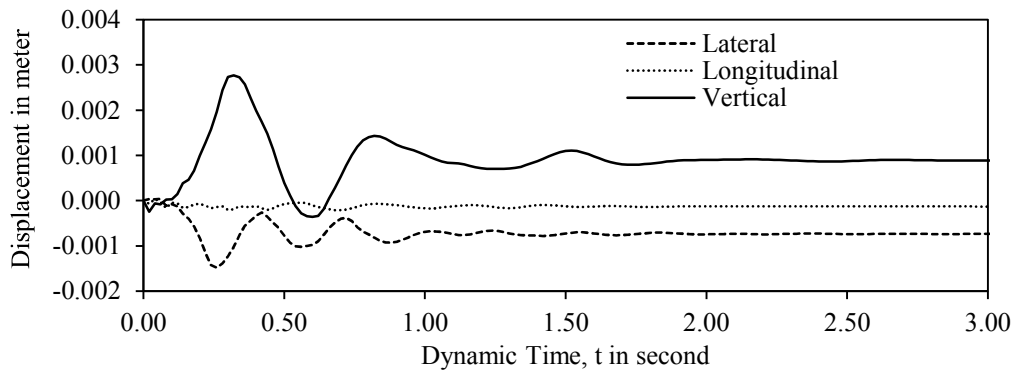
4.16 SURFACE DISPLACEMENT DURING SEISMIC SHAKING

Displacements are taken at a fixed point in surface. After two second, displacements are almost constant because of failure of soil particle at this point but overall not. Soil cluster not fail in case of failure of only one particle. So seismic shaking is not further proceed for this point. Surface displacements during seismic shaking are influenced to the surface structures. Surface displacements are changing with the variation of depths of tunnel crown which are shown in **Figure 4.49** for diameter D_1 . Displacements are taken nearly at a point such as (-3.5, 15.5, -1.5) for all depth of tunnel crown. Displacements are decreasing gradually with the increment of depths of tunnel crown and dynamic times. Maximum vertical displacement is 3.2 mm in 0.3s at A_1 for diameter, D_1 which indicates uplift. Maximum lateral

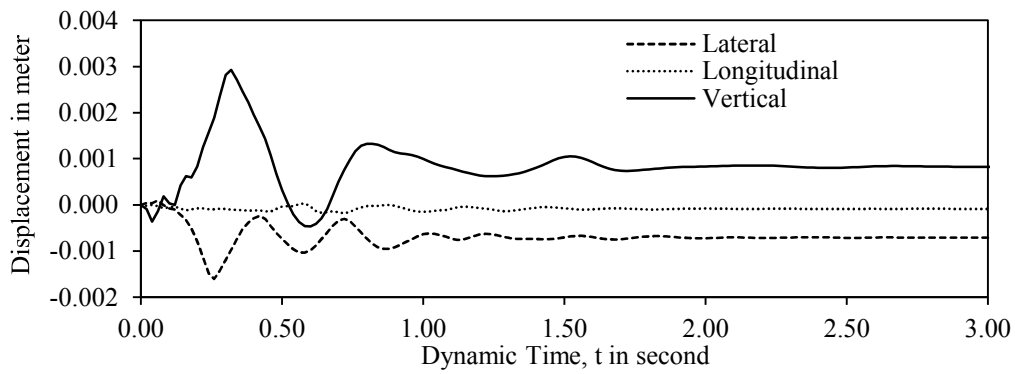
settlement is 1.8 mm in 0.25s at A_3 for diameter, D_1 . Vertical settlement is 0.6 mm in 0.65s at A_5 for diameter, D_1 .



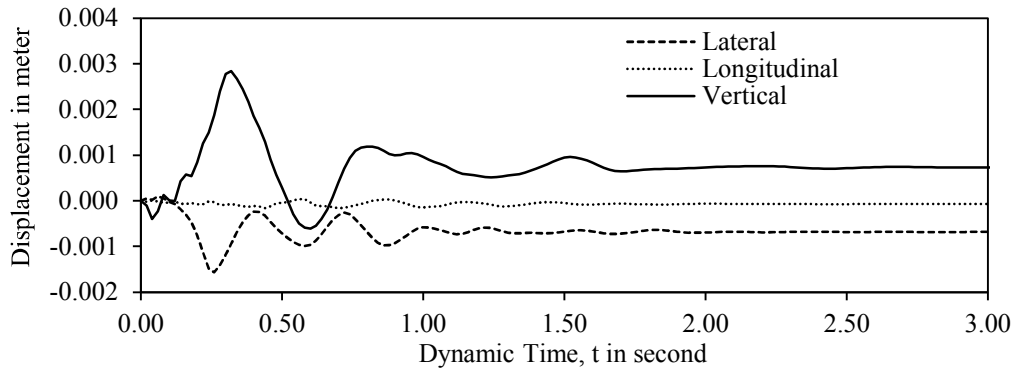
(a) Depth of tunnel crown, A_1



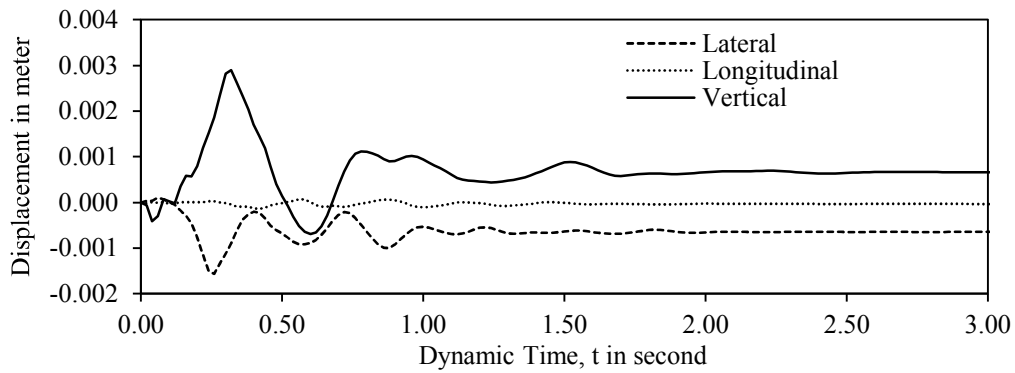
(b) Depth of tunnel crown, A_2



(c) Depth of tunnel crown, A_3



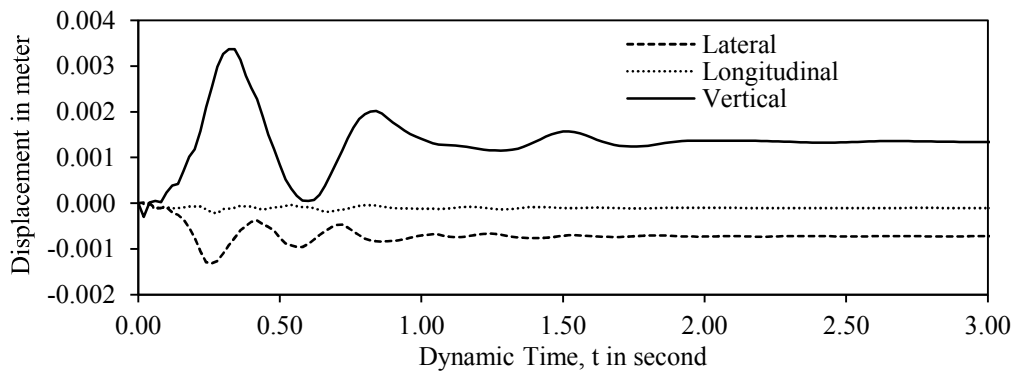
(d) Depth of tunnel crown, A_4



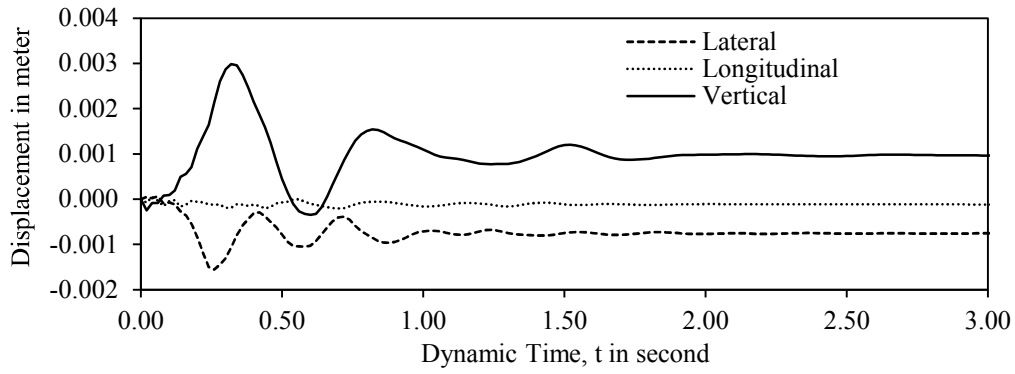
(e) Depth of tunnel crown, A_5

Figure 4.49: Surface displacement during seismic loading for diameter, D_1

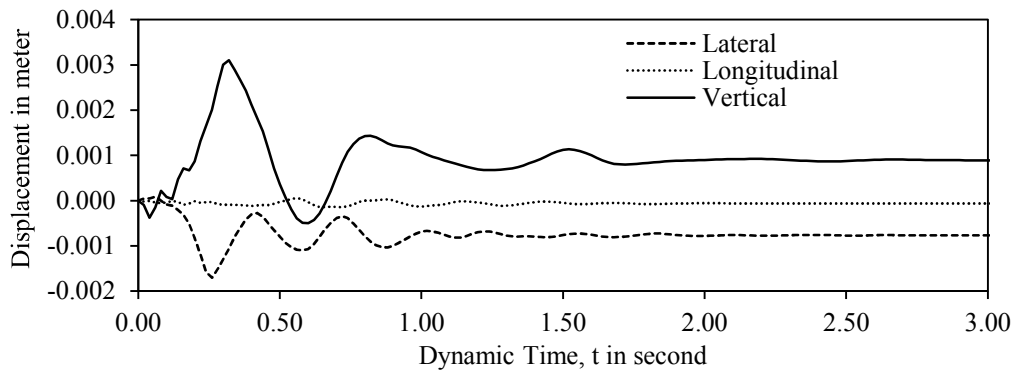
Surface displacements for Diameter D_2 are shown in **Figure 4.50**. Uplift decreases with the increment of depths of tunnel crown and also, it decreases with the increment of dynamic time. Maximum uplift is 3.4 mm at A_1 for diameter, D_2 . Vertical settlement is 0.65 mm at A_5 for diameter, D_2 .



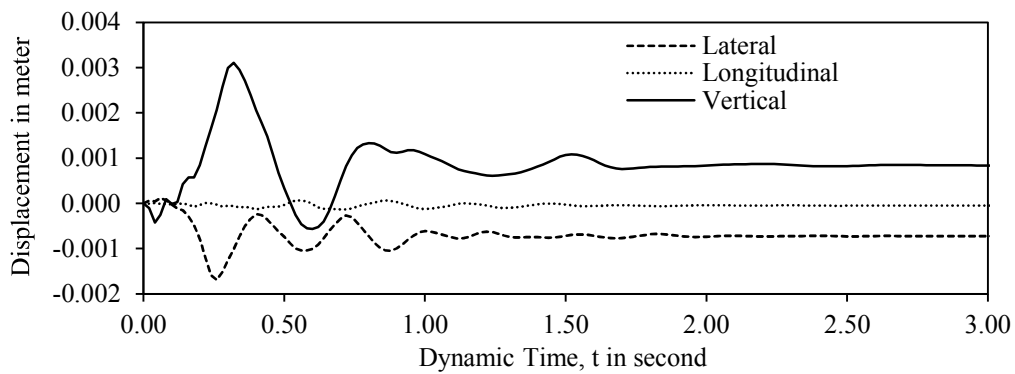
(a) Depth of tunnel crown, A_1



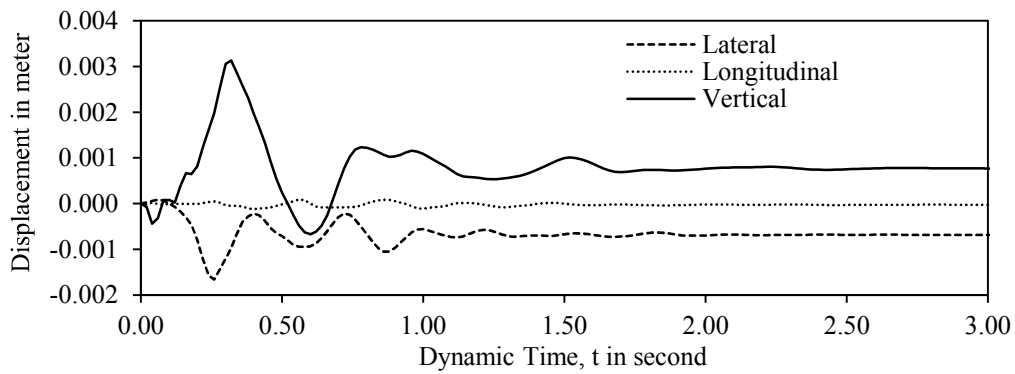
(b) Depth of tunnel crown, A_2



(c) Depth of tunnel crown, A_3



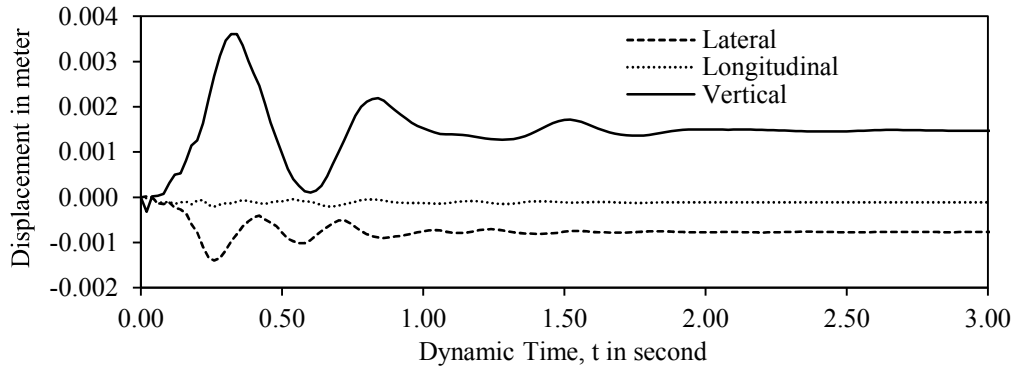
(d) Depth of tunnel crown, A_4



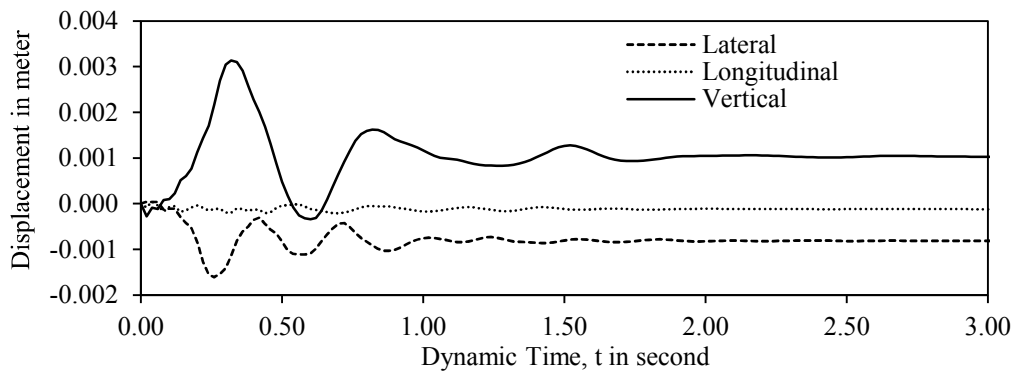
(e) Depth of tunnel crown, A_5

Figure 4.50: Surface displacement during seismic loading for diameter, D_2

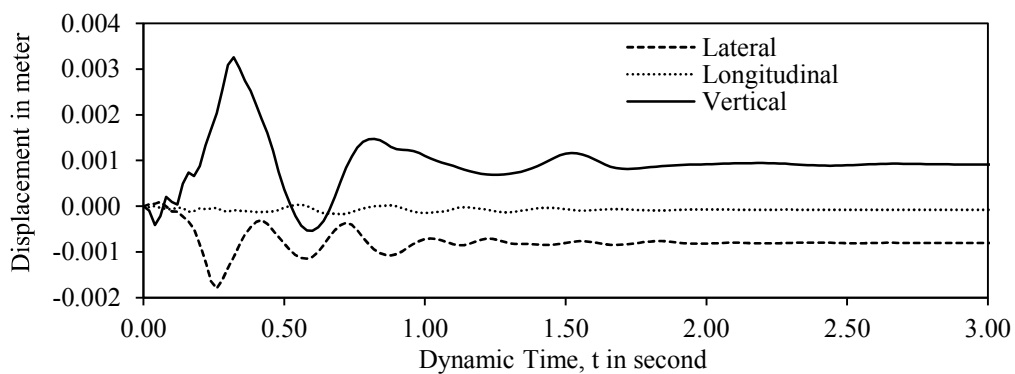
Surface displacements of diameter, D_3 are shown in **Figure 4.51**. Longitudinal surface displacement rates are very low because seismic shaking is applied along lateral directions. Maximum uplift is 3.6 mm at A_1 for diameter, D_3 . Vertical and lateral displacements are decreasing with increment of dynamic time. Vertical settlement is 0.6 mm at A_5 for D_3 .



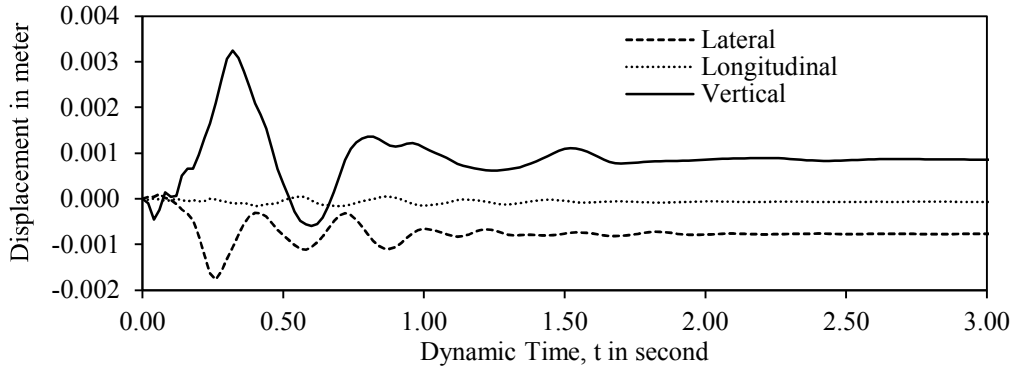
(a) Depth of tunnel crown, A_1



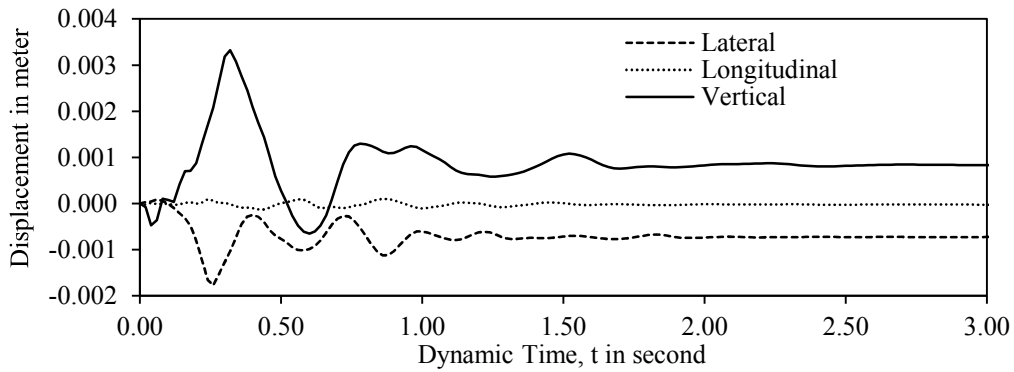
(b) Depth of tunnel crown, A_2



(c) Depth of tunnel crown, A_3



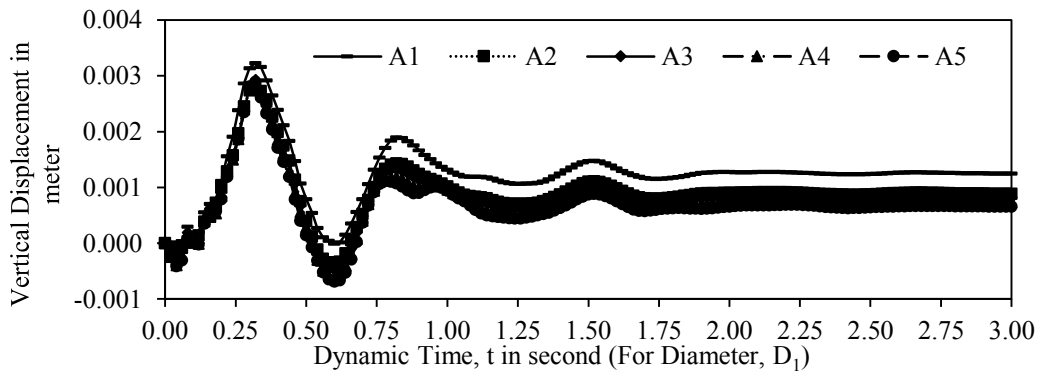
(d) Depth of tunnel crown, A₄



(e) Depth of tunnel crown, A₅

Figure 4.51: Surface displacement during seismic loading for diameter, D₃

Only vertical displacements are shown in **Figure 4.52** for diameter, D₁, D₂ and D₃. Maximum uplift is 3.7 mm in 0.35s at A₁ for D₃. Maximum settlement is 1.2 mm in 0.60s at A₅ location for diameter D₁. Settlements are nearly at zero after 2.5s. Minimum difference of settlements is 4.2 percent at dynamic time 0.6s. This difference consists of depths of tunnel crown such as A₄ and A₅.



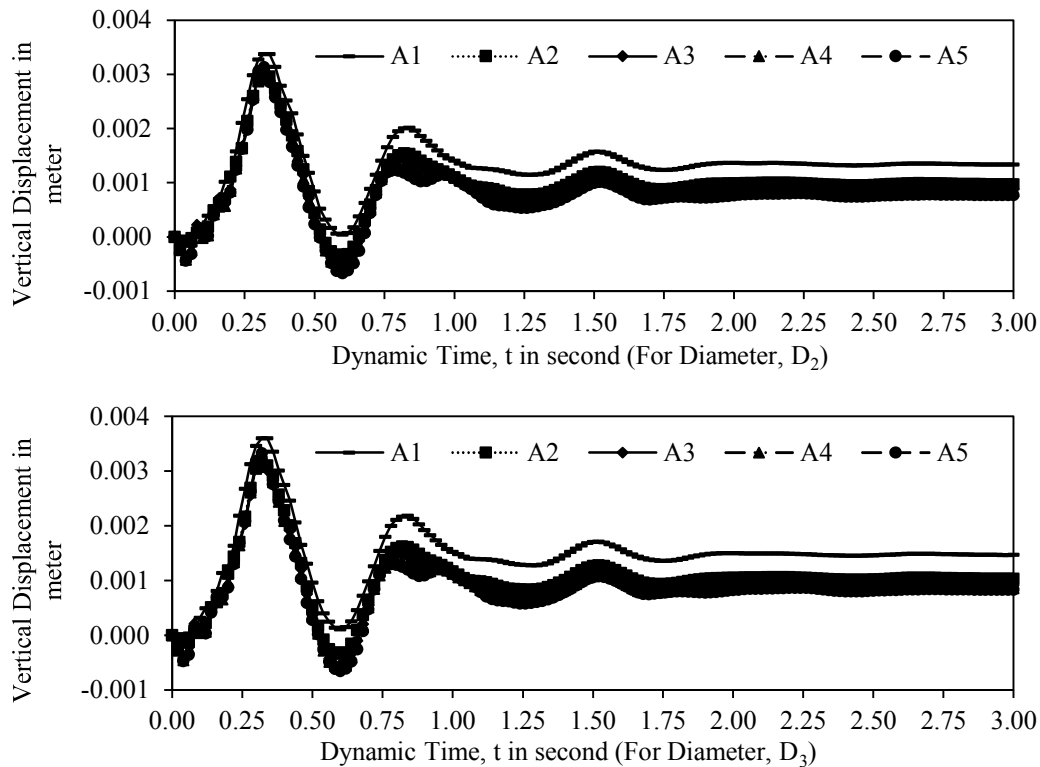


Figure 4.52: Vertical surface displacement of various relative depth during seismic loading

4.17 CONCLUSIONS

Numerical results are not exactly same with modified formulae results because modified formulae are developed based on plain strain consideration. Seismic loading has considered in analysis because evaluated behaviour of settlements under construction of TBM tunnel. Liquefaction has not occurred because variations of settlements are very low for various frequencies.

Differences of vertical surface settlements among various diameters have been found to be 7% at specific depth of tunnel crown, A₅ under static loading. Minimum vertical surface settlement is 5 mm at A₅/D₁ based on static loading and is 2 mm at A₅/D₁ based on seismic loading. Minimum differences of settlements among various lengths of tunnel have been found to be 2.5% for diameter, D₁ (10.5m) under static loading. Minimum value of total vertical settlement is 7 mm at A₄/D₃ based on seismic loading. Total vertical settlements are expressed uplift for static loading. Difference of settlement between static and seismic loading has been obtained to be 28% at depth of tunnel crown, A₅ for diameter D₁. Minimum lateral surface settlement is 2.5 mm at A₅/D₁ based on static loading and is 1.8 mm at A₅/D₁ based on seismic loading. Minimum differences of settlements among various lengths ($y_1 = 27\text{m}$, $y_2 = 29\text{m}$ and $y_3 = 31\text{m}$) of tunnel have been obtained to be 5% at depth of tunnel crown, A₅ (8.5m) for diameter, D₁ (10.5m) under static loading. Minimum value of total lateral settlement is 10 mm at A₅/D₁ location based on static and seismic loading. Differences of compressive settlements

among various lengths of tunnel have been obtained to be 13% at depth of tunnel crown, A_5 for diameter, D_1 under static loading. Minimum longitudinal surface settlement is 3 mm at A_5/D_1 based on static loading and is 0.2 mm at A_5/D_1 based on seismic loading. Minimum value of total longitudinal settlement is 11 mm at A_5/D_1 based on static loading and is 3 mm at A_5/D_1 based on seismic loading.

Minimum differences of volumetric strains among various lengths ($y_1 = 27\text{m}$, $y_2 = 29\text{m}$ and $y_3 = 31\text{m}$) of tunnel have been obtained to be 2.3% under static loading. Volumetric strain varies with the increment of relative depths of tunnel during seismic loading. On the basis of numerical analysis, minimum volumetric strain is 1.5 percent at A_5/D_1 for static loading and is 0.03 percent at A_5/D_1 for seismic loading.

Maximum major principle stress is 160 KPa at A_5/D_1 for static loading and is 158 KPa at A_5/D_1 for seismic loading. On the basis of numerical analysis, minimum volumetric strain is 0.002 percent at A_5/D_3 for static loading and is 0.0005 percent at A_n/D_n for seismic loading.

Lateral and longitudinal accelerations are relatively lower than vertical accelerations. Lateral surface accelerations in 0.25s is 0.9 m/s^2 at A_4/D_1 . Accelerations are fluctuating from zero to one second. This fluctuation rates are relatively high.

Vertical surface displacement is 1.2 mm in 0.6s at A_5/D_1 . Initially uplifts are occurred under seismic loading. Uplifts are higher than settlements. Rate of longitudinal surface settlements are lower than vertical surface settlements. Maximum value of lateral spreading is -1.8 mm at A_5/D_3 .

Longitudinal and lateral settlements are the function of vertical settlements. Based on above analysis results, it is to be noted that suitable depth of tunnel crown and tunnel diameter are 8.5 m (A_5) and 10.5 m (D_1).

CHAPTER FIVE

CONCLUSIONS AND RECOMMENDATIONS

5.1 CONCLUSIONS

Settlements are major issues for tunnel movements. Surface settlements above a tunnel affects the super structures. Settlements of bottom of tunnel generally express the overall (total) settlements of tunnel structures. Such types of settlements are calculated by modified formulae and PLAXIS 3D for long term (static) and seismic loading. Modified formulae are developed by the author, considering plain strain condition. Lateral and longitudinal settlements are the function of vertical settlement based on empirical and analytical formulae. In tunnel structure, strain induced volume losses are the function of settlements. Summary of this research are presented below:

Case study of a tunnel constructed in Barcelona Subway Network Extension Tunnel, Barcelona City, Spain has been used for validation purpose. The results of vertical surface settlements of that study are very close with modified empirical and analytical formulas of the researcher. Difference of vertical surface settlement using modified empirical formula and case study of the Barcelona Subway Network Extension Tunnel, Barcelona City, Spain has been found to be 0.7% under static loading. Case study of a tunnel constructed in Cairo Metro – Line III in Egypt has been used for validation purpose. The results of vertical surface settlement of that study is similar with PLAXIS 3D results of the present analysis. Difference of vertical surface settlement between PLAXIS 3D and the case study of Cairo Metro – Line III in Egypt has been found to be 0.1% under static loading. This result shows good accuracy of present model.

Modified empirical and analytical formulae results are expressed below. Minimum vertical surface settlement has been found to be 30mm at relative depth (ratio between depth of tunnel crown and diameter), A_5/D_1 using modified analytical formula under seismic loading. Vertical settlements of bottom of tunnel have been found to be 25mm and 100mm for seismic and static loading using modified analytical formulae. Minimum lateral surface settlement has been found to be 9 mm at relative depth, A_5/D_1 using modified analytical formulae under static and seismic loading. Minimum lateral settlement at bottom of tunnel has been found to be 10mm at relative depth, A_5/D_1 using modified analytical formulae under static and seismic loading. Minimum longitudinal surface settlement has been found to be 2.6mm at depth of tunnel crown, A_5 (8.5m) for diameter, D_1 based on modified empirical formula for static loading. Variations of longitudinal settlements at bottom of tunnel are constant along depth of tunnel for various diameters based on modified empirical formula. Minimum strain induced volume loss (volumetric strain) has been found to be 0.78% at depth of tunnel crown, A_5 (8.5m) for diameter,

D₁ (10.5m) under static loading. Strain induced volume losses are constant along depth of tunnel for various diameters under seismic loading.

Numerical analysis results by PLAXIS 3D are expressed below. Minimum vertical surface settlement has been found to be 5mm at depth of tunnel crown, A₅ for diameter, D₁ under static loading. Minimum vertical surface settlement has been found to be 2mm at depth of tunnel crown, A₅ for diameter, D₁ under seismic loading. Upward settlement at bottom of tunnel has been found to be 38mm at depth of tunnel crown, A₅ (8.5m) for diameter, D₁ (10.5m) under static loading. Minimum vertical settlement at bottom of tunnel has been found to be 7mm at depth of tunnel crown, A₄ (7.5m) for diameters D₂ (10.8m) and D₃ (11m) under seismic loading. Minimum lateral surface settlement has been found to be 2.5mm at relative depth, A₅/D₁ under static loading. Minimum lateral surface settlement has been found to be 1.8mm at relative depth, A₅/D₁ under seismic loading. Minimum lateral settlement at the bottom of tunnel has been found to be 10mm at depth of tunnel crown, A₅ for diameter, D₁ under static and seismic loading. Minimum longitudinal surface settlement has been found to be 3mm at relative depth, A₅/D₁ under static loading. Minimum longitudinal surface settlement has been found to be 0.2mm at depth of tunnel crown, A₅ (8.5m) for diameter, D₁ under seismic loading. Minimum longitudinal settlement at bottom of tunnel has been found to be 11mm at depth of tunnel crown, A₅ (8.5m) for diameter, D₁ (10.5m) under static loading. Minimum longitudinal settlement at bottom of tunnel has been found to be 3mm at depth of tunnel crown, A₅ (8.5m) for diameter, D₁ under seismic loading. Minimum value of volumetric strain has been obtained to be 1.5% at depth of tunnel crown, A₅ for diameter, D₁ under static loading. Minimum volumetric strain has been found to be 0.03% at depth of tunnel crown, A₅ for diameter, D₁ under seismic loading. Maximum major principle stress has been obtained to be 160 kN/m² for depth of tunnel crown, A₅ for diameter, D₁ under static loading. Maximum major principle stress has been found to be 158 kN/m² at depth of tunnel crown, A₅ for diameter, D₁ under seismic loading. Minimum lateral surface acceleration has been obtained to be 0.2 m/s² at depth of tunnel crown, A₅ for diameter, D₁ in dynamic time, 0.48s. Maximum vertical surface displacement has been found to be 1.2mm at depth of tunnel crown, A₅ for diameter, D₁ in dynamic time, 0.60s.

Maximum surface settlement generally varies from 10mm to 30mm for sandy soil. In this research, most of the surface settlements have been found to be less than 10mm based on numerical analysis under static and seismic loading at depth of tunnel crown, A₅ (8.5m) for diameter, D₁ (10.5m). In others depth of tunnel crown and diameters, settlements slightly differs from those required ranges.

5.2 RECOMMENDATIONS FOR FUTURE STUDIES

Breaking the limitation of this research, future studies have to be necessary. Probable types of future studies are shown in below:

- (1) Tunnel should be passes through the two or three layers that means replacement of homogenous layer with the heterogeneous layers.
- (2) Depth of sand layer should be takes as longer than present depth.
- (3) Tunnel should be analyses for strong seismic loading.
- (4) Inclination of tunnel should be consider for analysis and confliction of soil layer in longitudinal directions would be analyses.
- (5) Seismic fault reason should be consider for analysis and formulae should be develop for that case.
- (6) Lateral movement of tunnel should be consider for analysis.
- (7) More phase should be consider for analysis.
- (8) User define material model should be consider in analysis with the replacement of Mohr-Coulomb material model.
- (9) Small scale laboratory model should be perform for present studies.
- (10) Formulae would be developed for liquefaction analysis.

A lot of future studies are possible based on human thinking power. Such types of future studies are better effect upon underground space technology.

REFERENCES

Alexander, M. (1968) "Plasticity Theory and Application". Macmillan Series in Applied Mechanics Fred Landis, Editor. National Aeronautics and Space Administration. The Macmillan Company, New York.

Attewell, P. B., Yeates, J. & Selby, A. R. (1986). Soil Movements Induced by Tunnelling and their Effects on Pipelines and Structures, Glasgow, Blackie.

Attewell, P. B. & Woodman, J. P. (1982). Predicting the dynamics of ground settlement and its derivatives caused by tunnelling in soil. *Ground Engineering*, Vol.15, No. 8, 13-22 and 36.

BNBC 2006. Bangladesh National Building Code – 2006.

Bernhard M., Martin H., Ulrich M., Gerhard W., "Mechanised Shield Tunnelling", 2nd edition, 2011, Print ISBN: 978-3-433-02995-4, ePDF ISBN: 978-3-433-60150-1, ePub ISBN: 978-3-433-60149-5, mobi ISBN: 978-3-433-60148-8, o-Book ISBN: 978-3-433-60105-1, Ernst & Sohn, A wiley company.

Cording, E. J. (1991). Control of ground movements around a tunnel. General report, Proc. 9th Pan-Am Conf. on Soil Mechanics and Found. Engng., Chile.

Cording, E. J. & Hansmire, W. H. (1975). Displacement around soft ground tunnels. Proc. 5th Pan-Am Conf. on Soil Mech. and Found. Engng., Buenos Aires, Vol. 4, 571-633.

Clough, G. W. & Schmidt, B. (1981). Design and Performance of excavations and tunnels in soft clays. *Soft Clay Engineering*, Amsterdam, 269-276, Elsevier.

David M. Worley, Jack K. Odum, Robert A. Williams, and William J. Stephenson. (2002). A Test Of A Mechanical Multi-Impact Shear-Wave Seismic Source. Open-File Report 01-0440, USGS.

Dowding, C. H., and Rozen, A. (1978). Damage to Rock Tunnels from Earthquake Shaking, *Journal of the Geotechnical Engineering Division, ASCE*, Vol. 104, No. GT2.

Duddeck, H., *Empfehlungen zur Berechnung von Tunneln in Lockergestein* (1980). Herausgegeben vom Arbeitskreis Tunnelbau der Deutschen Gesellschaft für Erd- und Grundbau e.V., Essen, *Bautechnik* 57 (1980) 349- 356.

EUROCODE 8. (2003). Design of Structures for Earthquake Resistance, Draft No. VI, European Committee for Standardization, Brussels.

Franza, A., Marshall, A. M. & Zhou, B. (2018). Greenfield tunnelling in sands: the effects of soil density and relative depth. *Géotechnique* [<https://doi.org/10.1680/jgeot.17.P.091>].

Hashahsh, Y.M.A., Hook, J.J., Schmidt, B., Yao, J.I.C. (2001). Seismic design and Analysis of underground structure. *Tunnelling and Underground space Technology*, Vol. XVI, No.4, pp147-293, San Francisco, CA, USA.

Harris, D. L., Mair, R. J., Burland, J. B. & Standing, J. R. (2000). Compensation grouting to control tilt of Big Ben Clock Tower. *Int. Symposium on Geotechnical Aspects of Underground Construction in Soft Ground* (eds. Fujita, Kusakabe and Miyazaki), 225-232, Balkema.

Hill, R. (1950). *The Mathematical Theory of Plasticity*. Oxford University Press, London, U.K.

Hunt, D. (2004). *Predicting The Ground Movements Above Twin Tunnels Constructed In London Clay*. PhD Thesis. Department of Civil Engineering, School of Engineering, The University of Birmingham.

Kilany – EI M.E., Kasaby – EL E.A. and Mohab R.A. “Numerical Analysis of Tunnel Boring Machine in Soft Ground”, *Jokull Journal*, ISSN 0449 – 0576, vol. 67, No. 5, May 2017.

Loganathan, N. (2011). *An Innovative Method For Assessing Tunnelling-Induced Risks To Adjacent Structures*. PB 2009 William Barclay Parsons Fellowship Monograph 25.

Loganathan, N. & Poulos, H. G. (1998). Analytical Prediction For Tunnelling Induced Ground Movement In Clays. *Journal of Geotechnical and Geoenvironmental Engineering / September 1998*.

Marshall, A. M. & Franza, A. (2017). Discussion of “Observation of ground movement with existing pile groups due to tunneling in sand using centrifuge modelling” by Ittichai Boonsiri and Jiro Takemura. *Geotech. Geol. Engng* 35, No. 1, 535–539, <https://doi.org/10.1007/s10706-016-0083-x>.

Mair, R. J. & Taylor, R. N. (1997). Bored tunnelling in the urban environment. In *14th International conference on soil mechanics and foundation engineering*, pages 2353–2385. 5, 10, 14, 169.

Mair, R. J. (1993). Developments in geotechnical engineering research: application to tunnels and deep excavations *Proc. Inst. Civil Engineers, Civil Engineering*, Vol.93, 27-41.

Marto, A., Hajihassani, M., Makhtar, A. M. & Kasim, F. (2014). A Review on the Laboratory Model Tests of Tunnels in Soft Soils. *Malaysian Journal of Civil Engineering*. 26(1): 89-98.

O'Reilly, M. P. & New, B. M. (1982). Settlements above tunnels in the United Kingdom - their magnitude and prediction. In *Tunnelling 82, Papers Presented at the 3rd International Symposium*, London, England, Brighton, England. Inst of Mining and Metallurgy. 13, 14, 22.

O'Rourke, M.J. & Liu, X. (1999). Response of buried pipelines subject to Earthquake effects. Monograph No.III, MCEER (Multidisciplinary Center for Earthquake Engineering Research) Publications, University at Buffalo, Red Jacket Quadrangle, Buffalo, NY 14261.

Owen, G. N., and Scholl, R. E. (1981). *Earthquake Engineering of Large Underground Structures*, prepared for the Feral Highway Administration, FHWA/RD-80/195.

Paolucci, R., Pitikalis, k. (2007). Seismic risk assessment of underground structures under transient ground deformation. In Pitikalis, K. (editor). *Earthquake Geotechnical Engineering*. Chapter 18, pp 433-459. SpringerVienna.

Pescara, M., Gaspari G. M., & Repetto, L. (2011). Design of underground structures under seismic conditions: a long deep tunnel and a metro tunnel. Geodata Engineering SpA, Torino, Italy.

PLAXIS 3D, Reference Manual, Anniversary Edition.

PLAXIS, Material Models Manual, 2015.

PLAXIS, Scientific Manual, 2015.

Power, M. S., and Rosidi, D. (1998). *Seismic Vulnerability of Tunnels and Underground Structures Revisited*, North American Tunneling.

Power, M. S., Rosidi, D. & Kaneshiro, J. (1996). Strawman: screening, evaluation, and retrofit design of tunnels. Report Draft. Vol. III, National Center for Earthquake Engineering Research, Buffalo, New York.

Rankin, W. J. (1988). "Ground Movements Resulting from Urban Tunnelling: Predictions and Effects." *Engineering Geology of Underground Movements Geological Society*, 76-88.

Salimi, A.R., Esmaeili, M., & Salehi, B. (2013). Analysis of a TBM Tunnelling Effect on Surface Subsidence: A Case Study from Tehran, Iran. *International Journal of Environmental, Chemical, Ecological, Geological and Geophysical Engineering* Vol:7, No:6, 2013.

Sharma, S., & Judd, W. R. (1991). *Underground Opening Damage from Earthquakes*, Engineering Geology, Vol. 30, 1991.

Smith, I. M. and Griffiths, D. V. (1982). *Programming the Finite Element Method*. Jhon Willy & Sons, Chisester, U.K. Second Edition.

St. John, C. M., and Zahrah, T. F. (1987). *Aseismic Design of Underground Structures, Tunneling and Underground Space Technology*, Vol. 2, No. 2.

Szechy. (1969). K.: *Tunnelbau*. Springer, Wien.

Technical Manual for Design and Construction of Road Tunnels — Civil Elements. Publication No. FHWA-NHI-10-034. December 2009.

Verruijt, A. & Booker, J. R. (1996). Surface settlements due to deformation of a tunnel in an elastic half plane, *Geotechnique*, Vol. 46, No. 4, 753-756.

Vorster, T. E., Klar, A., Soga, K., & Mair, R. J. (2005). Estimating the effects of tunneling on existing pipelines. *Journal of Geotechnical and Geoenvironmental Engineering*, pages 1399–1410. 8, 22, 52, 65, 117.

Wang, J. N. (1993). *Seismic design of tunnel – A simple state of the art design approach*. Parson Brinckerhoff Quade & Douglas, Inc., New York, Monograph 7.

Zhou, B. (2014). *Tunnelling-induced ground displacements in sand*. PhD thesis, University of Nottingham (<http://eprints.nottingham.ac.uk/28394/1/2014%20Bo%20Zhou%20PhD%20thesis.pdf>).

APPENDIX A

A.1 Calculation of Maximum Vertical Surface Settlement for Long Term Loading by Modified Empirical Formula

Author modified equation of maximum vertical surface settlement is –

$$V_{(z),max.} = 0.0045 \frac{D^2}{H} \quad (A.1)$$

Taken some value such as

Diameter of Tunnel, $D = 10.5\text{m}$

Thickness of Tunnel, $t = 0.5\text{ m}$

Depth of Tunnel Crown, $A_1 = 4.5\text{m}$

Tunnel Depth, $H = 4.5 + (10.5/2) + 0.5 = 10.25\text{m}$

Now,

$$V_{(z),max.} = 0.0045 \frac{(10.5)^2}{10.25} = 0.0484\text{m} = 48.4\text{mm}$$

Maximum vertical surface settlement for long term loading is 48.4mm.

A.2 Calculation of Maximum Vertical Surface Settlement for Long Term Loading by Modified Analytical Formula

Author modified equation is –

$$V_{(z)max.} = \frac{5}{1000} R^2 H \left(\frac{1}{r_1^2} - \frac{1}{r_2^2} \right) + 0.001 R^2 H^3 \left[\frac{1}{r_1^4} - \frac{1}{r_2^4} \right] + \frac{0.01 R^2}{m} \left[\frac{(m+1)H}{r_2^2} \right] + \frac{0.002 R^2 H^3}{r_2^4} \quad (A.2)$$

Where,

Radius of Tunnel, $R = 10.5/2 = 5.25\text{m}$

Thickness of Tunnel, $t = 0.5$ m

Depth of Tunnel Crown, $A_1 = 4.5$ m

Tunnel Depth, $H = 4.5 + (10.5/2) + 0.5 = 10.25$ m

$$r_1^2 = (-10.25)^2 = 105.0625m^2$$

$$r_2^2 = (10.25)^2 = 105.0625m^2$$

$$r_1^2 = r_2^2$$

Soil poisson's ratio, $\nu = 0.250$

$$m = 1/(1 - (2 * 0.250)) = 2$$

Now,

$$\begin{aligned} V_{(z)max.} &= 0 + 0 + \frac{0.01(5.25)^2}{2} \left[\frac{(2 + 1)(10.25)}{105.0625} \right] + \frac{0.002(5.25)^2(10.25)^3}{11038.1289} = 0.04034 + 0.00538 \\ &= 0.0457m = 45.7mm \end{aligned}$$

Maximum vertical surface settlement for long term loading is 45.7mm.

A.3 Calculation of Maximum Vertical Surface Settlement for Seismic Loading by Modified Analytical Formula

Author modified equation is –

$$V_{(z)max.} = 0.005R^2H \left(\frac{1}{r_1^2} - \frac{1}{r_2^2} \right) + \frac{0.01R^2}{m} \left[\frac{(m + 1)H}{r_2^2} \right] \quad (A.3)$$

Where,

Radius of Tunnel, $R = 10.5/2 = 5.25$ m

Thickness of Tunnel, $t = 0.5$ m

Depth of Tunnel Crown, $A_1 = 4.5$ m

Tunnel Depth, $H = 4.5 + (10.5/2) + 0.5 = 10.25$ m

$$r_1^2 = (-10.25)^2 = 105.0625m^2$$

$$r_2^2 = (10.25)^2 = 105.0625m^2$$

$$r_1^2 = r_2^2$$

Soil poisson's ratio, $\nu = 0.250$

$$m = 1/(1 - (2 * 0.250)) = 2$$

Now,

$$V_{(z),max.} = 0 + \frac{0.01(5.25)^2}{2} \left[\frac{(2 + 1)(10.25)}{105.0625} \right] = 0.04034m = 40.34mm$$

Maximum vertical surface settlement for seismic loading is 40.34mm.

A.4 Calculation of Maximum Total Vertical Settlement for Long Term Loading by Modified Empirical Formula

Author modified equation is –

$$V_{(z),max.} = 0.0045 \frac{D^2}{(H - z)} \quad (A.4)$$

Where,

Diameter of Tunnel, $D = 10.5m$

Thickness of Tunnel, $t = 0.5 m$

Depth of Tunnel Crown, $A_1 = 4.5m$

Tunnel Depth, $H = 4.5 + (10.5/2) + 0.5 = 10.25m$

Any distance from free surface, $z = 4.5 + 10.5 + 1.0 = 16m$

Now,

$$V_{(z),max.} = 0.0045 \frac{(10.5)^2}{(10.25 - 16)} = -0.0863m = -86.3mm$$

Maximum total vertical settlement for long term loading is -86.3mm.

A.5 Calculation of Maximum Total Vertical Settlement for Long Term Loading by Modified Analytical Formula

Author modified equation is –

$$\begin{aligned}
 V_{(z)max.} = & -0.005R^2 \left(\frac{z_1}{r_1^2} + \frac{z_2}{r_2^2} \right) + 0.001R^2 \left[\frac{z_1(-z_2^2)}{r_1^4} + \frac{z_2(-z_1^2)}{r_2^4} \right] \\
 & + \frac{0.01R^2}{m} \left[\frac{(m+1)z_2}{r_2^2} + \frac{mz_1(-z_2^2)}{r_2^4} \right] \\
 & - 0.002R^2H \left[\frac{-z_2^2}{r_2^4} + \frac{m}{m+1} \frac{2zz_2(-z_2^2)}{r_2^6} \right]
 \end{aligned} \tag{A.5}$$

Where,

Radius of Tunnel, $R = 10.5/2 = 5.25\text{m}$

Thickness of Tunnel, $t = 0.5 \text{ m}$

Depth of Tunnel Crown, $A_1 = 4.5\text{m}$

Tunnel Depth, $H = 4.5 + (10.5/2) + 0.5 = 10.25\text{m}$

Any distance from free surface, $z = 4.5 + 10.5 + 1.0 = 16\text{m}$

$$z_1 = 16 - 10.25 = 5.75\text{m}$$

$$z_2 = 16 + 10.25 = 26.25\text{m}$$

$$z_1^2 = (5.75)^2 = 33.0625\text{m}^2$$

$$z_2^2 = (26.25)^2 = 689.0625m^2$$

$$r_1^2 = 33.0625m^2$$

$$r_2^2 = 689.0625m^2$$

$$r_1^4 = 1093.1289m^4$$

$$r_2^4 = 474807.1289m^4$$

$$r_2^6 = 327171787.3m^6$$

Soil poisson's ratio, $\nu = 0.250$

$$m = 1/(1 - (2 * 0.250)) = 2$$

Now,

$$\begin{aligned} V_{(z)max.} &= -0.005(5.25)^2 \left(\frac{5.75}{33.0625} + \frac{26.25}{689.0625} \right) \\ &+ 0.001(5.25)^2 \left[\frac{(5.75)(-689.0625)}{1093.1289} + \frac{(26.25)(-689.0625)}{474807.1289} \right] \\ &+ \frac{0.01(5.25)^2}{2} \left[\frac{(2+1)(26.25)}{689.0625} + \frac{(32)(-689.0625)}{474807.1289} \right] \\ &- 0.002(5.25)^2(10.25) \left[\frac{-689.0625}{474807.1289} + \frac{2}{2+1} \frac{(840)(-689.0625)}{327171787.3} \right] \\ &= -0.02922 - 0.10095 + 0.00935 + 0.00149 = -0.1193m = -119.3mm \end{aligned}$$

Maximum total vertical settlement for long term loading is -119.3mm.

A.6 Calculation of Maximum Total Vertical Settlement for Seismic Loading by Modified Analytical Formula

Author modified equation is –

$$V_{(z)max.} = -0.005R^2 \left(\frac{z_1}{r_1^2} + \frac{z_2}{r_2^2} \right) + \frac{0.01R^2}{m} \left[\frac{(m+1)z_2}{r_2^2} + \frac{mz(-z_2^2)}{r_2^4} \right] \quad (A.6)$$

Where,

Radius of Tunnel, $R = 10.5/2 = 5.25\text{m}$

Thickness of Tunnel, $t = 0.5\text{ m}$

Depth of Tunnel Crown, $A_1 = 4.5\text{m}$

Tunnel Depth, $H = 4.5 + (10.5/2)+0.5 = 10.25\text{m}$

Any distance from free surface, $z = 4.5 + 10.5 + 1.0 = 16\text{m}$

$$z_1 = 16 - 10.25 = 5.75\text{m}$$

$$z_2 = 16 + 10.25 = 26.25\text{m}$$

$$z_2^2 = (26.25)^2 = 689.0625\text{m}^2$$

$$r_1^2 = 33.0625\text{m}^2$$

$$r_2^2 = 689.0625\text{m}^2$$

$$r_2^4 = 474807.1289\text{m}^4$$

Soil poisson's ratio, $\nu = 0.250$

$$m = 1/(1 - (2 * 0.250)) = 2$$

Now,

$$\begin{aligned} V_{(z)max.} &= -0.005(5.25)^2 \left(\frac{5.75}{33.0625} + \frac{26.25}{689.0625} \right) \\ &\quad + \frac{0.01(5.25)^2}{2} \left[\frac{(2+1)(26.25)}{689.0625} + \frac{(32)(-689.0625)}{474807.1289} \right] = -0.02922 + 0.00935 \\ &= -0.01987\text{m} = -19.9\text{mm} \end{aligned}$$

Maximum total vertical settlement for seismic loading is -19.9mm.

A.7 Calculation of Maximum Lateral Surface Settlement for Long Term Loading by Modified Empirical Formula

Author modified equation is –

$$U_{(x),max.} = V_{(z),max.} \frac{A + D}{4H} \quad (A.7)$$

Taken some value such as

Diameter of Tunnel, $D = 10.5\text{m}$

Thickness of Tunnel, $t = 0.5\text{ m}$

Depth of Tunnel Crown, $A_1 = 4.5\text{m}$

Tunnel Depth, $H = 4.5 + (10.5/2) + 0.5 = 10.25\text{m}$

$$V_{(z),max.} = 48.4\text{mm}$$

Now,

$$U_{(x),max.} = 48.4 \frac{(4.5 + 10.5)}{4(10.25)} = 17.71\text{mm}$$

Maximum lateral surface settlement for long term loading is 17.71mm.

A.8 Calculation of Maximum Lateral Surface Settlement for Long Term Loading by Modified Analytical Formula

Author modified equation is –

$$\begin{aligned} U_{(x),max.} = & 0.00125R^2 \left(\frac{(A + D)}{r_1^2} + \frac{(A + D)}{r_2^2} \right) \\ & - 0.0000625R^2 \left[\frac{z_1((A + D)^2 - 16kz_1^2)}{r_1^4} + \frac{((A + D)^3 - (A + D)16kz_2^2)}{4r_2^4} \right] \\ & + \frac{0.0025(A + D)R^2}{m} \left(\frac{1}{r_2^2} \right) \\ & + \frac{0.001R^2(A + D)H}{(m + 1)} \left[\frac{z_2}{r_2^4} \right] \end{aligned} \quad (A.8)$$

Where,

Radius of Tunnel, $R = 10.5/2 = 5.25\text{m}$

Thickness of Tunnel, $t = 0.5\text{ m}$

Diameter of Tunnel, $D = 10.5\text{m}$

Depth of Tunnel Crown, $A_1 = 4.5\text{m}$

Tunnel Depth, $H = 4.5 + (10.5/2) + 0.5 = 10.25\text{m}$

$$z_1 = 0 - 10.25 = -10.25\text{m}$$

$$z_2 = 0 + 10.25 = 10.25\text{m}$$

$$z_2^2 = (10.25)^2 = 105.0625\text{m}^2$$

$$r_1^2 = \left[(0.25(4.5 + 10.5))^2 + (-10.25)^2 \right] \text{m}^2 = 119.125\text{m}^2$$

$$r_2^2 = 119.125\text{m}^2$$

$$r_2^4 = 14190.766\text{m}^4$$

Soil poisson's ratio, $\nu = 0.250$

$$m = 1/(1 - (2 * 0.250)) = 2$$

$$k = 0.250 (1 - 0.250) = 0.1875$$

Now,

$$\begin{aligned} U_{(x),max.} &= 0.00125(5.25)^2 \left(\frac{(4.5 + 10.5)}{119.125} + \frac{(4.5 + 10.5)}{119.125} \right) \\ &\quad - 0.0000625(5.25)^2 \left[\frac{(-10.25)((4.5 + 10.5)^2 - 315.1875)}{14190.766} \right. \\ &\quad \left. + \frac{((4.5 + 10.5)^3 - (4.5 + 10.5)(315.1875))}{56763.064} \right] \\ &\quad + \frac{0.0025(4.5 + 10.5)(5.25)^2}{2} \left(\frac{1}{119.125} \right) \\ &\quad + \frac{0.001(5.25)^2(4.5 + 10.5)(10.25)}{(2 + 1)} \left[\frac{10.25}{14190.766} \right] \\ &= 0.00868 - 0.00007 + 0.00434 + 0.00102 = 0.01397\text{m} = 14.0\text{mm} \end{aligned}$$

Maximum lateral surface settlement for long term loading is 14.0mm.

A.9 Calculation of Maximum Lateral Surface Settlement for Seismic Loading by Modified Empirical Formula

Author modified equation is –

$$\Delta_{(x),max.} = f \frac{a_1 g S C k}{C_s} (C_d - H) \quad (A.9)$$

Taken some value such as Diameter of Tunnel, $D = 10.5\text{m}$

Thickness of Tunnel, $t = 0.5\text{ m}$

Depth of Tunnel Crown, $A_1 = 4.5\text{m}$

Tunnel Depth, $H = 4.5 + (10.5/2) + 0.5 = 10.25\text{m}$

Factor, $a_1 = 0.30$

$g = 9.81\text{ m/s}^2$

Soil Factor, $S = 1.15$

Factor, $C = 0.9$

Factor, $k = 142\text{s}$

Modified Factor, $f = 10$

$C_s = 3\text{km/s}$

$C_d = 27.5\text{m}$

Now,

$$\Delta_{(x),max.} = 10 \frac{(0.30 * 9.81 * 1.15 * 0.9 * 142)}{3000} (27.5 - 10.25) = 24.87\text{mm}$$

Maximum lateral surface settlement for seismic loading is 24.87mm.

A.10 Calculation of Maximum Lateral Surface Settlement for Seismic Loading by Modified Analytical Formula

Author modified equation is –

$$U_{(x),max.} = 0.00125R^2 \left(\frac{(A + D)}{r_1^2} + \frac{(A + D)}{r_2^2} \right) + \frac{0.0025(A + D)R^2}{m} \left(\frac{1}{r_2^2} \right) \quad (A.10)$$

Where,

$$\text{Radius of Tunnel, } R = 10.5/2 = 5.25\text{m}$$

$$\text{Thickness of Tunnel, } t = 0.5 \text{ m}$$

$$\text{Diameter of Tunnel, } D = 10.5\text{m}$$

$$\text{Depth of Tunnel Crown, } A_1 = 4.5\text{m}$$

$$\text{Tunnel Depth, } H = 4.5 + (10.5/2) + 0.5 = 10.25\text{m}$$

$$z_1 = 0 - 10.25 = 10.25\text{m}$$

$$z_2 = 0 + 10.25 = 10.25\text{m}$$

$$r_1^2 = 119.125\text{m}^2$$

$$r_2^2 = 119.125\text{m}^2$$

$$\text{Soil poisson's ratio, } \nu = 0.250$$

$$m = 1/(1 - (2 * 0.250)) = 2$$

Now,

$$\begin{aligned} U_{(x),max.} &= 0.00125(5.25)^2 \left(\frac{(4.5 + 10.5)}{119.125} + \frac{(4.5 + 10.5)}{119.125} \right) \\ &+ \frac{0.0025(4.5 + 10.5)(5.25)^2}{2} \left(\frac{1}{119.125} \right) = 0.00868 + 0.00434 = 0.01302\text{m} \\ &= 13.02\text{mm} \end{aligned}$$

Maximum lateral surface settlement for seismic loading is 13.02mm.

A.11 Calculation of Maximum Total Lateral Settlement for Long Term Loading by Modified Empirical Formula

Author modified equation is –

$$U_{(x),max.} = V_{(z),max.} \frac{A + D}{4(H - z)} \quad (A. 11)$$

Taken some value such as

Diameter of Tunnel, $D = 10.5\text{m}$

Thickness of Tunnel, $t = 0.5\text{ m}$

Depth of Tunnel Crown, $A_1 = 4.5\text{m}$

Tunnel Depth, $H = 4.5 + (10.5/2) + 0.5 = 10.25\text{m}$

$$V_{(z),max.} = -86.3\text{mm}$$

Any distance from free surface, $z = 4.5 + 10.5 + 1.0 = 16\text{m}$

Now,

$$U_{(x),max.} = -86.3 \frac{(4.5 + 10.5)}{4(10.25 - 16)} = 56.3\text{mm}$$

Maximum total lateral settlement for long term loading is 56.3mm.

A.12 Calculation of Maximum Total Lateral Settlement for Long Term Loading by Modified Analytical Formula

Author modified equation is –

$$\begin{aligned}
U_{(x),max.} = & 0.00125R^2 \left(\frac{(A + D)}{r_1^2} + \frac{(A + D)}{r_2^2} \right) \\
& - 0.0000625R^2 \left[\frac{z_1((A + D)^2 - 16kz_1^2)}{r_1^4} + \frac{((A + D)^3 - (A + D)16kz_2^2)}{4r_2^4} \right] \\
& + \frac{0.0025(A + D)R^2}{m} \left(\frac{1}{r_2^2} - \frac{2mzz_2}{r_2^4} \right) \\
& + \frac{0.001R^2(A + D)H}{(m + 1)} \left[\frac{z_2}{r_2^4} + \frac{mz((A + D)^2 - 48z_2^2)}{16r_2^6} \right]
\end{aligned} \tag{A.12}$$

Where,

Radius of Tunnel, $R = 10.5/2 = 5.25\text{m}$

Thickness of Tunnel, $t = 0.5 \text{ m}$

Diameter of Tunnel, $D = 10.5\text{m}$

Depth of Tunnel Crown, $A_1 = 4.5\text{m}$

Tunnel Depth, $H = 4.5 + (10.5/2) + 0.5 = 10.25\text{m}$

$$z_1 = 16 - 10.25 = 5.75\text{m}$$

$$z_2 = 16 + 10.25 = 26.25\text{m}$$

$$z_2^2 = (26.25)^2 = 689.0625\text{m}^2$$

$$r_1^2 = 47.125\text{m}^2$$

$$r_2^2 = 703.125\text{m}^2$$

$$r_2^4 = 494384.766\text{m}^4$$

Soil poisson's ratio, $\nu = 0.250$

$$m = 1/(1 - (2 * 0.250)) = 2$$

$$k = 0.250 (1 - 0.250) = 0.1875$$

Any distance from free surface, $z = 4.5 + 10.5 + 1.0 = 16\text{m}$

$$r_2^6 = 347614288.3\text{m}^6$$

$$r_1^4 = 2220.766\text{m}^4$$

Now,

$$\begin{aligned} U_{(x),max.} &= 0.00125(5.25)^2 \left(\frac{(4.5 + 10.5)}{47.125} + \frac{(4.5 + 10.5)}{703.125} \right) \\ &\quad - 0.0000625(5.25)^2 \left[\frac{(5.75)((4.5 + 10.5)^2 - 99.1875)}{2220.766} \right. \\ &\quad \left. + \frac{((4.5 + 10.5)^3 - 31007.8125)}{1977539.064} \right] \\ &\quad + \frac{0.0025(4.5 + 10.5)(5.25)^2}{2} \left(\frac{1}{703.125} - \frac{1680}{494384.766} \right) \\ &\quad + \frac{0.001(5.25)^2(4.5 + 10.5)(10.25)}{(2 + 1)} \left[\frac{26.25}{494384.766} + \frac{32((4.5 + 10.5)^2 - 33075)}{5561828613} \right] \\ &= 0.01170 - 0.00054 - 0.00102 - 0.00019 = 0.00995\text{m} = 10\text{mm} \end{aligned}$$

Maximum total lateral settlement for long term loading is 10.0mm.

A.13 Calculation of Maximum Total Lateral Settlement for Seismic Loading by Modified Empirical Formula

Author modified equation is –

$$\Delta_{(x),max.} = f \frac{a_1 g S C k}{C_s} (C_d - (H - z)) \quad (A.13)$$

Taken some value such as

Diameter of Tunnel, $D = 10.5\text{m}$

Thickness of Tunnel, $t = 0.5\text{ m}$

Depth of Tunnel Crown, $A_1 = 4.5\text{m}$

Tunnel Depth, $H = 4.5 + (10.5/2)+0.5 = 10.25\text{m}$

Factor, $a_1 = 0.30$

$g = 9.81\text{ m/s}^2$

Soil Factor, $S = 1.15$

Factor, $C = 0.9$

Factor, $k = 142\text{s}$

Modified Factor, $f = 10$

$C_s = 3\text{km/s}$

$C_d = 27.5\text{m}$

Any distance from free surface, $z = 4.5 + 10.5 + 1.0 = 16\text{m}$

Now,

$$\Delta_{(x),max.} = 10 \frac{(0.30 * 9.81 * 1.15 * 0.9 * 142)}{3000} (27.5 - (10.25 - 16)) = 47.94\text{mm}$$

Maximum total lateral settlement for seismic loading is 47.94mm.

A.14 Calculation of Maximum Total Lateral Settlement for Seismic Loading by Modified Analytical Formula

Author modified equation is –

$$U_{(x),max.} = 0.00125R^2 \left(\frac{(A+D)}{r_1^2} + \frac{(A+D)}{r_2^2} \right) + \frac{0.0025(A+D)R^2}{m} \left(\frac{1}{r_2^2} - \frac{2mzz_2}{r_2^4} \right) \quad (A.14)$$

Where,

$$\text{Radius of Tunnel, } R = 10.5/2 = 5.25\text{m}$$

$$\text{Thickness of Tunnel, } t = 0.5 \text{ m}$$

$$\text{Diameter of Tunnel, } D = 10.5\text{m}$$

$$\text{Depth of Tunnel Crown, } A_1 = 4.5\text{m}$$

$$\text{Tunnel Depth, } H = 4.5 + (10.5/2) + 0.5 = 10.25\text{m}$$

$$z_1 = 16 - 10.25 = 5.75\text{m}$$

$$z_2 = 16 + 10.25 = 26.25\text{m}$$

$$z_2^2 = (26.25)^2 = 689.0625\text{m}^2$$

$$r_1^2 = 47.125\text{m}^2$$

$$r_2^2 = 703.125\text{m}^2$$

$$r_2^4 = 494384.766\text{m}^4$$

$$\text{Soil poisson's ratio, } \nu = 0.250$$

$$m = 1/(1 - (2 * 0.250)) = 2$$

$$k = 0.250 (1 - 0.250) = 0.1875$$

Any distance from free surface, $z = 4.5 + 10.5 + 1.0 = 16\text{m}$

$$r_2^6 = 347614288.3\text{m}^6$$

$$r_1^4 = 2220.766\text{m}^4$$

Now,

$$\begin{aligned} U_{(x),max.} &= 0.00125(5.25)^2 \left(\frac{(4.5 + 10.5)}{47.125} + \frac{(4.5 + 10.5)}{703.125} \right) \\ &+ \frac{0.0025(4.5 + 10.5)(5.25)^2}{2} \left(\frac{1}{703.125} - \frac{1680}{494384.766} \right) = 0.01170 - 0.00102 \\ &= 0.01068\text{m} = 10.7\text{mm} \end{aligned}$$

Maximum total lateral settlement for seismic loading is 10.7mm.

A.15 Calculation of Maximum Longitudinal Surface Settlement for Long Term Loading by Modified Empirical Formula

Author modified equation is –

$$U_{(y),max.} = \frac{V_{(z),max.}}{H} \quad (\text{A. 15})$$

Taken some value such as

Diameter of Tunnel, $D = 10.5\text{m}$

Thickness of Tunnel, $t = 0.5 \text{ m}$

Depth of Tunnel Crown, $A_1 = 4.5\text{m}$

Tunnel Depth, $H = 4.5 + (10.5/2) + 0.5 = 10.25\text{m}$

$$V_{(z),max.} = 48.4\text{mm}$$

Now,

$$U_{(y),max.} = \frac{48.4}{10.25} = 4.7mm$$

Maximum longitudinal surface settlement for long term loading is 4.7mm.

A.16 Calculation of Maximum Total Longitudinal Settlement for Long Term Loading by Modified Empirical Formula

Author modified equation is –

$$U_{(y),max.} = \frac{V_{(z),max.}}{(H - z)} \quad (A. 16)$$

Taken some value such as

Diameter of Tunnel, $D = 10.5m$

Thickness of Tunnel, $t = 0.5 m$

Depth of Tunnel Crown, $A_1 = 4.5m$

Tunnel Depth, $H = 4.5 + (10.5/2) + 0.5 = 10.25m$

$$V_{(z),max.} = -86.3mm$$

Any distance from free surface, $z = 4.5 + 10.5 + 1.0 = 16m$

Now,

$$U_{(y),max.} = \frac{-86.3}{(10.25 - 16)} = 15mm$$

Maximum total longitudinal settlement for long term loading is 15mm.

A.17 Calculation of Volumetric Strain for Long Term Loading by Modified Analytical Formula

Author modified equation is –

$$\varepsilon_{vl} = 0.01003 \exp \left[-\frac{0.69}{(1 + t + 0.5D)^2} \right] \quad (A.17)$$

Where,

Thickness of Tunnel, $t = 0.5\text{m}$

Diameter of Tunnel, $D = 10.5\text{m}$

Now,

$$\varepsilon_{vl} = 0.01003 \exp \left[-\frac{0.69}{(1 + 0.5 + 5.25)^2} \right] = 0.00988$$

Volumetric strain for long term loading is 0.00988.

A.18 Calculation of Volumetric Strain for Seismic Loading by Modified Analytical Formula

Author modified equation is –

$$\varepsilon_{vs} = \frac{V}{6000} + \frac{A_c(2t + D)}{36000000\sqrt{2}} \quad (A.18)$$

Where,

Seismic Wave Velocity, $V = 0.14472\text{m/s}$

Seismic Acceleration, $A_c = 3.5\text{m/s}^2$

Thickness of Tunnel, $t = 0.5\text{m}$

Diameter of Tunnel, $D = 10.5\text{m}$

Now,

$$\varepsilon_{vs} = \frac{0.14472}{6000} + \frac{3.5(1 + 10.5)}{36000000\sqrt{2}} = 0.000025$$

Volumetric strain for seismic loading is 0.000025.

APPENDIX B

B.1 Variation of Diameter

Symbol, D_n	Value in meter
D_1	10.5
D_2	10.8
D_3	11.0

B.2 Variation of Longitudinal Length of Tunnel

Symbol, y_n	Value in meter
y_1	27
y_2	29
y_3	31

B.3 Variation of Depth of Tunnel Crown

Symbol, A_n	Value in meter
A_1	4.5
A_2	5.5
A_3	6.5
A_4	7.5
A_5	8.5

B.4 Maximum Vertical Surface Settlement for Diameter, D_1 Above A Tunnel (mm)

Longitudi nal length of tunnel, y_n (m)	Ratio A_n/D_1	Long term loading (PLAXIS 3D)	Seismic loading (PLAXIS 3D)	Modified empirical formulae (long term loading) (2D)	Modified Analytical formulae (long term loading) (2D)	Modified Analytical formulae (seismic loading) (2D)
27.00	0.4286	-11.60	-2.30	50.60	48.10	42.40
	0.5238	-8.50	-1.90	45.90	43.60	38.50
	0.6190	3.60	1.60	42.00	39.90	35.20
	0.7143	4.70	1.70	38.70	36.80	32.40
	0.8095	6.70	1.70	35.90	34.10	30.10
29.00	0.4286	-14.00	-3.30	50.60	48.10	42.40
	0.5238	9.80	-2.60	45.90	43.60	38.50
	0.6190	-3.60	-2.30	42.00	39.90	35.20
	0.7143	-4.70	-2.00	38.70	36.80	32.40
	0.8095	6.70	1.80	35.90	34.10	30.10
31.00	0.4286	-15.70	-4.40	50.60	48.10	42.40
	0.5238	-10.70	-3.40	45.90	43.60	38.50
	0.6190	-4.60	-2.90	42.00	39.90	35.20
	0.7143	4.90	-2.60	38.70	36.80	32.40
	0.8095	6.80	-2.20	35.90	34.10	30.10

B.5 Maximum Vertical Surface Settlement for Diameter, D_2 Above A Tunnel (mm)

Longitudinal length of tunnel, y_n (m)	Ratio A_n/D_2	Long term loading (PLAXIS 3D)	Seismic loading (PLAXIS 3D)	Modified empirical formulae (long term loading) (2D)	Modified Analytical formulae (long term loading) (2D)	Modified Analytical formulae (seismic loading) (2D)
27.00	0.4167	-12.20	-2.40	52.70	50.10	44.20
	0.5093	-8.70	-2.90	47.80	45.50	40.10
	0.6019	-23.50	-1.80	43.80	41.70	36.80
	0.6944	5.20	1.80	40.40	38.40	33.90
	0.7870	7.30	1.90	37.50	35.70	31.50
29.00	0.4167	-14.70	-3.60	52.70	50.10	44.20
	0.5093	-10.00	-2.80	47.80	45.50	40.10
	0.6019	-27.90	-2.40	43.80	41.70	36.80
	0.6944	5.10	-2.10	40.40	38.40	33.90
	0.7870	7.30	1.90	37.50	35.70	31.50
31.00	0.4167	-16.70	-4.60	52.70	50.10	44.20
	0.5093	-11.10	-3.70	47.80	45.50	40.10
	0.6019	-30.90	-3.10	43.80	41.70	36.80
	0.6944	5.10	-2.70	40.40	38.40	33.90
	0.7870	7.30	-2.30	37.50	35.70	31.50

B.6 Maximum Vertical Surface Settlement for Diameter, D_3 Above A Tunnel (mm)

Longitudinal length of tunnel, y_n (m)	Ratio A_n/D_3	Long term loading (PLAXIS 3D)	Seismic loading (PLAXIS 3D)	Modified empirical formulae (long term loading) (2D)	Modified Analytical formulae (long term loading) (2D)	Modified Analytical formulae (seismic loading) (2D)
27.00	0.4091	-12.40	-2.50	54.10	51.40	45.40
	0.5000	-8.90	-2.10	49.20	46.80	41.30
	0.5909	-6.40	-1.80	45.10	42.90	37.80
	0.6818	5.70	1.90	41.60	39.60	34.90
	0.7727	7.60	2.00	38.60	36.70	32.40
29.00	0.4091	-15.00	-3.70	54.10	51.40	45.40
	0.5000	-10.30	-2.90	49.20	46.80	41.30
	0.5909	-7.20	-2.40	45.10	42.90	37.80
	0.6818	5.60	-2.20	41.60	39.60	34.90
	0.7727	7.60	2.00	38.60	36.70	32.40
31.00	0.4091	-17.20	-4.80	54.10	51.40	45.40
	0.5000	-11.50	-3.70	49.20	46.80	41.30
	0.5909	-7.70	-3.20	45.10	42.90	37.80
	0.6818	5.50	-2.70	41.60	39.60	34.90
	0.7727	7.60	-2.40	38.60	36.70	32.40

B.7 Maximum Total Vertical Settlement for Diameter, D_1 of a Tunnel (mm)

Longitudinal length of tunnel, y_n (m)	Ratio A_n/D_1	Long term loading (PLAXIS 3D)	Seismic loading (PLAXIS 3D)	Modified empirical formulae (long term loading) (2D)	Modified Analytical formulae (long term loading) (2D)	Modified Analytical formulae (seismic loading) (2D)
27	0.4286	-44.5	-13.3	-93.9	-138.1	-21.9
	0.5238	-42.7	-7.8	-93.9	-157.9	-22.1
	0.6190	-41	7.4	-93.9	-179.3	-22.3
	0.7143	-39.4	-5.5	-93.9	-202.2	-22.5
	0.8095	-37.8	-5.5	-93.9	-226.6	-22.7
29	0.4286	-46.8	12.5	-93.9	-138.1	-21.9
	0.5238	-44.7	8.9	-93.9	-157.9	-22.1
	0.6190	-42.9	-6.7	-93.9	-179.3	-22.3
	0.7143	-41.2	-6.8	-93.9	-202.2	-22.5
	0.8095	-39.3	-6.7	-93.9	-226.6	-22.7
31	0.4286	-48.5	-8.1	-93.9	-138.1	-21.9
	0.5238	-46.2	-7.8	-93.9	-157.9	-22.1
	0.6190	-44.3	-7.8	-93.9	-179.3	-22.3
	0.7143	-42.4	-7.7	-93.9	-202.2	-22.5
	0.8095	-40.4	-7.6	-93.9	-226.6	-22.7

B.8 Maximum Total Vertical Settlement for Diameter, D_2 of a Tunnel (mm)

Longitudinal length of tunnel, y_n (m)	Ratio A_n/D_2	Long term loading (PLAXIS 3D)	Seismic loading (PLAXIS 3D)	Modified empirical formulae (long term loading) (2D)	Modified Analytical formulae (long term loading) (2D)	Modified Analytical formulae (seismic loading) (2D)
27	0.4167	-46	14.1	-96.6	-139.6	-22.5
	0.5093	-43.7	9.6	-96.6	-159.2	-22.7
	0.6019	-41	9.2	-96.6	-180.4	-22.9
	0.6944	-40.3	6.5	-96.6	-203	-23.1
	0.7870	-38.5	-5.7	-96.6	-227	-23.3
29	0.4167	-48.5	13.1	-96.6	-139.6	-22.5
	0.5093	-45.8	10	-96.6	-159.2	-22.7
	0.6019	-45.9	-7	-96.6	-180.4	-22.9
	0.6944	-42.1	-6.9	-96.6	-203	-23.1
	0.7870	-40.1	-6.9	-96.6	-227	-23.3
31	0.4167	-50.3	8.7	-96.6	-139.6	-22.5
	0.5093	-47.4	-8.1	-96.6	-159.2	-22.7
	0.6019	-50.3	-8	-96.6	-180.4	-22.9
	0.6944	-43.2	-7.8	-96.6	-203	-23.1
	0.7870	-41.3	-7.7	-96.6	-227	-23.3

B.9 Maximum Total Vertical Settlement for Diameter, D_3 of a Tunnel (mm)

Longitudinal length of tunnel, y_n (m)	Ratio A_n/D_3	Long term loading (PLAXIS 3D)	Seismic loading (PLAXIS 3D)	Modified empirical formulae (long term loading) (2D)	Modified Analytical formulae (long term loading) (2D)	Modified Analytical formulae (seismic loading) (2D)
27	0.4091	-46.7	15.4	-98.4	-140.6	-22.8
	0.5000	-44.6	10.8	-98.4	-160.1	-23.1
	0.5909	-42.8	7.9	-98.4	-181.1	-23.3
	0.6818	-38.7	6.7	-98.4	-203.5	-23.5
	0.7727	-38.9	-5.8	-98.4	-227.3	-23.7
29	0.4091	-49	12.6	-98.4	-140.6	-22.8
	0.5000	-46.7	8.7	-98.4	-160.1	-23.1
	0.5909	-44.7	-7.1	-98.4	-181.1	-23.3
	0.6818	-40.4	-7	-98.4	-203.5	-23.5
	0.7727	-40.6	-6.9	-98.4	-227.3	-23.7
31	0.4091	-51	-8.5	-98.4	-140.6	-22.8
	0.5000	-48.3	-8.3	-98.4	-160.1	-23.1
	0.5909	-46.2	-8.1	-98.4	-181.1	-23.3
	0.6818	-41.3	-8	-98.4	-203.5	-23.5
	0.7727	-41.7	-7.7	-98.4	-227.3	-23.7

B.10 Maximum Lateral Surface Settlement for Diameter, D_1 Above A Tunnel (mm)

Longitudinal length of tunnel, y_n (m)	Ratio A_n/D_1	Long term loading (PLAXIS 3D)	Seismic loading (PLAXIS 3D)	Modified empirical formulae (long term loading) (2D)	Modified Analytical formulae (long term loading) (2D)	Modified Analytical formulae (seismic loading) (2D)	Modified empirical formulae (seismic loading) (2D)
27	0.4286	-3	-1.7	19.4	15.1	14.2	25.6
	0.5238	-2.3	-1.7	17.1	13.3	12.6	24.1
	0.6190	1.8	-1.7	15.2	11.9	11.3	22.7
	0.7143	2.2	-1.7	13.6	10.8	10.2	21.3
	0.8095	2.7	-1.6	12.4	9.8	9.3	19.8
29	0.4286	-3.8	-1.7	19.4	15.1	14.2	25.6
	0.5238	-2.9	-1.7	17.1	13.3	12.6	24.1
	0.6190	1.7	-1.7	15.2	11.9	11.3	22.7
	0.7143	2.1	-1.7	13.6	10.8	10.2	21.3
	0.8095	2.6	-1.6	12.4	9.8	9.3	19.8
31	0.4286	-4.6	-1.8	19.4	15.1	14.2	25.6
	0.5238	-3.4	-1.7	17.1	13.3	12.6	24.1
	0.6190	1.5	-1.7	15.2	11.9	11.3	22.7
	0.7143	2	-1.7	13.6	10.8	10.2	21.3
	0.8095	2.5	-1.6	12.4	9.8	9.3	19.8

B.11 Maximum Lateral Surface Settlement for Diameter, D_2 Above A Tunnel (mm)

Longitudinal length of tunnel, y_n (m)	Ratio A_n/D_2	Long term loading (PLAXIS 3D)	Seismic loading (PLAXIS 3D)	Modified empirical formulae (long term loading) (2D)	Modified Analytical formulae (long term loading) (2D)	Modified Analytical formulae (seismic loading) (2D)	Modified empirical formulae (seismic loading) (2D)
27	0.4167	-3.1	-1.8	20.4	15.7	14.9	25.4
	0.5093	-2.4	-1.8	17.9	13.9	13.2	23.9
	0.6019	-10.3	-1.8	15.9	12.5	11.8	22.5
	0.6944	2.4	-1.8	14.3	11.3	10.7	21
	0.7870	2.9	-1.7	13	10.3	9.7	19.6
29	0.4167	-4	-1.8	20.4	15.7	14.9	25.4
	0.5093	-3	-1.8	17.9	13.9	13.2	23.9
	0.6019	-12.5	-1.8	15.9	12.5	11.8	22.5
	0.6944	2.3	-1.8	14.3	11.3	10.7	21
	0.7870	2.8	-1.7	13	10.3	9.7	19.6
31	0.4167	-4.9	-1.9	20.4	15.7	14.9	25.4
	0.5093	-3.5	-1.8	17.9	13.9	13.2	23.9
	0.6019	-14.2	-1.8	15.9	12.5	11.8	22.5
	0.6944	2.2	-1.8	14.3	11.3	10.7	21
	0.7870	2.7	-1.7	13	10.3	9.7	19.6

B.12 Maximum Lateral Surface Settlement for Diameter, D_3 Above A Tunnel (mm)

Longitudinal length of tunnel, y_n (m)	Ratio A_n/D_3	Long term loading (PLAXIS 3D)	Seismic loading (PLAXIS 3D)	Modified empirical formulae (long term loading) (2D)	Modified Analytical formulae (long term loading) (2D)	Modified Analytical formulae (seismic loading) (2D)	Modified empirical formulae (seismic loading) (2D)
27	0.4091	-3.1	-1.8	21	16.2	15.3	25.2
	0.5000	-2.4	-1.8	18.4	14.4	13.6	23.8
	0.5909	1.9	-1.9	16.4	12.9	12.2	22.3
	0.6818	2.4	-1.8	14.8	11.6	11	20.9
	0.7727	3	-1.8	13.5	10.6	10.1	19.5
29	0.4091	-4	-1.8	21	16.2	15.3	25.2
	0.5000	-3	-1.8	18.4	14.4	13.6	23.8
	0.5909	-2.2	-1.9	16.4	12.9	12.2	22.3
	0.6818	2.4	-1.8	14.8	11.6	11	20.9
	0.7727	2.9	-1.8	13.5	10.6	10.1	19.5
31	0.4091	-5	-2	21	16.2	15.3	25.2
	0.5000	-3.6	-1.8	18.4	14.4	13.6	23.8
	0.5909	-2.6	-1.9	16.4	12.9	12.2	22.3
	0.6818	2.3	-1.8	14.8	11.6	11	20.9
	0.7727	2.8	-1.8	13.5	10.6	10.1	19.5

B.13 Maximum Total Lateral Settlement for Diameter, D_1 of a Tunnel (mm)

Longitudinal length of tunnel, y_n (m)	Ratio A_n/D_1	Long term loading (PLAXIS 3D)	Seismic loading (PLAXIS 3D)	Modified empirical formulae (long term loading) (2D)	Modified Analytical formulae (long term loading) (2D)	Modified Analytical formulae (seismic loading) (2D)	Modified empirical formulae (seismic loading) (2D)
27	0.4286	11.3	-10.4	67.1	11.5	12.1	47.2
	0.5238	10.4	9.4	71.5	11.7	12.4	47.2
	0.6190	9.6	10	76	11.9	12.6	47.2
	0.7143	9.5	10.6	80.5	12	12.8	47.2
	0.8095	9.3	11.2	85	12	12.9	47.2
29	0.4286	12.5	-10.5	67.1	11.5	12.1	47.2
	0.5238	11.4	9.4	71.5	11.7	12.4	47.2
	0.6190	9.5	10	76	11.9	12.6	47.2
	0.7143	10.2	10.6	80.5	12	12.8	47.2
	0.8095	9.8	11.1	85	12	12.9	47.2
31	0.4286	13.2	8.9	67.1	11.5	12.1	47.2
	0.5238	11.9	9.4	71.5	11.7	12.4	47.2
	0.6190	9.6	-4.1	76	11.9	12.6	47.2
	0.7143	10.7	10.6	80.5	12	12.8	47.2
	0.8095	10.4	11.1	85	12	12.9	47.2

B.14 Maximum Total Lateral Settlement for Diameter, D_2 of a Tunnel (mm)

Longitudinal length of tunnel, y_n (m)	Ratio A_n/D_2	Long term loading (PLAXIS 3D)	Seismic loading (PLAXIS 3D)	Modified empirical formulae (long term loading) (2D)	Modified Analytical formulae (long term loading) (2D)	Modified Analytical formulae (seismic loading) (2D)	Modified empirical formulae (seismic loading) (2D)
27	0.4167	11.9	9.4	68.4	11.8	12.4	47.4
	0.5093	10.5	9.9	72.9	12	12.7	47.4
	0.6019	-20.4	10.6	77.4	12.2	12.9	47.4
	0.6944	9.7	11.2	81.8	12.3	13.1	47.4
	0.7870	9.6	11.8	86.3	12.3	13.2	47.4
29	0.4167	12.9	9.4	68.4	11.8	12.4	47.4
	0.5093	11.5	10	72.9	12	12.7	47.4
	0.6019	-23.4	10.6	77.4	12.2	12.9	47.4
	0.6944	10.4	11.2	81.8	12.3	13.1	47.4
	0.7870	10.1	11.7	86.3	12.3	13.2	47.4
31	0.4167	13.8	9.4	68.4	11.8	12.4	47.4
	0.5093	12.2	10	72.9	12	12.7	47.4
	0.6019	-24	10.6	77.4	12.2	12.9	47.4
	0.6944	10.9	11.2	81.8	12.3	13.1	47.4
	0.7870	-10.7	11.7	86.3	12.3	13.2	47.4

B.15 Maximum Total Lateral Settlement for Diameter, D_3 of a Tunnel (mm)

Longitudinal length of tunnel, y_n (m)	Ratio A_n/D_3	Long term loading (PLAXIS 3D)	Seismic loading (PLAXIS 3D)	Modified empirical formulae (long term loading) (2D)	Modified Analytical formulae (long term loading) (2D)	Modified Analytical formulae (seismic loading) (2D)	Modified empirical formulae (seismic loading) (2D)
27	0.4091	12.1	9.8	69.3	12	12.6	47.6
	0.5000	10.9	10.3	73.8	12.2	12.9	47.6
	0.5909	10.4	11	78.3	12.4	13.2	47.6
	0.6818	9.4	11.6	82.7	12.5	13.3	47.6
	0.7727	9.8	12.2	87.2	12.6	13.5	47.6
29	0.4091	13.2	9.8	69.3	12	12.6	47.6
	0.5000	11.8	10.4	73.8	12.2	12.9	47.6
	0.5909	11.1	11	78.3	12.4	13.2	47.6
	0.6818	10	11.6	82.7	12.5	13.3	47.6
	0.7727	10.4	12.2	87.2	12.6	13.5	47.6
31	0.4091	14.1	9.8	69.3	12	12.6	47.6
	0.5000	12.5	10.4	73.8	12.2	12.9	47.6
	0.5909	11.8	11	78.3	12.4	13.2	47.6
	0.6818	10.5	11.6	82.7	12.5	13.3	47.6
	0.7727	10.9	12.2	87.2	12.6	13.5	47.6

B.16 Maximum Longitudinal Surface Settlement for Diameter, D_1 Above A Tunnel (mm)

Longitudinal length of tunnel, y_n (m)	Ratio A_n/D_1	Long term loading (PLAXIS 3D)	Seismic loading (PLAXIS 3D)	Modified empirical formulae (long term loading) (2D)
27	0.4286	6.7	0.6	5.2
	0.5238	4.2	0.5	4.3
	0.6190	1.4	0.4	3.6
	0.7143	-2.1	0.4	3
	0.8095	-2.7	0.3	2.6
29	0.4286	6.6	0.8	5.2
	0.5238	4	0.6	4.3
	0.6190	1.3	0.5	3.6
	0.7143	-2.7	0.5	3
	0.8095	-3.2	0.5	2.6
31	0.4286	6.3	1	5.2
	0.5238	3.7	0.8	4.3
	0.6190	1.3	0.7	3.6
	0.7143	-3.3	0.6	3
	0.8095	-3.6	0.5	2.6

B.17 Maximum Longitudinal Surface Settlement for Diameter, D_2 Above A Tunnel (mm)

Longitudinal length of tunnel, y_n (m)	Ratio A_n/D_2	Long term loading (PLAXIS 3D)	Seismic loading (PLAXIS 3D)	Modified empirical formulae (long term loading) (2D)
27	0.4167	7.1	0.7	5.3
	0.5093	4.4	0.5	4.4
	0.6019	5.8	0.4	3.7
	0.6944	-2.2	0.4	3.1
	0.7870	-2.9	0.3	2.7
29	0.4167	6.9	0.9	5.3
	0.5093	4.1	0.7	4.4
	0.6019	-6.6	0.6	3.7
	0.6944	-2.9	0.5	3.1
	0.7870	-3.4	0.5	2.7
31	0.4167	6.7	1.1	5.3
	0.5093	3.8	0.9	4.4
	0.6019	-9.7	0.7	3.7
	0.6944	-3.5	0.6	3.1
	0.7870	-3.8	0.6	2.7

B.18 Maximum Longitudinal Surface Settlement for Diameter, D_3 Above A Tunnel (mm)

Longitudinal length of tunnel, y_n (m)	Ratio A_n/D_3	Long term loading (PLAXIS 3D)	Seismic loading (PLAXIS 3D)	Modified empirical formulae (long term loading) (2D)
27	0.4091	7.2	0.6	5.4
	0.5000	4.5	0.5	4.5
	0.5909	2.4	0.4	3.8
	0.6818	-2.2	0.4	3.2
	0.7727	-3	0.4	2.8
29	0.4091	7	0.9	5.4
	0.5000	4.2	0.7	4.5
	0.5909	-2.2	0.6	3.8
	0.6818	-2.8	0.5	3.2
	0.7727	-3.5	0.5	2.8
31	0.4091	6.8	1.1	5.4
	0.5000	4	0.9	4.5
	0.5909	-3	0.8	3.8
	0.6818	-3.3	0.7	3.2
	0.7727	-3.9	0.6	2.8

B.19 Maximum Total Longitudinal Settlement for Diameter, D_1 of a Tunnel (mm)

Longitudinal length of tunnel, y_n (m)	Ratio A_n/D_1	Long term loading (PLAXIS 3D)	Seismic loading (PLAXIS 3D)	Modified empirical formulae (long term loading) (2D)
27	0.4286	10.1	4.8	17.9
	0.5238	-8.8	3.4	17.9
	0.6190	-8.5	3.1	17.9
	0.7143	-7	-3.7	17.9
	0.8095	-11	-3.1	17.9
29	0.4286	9.9	4.1	17.9
	0.5238	-8.6	3.4	17.9
	0.6190	-8.3	2.9	17.9
	0.7143	-6.9	-2.8	17.9
	0.8095	3.3	-3.7	17.9
31	0.4286	9.8	3.4	17.9
	0.5238	-8.4	2.4	17.9
	0.6190	-8.1	-2.6	17.9
	0.7143	-6.7	-3.5	17.9
	0.8095	-11.9	-4.3	17.9

B.20 Maximum Total Longitudinal Settlement for Diameter, D_2 of a Tunnel (mm)

Longitudinal length of tunnel, y_n (m)	Ratio A_n/D_2	Long term loading (PLAXIS 3D)	Seismic loading (PLAXIS 3D)	Modified empirical formulae (long term loading) (2D)
27	0.4167	-11.2	4.8	16.9
	0.5093	-9.5	4.4	16.9
	0.6019	8.2	-4.2	16.9
	0.6944	-7.1	3	16.9
	0.7870	-11.2	-3.3	16.9
29	0.4167	-11.1	4.5	16.9
	0.5093	-9.3	3.9	16.9
	0.6019	-8.2	3.3	16.9
	0.6944	-7	-2.9	16.9
	0.7870	-11.7	-3.9	16.9
31	0.4167	-10.8	3.9	16.9
	0.5093	-9.2	3.1	16.9
	0.6019	-12	-2.7	16.9
	0.6944	-6.9	-3.7	16.9
	0.7870	-12	-4.5	16.9

B.21 Maximum Total Longitudinal Settlement for Diameter, D_3 of a Tunnel (mm)

Longitudinal length of tunnel, y_n (m)	Ratio A_n/D_3	Long term loading (PLAXIS 3D)	Seismic loading (PLAXIS 3D)	Modified empirical formulae (long term loading) (2D)
27	0.4091	-11.2	4.9	16.3
	0.5000	-9.7	4.3	16.3
	0.5909	-8.9	3.5	16.3
	0.6818	-7.1	-3.4	16.3
	0.7727	-11.3	-3.4	16.3
29	0.4091	-11	4.3	16.3
	0.5000	-9.5	3.2	16.3
	0.5909	-8.7	3	16.3
	0.6818	-7	-3.1	16.3
	0.7727	-11.8	-3.8	16.3
31	0.4091	-10.8	3.6	16.3
	0.5000	-9.3	2.9	16.3
	0.5909	-8.5	-2.8	16.3
	0.6818	-6.8	-3.6	16.3
	0.7727	-12.3	-4.6	16.3

B.22 Maximum Volumetric Strain for Diameter, D_1

Longitudinal length of tunnel, y_n (m)	Ratio A_n/D_1	Long term loading (PLAXIS 3D)	Seismic loading (PLAXIS 3D)	Modified analytical formulae (long term loading) (2D)	Modified Analytical formulae (seismic loading) (2D)
27.0	0.4286	3.60	-0.037	0.9879	0.002491
	0.5238	3.30	-0.026	0.9879	0.002491
	0.6190	2.80	-0.045	0.9879	0.002491
	0.7143	3.00	-0.036	0.9879	0.002491
	0.8095	1.90	-0.032	0.9879	0.002491
29.0	0.4286	3.50	-0.033	0.9879	0.002491
	0.5238	3.20	0.029	0.9879	0.002491
	0.6190	2.70	-0.026	0.9879	0.002491
	0.7143	2.80	-0.029	0.9879	0.002491
	0.8095	1.80	-0.032	0.9879	0.002491
31.0	0.4286	3.70	-0.026	0.9879	0.002491
	0.5238	3.20	-0.028	0.9879	0.002491
	0.6190	2.70	-0.029	0.9879	0.002491
	0.7143	2.90	-0.033	0.9879	0.002491
	0.8095	2.00	-0.034	0.9879	0.002491

B.23 Maximum Volumetric Strain for Diameter, D_2

Longitudinal length of tunnel, y_n (m)	Ratio A_n/D_2	Long term loading (PLAXIS 3D)	Seismic loading (PLAXIS 3D)	Modified analytical formulae (long term loading) (2D)	Modified Analytical formulae (seismic loading) (2D)
27.0	0.4167	3.20	-0.038	0.9886	0.002493
	0.5093	2.60	-0.037	0.9886	0.002493
	0.6019	4.20	-0.038	0.9886	0.002493
	0.6944	1.60	0.036	0.9886	0.002493
	0.7870	2.10	-0.035	0.9886	0.002493
29.0	0.4167	3.40	-0.044	0.9886	0.002493
	0.5093	3.30	0.034	0.9886	0.002493
	0.6019	4.50	-0.028	0.9886	0.002493
	0.6944	2.50	0.036	0.9886	0.002493
	0.7870	2.00	0.029	0.9886	0.002493
31.0	0.4167	4.00	-0.047	0.9886	0.002493
	0.5093	3.30	-0.028	0.9886	0.002493
	0.6019	5.10	-0.032	0.9886	0.002493
	0.6944	2.50	0.036	0.9886	0.002493
	0.7870	2.00	-0.037	0.9886	0.002493

B.24 Maximum Volumetric Strain for Diameter, D_3

Longitudinal length of tunnel, y_n (m)	Ratio A_n/D_3	Long term loading (PLAXIS 3D)	Seismic loading (PLAXIS 3D)	Modified analytical formulae (long term loading) (2D)	Modified Analytical formulae (seismic loading) (2D)
27.0	0.4091	4.50	0.043	0.9890	0.002494
	0.5000	2.80	-0.034	0.9890	0.002494
	0.5909	2.00	-0.038	0.9890	0.002494
	0.6818	1.40	-0.035	0.9890	0.002494
	0.7727	1.50	0.040	0.9890	0.002494
29.0	0.4091	4.40	-0.050	0.9890	0.002494
	0.5000	3.40	-0.031	0.9890	0.002494
	0.5909	2.10	-0.031	0.9890	0.002494
	0.6818	2.30	-0.034	0.9890	0.002494
	0.7727	2.50	0.040	0.9890	0.002494
31.0	0.4091	4.30	-0.041	0.9890	0.002494
	0.5000	3.50	-0.036	0.9890	0.002494
	0.5909	3.70	-0.031	0.9890	0.002494
	0.6818	2.20	-0.035	0.9890	0.002494
	0.7727	2.40	0.040	0.9890	0.002494

APPENDIX C

C.1: Calculation of validation of modified empirical formula for maximum vertical surface settlement

Here, $H = 10\text{m}$, $D = 8\text{m}$

$$\text{Now, } V_{(z), \text{max.}} = (0.0045 * (8^2/10)) * 1000 = 28.8 \text{ mm [Use equation 3.1]}$$

C.2: Calculation of validation of modified analytical formula for maximum vertical surface settlement

Here, $z = 0$ (for surface); $z_1 = 0 - H = 0 - 10 = -10$; $z_2 = 0 + H = 0 + 10 = 10$;

$$r_1^2 = z_1^2 = (-10)^2 = 100; r_2^2 = z_2^2 = 10^2 = 100; R = D/2 = 8/2 = 4;$$

$$\text{Poisson Ratio, } \nu = 0.20; m = 1/(1-(2*0.20)) = 1.67$$

$$k = \nu/(1 - \nu) = 0.20/(1-0.20) = 0.25$$

$$\text{Now, } V_{(z), \text{max.}} = 0 + 0 + [(0.01*4^2)/2] * (((1.67 + 1) * 10)/100)] - [(0.002 * 4^2 * 10) * (-100/100^2)]$$

$$V_{(z), \text{max.}} = 0.02136 + 0.0032 = 0.0246\text{m} = 24.6\text{mm [Use equation 3.2]}$$

C.3: Calculation of validation of modified strain induced volume loss analytical formula for long term loading

Here, $t = 0$; means that inner and outer diameter of tunnel are same.

$$D = 8\text{m}; A = H - D/2 = 10 - (8/2) = 6\text{m}$$

$$\varepsilon_{vl} = 0.01003 \exp[-(0.69/(1+(8/(2*6))))^2] = 0.78\% \text{ [Use equation 3.9]}$$

C.4: Calculation of tunnel face pressure and grout pressure for CD test at $A_1 = 4.5\text{m}$, $D_1 = 10.5\text{m}$ (Bernhard et. al, 2011):

Lateral earth pressure coefficient, $K = 0.5$ (Duddeck (1980))

$$\text{(A) Tunnel Face Pressure, } \tau_f = \sigma_{h,\text{crown}} = [(\gamma_{1,\text{sat}} - \gamma_w)*(3.5)*(0.5) + (\gamma_{2,\text{sat}} - \gamma_w)*(1)*(0.5) + (\gamma_w * 3.5) + (\gamma_w * 1)] = [(18.9-9.81)*(3.5)*(0.5) + (20-9.81)*(1)*(0.5) + (9.81*3.5) + (9.81*1)]$$

$$\tau_f = \sigma_{h,\text{crown}} = 15.9 + 5.1 + 34.3 + 9.9 = 65.2 \text{ kN/m}^2$$

$$\sigma_{h,\text{invert}} = \sigma_{h,\text{crown}} + (\gamma_{2,\text{sat}} - \gamma_w)*(10.5)*(0.5) + (\gamma_w * 10.5) = 65.2 + 53.5 + 103 = 221.7 \text{ kN/m}^2$$

$$\text{Linear increment along depth of tunnel, } \tau_{f,\text{inc.}} = (\sigma_{h,\text{invert}} - \sigma_{h,\text{crown}})/D = [(221.7 - 65.2)/10.5]$$

$$\tau_{f,\text{inc.}} = 14.9 \text{ kN/m}^2/\text{m}$$

$$\text{(B) Grout Pressure, } \tau_g = \sigma_{v,\text{crown}} = [(\gamma_{1,\text{sat}} - \gamma_w)*(3.5) + (\gamma_{2,\text{sat}} - \gamma_w)*(1) + (\gamma_w * 3.5) + (\gamma_w * 1)] = [(18.9-9.81)*(3.5) + (20-9.81)*(1) + (9.81*3.5) + (9.81*1)]$$

$$\tau_g = \sigma_{v,\text{crown}} = 31.8 + 10.2 + 34.3 + 9.81 = 86.1 \text{ kN/m}^2$$

$$\sigma_{v,\text{invert}} = \sigma_{v,\text{crown}} + (\gamma_{2,\text{sat}} - \gamma_w)*(\pi D/4) + (\gamma_w * (\pi D/4))$$

$$= 86.1 + ((20-9.81)*((\pi*10.5)/4)) + (9.81 * ((\pi*10.5)/4)) = (86.1 + 84 + 80.9) \text{ kN/m}^2$$

$$\sigma_{v,\text{invert}} = 251 \text{ kN/m}^2$$

Linear increment along peripheral depth of tunnel, $\tau_{g,\text{inc.}} = (\sigma_{v,\text{invert}} - \sigma_{v,\text{crown}})/(\pi D/4)$

$$\tau_{g,\text{inc.}} = (251 - 86.1)/(10.5\pi/4) = 20 \text{ kN/m}^2/\text{m}$$

(C) Jacking Force, $T_{JF} = 68000 \text{ kN}$

$$\tau_{jF} = T_{JF}/(\pi D^2/4) = 68000/((\pi*10.5^2)/4) = 785.3 \text{ kN/m}^2$$

C.5: Calculation of axial increment of volume loss of tunnel

Length of tunnel boring machine = 12m

Surface contraction which equivalent to volume loss = 0.5%

Advancement of tunnel = 2m

Now, Axial increment = $0.5\%/(12-2) = 0.05\%/m$

C.6: Calculation of tunnel face pressure (Kilany et al. 2017)

(A) Tunnel Face Pressure, $\tau_f = \sigma_{h,\text{crown}} = [(15)*(2)*(0.5) + (16)*(2)*(0.5) + (18 - 9.81)*(1)*(0.5) + (17 - 9.81)*(3)*(0.5) + (9.81*1) + (9.81*3)]$; where, lateral earth pressure coefficient, $K = 0.5$

$$\tau_f = \sigma_{h,\text{crown}} = 90.1 \text{ kN/m}^2$$

$$\sigma_{h,\text{invert}} = \sigma_{h,\text{crown}} + (17 - 9.81)*(2)*(0.5) + (19 - 9.81)*(6)*(0.5) + (9.81 * 8) = 203.5 \text{ kN/m}^2$$

Linear increment along depth of tunnel, $\tau_{f,\text{inc.}} = (\sigma_{h,\text{invert}} - \sigma_{h,\text{crown}})/D = [(203.5 - 90.1)/8]$

$$\tau_{f,\text{inc.}} = 14.2 \text{ kN/m}^2/\text{m}$$

C.7: Calculation of maximum vertical settlement for $A_1 = 4.5\text{m}$, $D_1 = 10.5\text{m}$ by Mair (1993) empirical formula

$$V_s = 0.5\% = 0.005 \quad K = 34\% = 0.34 \quad D = 10.5\text{m} \quad H = 4.5 + (10/2) = 9.75\text{m}$$

Now, $V_{(z=0),\text{max.}} = 0.313 * [(V_s D^2)/(KH)]$

$$= 0.313 * [(0.005*(10.5^2))/(0.34*9.75)] * 1000 = 52.05\text{mm}$$

C.8: Calculation of maximum vertical settlement for $A_1 = 4.5\text{m}$, $D_1 = 10.5\text{m}$ by present research modified formula

$$D = 10.5\text{m} \quad H = 4.5 + (10/2) = 9.75\text{m} \quad z = 0 \text{ (for surface)}$$

Now, $V_{(z=0),\text{max.}} = 0.0045 * [D^2/(H - z)]$

$$= 0.0045 * [10.5^2/(9.75)] * 1000 = 50.88\text{mm}$$

THE END